Spring 5-15-2017

Diversity Oriented Synthesis, Characterization and Anti-Cancer Activity of Killer Peptide Nucleolipid Bioconjugates

Niki K. Rana
niki.rana@student.shu.edu

DIVERSITY ORIENTED SYNTHESIS, CHARACTERIZATION AND ANTI-CANCER ACTIVITY OF KILLER PEPTIDE NUCLEOLIPID BIOCONJUGATES

A thesis submitted to Seton Hall University in partial fulfillment of the requirements for the degree of Doctor of Philosophy

By

Niki K. Rana

May 2017

Department of Chemistry and Biochemistry

Seton Hall University

South Orange, NJ, USA

DISSERTATION COMMITTEE APPROVALS
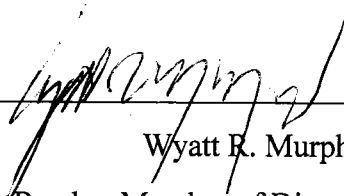
We certify that we read this thesis and in our opinion, it is sufficient in scientific scope and quality as a dissertation for the degree of Doctor in Philosophy.

APPROVED BY:
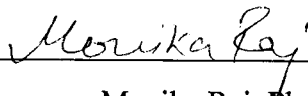
David Sabatino, Ph.D.

Research Mentor, Seton Hall University

Wyatt R. Murphy, Ph.D.

Reader, Member of Dissertation Committee,

Seton Hall University

Monika Raj, Ph.D.

Reader, Member of Dissertation Committee,

Seton Hall University

Cecilia Marzabadi, Ph.D.

Chair, Department of Chemistry and Biochemistry,

Seton Hall University

I dedicate this thesis to

my parents, Kamleshkumar, Nayanaben, and my sister, Urvi,

for their constant support and unconditional love.

ABSTRACT

The killer peptide sequence D-(KLAKLAK)$_2$ has been originally designed and developed as an antibacterial agent. Despite having excellent cytotoxicity towards bacteria, this sequence maintains low cell cytotoxicity in malignant mammalian cell types such as cancer. The chemical basis for its selectivity has been attributed to its poly(cationic) amphiphilic nature, which facilitates cell permeability across the negatively charged bacterial membrane, but with limited permeability across the zwitterionic membrane of mammalian cells. The positively charged D-(KLAKLAK)$_2$ sequence has been found to accumulate on the surface of the mitochondria causing dissipation of the negatively charged mitochondrial membrane potential. This charge disruption results in membrane lysis and the secretion of cell death markers that ultimately lead to programmed cell death. In order to overcome the limited activity of the D-(KLAKLAK)$_2$ sequence in malignant tumor cell types, we proposed that chemically robust and structurally pre-organized amphiphilic nucleolipids would function to enhance cell permeability and mitochondria localization in tumors, resulting in potent and long-lasting anti-cancer effects. In this study, thymidine-derived nucleolipids were rationally designed to contain 3'-lipid appendages and a reactive 5'-carboxy group. A diversity oriented synthesis approach featuring a reductive amination procedure was developed for making a small library of amphiphilic nucleolipids. Solid phase bioconjugation coupled the nucleolipids with the pro-apoptotic D-(KLAKLAK)$_2$ sequence for exploring structure-activity relationships. The peptide nucleolipid conjugates were found to self-assemble into amphiphilic nanoparticle formulations that promoted anti-cancer activity in a selected panel of cancer cells. This thesis will serve to highlight the most important findings towards the development of peptide-nucleolipid conjugates that effectively serve as potent anti-cancer agents.

ACKNOWLEDGEMENTS

I have always held a natural curiosity for the sciences. Growing up, I've always wondered how science can be used to answer nature's most mystifying questions. I marveled at the biology that led to flowers blossoming in the spring, the physics that rendered light possible in my room and the chemistry that surrounded the transformations I witnessed in living and non-living things. To help answer these fundamental questions, I relied on my parents, teachers, professors and textbooks for explanations. With their guidance, I was able to assign reason to my questions. This has inspired my desire to learn more about the sciences and to pursue my career in PhD research to unravel nature's greatest mysteries.

With this mission at heart, I decided to dedicate myself as a graduate student in the Department of Chemistry and Biochemistry at Seton Hall University under the mentorship of Dr. David Sabatino. I am truly thankful for Dr. Sabatino's help and guidance over the years and I would like to extend my warmest appreciation for being such a great mentor. Dr. Sabatino has always been patient and willing to assist me with my scheduling, research advice, and possible career paths. I could not have been as successful without his help every step of the way. Many thanks for your patient guidance, encouragement and advice. Since I joined the research group of Dr. Sabatino in the Spring of 2013, I've been able to expand my knowledge and develop high impact cancer research. I have been extremely lucky to have a supervisor who cared so much about my work and responded to my questions so promptly. Dr. Sabatino has guided my pursuit for knowledge and personal growth. For these important attributes, I'm very grateful. Without his unwavering support this dissertation would not have been possible. I thank him from the bottom of my heart for all of his continued help, support and guidance.

Kazakevich, Dr. James Hanson, Dr. Allan Blake, Dr. Joseph Maloy and Fr. Gerald Bounopane for their continuous support.

Furthermore, I would also like to thank the efforts of Dr. Uri Samuni, and PhD student Suying Huang for their collaboration at City University New York, Queen's College. With their expertise in DLS and TEM studies, we were able to complete important structural analyses of a peptide-nucleolipid conjugate which ultimately led to our first publication. I would also like to thank Maureen Grutt for all of the great administrative work she accomplishes for the Department and University. Maureen has also been especially kind and helpful for tracking my degree requirements and supporting my academic studies. Thank you for all of your efforts.

I feel proud to say that I have matured in a supportive and productive research environment. Working alongside colleagues that I consider friends who have played major roles in my academic studies. Firstly, I'd like to thank Pradeep Patel, a former graduate student from Dr. Sabatino's lab and one of my best friends for his peer advice in my first project and continuous guidance. There are few words that I can use to truly describe all of my appreciation for his help and support. Secondly, I'd like to thank Marianaaaaaaaa, Steve, Erik, Sunil, Gia, Claudia, Andrieh, Adah, Anthony and Chris for being part of my PhD lab life. For Mariana, I thank her from bottom of my heart to share each and every moment with her, including the maxima and minima of life. I wish that as we stepped into Seton Hall University together, we will find our way out together too. I'd like to thank all of my other friends in the Department, especially, Emi and Lauren. They have provided a zone of comfort in and out of school to help accomplish our graduate studies. Thank you to our neighboring group friends, Anu and Dr. Raj's students for all the time that we spent together over lunch or in meetings.

TABLE OF CONTENTS

CHAPTER 4: CONCLUSIONS AND CONTRIBUTIONS TO KNOWLEDGE

ABBREVIATIONS AND SYMBOLS

aRNA	Antisense RNA
Arg	Arginine
A549	adenocarcinoma cells
A_{260} or Abs	UV absorbance measured at 260 nm
A or Ala	Alanine
AON	Antisense oligonucleotide
ε-Ahx	aminohexanoic acid
AchR	acetylcholine receptor
Arg	Arginine
BSA	bovine serum albumin
BAIB	(Diacetoxyiodo)benzene
CTP	cancer targeting peptide
C or Cys	Cysteine
CD	Circular Dichroism
CO_2	Carbon dioxide
COSY	Correlation spectroscopy
CPG	Controlled pore glass
CTO	Cancer targeting oligonucleotide
Ca^{2+}	Calcium ion
CATB	Cetyl triethylammonium bromide
D or Asp	Aspartate
DAPI	diamidino-2-phenylindole

DIC	*N,N*-diisopropylcarbodiimide
DLS	dynamic light scattering
DCM	Dichloromethane
DMF	*N,N*-dimethyl formamide
DMSO	dimethyl sulfoxide
DNA	2′-deoxyribonucleic acid
DTPA	diethylenetriaminepentaacetic acid
DTT	Dithioreitol
DMAP	Dimethoxyaminopyridine
DU145	prostate cancer cell line
DMT	Dimethoxytrityl
EDTA	ethylene-diamine tetraacetate dehydrate
Ex/Em	excitation/emission
EDC	1-Ethyl-3-(3-dimethylaminopropyl)carbodiimide
ESI-MS	electrospray ionization mass spectrometry
EtOH	ethanol
ER	endoplasmic reticulum
^{19}F	Fluorine
FA	formic acid
FBOA	*p*-fluorobenzyloxime acetyl
FBS	fetal bovine serum
FDA	food and drug administration
FITC	fluorescein isothiocyanate

FGF-R	fibroblast growth factor receptor
Fmoc	Fluorenylmethyloxycarbonyl
G or Gly	glycine
g	Gram
g/mol	grams per mole
G-tetrads	G-tetraplexes
GRP78	glucose regulated protein 78 kDa
h	hours
HB	Hepatoblastoma
HCTU	O-(1H-6-Chlorobenzotriazole-1-yl)-1,1,3,3-tetramethyluronium hexafluorophosphate
HDFa	human dermal fibroblast
HATU	(1-[Bis(dimethylamino)methylene]-1H-1,2,3-triazolo[4,5-b]pyridinium 3-oxid hexafluorophosphate)
HepG2	human hepatoblastoma cell line
HER-2	human epidermal growth factor receptor 2
HIF-1	hypoxia-inducible factor 1
HOBt	1-hydroxybenzotriazole
hPTN	human pleiotrophin
HRP	horseradish peroxidase
HSP70	heat shock protein 70 kDa
HYD-1	hybrid peptide
^{123}I	iodine

Ile	Isoleucine
IC_{50}	concentration of inhibitor which causes 50% inhibition
K_D	dissociation constant
kDa	kilodalton
λ	wavelength
LC/MS	liquid chromatography mass spectrometry
Leu	Leucine
m/z	mass to charge ratio
Θ	molar ellipticity
mAb	monoclonal antibody
MeCN	acetonitrile
MeOH	Methanol
Me6652/4	melanoma cells
$MgCl_2$	magnesium chloride
MHC	major histocompatibility complex
MW	microwave
M.W.	molecular weight
μM	micromolar
μL	microliter
N:P	nitrogen to phosphate ratio
NK	natural killer
NMM	*N*-methylmorpholine
NMP	*N*-methylpyrrolidinone

NOTA	1,4,7-triazacyclononane-1,4,7-triacetic acid
OBOC	one-bead one compound
PAGE	polyacrylamide gel electrophoresis
PDA	photodiode array
Pbf	*N*-2,2,4,6,7-pentamethyldihydrobenzofuran-5-sulfonyl
PBS	phosphate buffered saline
Pep42-QD	Pep42-Quantum Dots
PET	positron emission tomography
PNA	peptide nucleic acid
Pro	proline
pIII	filamentous phage protein III
pVIII	filamentous phage protein VIII
PS-DVB	poly(styrene/divinyl benzene)
PSI	Peptide Scientific Inc.
PVDF	polyvinylidene difluoride
R	Arginine
RNA	ribonucleic acid
RNAi	RNA interference
RIPA	radioimmunoprecipitation assay
RP-HPLC	reverse-phase high performance liquid chromatography
RT	retention time
SEM	standard error of the mean
Sf-9	spodoptera frugiperda 9

siRNA	small interfering RNA
SJSA-1	osteosarcoma cells
SPPS	solid phase peptide synthesis
T or Thr	threonine
t-Bu	tertiary butyl
TAE	tris-acetate-EDTA
TBE	tris/boric acid/EDTA buffer
TE2A	Tetraazamacrocycles
TEM	transmission electron microscopy
TES	Triethylsilane
TETA	1,4,8,11-tetraazacyclotetradecane-1,4,8,11-tetraacetic acid
TFA	trifluroacetic acid
TFE	2,2,2-trifluoroethanol
TGF-β	transforming growth factor beta
™	trademark
TMB	3,3′,5,5′tetramethylbenzidine
Tris-HCl	tris(hydroxymethyl)aminomethane hydrochloride
Tyr	Tyrosine
UPR	unfolded protein response
UV-Vis	ultraviolet-visible
Val	Valine
VEGF	vascular endothelial growth factor
v/v	volume per volume

W or Trp   tryptophan

LIST OF FIGURES

CHAPTER 1

CHAPTER 3

CHAPTER 4

LIST OF SCHEMES

CHAPTER 1

CHAPTER 2

LIST OF TABLES

CHAPTER 1. BIO-ACTIVE PEPTIDES: AN OVERVIEW OF THEIR STRUCTURE-FUNCTION RELATIONSHIP FOR ANTI-CANCER ACTIVITY

1.1 ABSTRACT

Biologically active peptides exhibit a variety of beneficial effects, including anti-proliferative, antioxidant, anti-microtubule, and antibacterial properties. Their isolation from natural sources e.g. plant and marine sources, including algae and cyanobacteria have led to the development of many antibiotic and anti-cancer drugs. Vancomycin is among the most famous examples. Bioactive peptides have also been isolated as secondary metabolites derived from sponges, ascidians, tunicates and mollusks. For example, protein hydrolysates derived from the enzymatic digestion of aquatic and marine by-products are an important source of bioactive peptides. These exhibit antioxidant, antimicrobial activities and cytotoxic effects on malignant mammalian cancer types such as HeLa, AGS, and DLD-1 cells. Key to their biological activity are various amino acid residues that may be naturally occurring or modified, in addition to the incorporation of ions, small molecules and transition metal ligands that can tailor the structure-function properties of the peptides. An important class of biologically active peptides belong to the amphiphilic, α-helical cell penetrating peptides (CPPs). CPPs internalize within cells and traffic within endosomes until endosomal escape contributes to their delivery to various organelles. A common subcellular target for the positively charged CPPs is the negatively charged membrane surface of the mitochondria. Upon binding, depolarization of the negatively charged (-180 mV) mitochondrial membrane results in a loss of mitochondrial membrane integrity that stimulates the release of mitochondrial contents into the cytoplasm. The release of cell death effectors from the mitochondria, including cytochrome c, second mitochondrial derived activator of caspase and the apoptosis-inducing factor

(AIF) ultimately trigger programmed cell death. These desirable structure-function properties has led to the development of a new class of mitochondria penetrating peptides (MPPs) that exhibit potent activity against chronic diseases such as cancer.

1.2 INTRODUCTION

Short bioactive peptide sequences may exhibit efficient cellular uptake in mammalian cell types. These cell-penetrating peptides (CPPs) tend to have distinct structure-function properties. They include amphiphilic primary sequence compositions that typically include hydrophobic and positively charged amino acid residues. Moreover, the secondary structures of CPPs tends to be α-helical in nature. The amphiphilic peptide sequence has been shown to contribute to membrane affinity and translocation activity. Moreover, the α-helical peptide structure that has been found in many membrane spanning pore proteins has also been correlated as a secondary structure motif conducive to membrane transport and intracellular localization of soluble analytes [1]. A variety of cell translocation mechanisms have been attributed to the CPPs, including receptor and non-receptor mediated endocytosis, micro- and pinocytosis which encapsulates the peptides in membrane-bound endosomes for intracellular trafficking and release at the targeted site for activity [2]. A common target for the CPPs is the mitochondrion. The mitochondrion is a key organelle that performs essential cellular functions and plays pivotal roles in regulating cellular metabolism, senescence and survival. Thus, the mitochondria represents an entry point of interest for organelle-specific delivery of effector molecules used to treat metabolic, degenerative and hyperproliferative diseases [3]. In spite of their utility, mitochondria-targeting drugs remain hampered by a variety of side effects that limit their potential clinical utility. Therefore, the discovery of new drug-like molecules used to target the mitochondria in diseased cells and tissues is currently an urgent, un-met need. Towards this end, a series of short, amphiphilic peptides that penetrate the plasma

membrane and localize within the mitochondria for biological activity have served as promising leads. For example, the Tat peptide, (**Figure 1.1**) derived from the HIV transactivator protein is considered one of the first representative examples of a mitochondria-penetrating peptide (MPP) [4].

Figure 1.1. Primary sequence of the HIV-Tat peptide (48-60), GRKKRRQRRRGYKC, as a representative mitochondria-penetrating peptide. Figure adapted from reference Green, M., Loeweinstein, M. *Cell*, **1988**, *55, 1179 – 1188.*

Once internalized within cells, MPPs accumulate on the surface of the mitochondria and induce depolarization of the mitochondrial membrane. This depolarization commonly results in cell apoptosis [5]. For example, the depolarization and disruption of the mitochondrial membrane results in the release of the cell death markers such as the apoptosis inducing factor (AIF). Additionally, Ca^{2+} flux plays an important role for VDAC mediated calcium ion signaling. In compromised cells, unregulated Ca^{2+} flux leads to the release of caspase co-factors needed for the pro-apoptotic activity of the caspase enzymes. Similarly, the calcium signaling receptor- BCL-2 is a class of proteins found exclusively on the cell surface of the mitochondria that regulates cell death events [5]. The BCL-2 family of proteins constitutes a critical checkpoint in the apoptotic cascade. BAX, BH3, BAK are also pro-apoptotic checkpoints functioning with BCL-2 at the

mitochondrial membrane [6]. In cells with damaged mitochondria, BCL-2 signaling triggers the release of pro-apoptotic executors, including cytochrome c and reactive oxygen species. The formation of reactive oxygen species (ROS) aberrantly oxidizes biological molecules, altering their structure-function properties that ultimately impedes their normal cellular function [7]. Under these so-called "stressed conditions" protein misfolding also occurs and the unfolded-protein response (UPR) either rescues these proteins through chaperone activity or signals the release of caspase enzymes as pro-apoptotic executors in the absence of protein salvaging. Taken altogether, MPPs that serve to disrupt mitochondria structure and function can ultimately lead to programmed cell death by a variety of cell death signaling pathways (**Figure. 1.2**).

In order to improve the structure-function properties of the MPPs, small molecule and biological ligands that effectively target selected cell types and accumulate within the mitochondria have been developed. Small molecule ligands such as triphenylphosphine (TPP) and choline esters incorporated within MPPs improved their inner mitochondrial membrane (IMM) localization properties. For the incorporation of IMM-specific biologicals, including phospholipids, gramicidin S (GS)-based antioxidants have also improved activity, with the concomitant delivery of nitroxide ROS scavengers into the cellular matrix [8]. Organometallic complexes e.g. metalloporphyrin-MPP conjugates (**Figure. 1.3**), have also been developed as antioxidants within the mitochondria [9]. For example, the Mn-porphyrin-peptide stimulated superoxide dismutase (SOD) activity and decomposed peroxynitrite ($ONOO^-$), effectively scavenging NO-mediated apoptosis that resulted in increased cell viability in lipopolysaccharide [10] (LPS) stimulated macrophages RAW 264.7 cells.
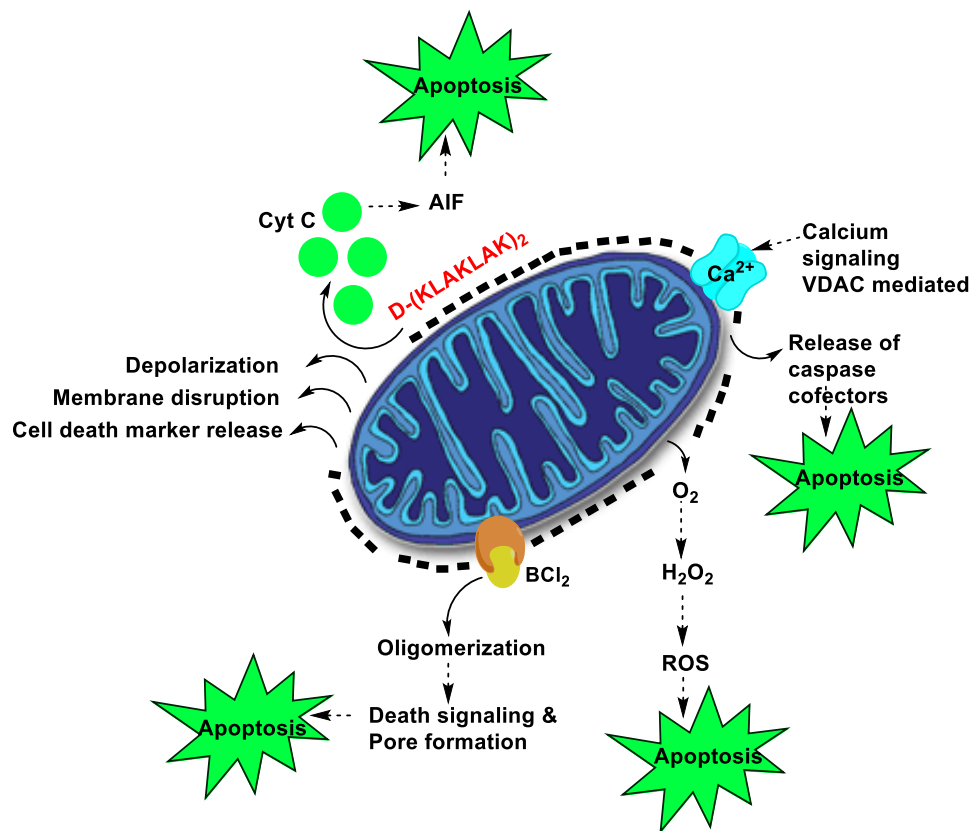
Figure 1.2. Possible cell death pathways triggered by the mitochondrial-targeting peptide D-(KLAKLAK)$_2$. Figure adapted from Farsinejad, S.; Gheisary, Z.; Ebrahimi, S.; Mohammad, A.A. *Tumor Bio*, **2015**, *36*, 5715-5725.

Short synthetic peptides that correspond to the BH3 pro-apoptotic effector domains e.g. BIDBH3 peptide sequence: EDIIRNIARHLAQVGDSMDR and BIMBH3 peptide sequence: MRPEIWIAQELRRIGDEFNA have also been designed and developed. These so-called "killer peptides" initiate the cell death cascade either by activating pro-apoptotic members or by counteracting anti-apoptotic members by displacing BH3 antagonists from their binding domains [11]. These killer peptides have been shown to trigger cell death in Jurkat leukemic cells.

Figure 1.3 Chemical structure of Mn-porphyrin modified with the mitochondria signaling peptide. Figure adapted from reference: Asayama, S., Kawamura, E., Nagaoka, S., Kawakamli, H. *Mol. Pharm.*, **2005**, *3*, 468-470.

1.3 D-(KLAKLAK)₂ ANTIMICROBIAL PEPTIDE: SYNTHESIS, CHARECTERIZATION AND BIOLOGICAL ACTIVITY.

The pro-apoptotic peptide D-(KLAKLAK)$_2$ is an antimicrobial peptide having the ability to internalize within bacteria and disrupt the mitochondrial membrane (**Figure 1.4**) [12]. The pro-apoptotic domain of the D-(KLAKLAK)$_2$ sequence is amphiphilic in nature and composed of hydrophobic leucine and alanine residues and with positively charged lysines. Moreover, in aqueous media, the peptide was found to adopt an α-helical secondary structure. These properties were found to be contributive to the biological activity of the peptide sequence, which readily penetrated the bacterial cell membrane. Inside cells, the peptide localized and disrupted the mitochondria leading to the selective cell death in bacteria and to a much lesser extent in mammalian cells. This selective activity is partly due to the higher affinity of the positively charged

D-(KLAKLAK)$_2$ peptide to the negatively charged bacteria cell surface, but to a lesser extent to the more neutral and hydrophobic composition of the mammalian cell surface [13].
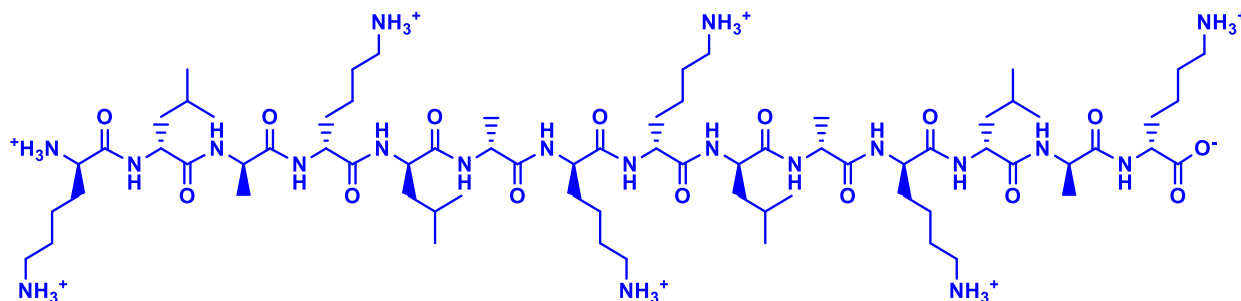
Figure 1.4. Primary sequence of the antimicrobial D-(KLAKLAK)$_2$ peptide at physiological pH=7.4. Figure adapted from reference Javadpour, M.M.; Juban, M.M.; Lo, W.C.; Bishop, S.M.; Alberty, J.B.; Cowell, S.M.; Becker, C.L.; McLaughlin, M.L. *J. Med. Chem.* **1996**, *39*, 3107-3113.

In order to improve the biological activity of the D-(KLAKLAK)$_2$ peptide within malignant mammalian cell types, cancer targeting peptides (CTP) or monoclonal antibodies have been incorporated to target and internalize the killer peptide sequence in cancer cells. For example a peptide comprised of a protein transduction domain (PTD), PTD-5, fused to an antimicrobial peptide, D-(KLAKLAK)$_2$ was able to trigger rapid apoptosis in a variety of cell lines *in vitro*. This included the MCA205 murine fibrosarcomas, the human head and neck tumors. A multifunctional theranostic nanoparticle has also been reported, where the CGKRK peptide provides the targeting function that takes the nanoparticles to tumor vascular cells and into their mitochondria. The nanoparticle uses the mitochondria-targeted D-(KLAKLAK)$_2$ peptide as the drug and iron oxide as a diagnostic component for MRI [14, 15].

In this study, the D-(KLAKLAK)$_2$ will be synthesized using the Fmoc-Solid Phase Peptide Synthesis (Fmoc-SPPS) method [16]. Upon completion of the synthesis cycle, the crude peptide will be analyzed and purified by reverse phase high performance liquid chromatography (RP HPLC). Characterization studies will be performed by electrospray ionization mass spectrometry (ESI MS) to confirm molecular weight identity. The biophysical and structural properties will be respectively analyzed by a combination of ultraviolet-visible (UV-Vis) and circular dichroism (CD) Spectroscopy. These structure-function relationships are important determinations for elucidating the biological activity of the killer D-(KLAKLAK)$_2$ peptide sequence and its conjugates within malignant cancer cell types.

1.3.1 SYNTHESIS AND CHARACTERIZATION OF D-(KLAKLAK)$_2$.

Solid phase peptide synthesis (SPPS) has been recognized as the most widely used technique for making short and long chain peptide sequences with natural and unnatural amino acids [17]. The use of an insoluble resin is key to this efficient method and provides a solid support for growing peptide sequences following coupling and deprotection steps of Fmoc-protected amino acids (**Scheme 1.1**).
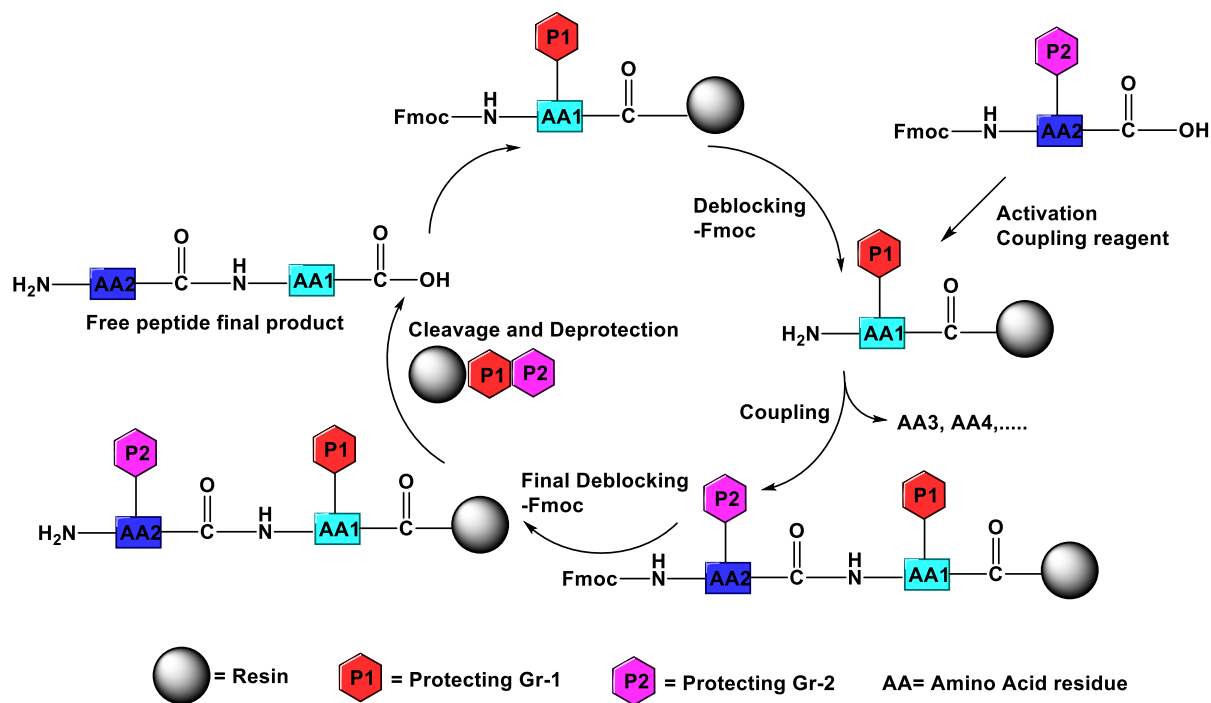
Scheme 1.1. Schematic diagram of the Fmoc-based solid phase peptide synthesis cycle. Synthesis cycle based on Behrendt, R.; White, P.; Offer, J. *J. Pept. Sci.* **2016**, *22*, 4-27.

The SPPS method was first invented by Nobel laureate Bruce Merrifield following the synthesis of the short peptide (LAGV) on polymer beads [18]. Since then, many short and long peptide sequences, including our target, D-(KLAKLAK)$_2$, have been synthesized for a wide range of applications in biology, chemistry and in medicinal chemistry [17]. The careful selection of the insoluble solid support (resin) is a crucial first step to a successful peptide synthesis strategy. The Merrifield-based polystyrene resin was first used in the synthesis of short peptide sequences. However, this solid support proved challenging for making lengthier, more hydrophobic peptides that aggregated during the course of peptide synthesis limiting coupling and deprotection efficiency. Consequently, new and improved resins, including the, TentaGel and NovaPEG resins [19,20] modified the polystyrene support with polyethylene glycol (PEG), (**Figure 1.5**). The incorporation of PEG improved the polar properties of the Merrifield resin, providing it with

9

greater swelling capabilities in *N,N*-dimethylformamide (DMF), the solvent of choice for SPPS

[20]. In addition, a suitable linker is incorporated in between the resin and the peptide sequence.

The linkers are especially useful for anchoring amino acids onto the solid support for peptide

synthesis but also for modifying the *C*-terminus of the sequence. For example, the Rink amide

linker has been incorporated for the generation of *C*-terminal peptide amides whereas the Wang

resin incorporates a linker that affords *C*-terminal peptide acids (**Figure 1.5**) [21]. Moreover, these

linkers also facilitate the removal of the peptide sequence from the solid support, which is typically

accomplished using concentrated trifluoroacetic acid (TFA) as opposed to the toxic hydrogen

fluoride (HF) gas initially used for the removal of peptides from the Merrifield resin.
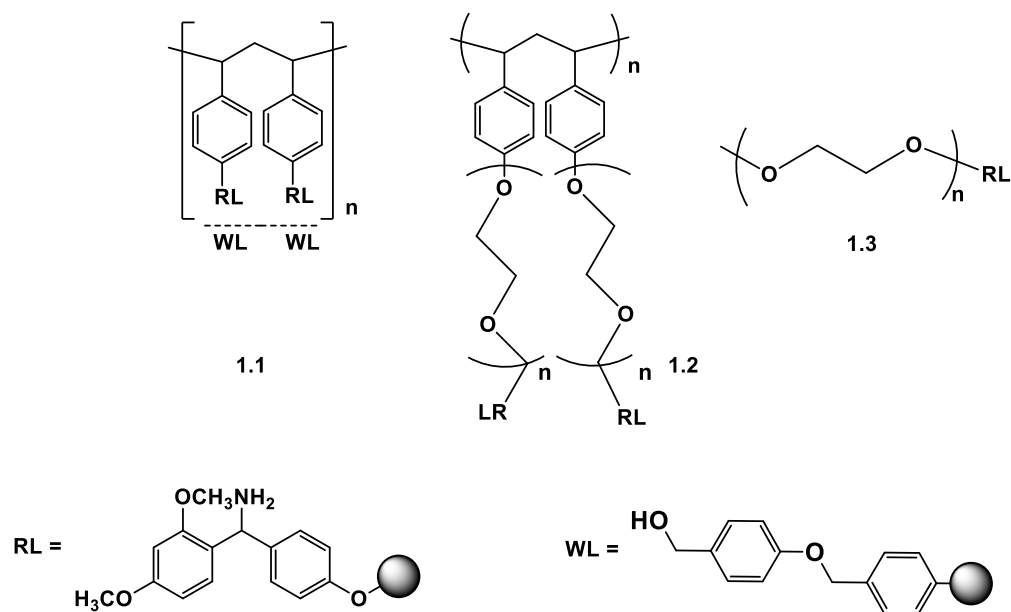
Figure 1.5. Solid supports and linkers for Fmoc-SPPS. Rink amide (RL) or Wang linked (WL) polystyrene-divinylbenzene (PS-DVB) **1.1**) Rink amide-linker polystyrene-graft-poly(ethylene glycol) resin (Tenta Gel, **1.2**) poly(ethylene glycol) (NovaPEG, **1.3**) Wang resin linker with solid support.

Following the judicious selection of an insoluble polymer support, and removal of the fluorenylmethoxycarbonyl (Fmoc) protecting group using piperidine as a base, the linker-bound support is ready for peptide synthesis. The *N*- Fmoc amino acids require orthogonal protection of side chain functional groups with TFA-labile protecting groups (e.g. Boc). A reactive coupling reagent effects the efficient coupling of amino acids to the linker-bound solid support. This coupling step typically functions to convert the *C*-terminal carboxylic acid to a reactive ester which favors coupling to the amino (peptide amides) or hydroxyl (peptide acids) groups on the solid support. Moreover, coupling reagents also facilitate the key peptide bond forming reactions between the *N*-terminal peptide bound support and the *C*-terminal active ester of the coupling *N*-Fmoc amino acid. Many coupling reagents for SPPS have been reported, including the carbodiimide-based couplings [22]. More reactive reagents for coupling have been developed to shorten the coupling times of *N*-Fmoc amino acids. These are particularly based on the uronium coupling reagents, such as, O-(1H-6-chlorobenzotriazole-1-yl)-1,1,3,3-tetramethyluronium hexafluorophosphate (HCTU) which worked particularly well in the solid phase synthesis of challenging peptides with coupling times as short as 1 minute [23].

The coupling procedure is followed by an Fmoc deprotection step, in which a secondary alkylamine is used to effect the elimination of the Fmoc group without concomitant epimerization of the peptide-bound support. Towards this goal, dilute solutions of alkylamines (*i.e.* 20% piperidine or 4-methylpiperidine in DMF, 10% piperidine in EtOH/NMP, 10:90 v/v, and piperazine/DBU) have been used to effectively un-mask the *N*-terminal amino groups for Fmoc-SPPS [24]. These steps have been incorporated within fully automated peptide synthesizers with and without microwave heating for rapid and high yielding coupling and deprotection steps. Following synthesis, cleavage of the peptide from the solid support and deprotection of side-chain

protecting groups are typically accomplished with concentrated trifluoroacetic acid (TFA) with minimal addition (<5%) of reaction scavengers (*i.e.* H_2O, triethylsilane, phenol and anisole). These conditions minimize side-product formation and improve yields of the crude peptide in solution for analysis and purification by RP HPLC. The identities of the isolated peptides are then confirmed by molecular weight analysis using ESI MS. With pure peptides in hand, structure-function properties are then investigated by a combination of spectroscopy, microscopy and chromatography for potential biological applications.

1.3.2 FMOC-SOLID PHASE PEPTIDE SYNTHESIS OF THE D-(KLAKLAK)$_2$ SEQUENCE

The goal of this study was to synthesize the antimicrobial killer peptide sequence D-(KLAKLAK)$_2$ by Fmoc-SPPS. Synthesis of this cationic peptide required the use of the PEGylated ChemMatrix Rink amide resin with a loading capacity of 0.47 mmol/g. A quantity of resin (300 mg) was used for a 0.1 mmol scale peptide synthesis that was anticipated to yield ~30-50 mg of the desired peptide sequence, sufficient for our structure-function relationship studies. Peptide synthesis was conducted either in a semi-automated PSI 200C Peptide Synthesizer (Fairfield, NJ) or within plastic PolyPrep cartridges. The resin was initially swollen in DMF and the addition of Fmoc-amino acids (3eq.), HCTU as coupling reagent (3eq.), NMM as base (6 eq.) and DMF as solvent (4-6 mL) were added to the resin to initiate the coupling reactions (**Scheme 1.2**). Typically, HCTU mediated coupling reactions of Fmoc-amino acids reach completion in 20-30 minutes at room temperature, while elevated temperatures (50-60 ^{o}C) and microwave irradiation allows for much faster reaction times, on the order of 2-5 min [25]. Coupling reactions for the D-(KLAKLAK)$_2$ sequence conducted at room temperature in order to minimize the likelihood of epimerization and side reactions at elevated temperatures [26]. Following coupling of Fmoc amino acids, deprotection of the *N*-terminal of Fmoc group was accomplished using basic piperidine in

DMF (20% piperidine in DMF, 4 mL). Complete Fmoc deprotection typically required successive additions of the piperidine reaction mixture. An initial treatment for 3-5 min removes most of the Fmoc group while a second, longer reaction for about 15 min was used to remove the remaining quantities of protecting group [20]. At the liberated *N*-terminus, coupling reactions were continued and followed by Fmoc deprtections until the desired, full-length peptide sequence was made on solid phase **Scheme 1.3.**

| 1.5 | 1.6 | 1.7 |
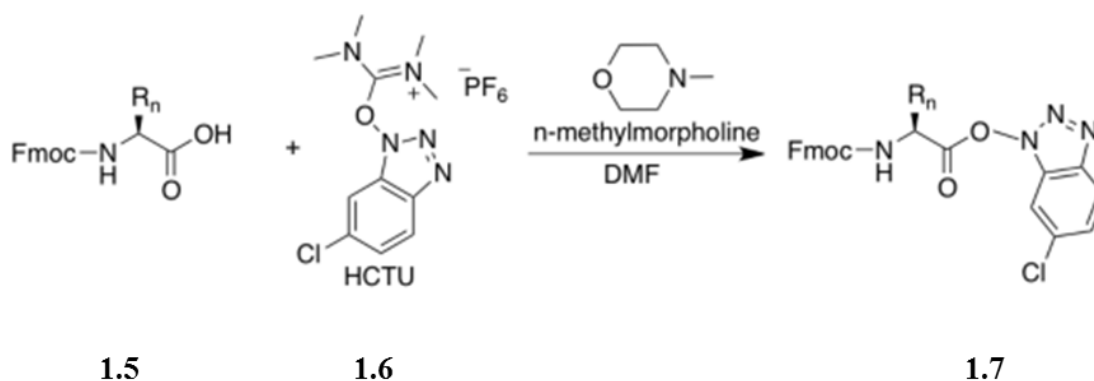
Scheme 1.2. HCTU activation of Fmoc-amino acids. Fmoc protected amino acid (**1.5**) reacts with the HCTU coupling reagent (**1.6**) and the base, *N*-methylmorpholine (NMM), to form the activated Fmoc-amino ester (**1.7**).
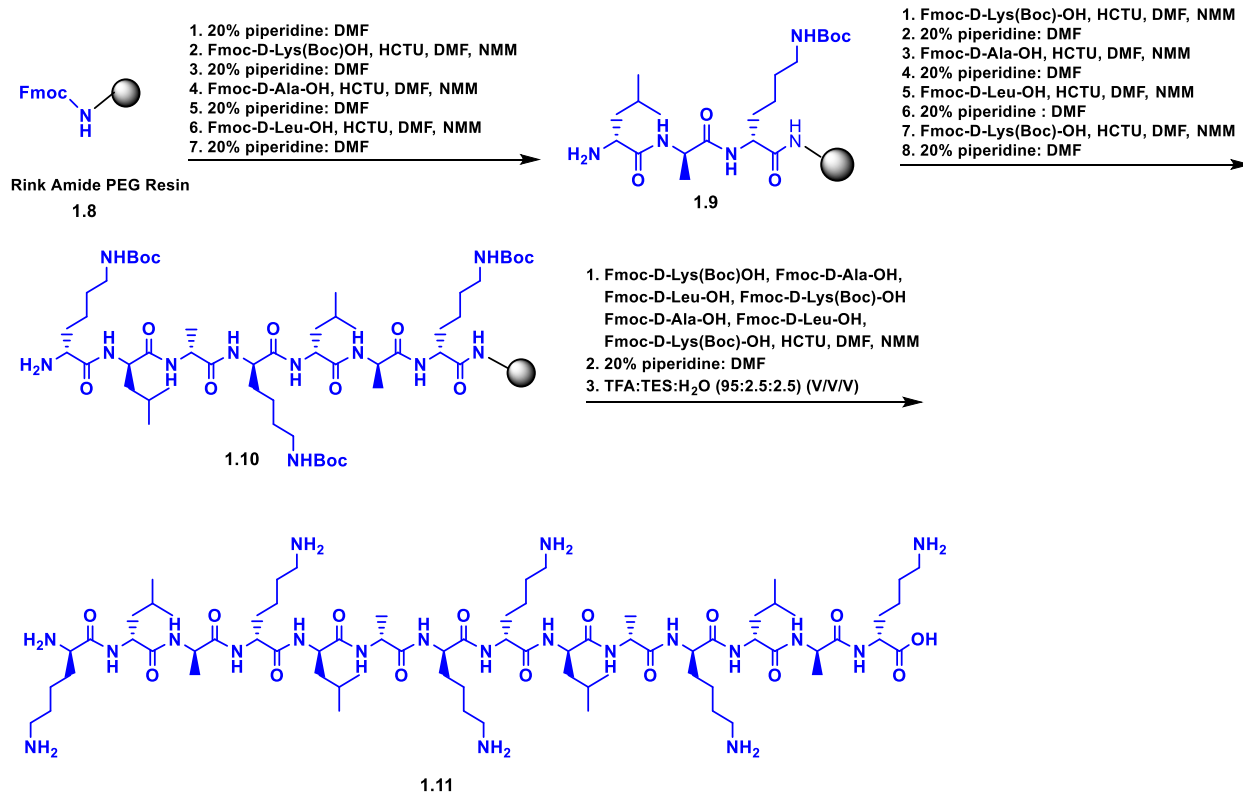
Scheme 1.3. Fmoc-SPPS of the D-(KLAKLAK)$_2$ peptide sequence.

Following peptide synthesis on solid phase, the cleavage and deprotection steps released the peptide from the solid support and removed all side-chain protecting groups. The cleavage and deprotection steps are effected by TFA (95%, 1-3 mL) with TES (2.5%, 25-75 μL) and water (2.5%, 25-75 μL) scavenging reactive intermediates. The cleavage and deprotection cocktail was concentrated under a stream of inert nitrogen. The crude peptide was then precipitated with cold ether (5-10 mL), vortexed and centrifuged to remove the supernatant and the crude peptide was isolated as a solid, white pellet, which washed twice more with cold ether. The crude peptide pellet was dried *in vacuo* and then resuspended in a mixture of MeCN:H$_2$O (1 mL, 50:50 v/v) with

minimal addition of an ion-pairing reagent (0.1% TFA or FA) to enhance dissolution for LC/MS analysis and purification.

1.3.3. ANALYSIS AND PURIFICATION OF D-(KLAKLAK)$_2$ SEQUENCE BY LC/MS

Following peptide synthesis, peptide crude purity and identity was assessed by LC/MS. A Waters C$_{18}$ symmetry shield column, (5.5 μM, 4.6 x150 mm) was used for the separation analysis. Moreover, an eluent gradient composed of: 2-83% MeCN or MeOH in water with (0.1% TFA) over 18 min was used for efficient peptide separation on the reverse phase column. Reaction progress was followed at 220 nm for amide bond absorptions using a photodiode array (PDA) detector. The crude peptide demonstrated a purity of 69% (**Figure 1.6**), while the purified peptide produced an isolated purity of >90% (**Figure 1.7**). The observed crude impurities were primarily due to failure sequences that accompanied incomplete coupling reactions of Fmoc-amino acids **Figure 1.6**. Following purification by RP-HPLC, the isolated peptide was found to have a purity of 93% in multiple eluent conditions composed of MeOH or MeCN in water and TFA (**Figure 1.7**). In order to confirm the identity of the purified, isolated peptide, ESI MS validated the molecular weight of the D-(KLAKLAK)$_2$ sequence, without detection of any significant impurities (**Figure 1.8**). The pure peptide was freeze-dried and lyophilized to dryness, stored in the freezer until further use.
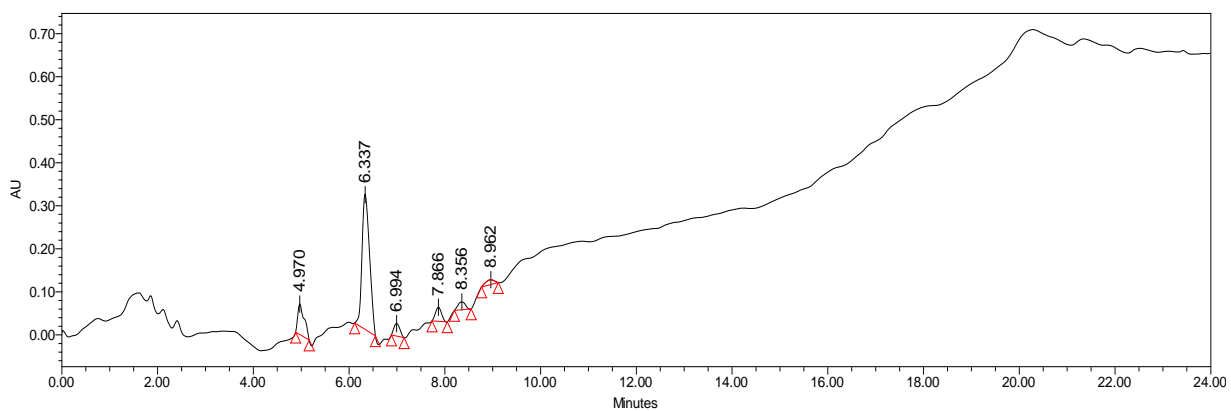
	Name	Retention Time	Area	% Area
1		4.970	672853	13.43
2		6.337	3456296	69.00
3		6.994	255399	5.10
4		7.866	285856	5.71
5		8.356	192441	3.84
6		8.962	146376	2.92

Figure 1.6. RP-HPLC chromatogram of the crude D-(KLAKLAK)$_2$. Linear gradient 2-83% MeOH (0.1% FA) over 18 min, with YMC Column-C18, (4.6 x 250 mm, 5.0 µm particle size) at 25 °C and flow rate of 1.0 mL/min with detection at 220 nm.
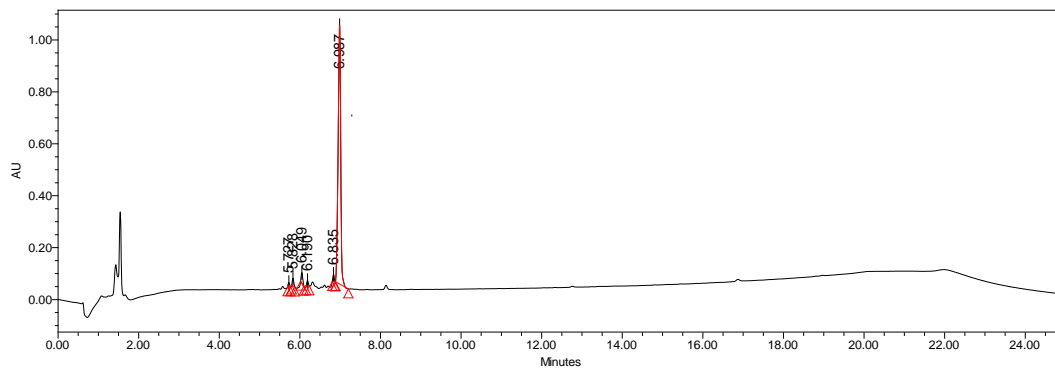
	Retention Time	Area	% Area	Height
1	5.727	40407	0.84	16862
2	5.828	71105	1.49	28974
3	6.049	108374	2.26	40163
4	6.190	51206	1.07	20630
5	6.835	65376	1.37	28942
6	6.987	4448515	92.97	998144

Figure 1.7. RP-HPLC chromatogram of the purified D-(KLAKLAK)$_2$. Linear gradient 2-83% MeOH (0.1% FA) over 18 min, with YMC Column-C18, (4.6 x 250 mm, 5.0 µm particle size) at 25 °C and flow rate of 1.0 mL/min with detection at 220 nm.
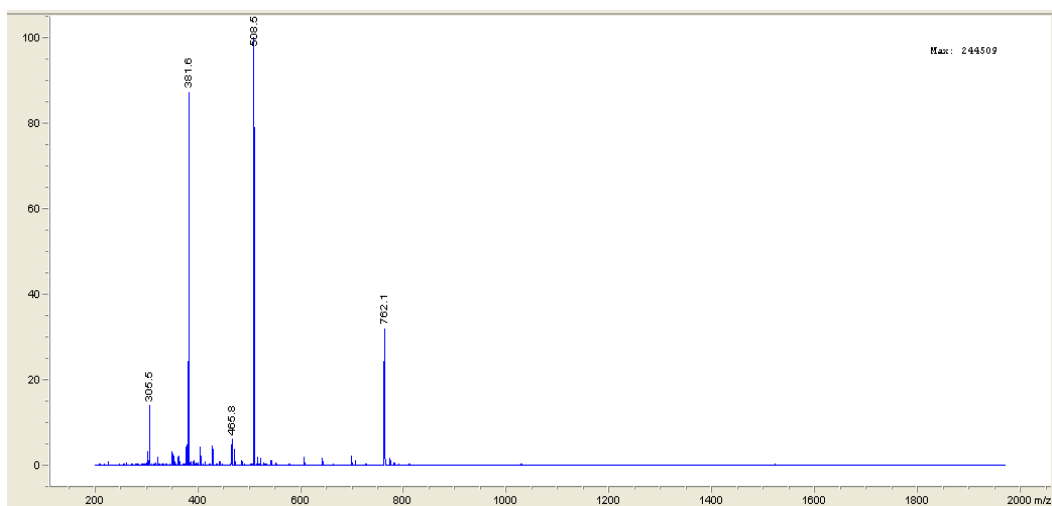
Figure 1.8. ESI –MS spectra of the purified, isolated D-(KLAKLAK)$_2$. MSD signal parameters: Threshold: 150, Step size: 0.15, Mode: scan, Polarity: Positive, Mass range: 500 to 3000, Fragmentation: 70, Gain: 1.0, Source: API-ES, Peak width: 0.10 min, Cycle time: 0.98 sec/cycle.

17

1.3.4 CHARECTERIZATION OF THE D-(KLAKLAK)₂ SEQUENCE BY CIRCULAR DICHROISM SPECTROSCOPY

Circular Dichroism (CD) spectroscopy provides important structural information of optically active chromophores over a wavelength range that is typically in the UV region (190-360 nm). CD spectroscopy aims to study chiral molecules of all types and sizes, but is used extensively in the study of large biological molecules, including in the determination of peptide structures. In relation to peptides, CD spectroscopy provides characteristic spectral traces that are consistent with peptide secondary and some tertiary structure arrangements. For example, peptide random coils or disordered structures exhibit a strong minimum band at 190 nm. Alternatively, ordered peptide secondary structures such as the α-helix (maximum at 190 nm, minima at 210, 230 nm), the β-sheets and turns (maximum at 200 nm, minimum at 220 nm) exhibit characteristic Cotton effects that helps distinguish between different types of secondary structures (**Figure 1.9**). These studies are also useful in determining structure, kinetics and thermodynamic stability of peptides in a wide range of solvent, pH and temperature conditions.
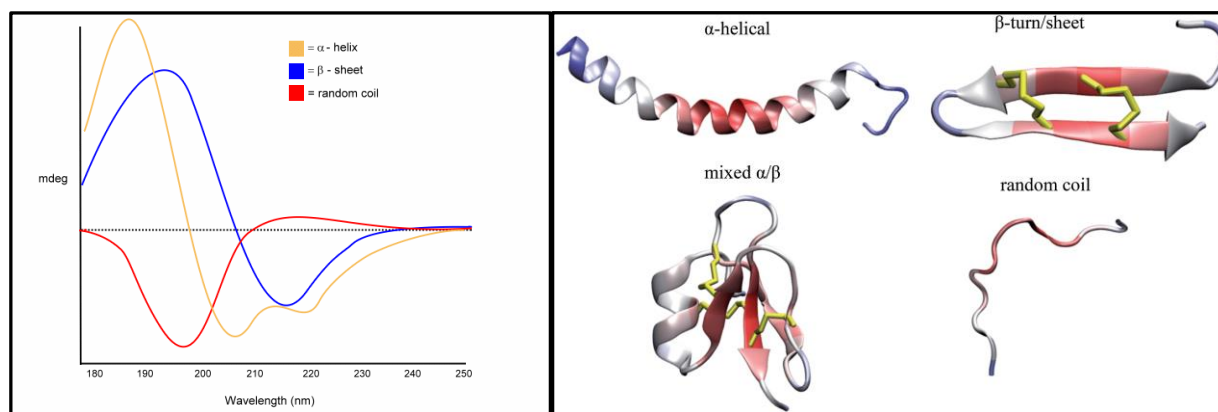
Figure 1.9. CD spectra and secondary peptide structures. The CD spectrum of poly-L-lysine in α-helix, β-sheet, and disordered (random coil) structures. 3D structural representation of

corresponding peptide secondary structures and random coils. Figure adapted from Dr. Ramy S. Farid- Discussion of CD Spectroscopy, a revised version of online lecture notes.

In this study, the structural properties of the isolated, pure D-(KLAKAK)$_2$ sequence was investigated on an Aviv Circular Dichroism (CD) Spectrophotometer (Model: 62A DS). The peptide samples (30 – 220 μM) dissolved in phosphate buffered saline (PBS), (8 g of NaCl, 0.2 g of KCl, 1.44 g of Na$_2$HPO$_4$, 0.24 g of KH$_2$PO$_4$, adjusted the pH to 7.4 with HCl, dissolved in 1 L of distilled H$_2$O). The CD spectra of the D-(KLAKAK)$_2$ sequence was collected from 190-260 nm using 1 nm bandwidth and 0.5 min step size at with 30 spectra points at 25 °C. Triplicate measurements were collected separately to ensure uniformity and reproducibility of the results. Spectra were blank corrected, smoothed and data converted to molar ellipticity values from the equation [θ] = θ /cl, where θ is the relative ellipticity (mdeg), c is the molar concentration of the peptides (μM) and l is the path length of the cell (1 cm). The data was imported into Microsoft Excel and the CD spectra plotted in terms of molar ellipticity *vs.* wavelength.

CD spectroscopy of D-(KLAKLAK)$_2$ sequence revealed a peptide sequence that exhibits α-helical character at lower (30 μM) concentration ranges that are expected to be physiologically relevant. At lower concentrations, the CD spectra suggests an α-helical peptide structure according to the minima observed at 210 and 230 nm with a strong maximum band apparent at 190 nm (**Figure 1.11**). Many α-helical proteins are present in the inner membranes of bacterial cells or the plasma membrane of eukaryotes, and sometimes in the outer membrane. They function as a major structural component of transmembrane proteins that facilitates the passage of molecules and ions in and out of the cell (i.e. transporter proteins). Interestingly, at higher concentrations (>100 μM)

the D-(KLAKLAK)$_2$ sequence is seemingly transitioning to a β-sheet or turn conformation with a strong negative band detected at around 230 nm and a positive one at around 200 nm (**Figure 1.10**). These results suggests the D-(KLAKLAK)$_2$ sequence contains a flexible secondary structure, capable of transitioning between different conformations as a function of concentration. This trend is anticipated to persist in different conditions, including variations in solvent, pH, ion strength and temperatures.
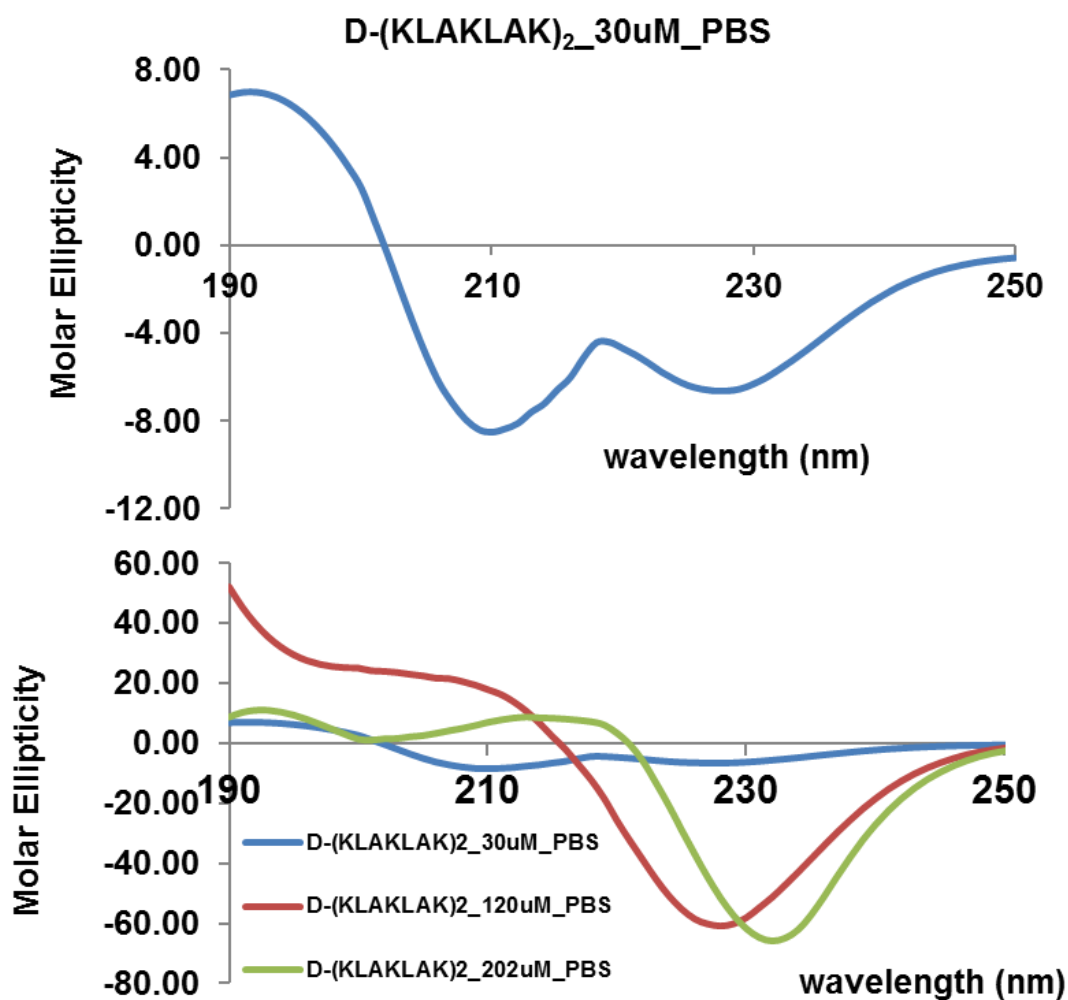
Figure 1.10. CD Spectra of the D-(KLAKLAK)$_2$ peptide sequence (30 – 120 μM) in PBS buffer.

1.4 BIOLOGICAL ACTIVITY OF D-(KLAKLAK)$_2$ SEQUENCE IN BACTERIA AND MAMMALIAN CELLS

Some antimicrobial peptides selectively inhibit and kill bacteria while maintaining low mammalian cell cytotoxicity [27]. This selectivity can be attributed to the membrane differences between bacteria and mammalian cell types. The exterior membranes of bacteria tend to be predominantly negatively charged due to a composition of anionic phospholipids and glycolipids. The mammalian cell exterior membranes are generally neutral in charge due to a mixed composition of complex biologicals, including the neutrally charged sphingolipids and cholesterol. Consequently, the positively charged D-(KLAKLAK)$_2$ sequence was found to have higher binding affinity and biological activity in bacteria *vs.* mammalian cell types.

Interestingly, the amphiphilic peptide sequence and α-helical secondary structure were also found to contribute to its cell translocation mechanism and localization onto the mitochondria. At the localized organelle, the peptide sequence was found to disrupt the mitochondria membrane integrity and biological function leading to its cytotoxic activity. Moreover, peptide translocation was postulated to occur by membrane fusion and translocation into the cytosol via endosomal transport and escape [14,15,28]. Alternatively, a receptor-mediated endocytic pathway was reported with the incorporation of a targeting vector or homing domain specific for a cell surface protein receptor (**Figure 1.11**) [29-33]. The latter is a crucial requirement for improving the mammalian cell cytotoxic activity of the D-(KLAKLAK)$_2$ sequence.
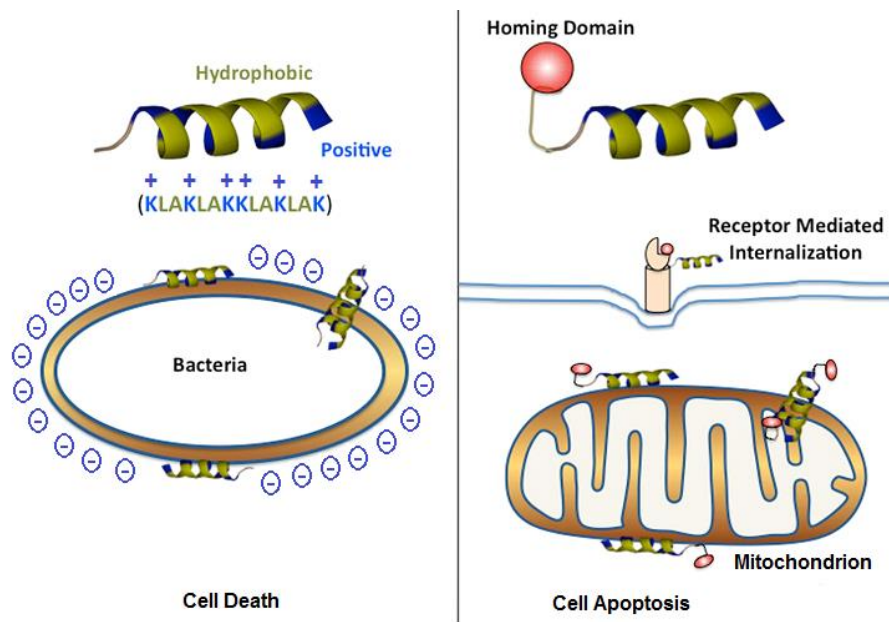
Figure 1.11. Schematic description of cell permeability and cytotoxicity of the D-(KLAKLAK)$_2$ sequence in bacteria and mammalian cell types.

1.5 DESIGN, SYNTHESIS, AND ANTI-CANCER ACTIVITY OF THE D-(KLAKLAK)$_2$ BIOCONJUGATES.

In order to enhance the cytotoxic activity of the killer D-(KLAKLAK)$_2$ sequence in malignant mammalian cell types, such as in cancers, modifications to the primary sequence composition and bioconjugation with small molecules, biologicals and cytotoxic drugs have been incorporated [14,15,28]. For example, a new dual-targeting pro-apoptotic peptide (DTP) was synthesized, characterized and evaluated for anti-cancer activity [29].
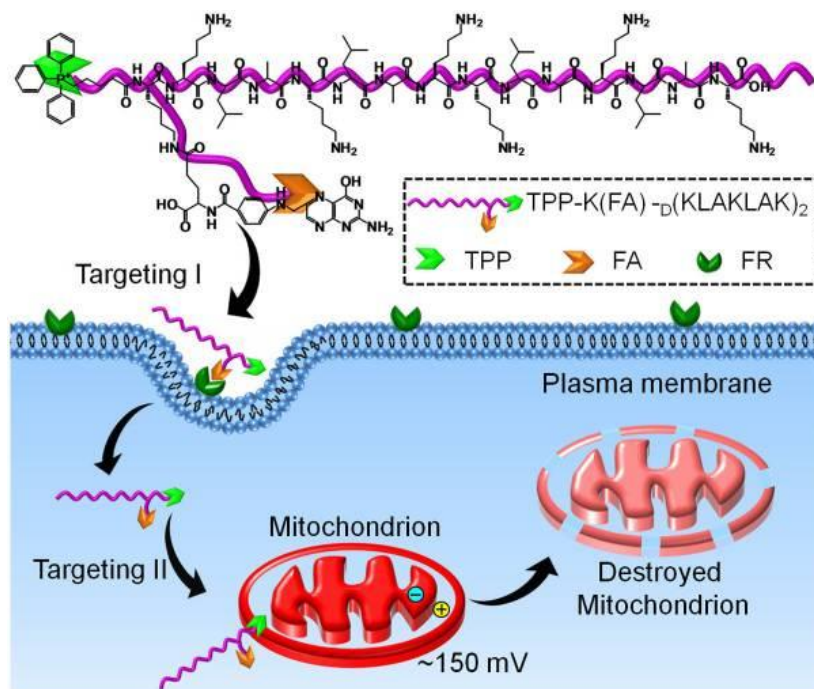
Figure 1.12. Dual targeting pro-apoptotic peptide and mechanism of action for the amphiphilic peptide: TPP-KFA-D-(KLAKLAK)$_2$. Figure adapted from reference Chen, W.H. *et. al. Sci. Rep.* **2013**, *3*, 3468.

This peptide bioconjugate combined three components within its bioactive form. Namely, the folic acid (FA) moiety for targeting the folate receptor (FR) overexpressed on the surface of cancer cells that facilitates receptor-mediated endocytosis. The positively charged and hydrophobic triphenylphosphine (TPP) moiety, facilitates cell permeability and mitochondria localization for the cytotoxic activity of the D-(KLAKAK)$_2$ sequence (**Figure 1.12**). This bioconjugate was synthesized by Fmoc-SPPS, isolated and characterized by LC/MS followed by its anti-cancer evaluation in KB, HeLa and COS7 cancer cells. Significantly, the bioconjugate was found to be more active than the native, D-(KLAKAK)$_2$ sequence, underscoring the importance of homing and penetrating vectors for mammalian cancer cell cytotoxic activity.

In a related example, the pH sensitive pHLIP peptide (GGEQNPIYWARY ADWLFTTPLLLLDLALLVDADEGTCG) was linked via a reducible disulfide bond to the D-(KLAKLAK)$_2$ sequence [30]. The synthesis of the wild type (WT) pHLIP sequence was accomplished by Fmoc-SPPS with the incorporation of a reactive cysteine residue at its *C* terminus. Subsequently, the D-(KLAKLAK)$_2$ sequence was also synthesized by Fmoc-SPPS with a reactive cysteine at the *N*-terminus for coupling onto the pHLIP sequence by disulfide bond formation. The pHLIP-S-S-D-(KLAKLAK)$_2$ bioconjugate was purified via reversed-phase high performance liquid chromatography (RP-HPLC). The purity of the peptides were determined by RP-HPLC, and their identities were confirmed via matrix-assisted laser desorption ionization time of flight mass spectrometry (MALDI-TOF-MS). Interestingly, the pHLIP peptide is a 36 residue sequence derived from the C helix of bacteriorhodopsin, a transmembrane spanning protein, [31] and shows the ability to insert across the lipid bilayer and form a transmembrane helix at lower pHs found within the acidic tumor microenvironment [31]. Thus, the pHLIP sequence contains tumor homing capabilities that would facilitate the delivery of cytotoxic agents directly within tumors. This is because at a pH corresponding to the extracellular pH of tumors, the pHilip sequence undergoes a pH-dependent conformational change driven by the protonation of aspartic acid residues, promoting the insertion of its *C*-terminus across the cell membrane to form a transmembrane α-helix [32]. In this manner, the (KLAKLAK)$_2$ sequence internalized within the cytosol of malignant tumor cells, such as, MDA-MB-231 breast cancer cell line and released by disulfide bond reduction by the reducing tumor cytosol for anti-cancer activity (**Figure 1.13**).
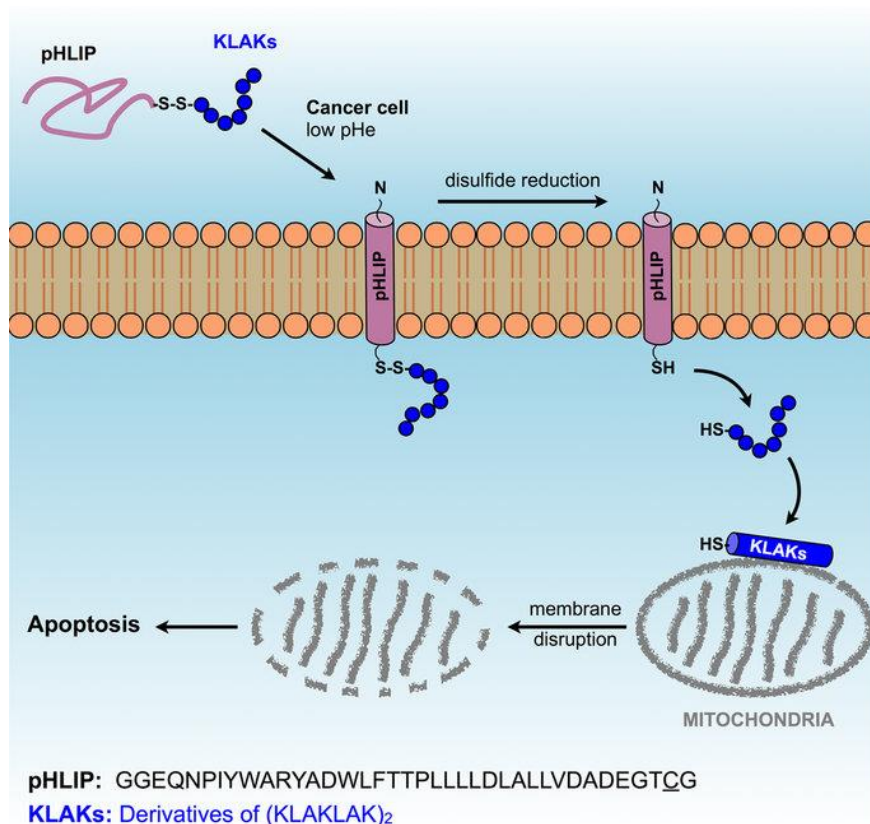
Figure 1.13. Schematic representation of the cell internalization and apoptosis activities of the pHilip–(KLAKLAK)$_2$ sequence. Figure adapted from Burns, K. E., McCleerey, T. P., Thevenin, D. *Sci. Rep.*, **2016**, *6*, 28465.

In a final example, the cytotoxic peptide D-(KLAKLAK)$_2$ conjugated to amphiphilic poly (β-thioester) copolymers were composed of ROS sensitive backbones and hydrophilic PEG side chains [33]. The conjugates were prepared by Fmoc-SPPS, and functionalization of the peptide onto the copolymer was accomplished by Michael addition of a reactive *N*-terminal Cys with the acrylate-derived copolymer backbone. In solution, the peptide-functionalized copolymer self-assembled into micelle-type nanoparticles due to the hydrophobic interactions of the copolymer backbone with the PEG and D-(KLAKLAK)$_2$ moieties (**Figure 1.14**). The self-assembled

polymer–peptide nanoparticles remarkably improved cellular internalization and accumulation of the therapeutic D-(KLAKLAK)$_2$ sequence in cancer cells. Compared to the free KLA peptide, the anti-tumor activity of the peptide-copolymer conjugate was significantly enhanced, up to ~400 times, suggesting the effectiveness in cancer treatment applications. The higher antitumor activity of the nanoparticles was attributed to the efficient disruption of mitochondrial membranes and subsequent excessive ROS production in cells. The ROS production around the mitochondria stimulated the swelling of nanoparticles and subsequent release of squaraine dyes. Squaraine dyes are a class of organic dyes showing intense fluorescence, typically in the near infrared region. They also form H-aggregates and significantly contribute to photoacoustic (PA) signaling for imaging the effects of ROS generation in live cells. In this manner, the self-assembled polymer peptide nanotherapeutics may hold great promise in medicinal chemistry applications.
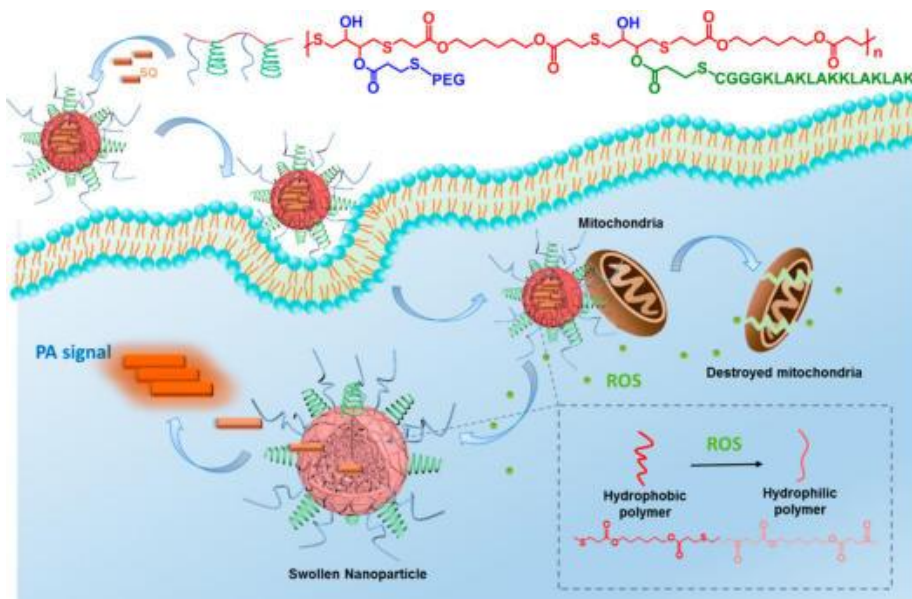
Fig.1.14. Self-assembled ROS-sensitive polymer-peptide conjugate (PPC) incorporating a reporter for enhanced tumor treatment. Figure adapted from Qiao, Z. Y.; Zhao, W. J.; Cong, Y.; Zhang, D.; Hu, Z.; Duan, Z. Y.; Wang, H. *Biomacromolecules*, **2016**, *17*, 1643–1652.

1.6 NUCLEOLIPIDS: COMPOSITION, SYNTHESIS, CHARACTERIZATION AND APPLICATIONS IN CANCER THERAPY

Nucleolipids are a special class of bioconjugates composed of a nucleoside and a lipophilic moiety e.g. alkyl chain, cholesterol, vitamin or fatty acid. A representative example of a naturally occurring nucleolipid consists of cytidinediphosphate diacylglycerol. This nucleolipid is composed of cytidine diphosphate functionalized with a diacylglycerol moiety at the 5'-diphosphate position. As such, the nucleolipid functions as a reactive intermediate for the functional group-transfer of the phosphatidic acid group. The nucleolipid is formed by the reaction of phosphatidic acid with cytidine-5-triphosphate resulting in the concomitant release of pyrophosphate (**Scheme 1.4**). By the transfer of the phosphatidic acid group onto OH groups of carbohydrates or proteins, glycolipids and lipoproteins are formed. Transfer to inosite or glycerol-3-phosphate results in the formation of the membrane components phosphatidylinosite and cardiolipin. Thus, the nucleolipid cytidinediphosphate diglycerol functions as a reactive intermediate in the biosynthesis of phospholipids, such as phosphatidylinositol, and regulates lipid-dependent signal transduction pathways [34]. Considering their relevance in biology, chemical synthesis methods have been developed for generating new nucleolipids for potential therapeutic applications.
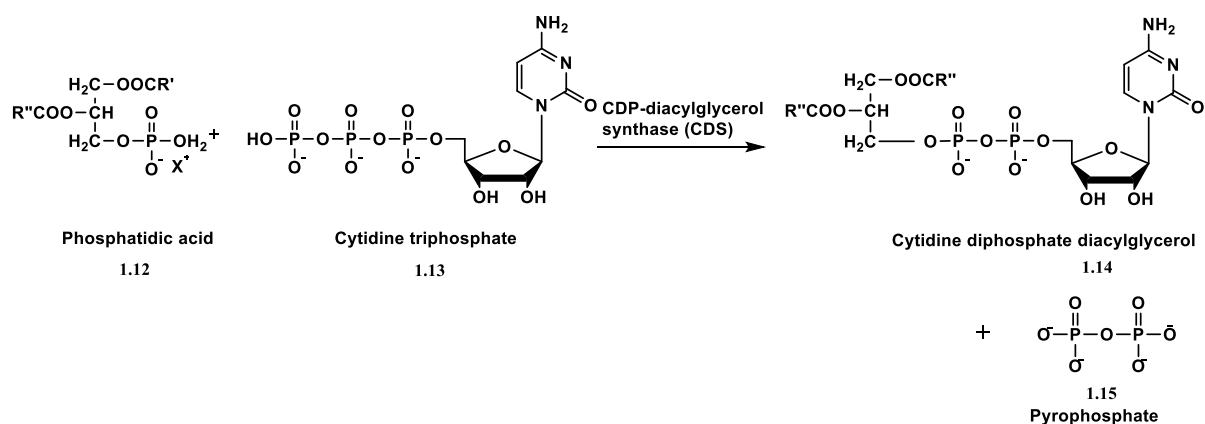
Scheme 1.4. Biosynthesis of Cytidinediphosphate diglycerol. Figure adapted from Liu, X.; Yin, Y.; Liu, Z. Nature, 2014, 5, 4244.

1.6.1 AMINO ACYLNUCLEOLIPID

The aminoacyl nucleolipids are an interesting class of synthetic amphiphilic nucleolipid bioconjugates. A variety of synthetic aminoacyl nucleolipids (**Figure 1.15**) have been prepared and found to self-assemble into higher-ordered biomaterials for applications in gene therapy, medicinal chemistry and biotechnology. These interesting properties stem from the amphiphilic nature of the bioconjugate, which readily self-assembles into high-order nanoparticle formulations or aggregates, which imparts its biological activity. For example, the synthetic guanosine aminoacyl nucleolipids (**1.16, 1.17**) displayed the ability to form stable G-tetraplexes (G-tetrads) in organic solvents [35], and were also found to behave as Li^+ and K^+ ion chelators. These materials were also found to facilitate transport of H^+/OH ions in the presence of an applied pH gradient [36]. Moreover, aminoacyl nucleolipids, **1.16** and **1.17** showed moderate to weak activity (IC_{50}: 17 - >103 µM) in an anti-proliferative assay across a panel of five tumor cell lines underscoring their potential in biomedical applications [36]. In a related case study, a cationic aminoacyl surfactant (**1.18**) demonstrated micelle forming capabilities in water according to DLS studies and modest cell toxicities (IC_{50}: 19 – 98 µM) relative to the cytotoxic cetyl triethylammonium bromide (CTAB) cationic amphiphile in a panel of human, rat and murine cell lines [37]. In light of their abilities to form stable cationic assemblies, the aminoacyl nucleolipids have been applied to gene delivery and treatment applications *in-vitro* [38]. The development of short interfering RNAs (siRNAs) have enabled the application of site-specific mRNA knockdown through the RNA interference (RNAi) pathway [34]. In spite of its potential in gene therapy applications, siRNAs remain limited by poor cell permeability. In an effort to overcome this limitation, siRNA delivery agents (transfection agents) have been developed to effectively condense and deliver siRNA across the amphiphilic cell membrane for RNAi activity.
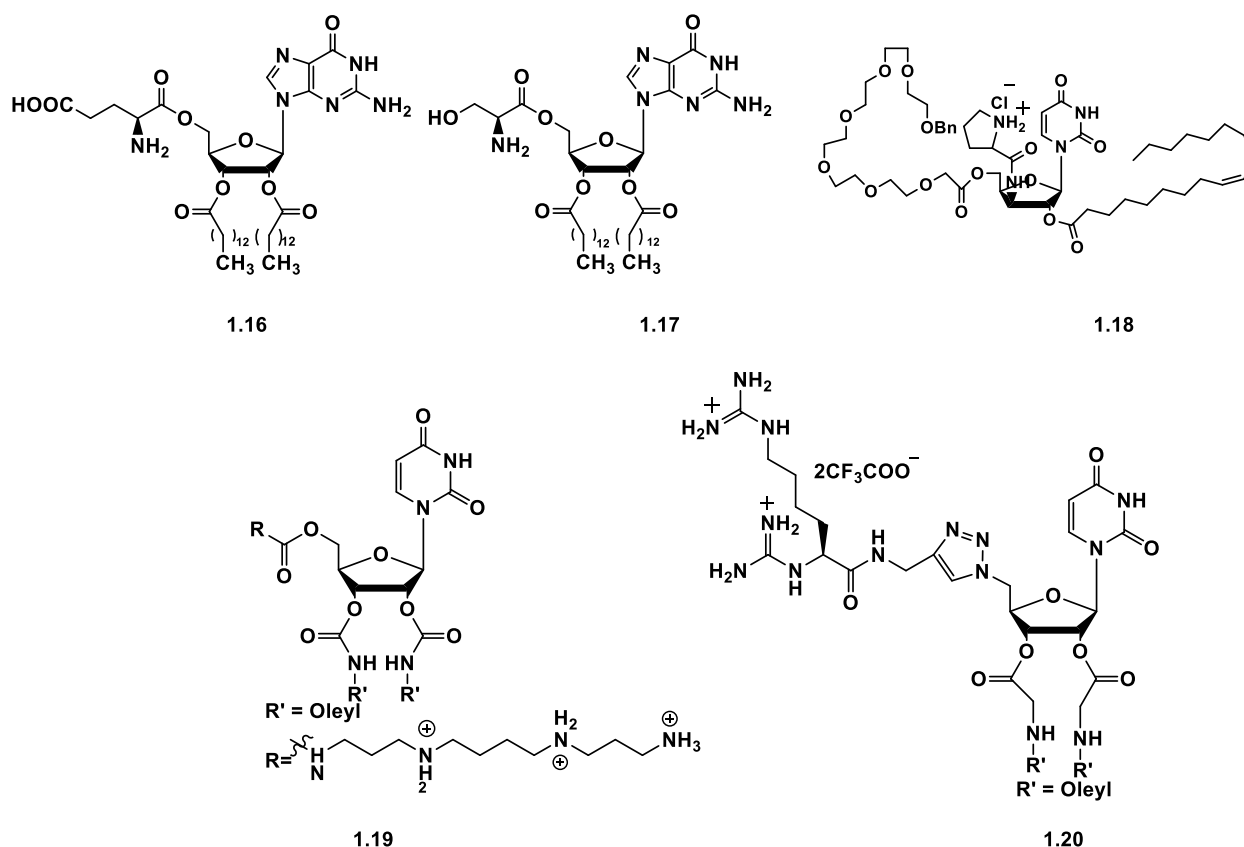
Figure 1.15. Structures of synthetic aminoacyl nucleolipids.

In this scope, a small library of synthetic polycationic nucleolipids have been formulated for siRNA transfection within HeLa cells for potent Vascular Endothelial Growth Factor (VEGF) knockdown [38]. The spermine derived aminoacyl nucleolipid (**1.19**) exhibited comparable siRNA transfection efficiencies (>90% VEGF knockdown) and cell death (~20%) as the benchmark Lipofectamine-based siRNA transfections, underscoring the utility of nucleolipids as siRNA transfection vectors. Moreover, metabolically stable variants of aminoacyl nucleolipids (**Figure 1.15**) have also been formulated for siRNA delivery applications in HeLa cells [39]. This cationic nucleolipid formed stable ionic complexes with anti-VEGF siRNA leading to potent VEGF knockdown (>90%) in HeLa cells [39]. These examples effectively demonstrate the fruitful

implementation of aminoacyl nucleolipids in condensing oligonucleotides and transporting them within cells for medicinal chemistry applications.

In our contribution, an aminoacyl nucleolipid was based on a guanine nucleoside, which contains the ability to participate in H-bonding interactions, an aminoacyl group for potential ionic bonding, and lipids which enable the self-assembly through non-polar interactions (**Figure 1.16**) [40]. The aminoacyl nucleolipid designed and synthesized in our study was anticipated to interact favorably with the promoter sequence of the GRP78 oncogene. This proposed DNA binding ligand was expected to unleash potent anti-cancer effects in GRP78 overexpressing tumors.
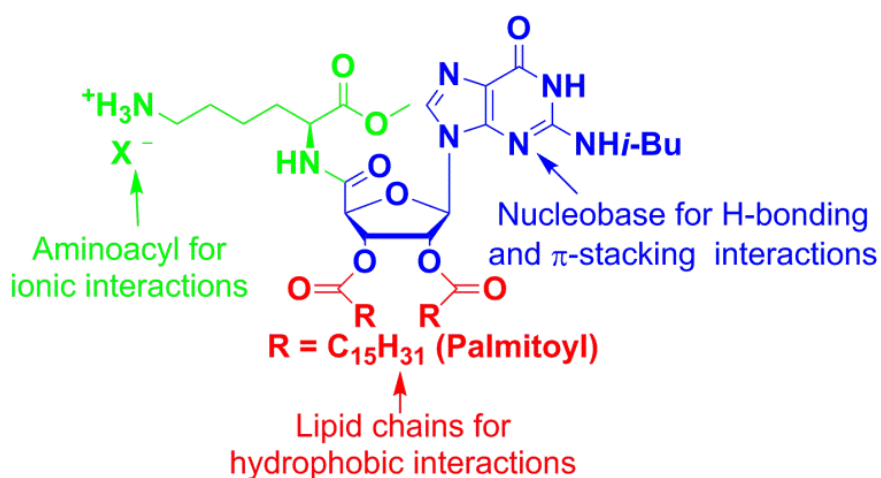
Figure 1.16. Chemical structure and DNA-binding interactions of an aminoacyl nucleolipid. Figure adapted from Patel, P.; Hanawa, E.; Yadav, R.; Samuni, U.; Marzabadi, C.; Sabatino, D. *Bioorg. Med. Chem. Lett.* **2013,** *23*, 5086-5090.

Our study began with the solution phase synthesis of an aminoacyl nucleolipid building block, **1.28**. The synthetic strategy involved the production of *N*-isobutyryl 5'-carboxy 2',3'-bis-*O*-(carbobenzyloxy) guanosine, **1.24,** (**Scheme 1.5**). *N*-isobutyrroyl 5'-dimethoxytrityl guanosine, **1.21**, was used to attach the Cbz protecting groups with benzylchloroformate and DMAP in DCM.

Following carbomylation, **1.22**, was detritylated using 3% trichloroacetic acid in DCM (3% TCA:DCM) affording the guanosie analog, **1.23**, in 98% yield. *N*-isobutyrryol-2',3'-bis-*O*-(carbobenzyloxy)guanosine, **1.23**, was then oxidized to the carboxylic acid, **1.24**, in 82% yield, using TEMPO oxidation.
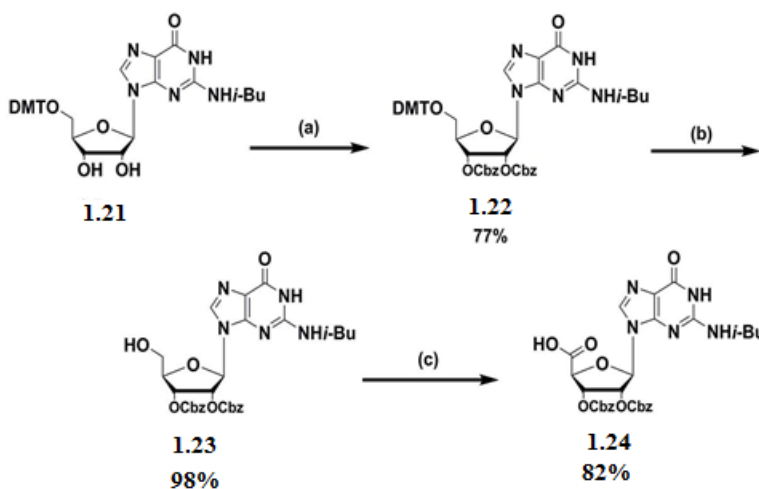
Scheme 1.5. Synthesis of *N*-isobutyryl 5'-carboxy 2',3'-bis-*O*-(carbobenzyloxy) guanosine, **1.24**. Conditions: (a) DMAP, benzyl chloroformate, DCM, 0_o C then r.t., 72 h, 77%, (b) 3%TCA:DCM, r.t., 15 min, 98%, (c) TEMPO, BAIB, MeCN:H_2O (50:50 v/v), r.t., 15 h, 82%.

Fmoc-Lys(Boc) was coupled at the 5'-carboxy position of **1.24** using *N*-ethoxycarbonyl 1,2-ethoxy-1,2-dihydroquinoline, EEDQ, (2 equiv) as coupling reagent and *N,N*-diisopropylethylamine, DIEA (2 equiv) as the base in DMF. The reaction produced the desired product in >99% yields. The Cbz protecting groups were deprotected using hydrogenolysis, generating diol **1.26** in quantitative yields (**Scheme 1.6**). The product was acylated with an excess of palmitoyl chloride to afford the protected aminoacyl nucleolipid **1.27** in >99% yield. The Boc-protecting group of **1.27** was removed using 50% TFA:DCM, followed by salt exchange to the hydrochloride salt with aqueous HCl. The desired aminoacyl nucleolipid, **1.28**, was obtained in

quantitative yields in this final reaction step and its purity and composition was ascertained by ^{1}H NMR, ^{13}C NMR, IR, UV/Vis, and MS techniques. A variety of experimental techniques, including gel shift mobility assays, thermal denaturation and CD spectroscopy were used to confirm the binding interactions of the aminoacyl nucleolipid with the GRP78 DNA.
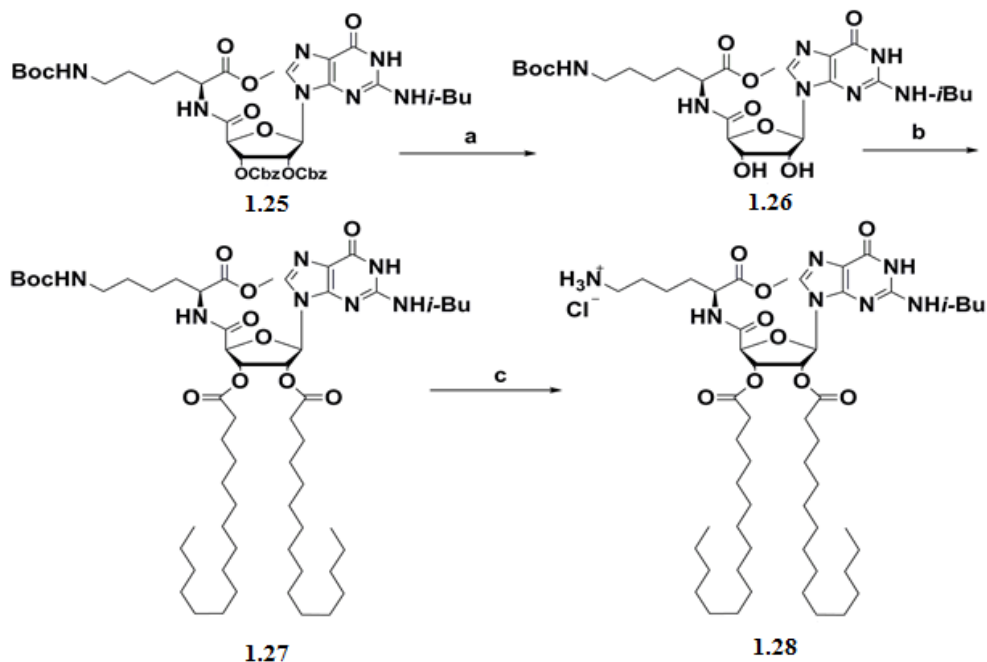
Scheme 1.6. Solution phase synthesis of aminoacyl nucleolipid. Conditions: (a) H$_2$, 10% Pd/C, EtOH, r.t., 1.5 h, >99% (b) palmitoyl chloride, DMAP, pyr., 2 h, >99% (c) 50% TFA:DCM, 2 h, r.t., then 1 M HCl, 3 h, >99%.

In order to assess the anti-cancer activity of the aminoacyl nucleolipid, a cancer cell line-screening assay was conducted against a panel of 60 cell lines at the National Cancer Institute (NCI). A single dose (10 μM) test was performed with the synthetic aminoacyl nucleolipid and cell viability was determined following 48 h incubation with cancer cells. A sulforhodamine B (SRB) cell viability assay was performed to determine cell death activity. The aminoacyl

nucleolipid was found to exhibit potent (90%) and selective anti-cancer activity against a SR human lymphoblastic leukemia cancer cell line (**Figure 1.17**). Interestingly, GRP78 is overexpressed in leukemic blasts of adult patients and in early relapse childhood leukemia suggesting a correlation between the GRP78 DNA binding affinity and the anti-leukemic activity of the aminoacyl nucleolipid. We are currently investigating the molecular basis for the potent and selective anti-cancer activity of the aminoacyl nucleolipid.
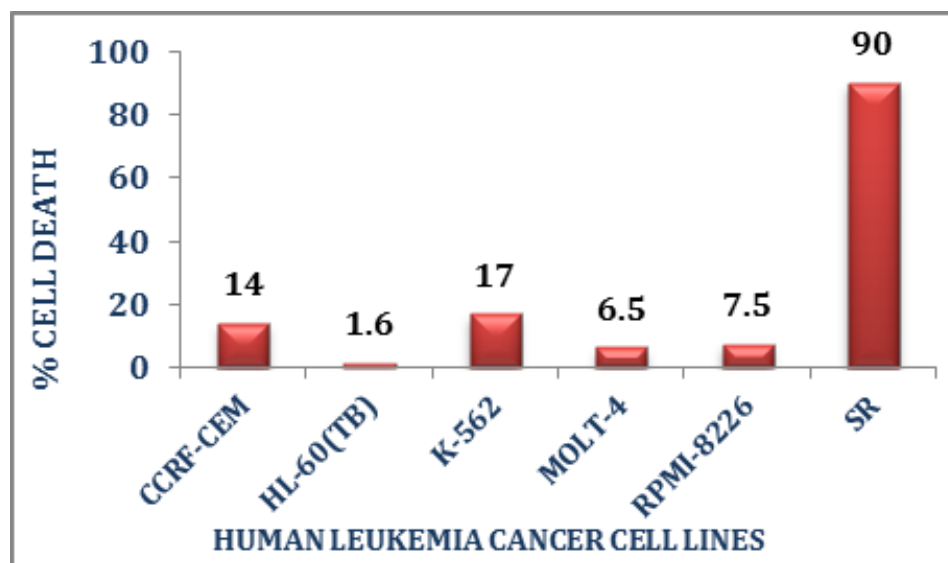
Figure 1.17. Cell death of human leukemia cell lines following treatment with aminoacylnucleolipid, **1.28**, (10 µM) for 48 h.

1.7. THESIS RESEARCH OBJECTIVES

In an effort to exploit the cell death effects of D-(KLAKLAK)$_2$, and improve its 'drug-like' properties, chemically robust and structurally pre-organized amphiphilic nucleolipids are proposed to enhance cell permeability and mitochondria localization in tumor cell types for potent and long-lasting anti-cancer effects (**Figure 1.18**). These amphiphilic nucleolipids are inspired from our previous study on the so-called aminoacyl nucleolipid [40]. Building upon this work, the novel

nucleolipids described in this thesis are rationally designed to contain a reactive 5'-carboxy group for introduction within the pro-apoptotic D-(KLAKLAK)$_2$ sequence by solid phase peptide synthesis. The nucleolipid is based on a thymidine nucleoside that provides a chemically resilient and structurally pre-organized scaffold, and long chain alkylamines that are proposed to facilitate cell penetration and mitochondria localization within tumor cell.
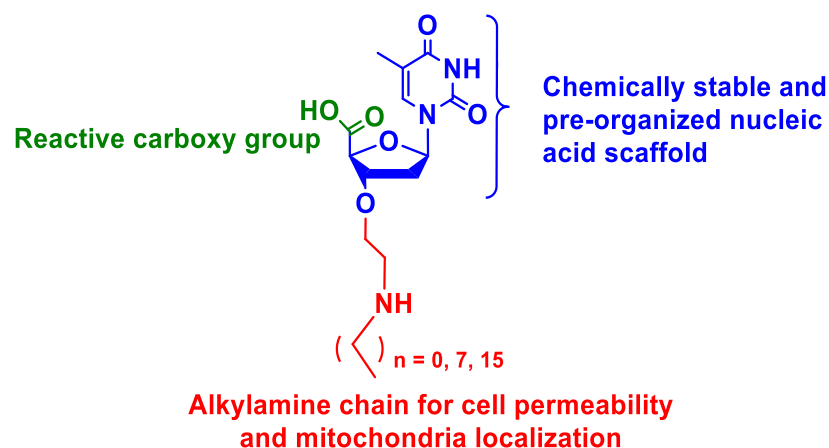
Figure 1.18. Design and structure of the amphiphilic nucleolipids synthesized in this study.

In this study, the design, synthesis, characterization, and cancer cell death activity of a new class of peptide nucleolipids is described. This thesis will present a new class of palmitamide and nucleolipid derived D-(KLAKLAK)$_2$ bioconjugates in Chapter 2. A presentation of its synthesis, biophysical and anti-cancer activity is described and related to the native, peptide sequence. Chapter 3 will describe a diversity oriented synthesis approach for making chemically diverse nucleolipids that may be useful in exploring structure-function relationships of the bioconjugates and their cancer cell targets. This chapter will also highlight the potential of this methodology; in building libraries from libraries of nucleolipid derivatives that may be easily incorporated within other lead biologicals or in themselves present an element of anti-cancer activity. Finally, the D-(KLAKAK)$_2$-nucleolipid conjugates may also be functionalized with tumor homing vectors, for

selective and effective treatment of cancer cell types. The latter forms an important part of the precision medicine initiative currently in progress in our group for the rapid and selective diagnosis and treatment of cancer. These contributions to knowledge (Chapter 4) and supporting information (Appendix) will be presented as the final sections of this thesis.

1.8 REFERENCES

1. Alberts, B.; Johnson, A.; Lewis, J. *Molecular Biology of the Cell*, 4th edition, New York: Garland Science; **2002,** Membrane Proteins.

2. Suzuki, T.; Futaki, S.; Niwa, M.; Tanaka, S.; Ueda, K.; Sugiura, Y. *J Biol Chem.* **2002**, *277*, 2437-2443.

3. Fantin, V.R.; Leder, P. *Oncogene*, **2006,** *25*, 4787–4797.

4. Green, M.; Loeweinstein, M. *Cell*, **1988**, *55*, 1179 – 1188.

5. Frantz, M.; Wipf, P. *Environ Mol Mutagen*, **2010,** *51*, 462–475.

6. Letai, A.; Bassik, M.C.; Walensky, L.D.; Sorcinelli, M.D.; Weiler, S.; Korsmeyer, S.J. *Cancer Cell,* **2002**, *2*, 183-192.

7. Zorov, D.B.; Juhaszova, M.; Sollott, S.J. *Physiol Rev.* **2014**, *94*, 909-950.

8. Kagan, V.E. *Adv. Drug Deliv. Rev.* **2009**, *61*, 1375–1385.

9. Asayama, S.; Kawamura, E.; Nagaoka, S.; Kawakamli, H. *Mol. Pharm.*, **2006**, *3*, 468-470.

10. Kulp, A.; Kuehn, M.J. *Annual review of microbiology*. **2010**, *64*, 163-184.

11. Letai, A.; Bassik, M.C.; Walensky, L.D.; Sorcinelli, M.D.; Weiler, S.; Korsmeyer, S.J. *Cancer Cell*, **2002**, *2*, 183-192.

12. Javadpour, M.M.; Juban, M.M.; Lo, W.C.; Bishop, S.M.; Alberty, J.B.; Cowell, S.M.; Becker, C.L.; McLaughlin, M.L. *J. Med. Chem.* **1996**, *39*, 3107-3113.

13. Reinhardt, A.; Neundorf, I.; *Int J Mol Sci.* **2016**, *17*, 701.

14. Mai, J.C.; Mi, Z.; Kim, S.; Ng, B.; Robbins, P.D. *Cancer Res.* **2001,** 61, 7709-7712.

15. Agemy, L.; Friedmann-Morvinski, D.; Kotamraju, V.R.; Roth, L.; Sugahara, K.N.; Girard, O.M.; Mattrey, R.F.; Verma, I.M.; Ruoslahti, E. *Proceedings of the National Academy of Sciences of the United States of America*, **2011**, *108*, 17450-17455.

16. Behrendt, R.; White, P.; Offer, J.J. *Pept Sci.* **2016**, *22*, 4-27.

17. Mäde, V, Els-Heindl S, Beck-Sickinger, A.G. *J Org Chem.* **2014**, *10*, 1197-1212.

18. Merrifield, R.B. *J. Am. Chem. Soc.*, **1963**, 85, 2149–2154.

19. Rapp, W.; Zhang, L.; Habish, R.; Bayer, E. *In Peptides: Proceedings of the 20 European Peptide Symposium.* **1988**, 21, 199-201. (b) Zalipsky, S.; Chang, J.L.; Albericio, F.; Barany, G. React. Polym. **1994**, *22*, 243-258.

20. Garcia-Martin, F.; Quintanar-Audelo, M.; Garcia-Ramos, Y.; Cruz, L.J.; Gravel, C.; Furic, R.; Cote, S.; Tulla-Puche, J.; Albericio, F. *J. Comb. Chem.* **2006**, *8*, 213-220.

21. Chantell, C.A.; Onaiyekan, M.A.; Menakuru, M. *J. Pept. Sci.* **2012**, *18*, 88.

22. Liu, X.; Yin, Y.; Liu, Z. *Nature*, **2014**, *5*, 4244.

23. Hood, C.A.; Fuentes, G.; Patel, H.; Page, K.; Menakuru, M.; Park, J.H. *J. Pept. Sci.* **2008**, *14*, 97.

24. a) Ralhan, K.; KrishnaKumar, V.G.; Gupta, S. *RSC Adv*. **2015**, *5*, 104417-104425. b) Luna, O.F.; Gomez, J.; Cárdenas, C.; Albericio, F.; Marshall, S.H.; Guzmán, F. *Molecules*, **2016**, *21*, 1542.

25. Basca, B.; Horvati, K.; Bosze, S.; Andrea, F.; Kappe, C.O. *J. Org. Chem.* **2008**, *73*, 7532-7542.

26. Geiger, T.; Clarke, S. *J. Biol. Chem*. **1987**, *262*, 785-794.

27. Matsuzaki, K. *Biochim. Biophys. Acta.* **2009**, *1788*, 1687-1692.

28. Horton, K.L.; Kelley, S.O. *J. Med. Chem.* **2009**, *52*, 3293-3299

29. *Chen*, *W.H.; Xu*, *X.D.*; *Luo*, *G.F.; Jia*, *H.Z.*; *Lei, Q.; Cheng*, *S.X.*; *Zhuo*, *R.X.*; *Zhang*, *X.Z. Sci. Rep. 2013*, *3*, *3468.*

30. Burns, K. E.; McCleerey, T.P.; Thevenin, D. *Sci. Rep.*, **2016**, *6*, 28465

31. Reshetnyak, Y.K.; Segala, M.; Andreev, O.A.; Engelman, D.M. *Biophys. J.* **2007,** *93***,** 2363–2372.

32. Hunt, J.F.; Rath, P.; Rothschild, K.J.; Engelman, D.M. *Biochemistry*, **1997**, *36*, 15177-15192.

33. Qiao, Z.Y.; Zhao, W.J.; Cong, Y.; Zhang, D.; Hu, Z.; Duan, Z. Y.; Wang, H. *Biomacromolecules*, **2016**, *17*, 1643–1652.

34. Liu, X.; Yin, Y.; Liu, Z. *Nature*, **2014**, *5*, 4244.

35. Doluca, O.; Withers, J.M.; Filichev, V.V. *Chem. Rev.* **2013**, *113*, 3044-3083.

36. Simeone, L.; Milano, D.; De Napoli, L.; Irace, C.; Di Pascale, A.; Boccalon, M.; Tecilla, P. *Chemistry,* **2011**, *17*, 13854-13865.

37. Patil, S.P.; Yi, J.W.; Bang, E.K.; Jeon, E.M.; Kim, B.H. *Med. Chem. Commun.* **2011**, *2*, 505-508.

38. Agrawal, N.; Dasaradhi, P.V.; Mohmmed, A.; Malhotra, P.; Bhatnagar, R.K.; Mukherjee, S.K. *Microbiol. Mol. Biol. Rev.* **2003**, *67*, 657-685.

39. Yang, H.W.; Yi, J.W.; Bang, E.K.; Jeon, E. M.; Kim, B. H. *Org. Biomol. Chem.* **2011**, *9*, 291-296.

40. Patel, P.; Hanawa, E.; Yadav, R.; Samuni, U.; Marzabadi, C.; Sabatino, D. *Bioorg Med Chem Letters.* **2013**, *23*, 5086-5090.

CHAPTER 2. SYNTHESIS, CHARACTERIZATION AND ANTI-CANCER ACTIVITY OF A PEPTIDE-NUCLEOLIPID BIOCONJUGATE

2.1 ABSTRACT

The nucleolipids form an interesting class of bioconjugates displaying desirable bio-physical and biological properties for applications in cancer detection and therapy. They own the ability to self-assemble into amphiphilic higher-order nanostructures which contributes to their biological relevance in medicinal chemistry. Therefore, nucleolipids have also been used in the delivery of hydrophobic drugs, biologicals and fluorescent probes for the detection and treatment of malignant cells. Structurally, the amphiphilic nucleolipids are composed of hydrophobic lipid appendages that are connected to a nucleoside core forming an amphiphile that may be further functionalized for medicinal chemistry applications. In spite of their utility, the nucleolipids remain limited by tedious total synthesis strategies, solubility issues in biological media and the susceptibility towards aggregation that may limit their biological function in live cells. In order to address these limitations, this chapter describes the synthesis, characterization and anti-cancer activity of a new class of amphiphilic peptide-nucleolipid bioconjugate. The approach began with the synthesis of a reactive carboxy-derived thymidine nucleolipid. The nucleolipid is based on a thymidine nucleoside that provides a chemically resilient and structurally pre-organized scaffold, and long chain alkylamines that are proposed to facilitate cell penetration and mitochondria localization for anti-cancer activity within tumor cells. Key to the synthesis strategy is a reductive amination procedure for installing the alkylamines onto the 3'-aldehyde derived thymidine building block. In this manner, a diversity oriented approach may be envisioned for the generation of functionally diverse nucleolipids. Deprotection and oxidation afforded the 5'-carboxy-derived nucleolipid which was then conjugated to the D-(KALAKLAK)$_2$-AK sequence. This peptide sequence is known as the killer peptide due to its ability to disrupt mitochondria structure and

function ultimately leading to apoptosis. The nucleolipid is anticipated to function as a vector, facilitating the penetration of the D-(KALAKLAK)$_2$-AK in tumors for potent anti-cancer activity. This chapter will further describe the outcome of a first representative example of a peptide-nucleolipid bioconjugate.

2.2 CHAPTER OBJECTIVES

This thesis chapter aims to describe the design, synthesis and characterization of a new class of peptide nucleolipid bioconjugates for anti-cancer applications. In order to accomplish these research objectives, a simple, reliable and reproducible synthesis strategy for making a 5'-carboxy 3'-hexadecylamine thymidine nucleolipid has been developed. This synthesis strategy features a key reductive amination step that was used to install hexadecylamine onto the 3'-aldehyde derived thymidine. This reaction afforded the desired nucleolipid in good yields and purities. Additionally, it may also be extended to other alkylamines for making libraries of functionally diverse nucleolipids for exploring structure-activity relationships with malignant cellular targets. Following deprotection and oxidation of the 5'-OH to the 5'-CO$_2$H, the carboxy-derived nucleolipid was characterized by a combination of chromatography and spectroscopy to ascertain identity and purity. The second objective is related to the solid phase peptide synthesis of the antimicrobial peptide D-(KLAKLAK)$_2$. In spite of its antiseptic activity, the D-(KLAKLAK)$_2$ sequence lacks mammalian cell permeability and cytotoxicity. Many efforts have been developed to improve the cytotoxic activity of the D-(KLAKLAK)$_2$ sequence in malignant mammalian cell types. Among the most commonly used methods is conjugation of the peptide with amphiphilic vectors that improve permeability across the mammalian cell membrane and promote localization at the mitochondria for cytotoxic activity. In the second objective, a solid phase synthesis approach has been developed for making an orthogonally protected D-

(KLAKLAK)$_2$-AK sequence. Liberation of the *C*-terminus amino group from the Lys side chain facilitated the development of a HCTU-based coupling reaction in between the peptide and carboxy derived nucleolipid to generate the peptide-nucleolipid bioconjugate. The desired peptide nucleolipid bioconjugate was then characterized by a combination of chromatography, spectroscopy and microscopy to fulfill the requirement of our third research objective, related to the characterization of the peptide-nucleolipid bioconjugate. In collaboration with Suing Huang (Ph.D. student) in the laboratory of Dr. Uri Samuni (Department of Chemistry, Queen's College) dynamic light scattering (DLS) and transmission electron microscopy (TEM) experiments were accomplished in order to validate the higher-order nanoparticle formulation of the bioconjugate. The final research objective in this study was aimed towards investigating the potential anti-cancer activity of the peptide nucleolipid bioconjugate. A screening assay was performed at the National Cancer Institute (NCI), in which a single dose treatment of the peptide nucleolipid bioconjugate was administered to 60 different cancer cell lines to determine inhibitory growth effects and cytotoxicity. Completion of these research objectives led to the identification of a lead peptide nucleolipid bioconjugate that may have anti-cancer utility in a selected panel of cancer cells lines. This thesis chapter will provide additional insights to the completion of the research objectives towards the synthesis, characterization and anti-cancer evaluation of a newly developed peptide-nucleolipid bioconjugate.

2.3 INTRODUCTION

The so-called "killer" peptide sequence D-(KLAKLAK)$_2$ has been originally designed and developed as an antimicrobial agent [1]. This peptide sequence was found to maintain selective cytotoxic activity towards bacteria, but not in mammalian cell types. The chemical basis for its selectivity has been attributed to its poly(cationic) amphiphilic nature, which facilitates

translocation across the negatively charged bacterial cell membrane, but with limited permeability across the zwitterionic membrane of mammalian cell types [2]. Once internalized within cells, the positively charged D-(KLAKLAK)$_2$ sequence has been found to associate to the surface of the mitochondria causing dissipation of the negatively charged mitochondrial membrane potential [3]. This depolarization resulted in a loss of mitochondrial structure integrity that caused membrane rupture and the release of mitochondrial contents into the cytoplasm. The release of the cell death effectors from the mitochondria, including cytochrome c, the second mitochondrial-derived activator of caspase (Smac/DIABLO) and the apoptosis-inducing factor (AIF) ultimately resulted in programmed cell death [4]. In an effort to exploit the cell death effects of D-(KLAKLAK)$_2$, modifications to the primary sequence [5] and conjugation with cell penetrating, targeting peptides and proteins [6-14] have resulted in improved cell translocation and cytotoxic activity within malignant mammalian cell types, such as in human cancers. In spite of their utility, effective methods for the safe and long-lasting administration of peptide-based therapeutics are still in widespread demand. Limitations which include poor peptide cell permeability, minimal exposure and resident time at the target tumor site for activity have impeded the translation of bio-active peptides such as the D-(KLAKLAK)$_2$ sequence from pre-clinical to clinical use. In an effort to mitigate these limitations and improve the 'drug-like' properties of the pro-apoptotic D-(KLAKLAK)$_2$ sequence, an amphiphilic nucleolipid is proposed to enhance cell permeability and mitochondria localization in tumors, resulting in potent and long-lasting anti-cancer effects.

The nucleolipids represent an interesting class of bioconjugates with the ability to form stable, higher-ordered nanostructure formulations for potential applications in medicinal chemistry [15, 16]. For example, they have been shown to form complexes with short-interfering RNA (siRNA), facilitating siRNA transfection across cell membranes and leading to the down-

regulation of mRNA expression in cancer cells [17-19]. Moreover, the synthesis, GRP78 oncogene binding and selective anti-cancer activity of a novel aminoacyl nucleolipid bioconjugate within the SR human leukemia cancer cell line has been described [20]. Thus, the nucleolipids have effectively served as robust delivery vehicles for biologicals and as potent cytotoxic agents for enhancing the cell death responses in cancer. In this study, a thymidine-derived nucleolipid is rationally designed to contain a reactive carboxy group for coupling with the pro-apoptotic D-(KLAKLAK)$_2$ sequence. This strategy will enable the introduction of functionally diverse nucleolipids within the D-(KLAKLAK)$_2$ sequence in order to improve structure-activity relationships in malignant cancer cell types.

2.3.1 SYNTHESIS, CHARACTERIZATION AND ANTI-CANCER ACTIVITY OF A PEPTIDE NUCLEOLIPID BIOCONJUGATE

Niki Rana[a], Suiying Huang[b], Pradeepkumar Patel[a], Uri Samuni[b], and David Sabatino[a,*]

[a]*Department of Chemistry and Biochemistry, Seton Hall University, 400 South Orange Avenue, South Orange, New Jersey 07079, United States*
[b]*Department of Chemistry, Queens College, City University of New York, 65-30 Kissena Blvd, Flushing , New York 11367, United States and the Ph.D. Programs in Chemistry and Biochemistry, The Graduate Center of the City University of New York, New York, NY 10016*
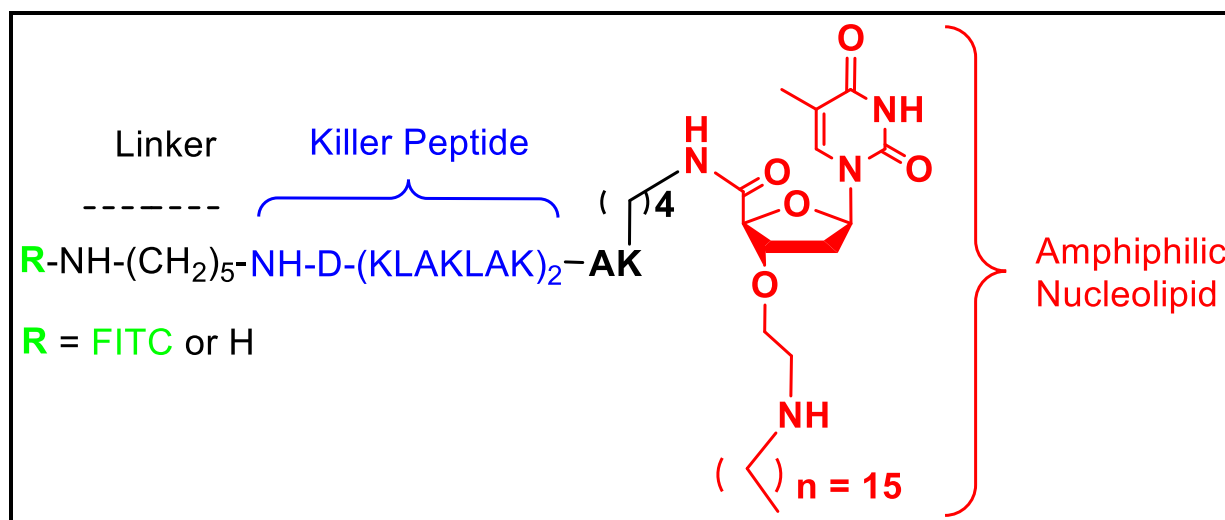
Figure 2.1. Graphical abstract of the peptide-nucleolipid bioconjugate developed in this study.

Figure adapted from Rana, N., Huang, S.; Patel, P.; Samuni, U.; Sabatino, D. *Bioorg. Med. Chem. Lett.*, **2016,** *26***,** 3567–3571.

2.3.2. RESULTS AND DISCUSSION

2.3.3. SYNTHESIS OF A 5'-CARBOXY 3'-HEXADECYLAMINE THYMIDINE DERIVED NUCLEOLIPID

The synthesis of nucleolipid **2.6** (**Scheme 2.1**) was initiated by the regioselective attachment of the allyl group at the 3'-hydroxyl of commercially available 5'-*O*-(4-

dimethoxytrityl) DMT- thymidine, **2.1**. The allylation reaction proceeded smoothly with sodium hydride (NaH) as base, and allyl bromide as alkylating reagent resulting in 87% yield of the mono-allylated nucleoside, **2.2**, and without any observable allylation on thymine. The allyl group in **2.2** was then oxidized to the aldehyde, **2.3**, and isolated in 84% yields following silica gel column chromatography. The reactive 3'-aldehyde was subsequently condensed with hexadecylamine and reduced using sodium cyanoborohydride to yield the alkylamine–derived thymidine, **2.4**. This two-step one-pot reductive amination reaction favored the formation of the desired intermediate, **2.4**, in 43% yields. In this reaction, the conversion of the imine to secondary amine was closely monitored by ^{1}H NMR which confirmed the disappearance of the iminium proton (δ: 6.85 ppm) upon complete reduction of the Schiff base. Following quantitative removal of the 5'-DMT group using trichloroacetic acid (TCA), a TEMPO-mediated oxidation reaction converted the 5'-hydroxy to the carboxylic acid, **2.6**, in 50% yield. Each reaction intermediate and the final product, **2.6**, were characterized by NMR, IR spectroscopy and by MS to confirm purities and identities.
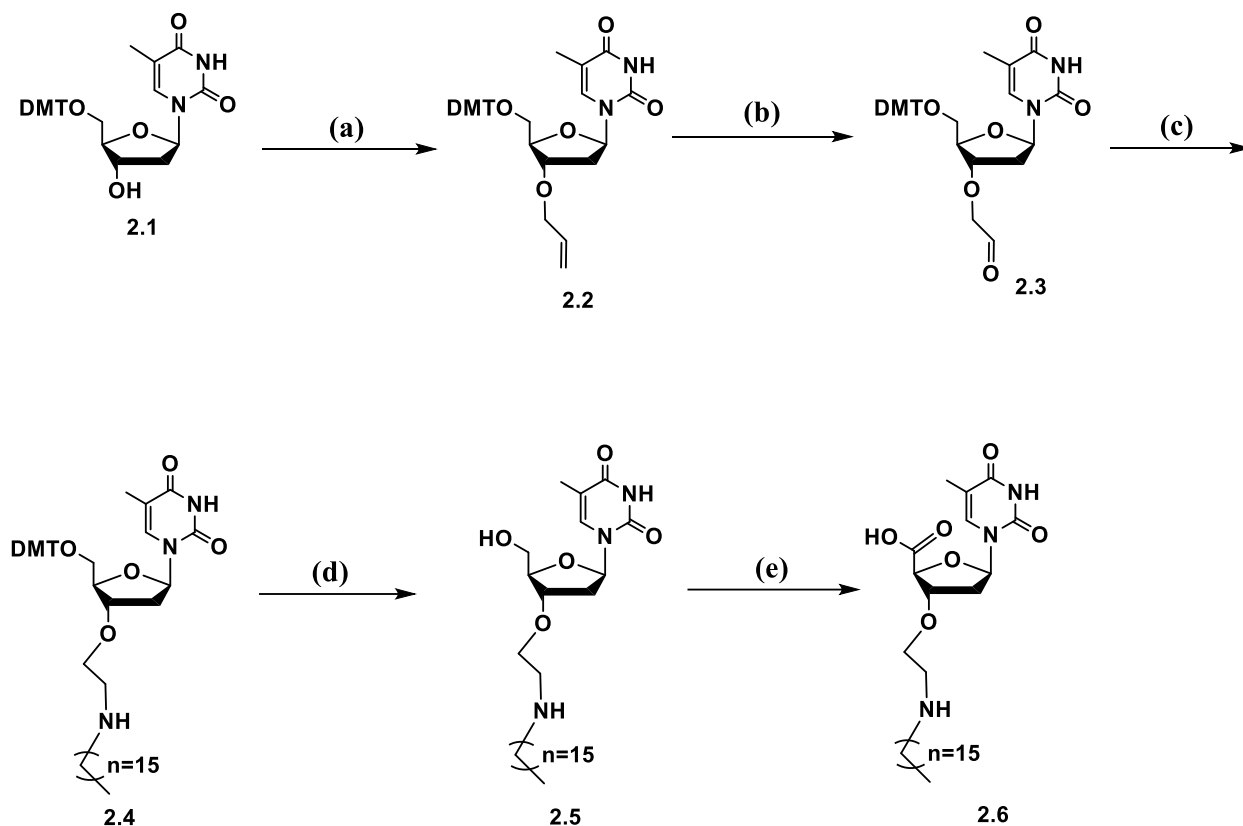
Scheme 2.1. Synthesis of 5'-carboxy-derived thymidine nucleolipid, **2.6**

Conditions: (a) allyl bromide, NaH, THF, sonication, r.t., 3hr, 87%, (b) 4% OsO_4 in t-BuOH, NMO, $Na_2S_2O_4$, $NaIO_4$, acetone:phosphate buffer (3:1 v/v), 84%, (c) i) 1-hexadecylamine, THF, r.t., 20 min, ii) $NaBH_3CN$, THF, r.t., 4hr, 43% (d) 3% TCA:DCM, r.t., 4h, >99%, (e) i) TEMPO, BAIB, DCM, r.t., 2h, ii) MeCN:Water r.t., 24 hr, 50%.

2.3.4 DESIGN AND SYNTHEIS OF D-(KLAKLAK)₂-AK PEPTIDE SEQUENCE AND ITS RELATED ANALOGUES.

The thymidine derived nucleolipid was rationally designed and synthesized to contain a reactive carboxy group for coupling with the pro-apoptotic D-(KLAKLAK)₂ sequence, to afford the desired peptide-nucleolipid bioconjugate (**Figure 2.1**). The thymidine nucleoside provides a chemically resilient and structurally pre-organized scaffold [21] while the long chain alkylamine

is anticipated to enhance cell permeability and mitochondria localization of the D-(KLAKLAK)$_2$-AK sequence for potent anti-cancer activity. Moreover, the native peptide, D-(KLAKLAK)$_2$-AK, and the palmitamide-derived D-(KLAKLAK)$_2$-AK sequences were also synthesized and used as controls to evaluate the influence of the nucleolipid on the biophysical, structural and biological properties of the D-(KLAKLAK)$_2$-AK sequence (**Figure 2.2A**).
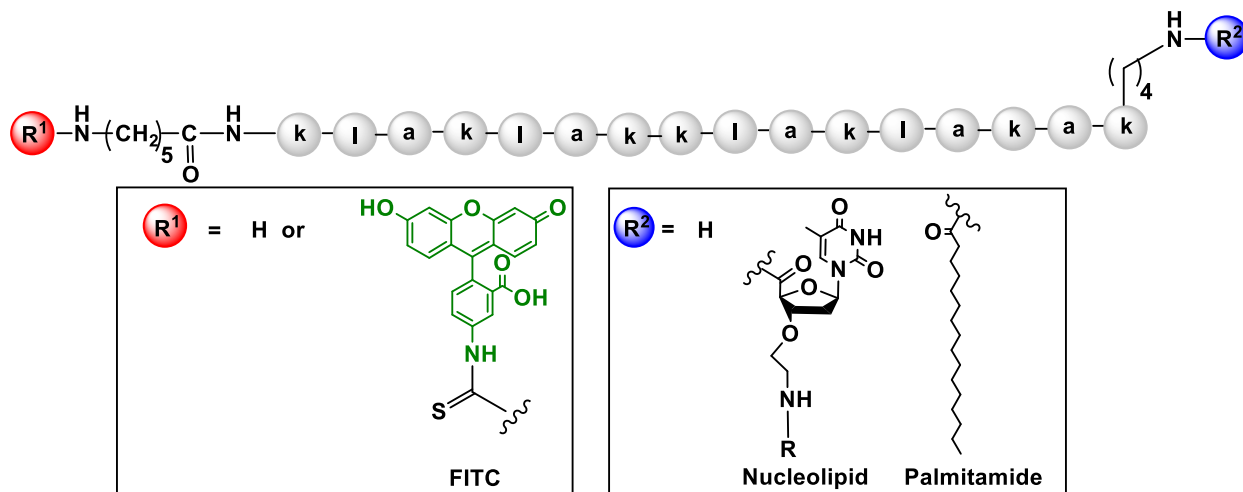
Figure 2.2 A. Peptide structures. The D-(KLAKLAK)2-AK peptide scaffold with R^1(red) = H or FITC, R^2(blue) = H, Nucleolipid or Palmitamide. R^1, R^2 = H, **2**, R^1 = FITC, R^2 = H, **5**, R^1 = H, R^2 = Palmitamide, **3**, R^1 = H, R^2 = Nucleolipid, **4**, R^1 = FITC, R^2 = Palmitamide, **6**, R^1 = FITC, R^2 = Nucleolipid, **7**. All amino acids are in their D-configuration.

The synthesis of the D-(KLAKLAK)$_2$-AK sequence, **2.7**, was accomplished by conventional Fmoc-solid phase peptide synthesis on a Rink amide hydrophilic poly(ethylene glycol) resin (Nova PEG, 0.47 mmol/g) [22]. At the *N*-terminus of the peptide sequence an aminohexanoic acid (AHx) linker was attached for the incorporation of fluorescein isothiocyanante (FITC) [23]. Following cleavage and deprotection, the FITC-labeled peptide sequence, **2.10**, was

isolated by RP-HPLC for characterization studies. At the *C*-terminus, an orthogonally protected Lys(Dde) residue was selectively deprotected on solid-phase using hydroxylamine hydrochloride buffered with imidazole. These mild conditions have been shown to cleave the Dde group without concomitant Fmoc-deprotection that has been shown to occur when hydrazine is used as Dde deblocking reagent [24]. Bioconjugation was first attempted by coupling palmitic acid at the *C*-terminus of the partially deprotected peptide sequence, **2.14**, bound to the solid support (**Scheme 2.2**). Optimized conditions for peptide coupling reactions using HCTU as coupling reagent and NMM as base were adopted for making the desired bioconjugates on solid support.

The palmitamide-derived D-(KLAKLAK)$_2$-AK sequence was Fmoc-deprotected and either coupled with FITC at the *N*-terminus, followed by cleavage and deprotection from solid-phase, or was directly cleaved and deprotected for LCMS analysis and purification. The palmitamide-derived D-(KLAKLAK)$_2$-AK sequence, **2.9**, and the FITC-labeled sequence, **2.12**,
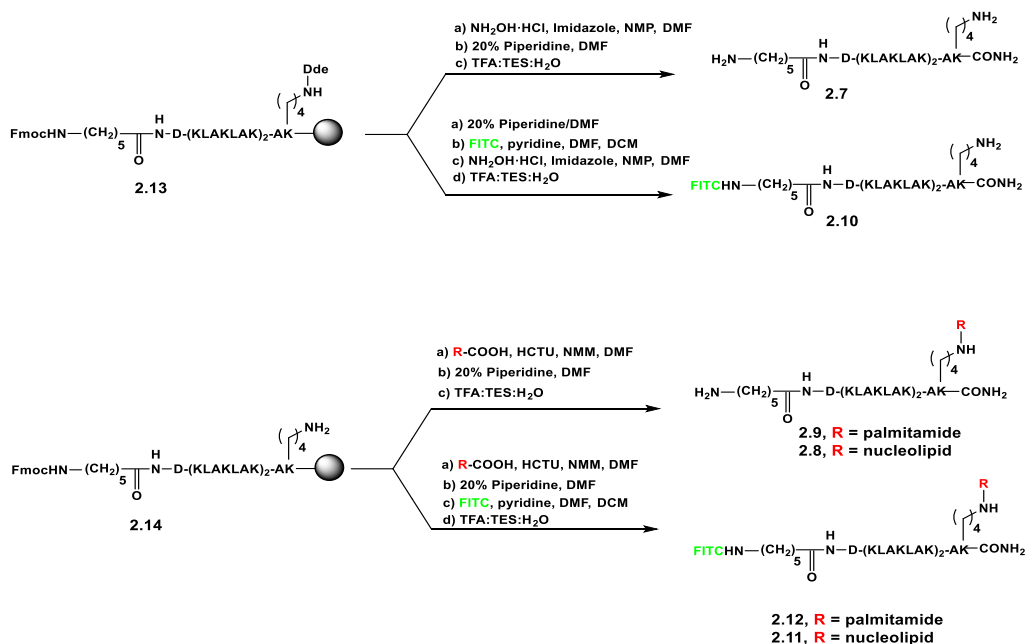

Scheme 2.2. Synthesis of FITC and non-FITC labeled D-(KLAKLAK)$_2$-AK conjugated with nucleolipid **2.6** or with palmitic acid.

were isolated by RP-HPLC and their identities were confirmed by MS. These coupling conditions were adopted for the synthesis of the nucleolipid-derived D-(KLAKLAK)$_2$-AK sequence, which was also produced respectively **2.8** and **2.11**, without and with the FITC label. In either cases, the peptide bioconjugates were isolated in sufficient yields (10-33%) and purities ($\geq$96%) for the structure-activity relationship studies.

2.4 CHARACTERIZATION OF D-(KLAKLAK)$_2$-AK AND ITS RELATED ANALOGUES.

The peptide bioconjugates were anticipated to display greater hydrophobicity relative to the native D-(KLAKLAK)$_2$-AK sequence. The enhanced hydrophobic character of cell-penetrating peptides has been shown to improve their membrane translocation, presumably due to the favorable non-polar interactions in between the hydrophobic side-chain residues of the peptides and the long-chain alkyl groups found within the lipid bilayer [25]. Comparison of the retention times on RP-HPLC (**Figure 2.2. B**) for the native, D-(KLAKLAK)$_2$-AK sequence, **2.7**, RT = 6.5 min, with the palmitamide-derived D-(KLAKLAK)$_2$-AK, **2.9**, RT = 17.6 min, and the nucleolipid-derived D-(KLAKLAK)$_2$-AK, **2.8**, RT = 11.3 min, confirmed that the palmitamide, followed by the nucleolipid produced the greatest hydrophobic effects onto the native D-(KLAKLAK)$_2$-AK sequence.
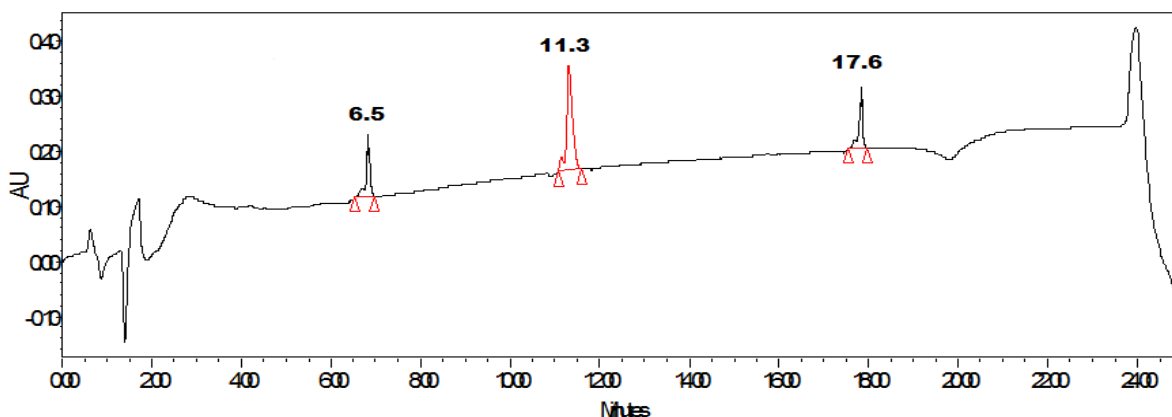
Entry	Sample Sequence	Rt(min)	% Purity
2.	AHx-D-(KLAKLAKKLAKLAK)-AK	6.5 min	> 99 %
3.	AHx-D-(KLAKLAKKLAKLAK)-AK-$C_{16}H_{31}O$ (Palmitamide)	17.6 min	> 99 %
4.	AHx-D-(KLAKLAKKLAKLAK)-AK-$C_{28}H_{48}N_3O_5$ (Nucleolipid)	11.3 min	96 %

Figure 2.2 B. RP-HPLC comparison study of the native, nucleolipid and palmitamide-derived D-(KLAKLAK)$_2$-AK biooconjugates. Column: Waters Symmetry Shield C$_{18}$, 5µm, 4.6x150 mm Mobile Phase: 2-80% MeCN:H$_2$O_0.1%FA PDA detection at: 220 nm.

The complete LC/MS characterization data for the peptides synthesized in this study is provided in **Table 2.1**. Of note, pure peptides were isolated following RP HPLC purification in purities>95%. Peptide purities were also confirmed in two different eluent systems which indicated single isolated peptide peaks at their characteristic retention times. The molecular weight identities of the peptides were confirmed as their mass:charge, in which multiple charge states, presumably due to the positively charged Lys ammonium groups were detected on ESI MS. Nonetheless, the peptides were isolated and characterized by LC/MS in sufficient quantities and purities for investigating their biophysical, structural and biological properties.

50

Table 2.1 Characterization data of peptides

Entry	Sequence	[a] Crude Purity (%)	[b] Isolated Purity (%)	[h] Isolated Yield(%/mg)	[i] M.W. (g/mol) Expt(Theoratical)	[j] Z	[k] RT (min)	[l] RT (min)
1	D-(KLAKLAKKLAKLAK)	93	[c]>99	56/(21.4)	508.5(507.0)	3	[f]7.5	[c]6.9
2	AHx-D-(KLAKLAKKLAKLAK)-AK	68	[d]>99	64/(29)	459.7(459.0)	4	[f]6.5	[d]4.2
3	AHx-D-(KLAKLAKKLAKLAK)-AK-$C_{16}H_{31}O$ (Palmitamide)	49	[e]>99	33/(8.3)	518.5(519.3)	4	[g]17.6	[e]13.8
4	AHx-D-(KLAKLAKKLAKLAK)-AK-$C_{28}H_{48}N_3O_5$ (Nucleolipid)	42	[f]96	10/(2.1)	468.8(468.4)	5	[f]11.3	[d]6.3
5	FITC-AHx-D-(KLAKLAKKLAKLAK)-AK	93	[f]>99	20/(4.0)	445.8(445.0)	5	[f]10.5	[d]6.0
6	FITC-AHx-D-(KLAKLAKKLAKLAK)-AK-$C_{16}H_{31}O$ (Palmitamide)	93	[g]>99	5/(2.0)	493.6(492.6)	5	[g]15.4	[e]5.7
7	FITC-AHx-D-(KLAKLAKKLAKLAK)-AK-$C_{28}H_{48}N_3O_5$ (Nucleolipid)	82	[g]96	30/(4.8)	546.9(546.2)	5	[g]10.5	[e]10.5

[a]Crude purities by RP-HPLC at 220 nm. [b]Isolated purities by RP-HPLC at 220 nm using [c]2-83% MeCN/H_2O with 0.1% TFA over 18 min, [d]2-80% MeCN/ H_2O with 0.1% FA over 17 min, [e]20-80 MeCN/ H_2O with 0.1% FA over 17 min, [f]2-80% MeOH/ H_2O with 0.1% FA over 17 min, [g]20-80 MeOH/H_2O with 0.1% FA over 17 min. [h]Isolated yields based on the resin loading. [i]Observed mass (expected mass) as [M+H]+/Z as detected by LCMS. [j]Charged state of the peptides as detected by LCMS in positive mode. [k]Retention times using methanol/water. [l]Retention times using acetonitrile/water. ([c]2-83% MeCN/H_2O with 0.1% TFA over 18 min, [d]2-80% MeCN/ H_2O with 0.1% FA over 17 min, [e]20-80 MeCN/ H_2O with 0.1% FA over 17 min, [f]2-80% MeOH/ H_2O with 0.1% FA over 17 min, [g]20-80 MeOH/H_2O with 0.1% FA over 17 min.)

The hydrophobicity of the peptide bioconjugates was also confirmed by the DLS zeta potential measurements and the logP values evaluating the octanol:water partition coefficients of the FITC-labeled peptides at 490 nm **(Table 2.2)**. Furthermore, UV-Vis spectroscopy also confirmed the characteristic absorption bands of the peptide bonds ($\lambda_{max} \sim 220$ nm) and the thymine base ($\lambda_{max} \sim 260$ nm) corresponding to the nucleolipid-derived D-(KLAKLAK)$_2$-AK, **2.8**, (**Figure 2.2C**).
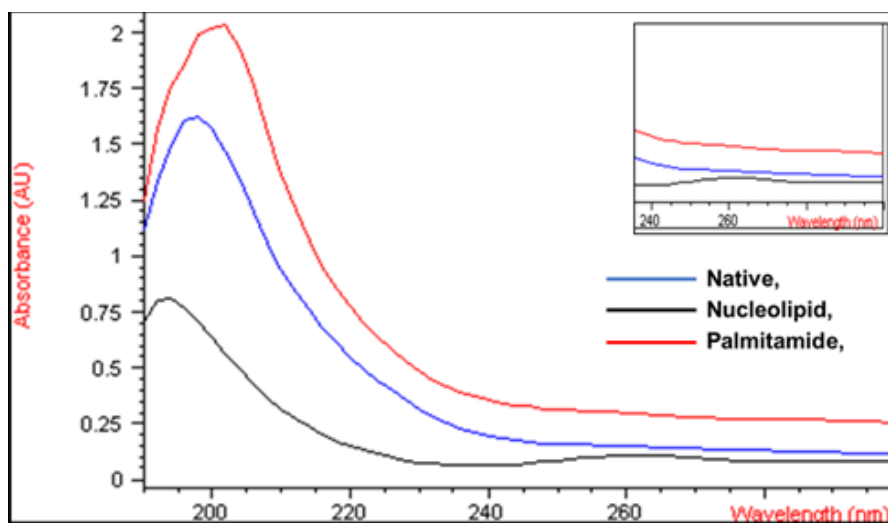

Figure 2.2C. UV/Vis spectroscopy (190–300 nm) of the peptides. Inset shows the nucleolipid-derived D-(KLAKLAK)2-AK, absorbance at 260 nm.

CD spectroscopy was then used to evaluate the secondary structures (if any) of the peptides in H$_2$O:TFE. The combination of H$_2$O:TFE has been especially useful in mimicking the amphiphilic lipid bilayer microenvironment that has served to stabilize peptide secondary structures in solution [26]. In this study, the native, D-(KLAKLAK)$_2$-AK sequence, **2.7**, displayed a stable, α-helical secondary structure (65% helicity), while the palmitamide-derived D-(KLAKLAK)$_2$-AK, **2.9**, displayed enhanced helicity (76%) and the nucleolipid-derived D-

(KLAKLAK)$_2$-AK **2.8**, demonstrated a less stable (42%) α-helical secondary structure (**Figure 2.2D** and **Table 2.2**).
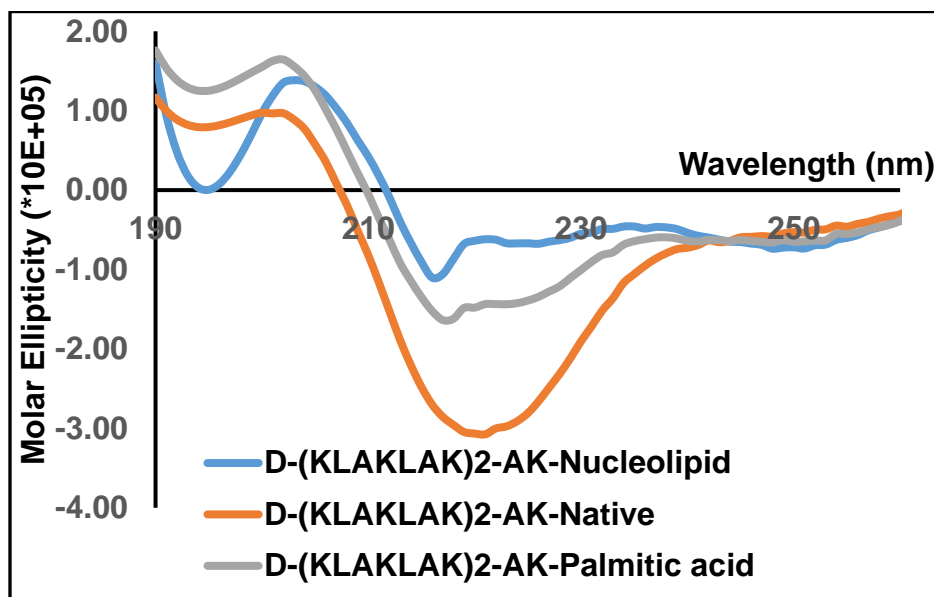

Figure 2.2D. CD spectra of peptides at 12.5 µM in H$_2$O: TFE (50:50, v/v)

Many amphiphilic cell-penetrating peptides adopt α-helical secondary structures. In certain cases, this peptide motif functions as a recognition site with other membrane spanning proteins (such as the pore proteins) and facilitates cellular translocation activity [27]. The amphiphilic α-helical peptides, **2.7**, **2.9** and **2.8**, were subsequently analyzed by DLS and TEM to determine ionic charge, size, shape and particle distributions (**Figure 2.3**). The DLS data (**Table 2.2** confirmed positively charged peptide ionic structures according to the zeta-potential measurements obtained in H$_2$O. The size distributions (60 – 300 nm) detected by DLS and TEM were found to be comparable and indicated a single, major population of nanoparticles for each formulation (**Figure 2.3**).

Table 2.2. Structural and biophysical properties of the peptide sequences.

Sequence[a]	% Helicity[b]	#of Helical residues[c]	Hydrophobicity[d]		Size(nm)		Zeta potential [g](mV)
			%AcN elution	cLogP	DLS [e]	TEM [f]	
AHx-D-(KLAKLAK)$_2$-AK	65	9	17	n.a.	270±80	70-150	30
AHx-D-(KLAKLAK)$_2$-AK-R^1	76	11	32	n.a.	190±70	70-150	7
AHx-D-(KLAKLAK)$_2$-AK-R^2	42	6	25	n.a.	310±90	60-120	6
FITC-AHx-D-(KLAKLAK$_2$-AK	n.a.	n.a.	24	-1.44±0.40	n.a.	n.a.	n.a.
FITC-AHx-D-(KLAKLAK)$_2$ AK-R^1	n.a.	n.a.	22	-0.36±0.02	n.a.	n.a.	n.a.
FITC-AHx-D-(KLAKLAK)$_2$)-R^2	n.a.	n.a.	42	-0.41±0.05	n.a.	n.a.	n.a.

Structure and comparison of hydrophobicity and helicity of the D-(KLAKLAK)$_2$-AK analogues. [a]Sequence compositions D-(KLAKLAK)$_2$-AK with R^1 = palmitamide, R^2 = nucleolipid, and FITC, [b]% Helicity calculated from observed ellipticity [Θ] at 222 nm using CD spectroscopy, [c]# of helical residues calculated from the % helicity determined using CD spectroscopy, [d]Hydrophobicity measured as % acetonitrile elution from the RP-HPLC C$_{18}$ column, LogP values (average and standard deviation of three independently conducted experiments) calculated from partitioning between 1-octanol and 10mM Tris pH 7.4 measured for the FITC-labeled (KLAKLAK)$_2$ peptides using UV-Vis spectroscopy at 492 nm, [e,f]Reported size of the peptide-based nanoparticle formulations based on DLS and TEM measurements. [g]Zeta potential measurements for the peptide samples obtained in water at 25ºC.

For example, the native D-(KLAKLAK)$_2$-AK sequence, **2.7**, displayed, uniform, square shaped particles ranging in sizes from 70 – 270 nm. The palmitamide-peptide bioconjugate, **2.9**, produced smaller, spherical-shaped particle sizes (70 – 190 nm), while the nucleolipid-peptide bioconjugate **2.8**, demonstrated the largest particle size formulation (60 – 310 nm). Taken altogether, these results suggests that the peptides may exhibit favorable biophysical and structural properties for their applications in molecular cancer cell biology. Considering the self-assembly

and nanoparticle formulation of similar amphiphilic D-(KLAKLAK)$_2$ sequences have led to significant anti-cancer effects [28] the cancer cell line toxicities of the peptides were subsequently evaluated.
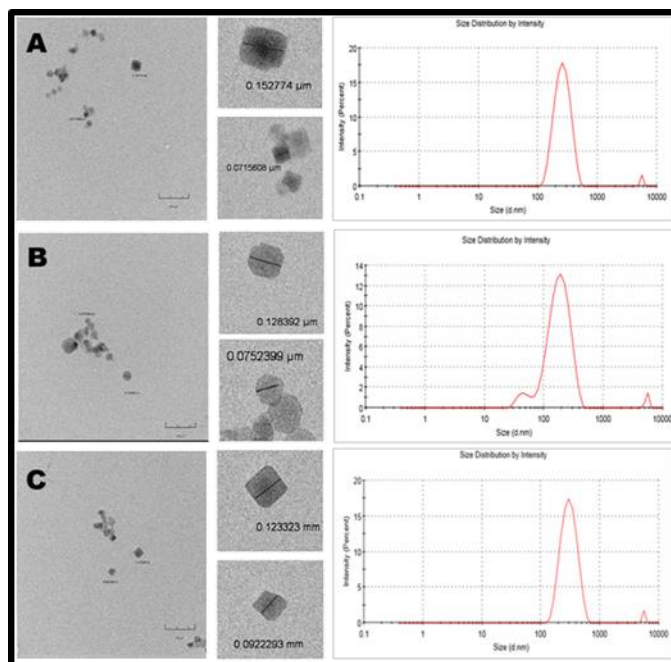

Figure 2.3. TEM images and DLS particle diameter size distributions of A) The native D-(KLAKLAK)$_2$-AK sequence, **2.7,** B) the palmitamide-derived D-(KLAKLAK)$_2$-AK sequence, **2.9**, and C) the nucleolipid-derived D-(KLAKLAK)$_2$-AK sequence, **2.8**.

2.5 BIOLOGICAL EVALUATION OF THE D-(KLAKLAK)2-AK SEQUENCE AND ITS RELATED ANALOGUES

A lethality assay was performed against a panel of 60 cancer cell lines at National Cancer Institute (NCI) [29]. A single dose screen was performed with the native, D-(KLAKLAK)$_2$-AK sequence, **2.7**, (10 μM), the palmitamide-derived D-(KLAKLAK)$_2$-AK sequence, **2.9**, (7.25 μM), and the nucleolipid-derived D-(KLAKLAK)$_2$-AK sequence, **2.8**, (2.13 μM). The cell growth data

(**Figures 2.4-2.6**) indicated that the peptides were found to be most active towards a panel of non-small cell lung carcinoma (NSCLC). Interestingly, the palmitamide and nucleolipid-derived D-(KLAKLAK)$_2$-AK sequences, **2.9** and **2.8**, showed the highest toxicity (~30%) within the A549 NSCLC cell line, resulting in a 1.5-fold enhancement relative to the native D-(KLAKLAK)$_2$-AK sequence, **2.7**, (~20%) (**Table 2.3**).

Table 2.3. NCI-60 cancer cell line screen lethality (% cell death) data for a selection of human Non-Small Cell Lung Cancer cell lines.

Lethality (% cell death) in NSCLC			
Sequence	**A549**	**NCI-H226**	**NCI-H522**
Native, **2.7**	19	1	14
Palmitamide, **2.9**	32	0	16
Nucleolipid, **2.10**	31	4	11

These results correlate nicely with the recently reported anti-cancer effects of the amphiphilic D-(KLAKLAK)$_2$-phospholipid liposome formulation which enhanced the cytotoxicity of the killer peptide sequence within the A549 lung cancer cells and within the drug-resistant lung cancer A549/Taxol cell line [30]. Thus, the amphiphilic palmitamide or nucleolipid-derived D-(KLAKLAK)$_2$-AK sequences represents an interesting class of bioconjugates that have served to potentiate the cancer cell death response of the native D-(KLAKLAK)$_2$-AK within the A549 lung cancer cell line. Furthermore, the cytotoxic selectivity for cancer cell lines over normal tissues for bioconjugates **2.8** and **2.9** is unanticipated but may be introduced by the incorporation of cancer cell targeting ligands [6,7,9,12-14].
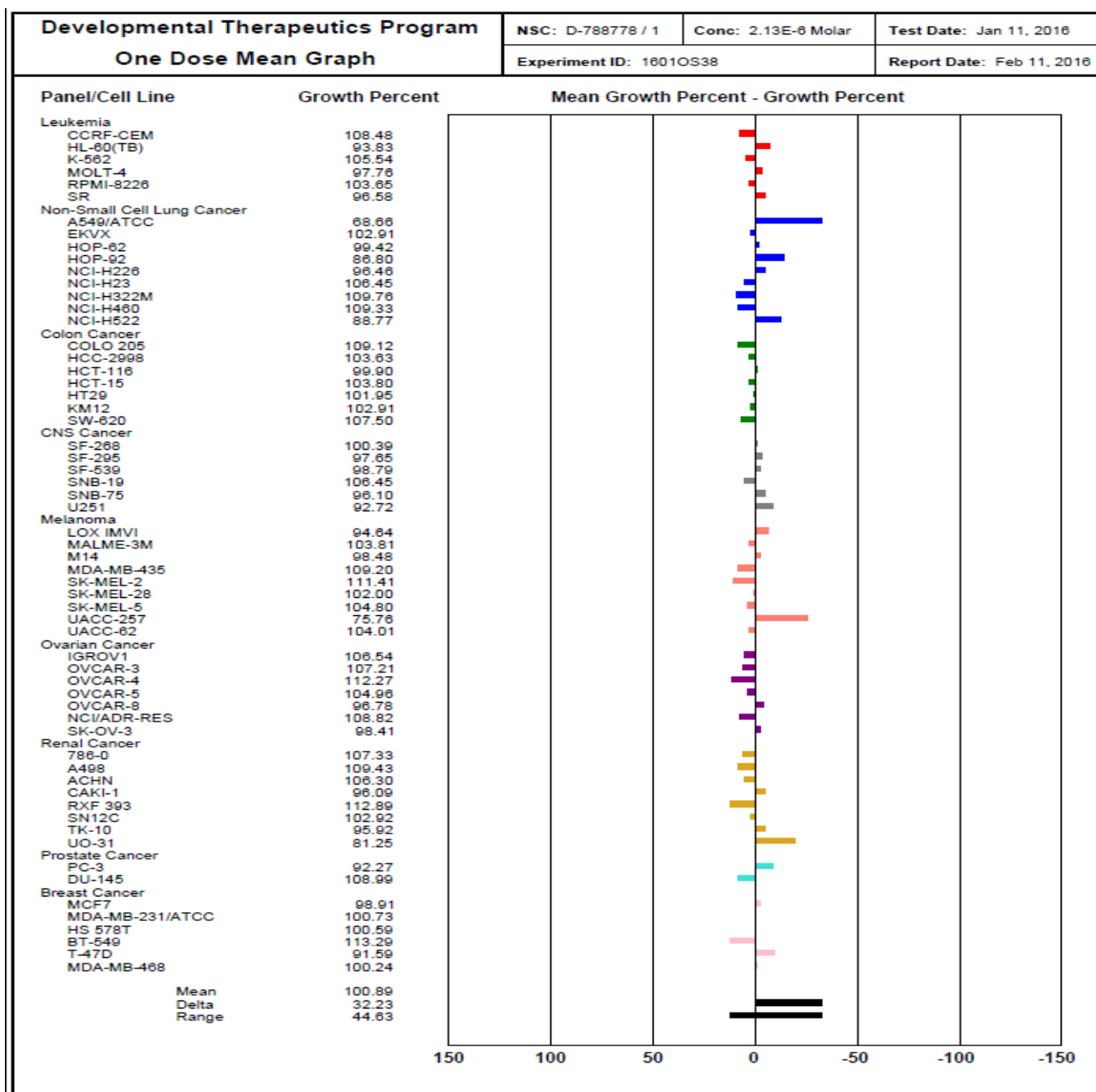
Developmental Therapeutics Program
One Dose Mean Graph

NSC: D-788778 / 1	Conc: 2.13E-6 Molar	Test Date: Jan 11, 2016
Experiment ID: 1601OS38		Report Date: Feb 11, 2016

Panel/Cell Line	Growth Percent
Leukemia	
CCRF-CEM	108.48
HL-60(TB)	93.83
K-562	105.54
MOLT-4	97.76
RPMI-8226	103.65
SR	96.58
Non-Small Cell Lung Cancer	
A549/ATCC	68.66
EKVX	102.91
HOP-62	99.42
HOP-92	86.80
NCI-H226	96.46
NCI-H23	106.45
NCI-H322M	109.76
NCI-H460	109.33
NCI-H522	88.77
Colon Cancer	
COLO 205	109.12
HCC-2998	103.63
HCT-116	99.90
HCT-15	103.80
HT29	101.95
KM12	102.91
SW-620	107.50
CNS Cancer	
SF-268	100.39
SF-295	97.65
SF-539	98.79
SNB-19	106.45
SNB-75	96.10
U251	92.72
Melanoma	
LOX IMVI	94.64
MALME-3M	103.81
M14	98.48
MDA-MB-435	109.20
SK-MEL-2	111.41
SK-MEL-28	102.00
SK-MEL-5	104.80
UACC-257	75.76
UACC-62	104.01
Ovarian Cancer	
IGROV1	106.54
OVCAR-3	107.21
OVCAR-4	112.27
OVCAR-5	104.96
OVCAR-8	96.78
NCI/ADR-RES	108.82
SK-OV-3	98.41
Renal Cancer	
786-0	107.33
A498	109.43
ACHN	106.30
CAKI-1	96.09
RXF 393	112.89
SN12C	102.92
TK-10	95.92
UO-31	81.25
Prostate Cancer	
PC-3	92.27
DU-145	108.99
Breast Cancer	
MCF7	98.91
MDA-MB-231/ATCC	100.73
HS 578T	100.59
BT-549	113.29
T-47D	91.59
MDA-MB-468	100.24
Mean	100.89
Delta	32.23
Range	44.63

Mean Growth Percent - Growth Percent

Axis: 150 100 50 0 -50 -100 -150

Figure 2.4. NCI 60 cancer cell line screen for determining growth inhibition and cytotoxic activity for a single dose (2.13 μM) treatment of nucleolipid-derived D-(KLAKLAK)$_2$-AK, **2.8**.
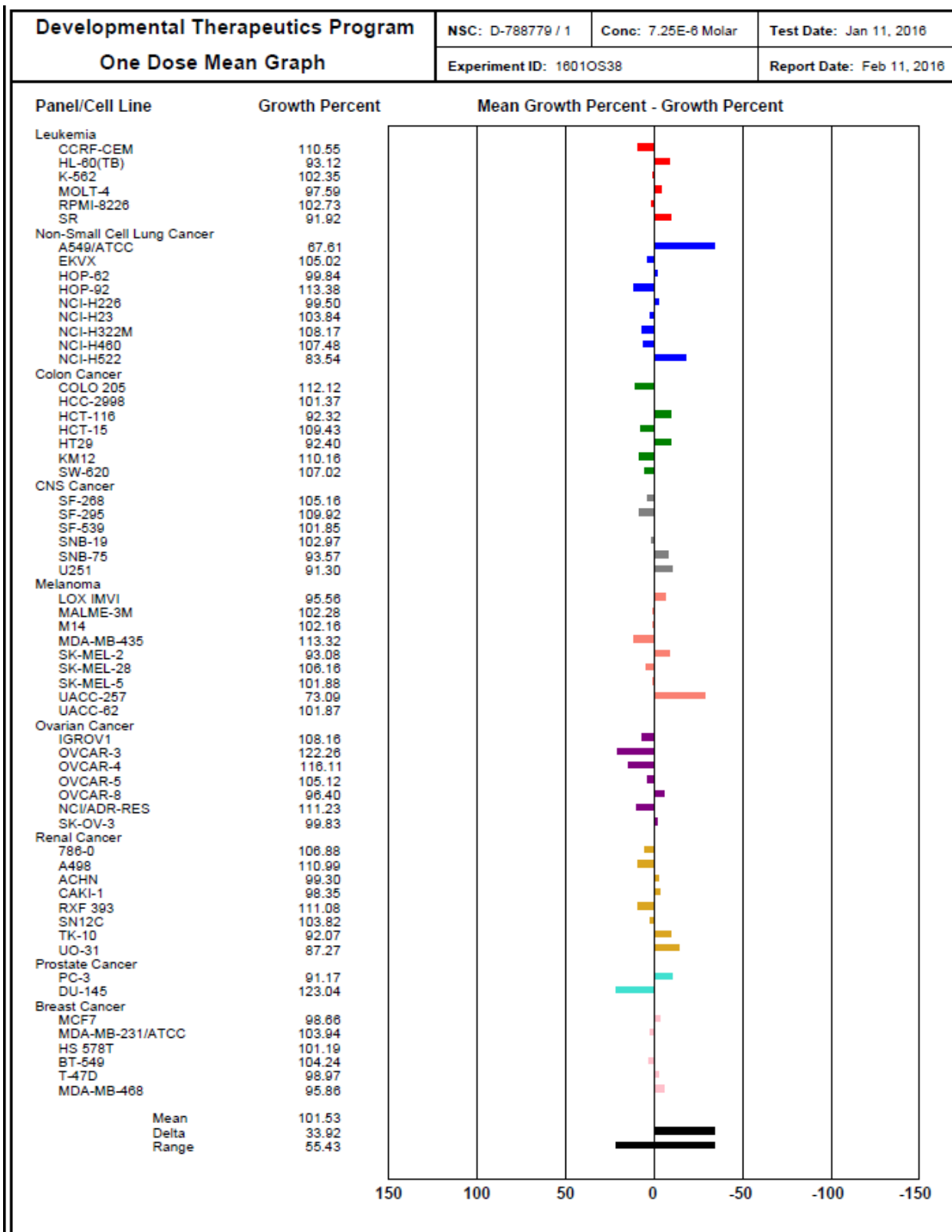
Figure 2.5. NCI 60 cancer cell line screen for determining growth inhibition and cytotoxic activity

for a single dose (7.25 μM) treatment of palmitamide-derived D-(KLAKLAK)$_2$-AK, **2.9**.
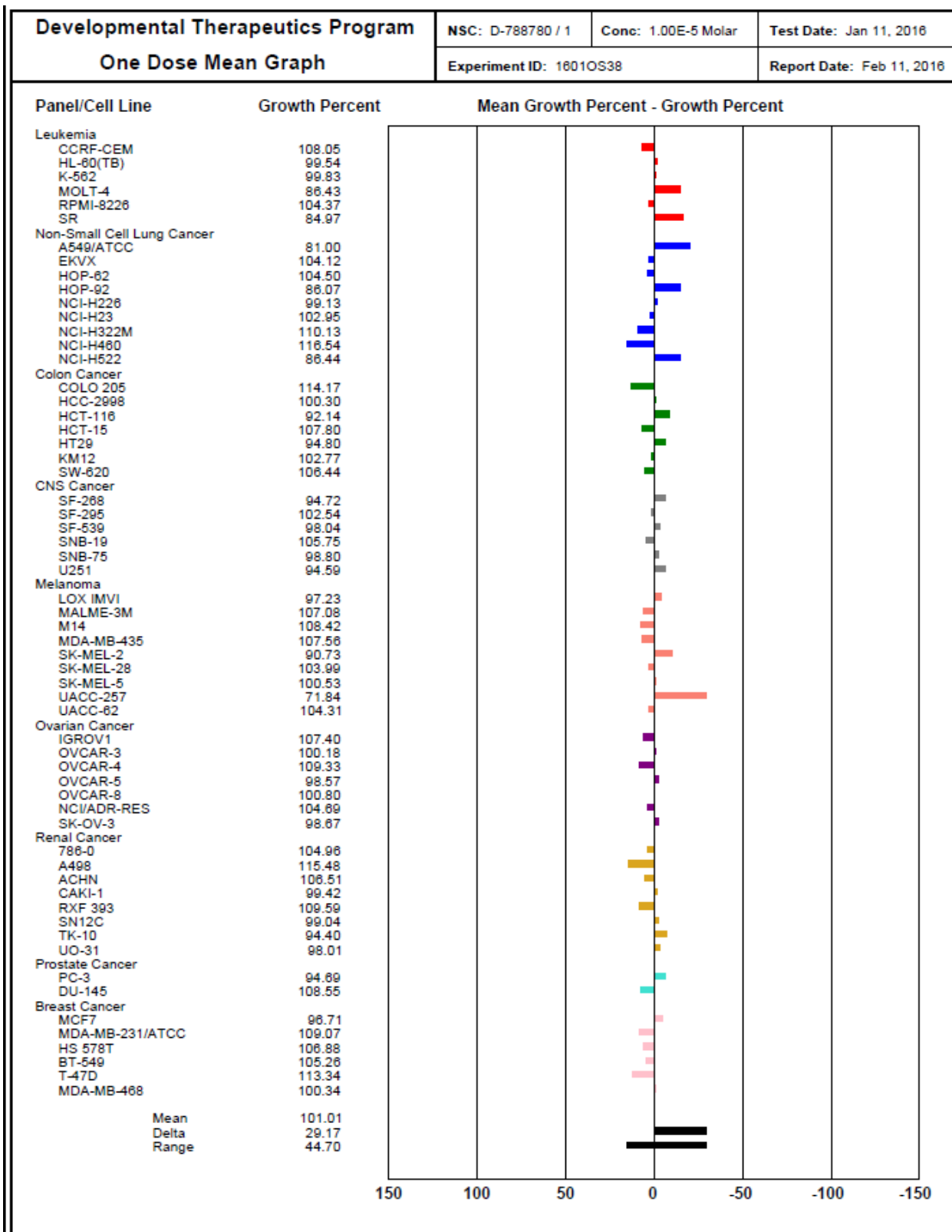
Figure 2.6. NCI 60 cancer cell line screen for determining growth inhibition and cytotoxic activity

for a single dose (10 μM) treatment of D-(KLAKLAK)$_2$-AK, **2.7**

2.6 CONCLUSIONS

In conclusion, the synthesis, characterization and anti-cancer activity of a new class of killer peptide bioconjugates are reported in this chapter. The peptide bioconjugates were found to be more hydrophobic relative to the native sequence. Moreover, the peptide bioconjugates displayed α-helical structures and cationic nanoparticle formulations that were contributive towards their anti-cancer activities. Within a NCI-60 cancer cell line screen, the peptide bioconjugates displayed enhanced cell death activity relative to the native sequence within the human A549 lung cancer cell line. These results validates the anti-cancer utility of the new amphiphilic peptide bioconjugates and paves the way for a cancer cell biology study that may ultimately unveil their mechanism of action. Moreover, the development of a key reductive amination procedure for making nucleolipids provides an opportunity for the generation of a diversity oriented synthesis approach. The latter is envisioned for making a library of functionally diverse nucleolipids for their incorporation into a lead, such as the D-(KLAKAK)$_2$ sequence, and for improving its structure-function properties in cancer cell types. Moreover, the peptide nucleolipid bioconjugate may also be functionalized with cancer-targeting peptide sequences for the development of a selective anti-cancer approach. The latter is of current research interest and some preliminary work detailing their development is presented in Chapter 3 of this thesis.

2.7. EXPERIMENTAL SECTION

General Methods:

All non-aqueous reactions were performed under inert atmosphere (nitrogen) unless otherwise specified. All glassware was cleaned and stored in a pre-heated oven (160 $^{\circ}$C) for drying

and cooled in a dessicator prior to use. Anhydrous solvents and reagents were purchased from Aldrich (St. Louis, MO) and used as received. Analytical thin-layer chromatography (TLC) was performed on aluminum-backed silica gel plates (Merck 60 F254). TLCs were visualized under UV shadowing (260 nm) or staining (10% H_2SO_4/MeOH). Compound purification using silica gel chromatography was performed on a 230-400 mesh silica (Sorbent Technologies). Melting points were obtained on a Thermo Melt apparatus. Specific rotations measurements were recorded on a DigiPol 781 Automatic Polarimetry (Rudolph Instruments, Fairfield, NJ, USA) and collected as an average of five measurements per compound. Data are reported as follows: [α]λ temp, concentration (c in g/100 mL), in Acetone, MeOH, DCM or $CHCl_3$. Molecular weights were measured as direct injections on a Hewlett Packard series 1100 MSD equipped with ESI as ion-source in positive mode using 50/50 v/v MeOH/H_2O at a flow-rate of 1 mL/min. Infrared (IR) spectra were obtained on a Nicolet 4700 FT-IR (ThermoElectron Co.) coupled with OMNIC software (driver version: 7.1). The compounds were deposited on a KBr plate with the cast film technique and the data was collected as an average of 3 scans in wavenumbers (cm^{-1}). Nuclear magnetic resonance spectra (^{1}H, ^{13}C, COSY NMR) were recorded on an Varian Inova NMR AS500 spectrophotometer. The NMR spectra were obtained at ambient temperature using an indirect pulse-field gradient (ID-PFG) probe. The obtained data was processed using VNMRJ software (version 2.2). The ^{1}H and ^{13}C assignments were based on gCOSY and gHMQC NMR correlation experiments.

Synthesis:

3'-*O*-(allyl)-5'-*O*-(dimethoxytrityl) thymidine (2.2): To a suspension of 60% NaH (220 mg, 9.19 mmol) in anhydrous THF (20 mL) under argon at 0 °C was added 5'-*O* (dimethoxytrityl) thymidine (2 g, 3.67 mmol). After sonication for 20 min, allyl bromide (792 μL, 9.17 mmol) was added and

the reaction mixture was stirred at r.t. for 3 h. The mixture was poured into saturated $NaHCO_3$ (40 mL) and extracted with EtOAc (3 × 20 mL). The combined organic layers were then washed with brine (30 mL), dried over $MgSO_4$, filtered and concentrated. Purification by flash column chromatography (EtOAc–petroleum ether, 1:1 v/v, 1% Et_3N) afforded 3'-*O*-(allyl)-5'-*O*-(dimethoxytrityl)thymidine as a white solid; yield: 1.65 g (87 %); m.p. 83 °C. $[\alpha]_{589}^{23}$: +15.29 (c 0.01, Acetone). R_f = 0.44 (EtOAc–petroleum ether, 7:3 v/v). IR (KBr) υ_{max} (cm^{-1}) = 3182.1, 3059.1, 2929.9, 2836.8, 1693.4, 1607.7, 1582.3, 1508.9, 1464.5, 1364, 1273.5, 1251.1, 1177.1, 1105.4, 1063.1, 1033.5, 915.8, 829.1, 791.1, 755.8, 727.0, 702.1.^{1}H NMR (500 MHz, acetone-d_6): δ = 1.52 (s, 3H), 2.42 (m, 2H), 3.43 (m, 2H), 3.82 (s, 6H), 4.07 (m, 2H), 4.10 (d, J = 3.0 Hz, 1H), 4.40 (t, J = 3.0 Hz, 1H), 5.17 (dd, J = 1.5, 10.5 Hz, 1H), 5.29 (dd, J = 1.5, 17.25 Hz, 1H), 5.93 (m, 1H), 6.33 (dd, J = 6.0, 8.0 Hz, 1H), 6.94 (d, J = 8.5 Hz, 4H), 7.28 (t, J = 7.5 Hz, 1H), 7.35–7.41 (m, 6H), 7.52 (d, J = 7.0 Hz, 2H), 7.64 (d, J = 1.0, 1H). 10.03 (bs, 1H). ^{13}C NMR (126 MHz, acetone-d_6): δ = 11.34, 37.36, 54.69, 63.97, 69.76, 79.04, 83.79, 84.49, 86.68, 110.2, 113.2, 116.1, 126.9, 127.9, 128.2, 130.1, 135.0, 135.5, 135.7, 135.8, 145.0, 150.4, 151.7, 158.9, 163.4, 179.2. ESI MS (m/z) calculated for $C_{34}H_{36}N_2O_7$ [M+Na], 607.2; found 607.2.

3'-*O*-(formylmethyl)-5'-*O*-(dimethoxytrityl) thymidine (2.3): To a solution of **2.2** (1.63 g, 2.79 mmol) in a mixture of acetone–H_2O (12 mL, 3:1 v/v) was added NMO (0.65 g, 5.58 mmol) and a solution of 2.5% OsO_4 in *t*-BuOH (1.8 mL). The mixture was stirred at r.t. for 2 h, then treated with $Na_2S_2O_5$ (0.98 g, 5.15 mmol) and stirred for 30 min. The reaction mixture was then treated with H_2O (50 mL) and the aqueous layer was extracted with EtOAc (3 × 50 mL). The combined organic layers were washed with brine (100 mL), dried over $MgSO_4$, filtered and concentrated. The residue was dissolved in a mixture of acetone phosphate buffer pH 7 (22 mL, 3:1 v/v), and

NaIO$_4$ (1.50 g, 7.02 mmol) was added. The mixture was stirred at r.t. for 2 h, and then filtered, and the precipitate was washed with EtOAc (50 mL). The separated aqueous layer was extracted with EtOAc (2 × 50 mL) and then the combined organic layers were washed with brine (100 mL), dried over MgSO$_4$, filtered and concentrated. The crude product 3'-O-(formylmethyl)-5'-O-(dimethoxytrityl) thymidine (solid; 1.50 g, 84%) was used directly as recovered. m.p. 123 °C. $[\alpha]_{589}^{23}$: +3.61 (c 0.80, acetone). R$_f$ = 0.55 (CH$_2$Cl$_2$–MeOH, 9:1). IR (KBr) υ_{max} (cm^{-1}) = 3307, 3066.8, 3007.3, 2953.4, 2929.6, 2856.5, 1736.7, 1698.6, 1660.3, 1610.8, 1557.2, 1509.6, 1485.4, 1445.8, 1382.6, 1300.8, 1253.5, 1217.4, 1176.1, 1109.9, 1072, 1034.8, 1002.6, 968.5, 936.6, 890.7, 863.6, 755.8, 704.6, 667.9 ^{1}H NMR (500 MHz, DMSO-d$_6$): δ = 1.44 (s, 3H), 2.29-2.38 (m, 2H), 3.36 (dd, J = 3.0, 10.8 Hz, 1H), 3.45 (dd, J = 3.0, 10.8 Hz, 1H), 3.79 (s, 6 H), 4.06–4.10 (m, 2H), 4.18 (d, J = 2.5 Hz, 1H), 4.24 (d, J = 6.0 Hz, 1H), 6.19 (t, J = 2.0 Hz, 1H), 6.91 (dd, J = 1.0, 9.30 Hz, 4H), 7.23–7.28 (m, 7H), 7.40 (d, J = 7.0 Hz, 1H), 7.52 (d, J = 1.5 Hz, 1H), 9.55 (s, 1H), 11.4 (s, 1H). ^{13}C NMR (126 .9 MHz, DMSO-d$_6$): δ = 12.1, 14.5, 14.6, 21.2, 36.8, 39.4, 39.6, 39.7, 40.0, 40.1, 40.2, 40.4, 55.5, 60.2, 64.2, 74.7, 80.4, 83.3, 84.1, 84.2, 87.0, 110.2, 114.0, 113.7, 127.2, 128.1, 128.4, 130.1, 130.2, 135.6, 135.8, 136.0, 145.1, 151.0. ESI MS (m/z) calculated for C$_{33}$H$_{34}$N$_2$O$_8$ [M+H], 586.2; found 586.2.

3'-O-(hexadecylaminoethyl)-5'-O-(dimethoxytrityl) thymidine (2.4): The starting material **2.3** (250 mg, 0.04 µmol) and 1-hexadecylamine (194 mg, 0.036 µmol) were dissolved in 3 mL of dry THF. The reaction was stirred for 20 min at room temperature and sodium cyanoborohydride (80 mg, 0.05 µmol, 1.5 equiv) was added to reaction mixture and stirred for 4 hrs. The reaction was then concentrated *in vacuum* and purified by flash column chromatography using EtOAc:Petroleum ether (6:4 v/v) to yield a white foamy product **2.4** in 43% yield. m.p. 70 °C.

$[\alpha]_{589}^{23}$: +9.11 (c 0.01, DCM). R_f = 0.50 (EtOAc–petroleum ether, 6:4 v/v). IR (KBr) υ_{max} (cm^{-1}) = 3168.8, 3060.7, 2924.4, 2853.1, 2421.0, 1843.9, 1791.9, 1771.9, 1761.2, 1750.2, 1733.4, 1691.9, 1678.5, 1635.7, 1607.4, 1583.0, 1550.2, 1540.5, 1510.6, 1467.2, 1418.9, 1363.3, 1295.9, 1275.0, 1251.7, 1177.1, 1100.7, 1035.5, 964.0, 902.1, 829.4, 790.9, 754.8, 727.2, 702.0, 585.3, 492.7, 418.6. ^{1}H NMR (499.84 MHz, CD$_2$Cl$_2$): δ = 0.91 (t, J = 7.0 Hz, 3H), 1.30 (t, J = 10.5 Hz, 28H) , 1.50 (d, J = 12.0 Hz, 3H), 1.57 (s, 1H), 2.23 (m, 1H), 2.46 (t, J = 6.0 Hz, 1H), 2.81 (d, J = 8.0 Hz, 1H), 3.00 (m, 2H), 3.33 (m, 1H), 3.44 (d, J = 11 Hz, 1H), 3.64 (m, 1H), 3.75–3.83 (m, 8H), 4.11 (dd, J = 2, 14.5 Hz, 1H), 4.21 (d, J = 5.0 Hz, 1H), 6.29 (m, 1H), 6.85 (m, 4H), 7.24-7.33 (m, 7H), 7.41 (d, J = 10.0 Hz, 2H), 7.46 (s, 1H). ^{13}C NMR (125.6 MHz, CD$_2$Cl$_2$): δ = 22.6, 25.7, 25.8, 26.5, 29.1, 29.3, 29.4, 29.5, 29.6, 31.9, 53.0, 53.1, 53.4, 53.6, 53.8, 55.2, 55.3, 111.1, 113.2, 128.0, 130.0, 131.0, 135.3, 135.4, 158.9. ESI MS (m/z) calculated for C$_{49}$H$_{69}$N$_3$O$_7$ [M+H], 812.5; found 812.1

3'-*O*-(hexadecylaminoethyl)-thymidine (2.5): A solution of 3% TCA in DCM (10 mL) was added dropwise at room temperature to **2.4** (100 mg, 0.123 mmol). The reaction was continued for 3 hr, the mixture was concentrated and loaded directly onto a column chromatography for purification. The crude was purified (EtOAc:Petroleum ether, 3:2 v/v) to obtain >99% of a white foamy product. m.p. 79 °C. $[\alpha]_{589}^{23}$ -3.088 (c 0.01, DCM). R_f = 0.10 (EtOAc–Petroleum ether, 6:4). IR (KBr) υ_{max} (cm^{-1}) = 3632.9, 3572.0, 3410.1, 2923.6, 2853.2, 2424.5, 1733.4, 1709.2, 1703.0, 1692.0, 1678.0, 1665.7, 1659.0, 1642.3, 1468.4, 1378.1, 1276.8, 1098.1, 821.3, 775.2, 675.1. ^{1}H NMR (499.9 MHz, DMSO-d_6): δ = 0.87 (t, J = 6.75 Hz, 2H), 1.24 (s, 19H), 1.60 (bs, 1H), 1.79 (s, 3H), 2.14 (d, J = 6.5 Hz, 1H), 2.22-2.25 (m, 1H), 2.52 (s, 2H), 2.69 (d, J = 5.0 Hz, 1H), 2.76 (t, J = 5.25 Hz, 1H), 2.90 (t, J = 4.25 Hz, 2H), 3.60 (s, 1H), 3.70 (s, 1H), 4.0 (m, 1H),

4.10 (d, J = 3.0 Hz, 1H), 6.51 (bs, 1H), 6.14-6.17 (m, 1H), 7.71 (s, 1H), 11.2 (s, 1H). ^{13}C NMR (126.9 MHz, DMSO-d_6): δ = 12.7, 14.3, 14.4, 22.5, 24.9, 26.8, 29.0, 29.1, 36.6, 52.0, 53.2, 62.0, 64.4, 68.0, 80.2, 80.2, 80.3, 84.2, 84.3, 84.8, 84.9, 85.0, 110.0, 136.3, 136.4, 151.0, 164.1, 165.2. ESI MS (m/z) calculated for $C_{28}H_{51}N_3O_5$ [M-H], 509.7; found 510.5.

3'-O-(hexadecylaminoethyl)-5'-carboxy-thymidine (2.6): To a solution of **2.5** (124 mg, 0.258 mmol) in CH_2Cl_2 (1.3 mL) was added 2,2,6,6-tetramethyl-1-piperidinyloxy, free radical (TEMPO) (9 mg, 0.06 mmol), and iodobenzene diacetate (BAIB) (184 mg, 0.570 mmol) at room temperature. After the mixture was stirred for 2 h, a mixture of MeCN:H_2O (1:1 v/v, 140 μL) was added to the reaction mixture and stirred for 24 h. After evaporation of the solvent, the residue was purified by flash chromatography ($CHCl_3$:MeOH 9:1 v/v). The pure product was obtained as white powder in 50% yield. $[\alpha]_{589}^{23}$ (c 0.01, DCM), R_f = 0.20 ($CHCl_3$: MeOH 9:1 v/v). ^{1}H NMR (499.8 MHz, DMSO): δ= 1.14 (t, J = 6.75 Hz, 3H), 1.56 (t, J = 13.2 Hz, 30H), 2.79-2.80 (m, 7H), 3.28-3.37 (m, 1H), 3.6 (bs, 1H), 3.98-4.05 (m, 2H), 4.44-4.45 (m, 1H), 4.51 (d, J = 1.5 Hz, 1H), 6.43-6.46 (m, 1H), 9.37 (s, 1H), 11.46 (bs, 1H). ^{13}C NMR (125.69 MHz, DMSO-d_6): δ= 13.0, 14.3, 22.5, 26.2, 27.0, 29.1, 29.5, 31.7, 39.5, 39.6, 40.0, 40.02, 40.1, 40.2, 40.3, 40.5, 83.2, 84.4, 86.0, 109.0, 139.0, 151.0, 164.4, 173.4. ESI MS (m/z) calculated for $C_{28}H_{49}N_3O_6$ [M-H], 522.3; found 522.4

Solid phase peptide synthesis:

Synthesis of peptides was performed on a PSI 200 Peptide Synthesizer (Peptide Scientific Inc.) on a Rink amide poly(ethylene glycol) resin (Nova PEG, 0.47 mmol/g). Fmoc-D-amino acids (3 eq.) were dissolved in DMF (4 mL) along with NMM (6 eq.) and HCTU (3 eq.). The reaction

mixture was agitated for 5 min and added to the solid support for automated coupling and deprotection. Coupling times were set to 20 min followed by deprotection of the Fmoc protecting group (30 min) with 20% piperidine in DMF. Washing (MeOH and DMF) and drying of the peptide bound support with $N_{2(g)}$ were accomplished prior to the recovery of the peptide bound to resin. At the *N*-terminus, Fmoc-aminohexanoic acid (Ahx, 3 eq.) was coupled and Fmoc-deprotected. Labeling of the Ahx-peptide *N*-terminus with fluorescein isothiocyanate (FITC, 1.1 eq.) in pyridine:DMF:DCM (12:7:5 v/v/v) was accomplished in the dark, overnight at room temperature. Following synthesis, peptide cleavage from the solid support and deprotection of the side-chain protecting groups were accomplished with concentrated trifluoroacetic acid (TFA, 95%) with minimal addition (5%) of reaction scavengers (*i.e.* H_2O, triethylsilane). The cleavage and deprotection reaction was completed in 2 hr at room temperature. Peptide samples were concentrated, precipitated in cold diethyl ether, and isolated as white pellets for LC/MS analyses and purification.

Solid-phase bioconjugation:

Solid-phase bioconjugation of peptide nucleolipid and palmitamide were performed on an oil bath reaction apparatus with stirring block. Rink amide poly(ethylene glycol) resin (Nova PEG, 0.47 mmol/g) was transferred to a reaction vessel and swollen with 500 µl, DMF at 60 ℃ for 2 hr. The resin was filtered, washed and dried under $N_{2(g)}$ prior to the reaction. Nucleolipid or palmitamide (3 eq.) were added in DMF (500 µl) along with NMM (6 eq.) and HCTU (3 eq.). The reaction mixture was preactivated for 7 min before slowly added and agitated for 14 h at 60 ℃ with peptide bound to solid support. Coupling times were set at 20 min followed by deprotection of the Fmoc protecting group (30 min) with 20% piperidine in DMF. Washing (MeOH, DMF and DCM) and drying of the peptide bound support with $N_{2(g)}$ were accomplished prior to the recovery of the

peptide bound to resin. Labeling of the Ahx-peptide *N*-terminus with fluorescein isothiocyanate (FITC, 1.1 eq.) in pyridine:DMF:DCM (12:7:5 v/v/v) was accomplished in the dark, overnight at room temperature. Following synthesis, peptide cleavage from the solid support and deprotection of the side-chain protecting groups were accomplished with concentrated trifluoroacetic acid (TFA, 95%) with minimal addition (5%) of reaction scavengers (*i.e.* H_2O, triethylsilane). The cleavage and deprotection reaction was completed in 2 h at room temperature. Peptide samples were concentrated, precipitated in cold ether, and isolated as white pellets for LC/MS analyses and purification.

Characterization of peptides by LC/MS:

Crude peptide pellets were dissolved in MeOH/H_2O (50:50 v/v, 1 mL) for LCMS analyses. Sample analyses were performed on an Agilent 1100 series ESI-LCMS with a single quadrupole mass analyzer and LC conditions used a linear binary gradient 20-80% or 2-82% MeCN/H_2O, 0.1% FA, over 17 min at 25°C. Analytical RP-HPLC was performed using a Waters 2695 Symmetry® C18 column (3.9 x 150 mm, 5 μm particle size) using a linear binary gradient, 20-80% or 2-82% MeCN/H_2O, 0.1% FA, over 17 min at 25°C, with a 1 mL/min flow rate and detection at 220 nm and 260 nm. Samples collected after purification were lyophilized to a white solid and re-dissolved in 50:50 v/v H_2O:MeOH to confirm purity and identity by LCMS analyses.

Circular Dichroism (CD) Spectroscopy:

Samples were prepared 12-16 hr ahead of time in H_2O:TFE (50:50, v/v, 1 mL) and stored at 5 °C. CD spectra were collected as an average of 3 scans on an Aviv Circular Dichroism (CD) spectrophotometer (Model: 62A DS) from 190-260 nm, using 1 nm bandwidth and 0.5 min step size at 25 °C. Samples were blank corrected, the data was smoothed and converted to molar

ellipticity values from the equation $[\theta] = \theta/cl$, where θ is the molar ellipticity (mdeg), c is the molar concentration of the peptides (12.5 µM) and l is the path length of the cell (1 cm). The data was imported into Microsoft Excel and the CD spectra were plotted in terms of molar ellipticity *vs* wavelength.

UV/Vis Spectroscopy:

The final concentrations of the peptide solutions was determined by UV/Vis spectrophotometry at 214 nm (ε value of peptides and calculated from the equation:

$$\varepsilon_{214} = (\varepsilon_{peptidebond})(n_{peptidebonds}) + \Sigma\,(\varepsilon_{aminoacid(i)})(n_{aminoacid(i)}).$$

The analyses were conducted on an 8452A Diode Array Spectrophotometer from Hewlett Packard, with wavelength range set from 190 – 600 nm with maximum absorption collected at 220 and 260 nm in addition to 490 nm for the FITC-labeled peptides. Peptide concentrations were standardized at 12.5 µM.

Log P values were measured via octanol partitioning by a modification of the shake-flask method. An aliquot (200 µL, 0.16 mM) of the FITC-labeled peptide samples in Tris buffer (10 mM, pH 7.4) and 1-octanol (200 µL) were added to a 0.5 mL micro tube. Samples were vortexed (1 min) and centrifuged. An aliquot of each layer (150 µL) was removed and diluted (850 µL, 3:1 v/v methanol:Tris or methanol:octanol) to a final composition of 3:1:1 v/v/v methanol:octanol:Tris buffer. The aqueous layer was diluted (30 µM) and a series of three serial dilutions were prepared for each phase. The log of the partition coefficient (FITC$_{490nm}$ of the organic layer *vs.* FITC$_{490nm}$ of the aqueous layer) yielded log P values according to UV absorption measurements made at 490 nm. For compounds with very low lipophilicity (log P $\leq$ 2.3), the volume of the octanol and water was increased from (100 to 125 µL), and the absorbance of the octanol layer was measured without

any additional dilutions. This procedure was repeated a minimum of three times per sample to calculate the mean log P and standard error. All absorbance measurements used were within the linear range of the instrument and blank corrected with Tris buffer and distilled water.

Dynamic Light Scattering (DLS):

DLS measurements were performed on Malvern Zetasizer (Malvern Instruments Limited ZEN3600). All samples were diluted with pico pure water by ratio of 1:1, 1:4, 1:8, and 1:16. Samples were sonicated for 15 minutes before measurement. Results were chosen from the major population of the highest quality measurement.

Transmission Electron Microscopy (TEM):

Dilute samples used for DLS measurements were mixed in a 1:1 ratio with 1% uranyl acetate, sonicated for 10 minutes. An aliquot (5 µL) was put on a carbon film coated copper grid, 300 mesh (electron microscopy sciences, Hatfield, PA) and the excess solution was removed immediately using absorbent paper. The grids were dried overnight and viewed under the transmission electron microscope (JEOL, model JEM-1200 EX). Images were taken with a SIA–L3C CCD camera (Scientific Instruments and Applications, Inc.) using the software Maxim DL5 (Diffraction Limited, Ottawa, Canada).

Cell Viability:

NCI 60 testing is performed in two parts: first a single concentration is tested in all 60 cell lines at a single dose of about 10^{-5} molar or 15 µg/ml. If the results obtained meet the selection criteria, then the compound is tested again in all 60 cell lines in 5 x 10 fold dilutions with the top dose being about 10^{-4} molar or 150 µg/ml.

Concentration Requirements – 1-dose/cancer in vitro program

Peptide samples were prepared in DMSO:glycerol 9:1 v/v at a concentration of about 4 mM for the one dose assay and about 40 mM for the 5-dose assay. In both cases the solution is diluted 1:400, giving a High Test concentration of about 10 or 100 µM, respectively.

Volume requirements – Pre-screen/cancer in vitro program

The cancer screen requires 100 µL for 1 log, 5-dose dilutions of regular compounds and 75 µL for 1-dose testing. 1-dose testing is done at 1/10th the high concentration of 5-dose testing, so the volume requirement is 210 µl + 20% at 40 mM for compounds with molecular weights or 210 µL + 20% at 60,000 µg/ml = 250 µL for compounds without molecular weights (macromolecules) (i.e. less than 10 mg for MW = 1000 or 15 mg for compounds tested as weight/volume).

For 1-dose 60 cell testing: On the day of or the day before drug addition to growing cells in tissue culture, a strip of standards (Adriamycin, NSC 123127 prepared and stored the same as the compounds) is added to the detachable well plate, and 90 µL DMSO is added to each well (4 mM solution), and mixed/sonicated and 75 µL is transferred, using a 12 channel hand pipettor, to a 12 channel reservoir plates (column plates), which is sealed and stored under nitrogen in a desiccator box until delivered to the testing lab. The labels are placed at the right and the left of the front of the reservoir plate. It will be the first and the last NSC number in the row. Rows are transferred from detachable plate to columns 3-12 of column plates. Plates are sealed and stored under nitrogen no more than 24 hours prior to drug addiction.

Interpretation of One-Dose Data

The one-dose data will be reported as a mean graph of the percent growth of treated cells and will be similar in appearance to mean graphs from the 5-dose assay. The number reported for

the one-dose assay is growth relative to the no-drug control, and relative to the time zero number of cells. This allows detection of both growth inhibition (values between 0 and 100) and lethality (values less than 0). This is the same as for the 5-dose assay, described below. For example, a value of 100 means no growth inhibition. A value of 40 would mean 60% growth inhibition. A value of 0 means no net growth over the course of the experiment. A value of -40 would mean 40% lethality. A value of -100 means all cells are dead. Information from the one-dose mean graph is available for COMPARE analysis.

2.8 REFERENCES

1. Javadpour, M. M.; Juban, M. M.; Lo, W. C.; Bishop, S. M.; Alberty, J. B.; Cowell, S. M.; Becker, C. L.; McLaughlin, M. L. *J. Med. Chem.* **1996**, *39*, 3107.

2. Glukhov, E.; Stark, M.; Burrows, L. L.; Deber, C. M. *J. Biol. Chem.* **2005**, *280*, 33960.

3. McGrath, D. M.; Barbu, E. M.; Driessen, W. H.; Lasco, T. M.; Tarrand, J. J.; Okhuysen, P. C.; Kontoyiannis, D. P.; Sidman, R. L.; Pasqualini, R.; Arap, W. Proc. *Natl. Acad. Sci. USA,* **2013**, *110*, 3477.

4. Costantini, P.; Jacotot, E.; Decaudin, D.; Kroemer, G. *J. Natl Cancer Inst.* **2000**, *92*, 1042.

5. Horton, K. L.; Kelley, S. O. *J. Med. Chem.* **2009**, *52*, 3293.

6. Ellerby, H. M.; Arap, W.; Ellerby, L. M.; Kain, R.; Andrusiak, R.; Rio, G. D.; Krajewski, S.; Lombardo, C. R.; Rao, R.; Ruoslahti, E.; Bredesen, D. E.; Pasqualini, R. *Nat. Med.* **1999**, *5*, 1032.

7. Liu, Y.; Steiniger, S. C.; Kim, Y.; Kaufmann, G. F.; Felding-Habermann, B.; Janda, K. D. *Mol. Pharm.* **2007**, *4*, 435.

8. Mai, J. C.; Mi, Z.; Kim, S. H.; Ng, B.; Robbins, P. D. *Cancer Res.* **2001**, *61*, 7709.

9. Marks, A. J.; Cooper, M. S.; Anderson, R. J.; Orchard, K. H.; Hale, G.; North, J. M.; Ganeshaguru, K.; Steele, A. J.; Mehta, A. B.; Lowdell, M. W.; Wickremasinghe, R. G. *Cancer Res.* **2005**, *65*, 2373.

10. Law, B.; Quinti, L.; Choi, Y.; Weissleder, R.; Tung, C. H. *Mol. Cancer Ther*, **2006**, *5,* 1944-9.

11. Zurita, A. J.; Troncoso, P.; Cardó-Vila, M.; Logothetis, C. J.; Pasqualini, R.; Arap, W. *Cancer Res.* **2004**, *64*, 435.

12. Rege, K.; Patel, S. J.; Megeed, Z.; Yarmush, M. L. *Cancer Res.* **2007**, *67*, 6368.

13. Cai, H.; Yang, H.; Xiang, B.; Li, S.; Liu, S.; Wan, L.; Zhang, J.; Li, Y.; Cheng, J.; Lu, X. *Mol. Pharm.* **2010**, *7*, 586.

14. Agemy, L.; Friedmann-Morvinski, D.; Kotamraju, V. R.; Roth, L.; Sugahara, K. N.; Girard, O. M.; Mattrey, R. F.; Verma, I. M.; Ruoslahti, E. *Proc. Natl. Acad. Sci. USA* **2011**, *108*, 17450.

15. Simeone, L.; Irace, C.; Di Pascale, A.; Ciccarelli, D.; D'Errico, G.; Montesarchio, D. Eur. J. *Med. Chem.* **2012**, *57*, 429.

16. Arigon, J.; Prata, C. A.; Grinstaff, M. W.; Barthélémy, P. *Bioconjug. Chem.* **2005**, *16*, 864.

17. Patil, S. P.; Yi, J. W.; Bang, E. K.; Jeon, E. M.; Kim, B. H. *Med. Chem. Commun*. **2011**, *2*, 505.

18. Yang, H. W.; Yi, J. W.; Bang, E. K.; Jeon, E. M.; Kim, B. H. *Org. Biomol. Chem.* **2011**, *9*, 291.

19. Ceballos, C.; Prata, C. A. H.; Giorgio, S.; Garzino, F.; Payet, D.; Barthélémy, P.; Grinstaff, M.; Camplo, M. *Bioconjug. Chem*. **2009**, *20*, 193.

20. Patel, P.; Hanawa, E.; Yadav, R.; Samuni, U.; Marzabadi, C.; Sabatino, D. *Bioorg. Med. Chem. Lett.* **2013**, *23*, 5086.

21. Hart, P. A.; Davis, J. P. *J. Am. Chem. Soc*. **1969**, *91*, 512.

22. Chantell, C. A.; Onaiyekan, M. A.; Menakuru, M. *J. Pept. Sci*. **2012**, *18*, 88.

23. Jullian, M.; Hernandez, A.; Maurras, A.; Puget, K.; Amblard, M.; Martinez, J.; Subra, G. *Tetrahedron Lett*. **2009**, *50*, 260.

24. Diaz-Mochon, J. J.; Bialy, L.; Bradley, M. *Org. Lett*. **2004**, *6*, 1127.

25. Avrahami, D.; Oren, Z.; Shai, Y. *Biochemistry*, **2001**, *40*, 12591.

26. Ozdirekcan, S.; Nyholm, T. K.; Raja, M.; Rijkers, D. T.; Liskamp, R. M.; Killian, *J. A. Biophys. J.* 2008, **94**, *1315*.

27. Epand, R.; Shai, Y.; Segrest, J. P.; Anantharamaiah, G. M. *Pept. Sci*. **1995**, *37*, 319.

28. Standley, S.M.; Toft, D.J.; Cheng, H.; Soukasene, S.; Chen, J.; Raja, S.M.; Stupp, S.I. *Cancer Res.*, **2010**, *70*, 3020.

29. Shoemaker, R.H. *Nat. Rev. Cancer* **2006***, 6*, 813-823.

30. Jiang, L.; Li, L.; He, X.; Yi, Q.; He, B.; Cao, J.; Pan, W.; Gu, Z. *Biomaterials*. **2015**, *52*, 126.

CHAPTER 3: DIVERSITY ORIENTED SYNTHESIS OF KILLER PEPTIDE NUCLEOLIPID BIOCONJUGATES AND THEIR STRUCTURE-ACTIVITY RELATIONSHIP STUDIES

3.1 GENERAL INTRODUCTION

Nucleolipid bioconjugates have a wide range of applications including gene therapy, medicinal chemistry and for the formulation of biomaterials for the development of biotechnologies [1,2]. Their exceptional utility stems from an amphiphilic structure which facilitates self-assembly into supramolecular nanoparticle formulations in aqueous and organic solutions [3]. The structural features of nucleolipid bioconjugates includes a nucleoside core that may participate in H-bonding interactions and hydrophobic lipid appendages which may facilitate self-assembly through non-polar interactions. Moreover, nucleolipids may be functionalized with reactive functional groups, including carboxylic acids that may participate in amide couplings, azide and alkynes that can be used for dipolar cycloaddition chemistry in addition to the incorporation of a wide range of electrophiles that may be prone towards nucleophilic substitution or cross coupling reactions.

For example, an amino acyl nucleolipid was synthesized following an optimized EEDQ-coupling strategy in which a reactive 5'-carboxy derived guanosine derivative was effectively coupled to Lys(Boc)CO$_2$Me [4]. The subsequent deblocking of the 2' and 3'-CBz protecting groups by hydrogenolysis followed by esterification of the 2' and 3'-OH groups with palmitoyl chloride afforded the aminoacylnucleolipid. The side-chain Lys(Boc) protecting group was removed using acidic conditions to afford a partially protected cationic aminoacyl nucleolipid that showed the ability to bind to GRP78 DNA and elicit selective and potent cell death (>90%) in a SR leukemia cell line at 10 μM [4]. The free-form guanosine aminoacyl nucleoplipids retain the

ability to form stable G-tetraplexes in solution [5], while chelating with Li^+ and K^+ metal ions. Interestingly, the self-assembled amphiphiles also produced H^+/OH^- ion flux in the presence of a pH gradient making them potentially useful transporter ligands [5]. In anti-proliferative assays in a selected panel of cancer cell lines, the nucleolipids showed modest activities (IC_{50}: 17 - $>10^3$ µM) in the MCF-7 breast cancer cells [5]. Similarly, a cationic aminoacyl surfactant was formed through a multi-step synthesis strategy, ultimately featuring Mitsonoubu chemistry which yielded the reactive 3'-azido xylouracil derivative which was subsequently reduced to the free amino and coupled to *N*-Boc-Pro using carbodiimide coupling conditions [6]. Carbodiimide couplings were also used to functionalize the 2'-OH with oleic acid and the 5'-OH with a poly(ethylene) glycol chain. The deprotection of the Boc group yielded a cationic amphiphile which formed micelles in water and produced weak activities (IC_{50}: 19 – 98 µM) relative to the control cetyl triethylammonium bromide (CTAB) in a panel of human, rat and murine cell lines [6]. The biological activity of the aminoacyl nucleolipid, was found to occur at concentrations nearing its critical micelle concentration (cmc: 40 µM), underscoring the importance of a self-assembled nanoparticle formulation for biological activity. Moreover, nucleolipid bioconjugates have been used in gene delivery applications [7,8]. For example, synthetic polycationic nucleolipids generated by carbonyldiimidazole couplings have been combined siRNA for the formation of stable ionic complexes that facilitated delivery and release of siRNA within HeLa cells for Vasuclar Endothelial Growth Factor (VEGF) knockdown [7]. The spermine derived amino acyl nucleolipid was found to effectively transfect siRNA (>90% VEGF knockdown) which ultimately led to apoptosis (~20%) in HeLa cells. The arginine-linked nucleolipid synthesized from a 1,3-dipolar cycloaddition formed stable ionic complexes with anti-VEGF siRNA resulting in potent VEGF knockdown (>90%) which paralleled the Lipofectamine-based siRNA transfections in

HeLa cells [8]. The glycosyl nucleolipids have also formed an interesting class of amphiphiles. In a relevant study, a glycosyl nucleolipid was synthesized by the Huisgen copper catalyzed azide-alkyne 1,3-dipolar cyloaddition reaction which also facilitated the incorporation of alkyne-derived fatty alcohols, steroids, terpenoids, fatty esters, amides and fluorinated amides [9]. The glycosyl nucleolipids exhibited complementary H-bonding, π-π stacking and hydrophobic interactions which contributed to their cytotoxicities (>70%) even after 72 h incubation with the human hepatocarcinoma (Huh-7) cell line. Interestingly, the amphiphiles formed hydrogels with distinctive supramolecular self-assemblies, including nanofibers, spheres and semitubular objects that were speculated to contribute to their cytotoxicities. Therefore, functionally diverse nucleolipids have shown the ability to self-assemble into amphiphilic supramolecular structures that were found to be contributive to their anti-cancer activities.

Additional nucleolipids containing various modifications are represented in **Figure 3.1**. The nucleotide-based amphiphiles (**3.1**) were formed from an extension of phosphoramidite chemistry, by tetrazole-mediated couplings with fatty long chain alcohols [10]. The resulting amphiphiles displayed the capabilities of forming lamellar-type structures held together by H-bonding interactions as discerned from FT-IR spectroscopy and X-ray diffraction studies. In a related example, uridine phosphocholine-based amphiphiles were prepared with myristic, palmitic, stearic, arachidic and oleic acids, **3.2** [11]. TEM imaging revealed the formation of small, unilamellar vesicles and nanofibers capable of entrapping DNA for potential gene delivery applications. More specifically, a uridine based nucleolipid, **3.3**, was prepared via a synthetic strategy featuring nucleophilic displacement of a reactive 5'-tosylate with trimethylamine to form the quaternary ammonium tosylate salt. At the 2' and 3'-OH groups, carbodiimide couplings installed the dioleolyl groups. The cationic nucleolipid formed worm-like structures in aqueous

solution and formed multilamellar structures with calf thymus DNA, which was found to be intercalated in between the lipid bilayers [12]. In a similar application, a phosphocholine nucleolipid, **3.4**, was synthesized in a 4-step procedure and was found to effectively form vesicles with plasmid DNA [13]. The ability for cationic amphiphilic nucleolipids to readily condense nucleic acids into stable nanoparticle formulations paves the way for gene delivery applications in gene therapy, biotechnology and in molecular cell biology.
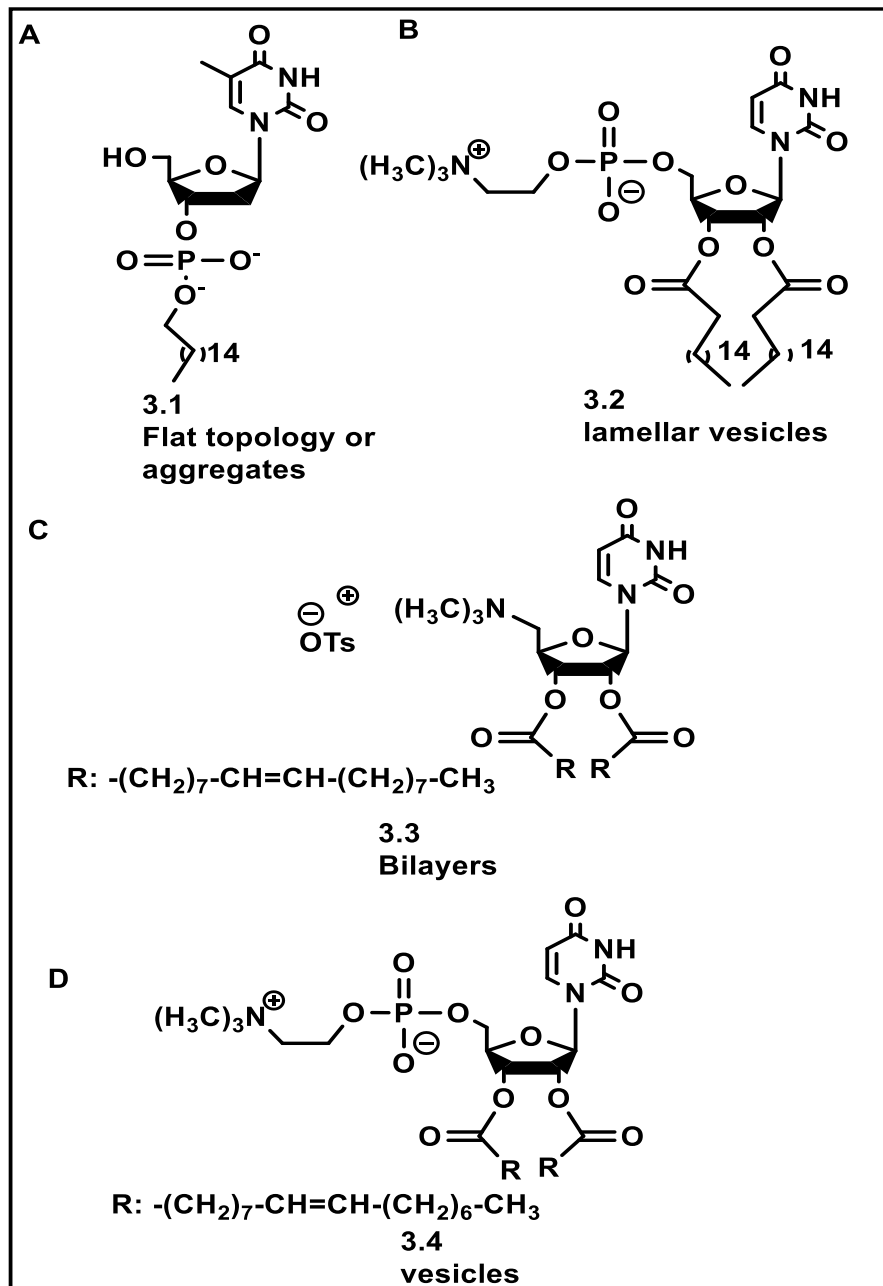
Figure 3.1. Synthetic nucleolipids scaffolds (A) deoxythymidine palmitoylphosphate [10] (B) 1,2-dipalmitoyluridinophosphocholine (DPUPC) [11] (C) (*N*-[5',(2',3'-dioleoyl)uridine-*N',N',N'*-trimethylammonium tosylate (DOTAU) [12] (D) *O*-ethyl-dioleylphosphatidylcholinium-uridine (*O*-ethyl-DOUPC) [13].

The nucleolipids are based on non-ionic, zwitterionic, and ionic structures that are adaptive towards self-assembly and nanoparticle formulation. The alkylamine hydrophobic chain was also found to play an important role in the self-assembly process. It provided hydrophobic character to the amphiphile that resulted in the self-assembly of topologically defined structures (**Figure 3.2**). Cryo-TEM reveals high resolution imaging of phospholipid nucleosides, including the self-assembly of polydisperse wormlike micelles for 1,2-dilauroyl-*sn*-glycerophosphatidyluridine (DLPU) in aqueous solution (**Figure 3.2 A**) [18]. Spontaneous formation of helical structures has also been observed for dimyristoyl-5'-phosphatidyldeoxycytidine (DMPcyt) (**Figure 3.2 B**). The electron micrograph of the super helical strands served as proof of self-assembly and formulation into discrete, well-defined structures [19]. Related examples include, a palmitoyl phosphate nucleolipid, which was found to self-assemble into flat and aggregated motifs, the choline-based nucleolipids produced quasi-spherical micelles, whereas the 5'-substituted nucleolipids produced micelles, flexible cylindrical aggregates and bilayers based on alkylamine chain length. Short chain alkylamines (e.g. $(CH_2)_6$ to $(CH_2)_9$) formed quasi-spherical micelles and long chain alkylamine (e.g. $(CH_2)_{10}$ to $(CH_2)_{20}$) nucleolipids formed flat structures [14-19]. These examples serve to illustrate the functionally diverse nature of amphiphilic nucleolipids. Synthetic methods have not only facilitated their production but also improved their applications. As such, nucleolipid bioconjugates form an interesting class of amphiphiles that retain the ability to self-assemble into well-defined high-order nanostructure formulations for a wide range of applications. These include but are not limited to their use as responsive biomaterials, as diagnostic and therapeutic probes.
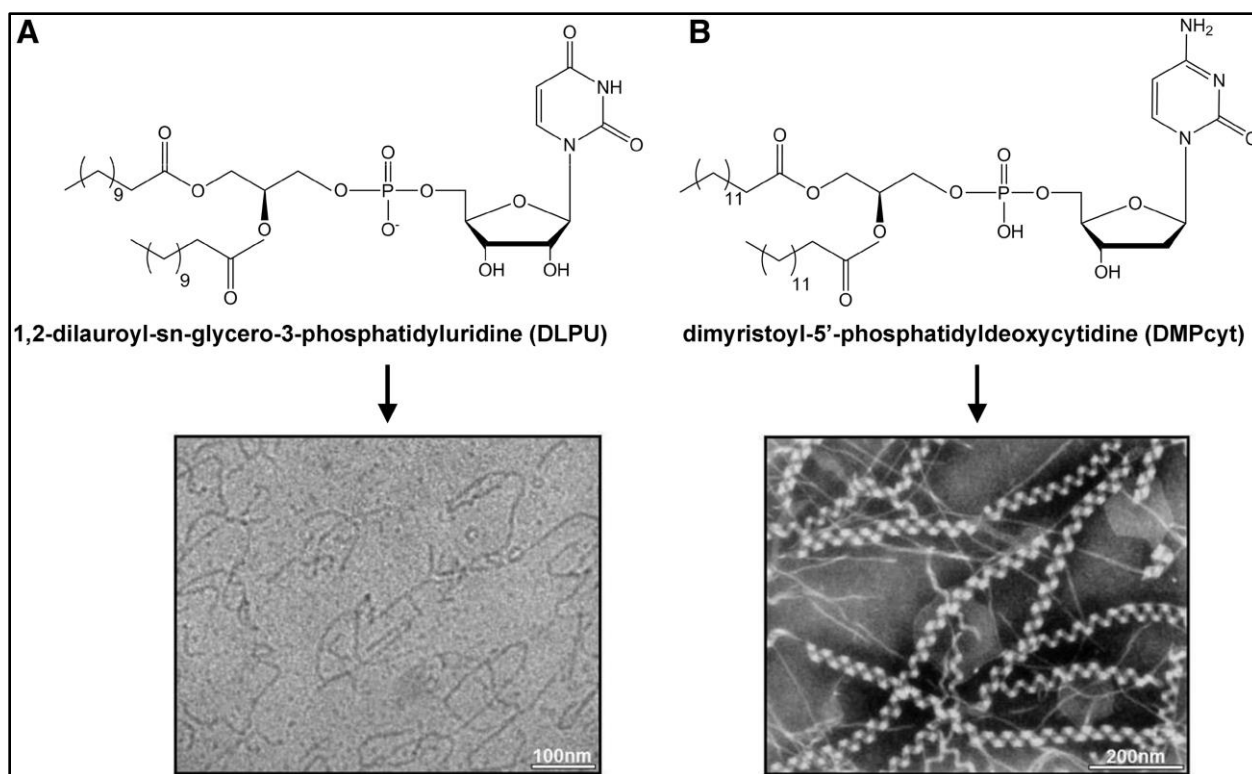
Figure 3.2. Phospholipid-nucleolipid self-assembly into higher-ordered nanostructures. TEM images adapted from Allain, V.; Bourgaux, C.; Couvreur, P. *Nucleic Acids Res.* **2012**, *40*, 1891-1903.

3.2 CHAPTER OBJECTIVES

The synthesis, characterization and anti-cancer activity of a new class of killer peptide bioconjugates was reported in Chapter 2. The nucleolipid derived D-(KLAKLAK)$_2$-AK sequence retained an amphiphilic, α-helical structure which displayed greater anti-proliferative effects in a selective panel of NSCLC when compared to the palmitamide derived peptide and the wild type sequence. In the search for more potent peptide-based anti-cancer conjugates the development of new and improved nucleolipid derived D-(KLAKLAK)$_2$-AK sequences are desired. Towards this goal, this chapter describes the diversity oriented synthesis of new peptide-nucleolipid conjugates

for structure-activity relationship studies (SARs) against cellular tumor targets. Considering a reductive amination approach was successfully developed for the synthesis of a hecadecylamine-derived nucleolipid-peptide conjugate, this approach may be perfectly suitable for the incorporation of various small, medium, large chain alkylamine, diamines, unsaturated amines or polyamines for exploring SARs. More specifically, these modifications are expected to fine tune the amphiphilic poly(cationic) α-helical properties of the peptide nucleolipids. These requirements are anticipated to improve binding and permeability across the lipid bilayer of malignant tumor types. These characteristics are also anticipated to improve peptide accumulation at the mitochondria that results in the dissipation of charge, the disruption of organelle integrity and the release of pro-apoptotic executors that effect cancer cell death. The proposed mechanism of action is described in **Figure 3.3**.
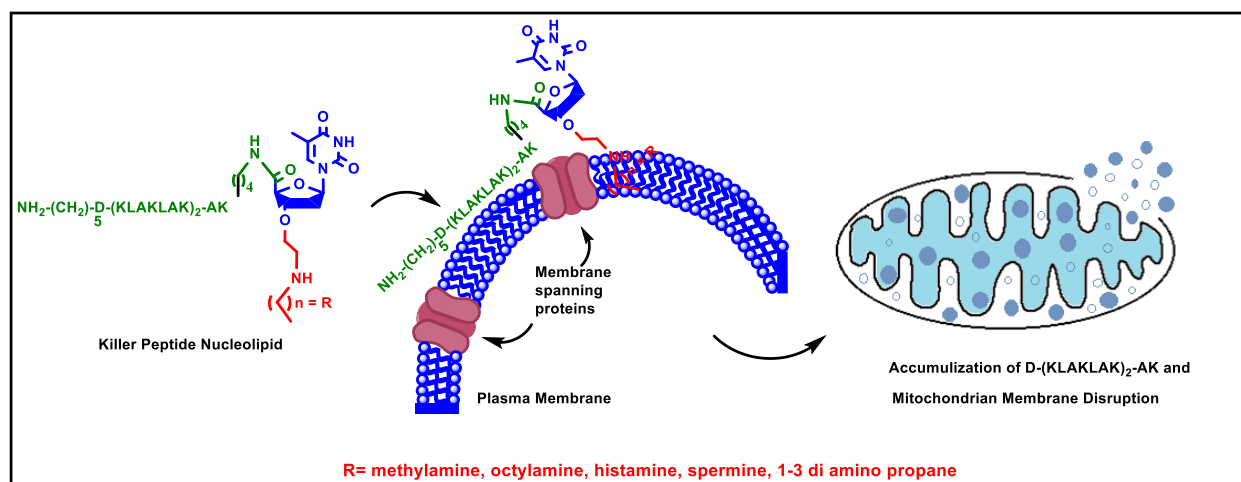
Figure 3.3. Proposed mechanism of action for the peptide nucleolipid bioconjugates.

The judicious selection of different alkyl amines, including methylamine and octylamine was based on their capabilities to fine tune peptide hydrophobicity and to provide a comparative study investigating the influence of alkyl chain length on peptide structure, biophysical and

biological properties. Moreover, histamine modifications have also been incorporated for boosting immune responses while acting as neurotransmitters by binding to the G-protein coupled histamine receptor [14-16]. Thus, histamine derived peptide nucleolipids are expected to trigger multiple biological responses in live cancer cells. Polyamines such as 1,3-diamino propane and spermine are expected to generate poly(cationic) nucleolipids at physiological pH. This feature is not only expected to facilitate peptide internalization and mitochondria localization but also in the delivery of poly(anionic) cargo, such as in the delivery of siRNA for RNAi applications. Thus, this chapter describes the diversity oriented synthesis strategy for the development of functionally diverse carboxy-derived nucleolipids that may then be combined with the killer peptide sequence by our well-established solid-phase bioconjugation approach. Peptide nucleolipid bioconjugates will be analyzed and purified by LC/MS. Peptide biophysical studies will be determined by RP HPLC and UV-Vis spectroscopy while CD spectroscopy will shed insights on the structural properties of the bioconjugates. The anti-cancer screen of the bioconjugates will take place in collaboration with Hackensack University Medical Center, under the supervision of Dr. Robert Korngold. Mariana Phillips (PhD student in the Sabatino group located in the Department of Chemistry and Biochemistry) will conduct cell based cytotoxicity studies in the selected tumor cells in order to validate a lead peptide-nucleolipid bioconjugate. Taken altogether, these important SAR studies are not only pivotal to the identification of peptide-nucleolipid combinations that can effect potent cancer cell death, but also in the selection of a lead bioconjugate that can be functionalized with cancer-targeting ligands for the selective treatment of tumors. The latter is a focus of current and future studies aimed towards the development of selective and potent peptide anti-cancer drugs (Chapter 4).

3.3 SYNTHESIS AND CHARECTERIZATION OF PEPTIDE-NUCLEOLIPID BIOCONJUGATES.

3.3.1. RATIONAL DESIGN OF PEPTIDE-NUCLEOLIPID BIOCONJUGATES

The rational design of a library of peptide-nucleolipid bioconjugates was developed in this study (**Figure 3.4**). The nucleolipid scaffold was designed with diverse functional groups including alkylamines with varying chain lengths (e.g. methylamine, octylamine and hexadecylamine) to explore the influence of hydrophobicity on peptide structure and activity. Moreover, alkyl diamines and polyamines (e.g. diamino propane and spermine) were also included as functional groups that were anticipated to bear polycations at physiological pH. The latter encompasses an important requirement for cell permeability and mitochondrial localization that ultimately results in cellular cytotoxicity [20]. Furthermore, cyclic amines such as histamine were also included in our proposed design to fine-tune the amphiphilic nature of the nucleolipid while potentially triggering interesting biological activities inside cells [21]. The functionally diverse nucleolipids were also designed with a reactive 5'-carboxy group which would facilitate coupling to the ε-amino group of the *C*-terminal Lys within the D-(KLAKLAK)$_2$-AK sequence. At the *N*-terminus, the peptide sequence is lengthened by an aminohexanoic acid linker (AHx) which is necessary for the efficient incorporation of the fluorescein isothiocyanate (FITC) fluorescent tag for imaging biological activity inside cells [22]. In this manner, the newly designed D-(KLAKLAK)$_2$-AK nucleolipid bioconjugates (**Figure 3.4**) would serve to explore the influence of structurally diverse nucleolipids on the biological activity of the killer peptide sequence. These studies are not only important for determining structure-activity relationships but also in identifying a lead that can be further optimized into an anti-cancer therapeutic.
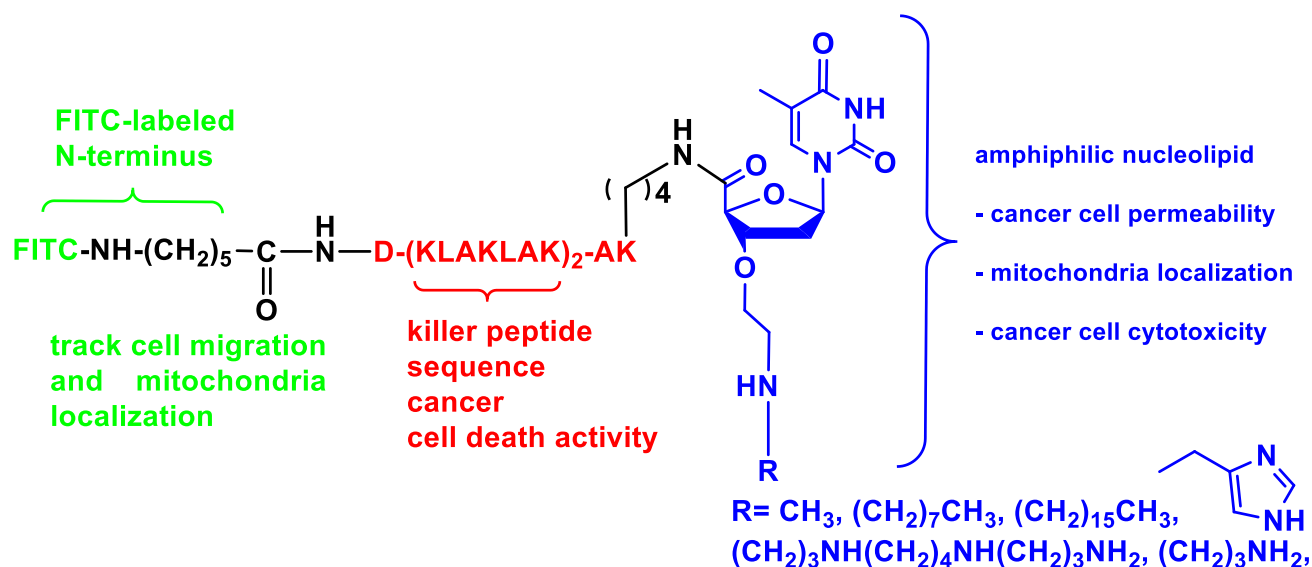
Figure 3.4. Design of killer peptide nucleolipid bioconjugates. Figure adapted from Rana, N., Huang, S.; Patel, P.; Samuni, U.; Sabatino, D. *Bioorg. Med. Chem. Lett.*, **2016**, *26*, 3567–3571.

3.3.2. DIVERSITY ORIENTED SYNTHEIS OF NUCLEOLPIDS

The 3'-aldehyde derived thymidine, **3.5**, was selected as the reactive precursor for the diversity oriented synthesis of functionally diverse nucleolipids (**Figure 3.5**). In this synthesis method, the reductive amination approach was optimized with functionally diverse amines for yielding nucleolipids **3.6**-**3.10**. The reductive amination with methylamine and octylamine proceeded smoothly according to TLC. However, difficulties associated with extraction and chromatographic purification limited yield recoveries. Nonetheless, the alkylamine-derived nucleolipids, **3.6**-**3.7**, were recovered in sufficient quantities (14-32% yields) for their conversion into the desired 5-carboxy derived nucleolipids as described in **Scheme 3.1**. The histamine, spermine and *N*-Boc diaminopropoane derived nucleolipids (**3.8**-**3.10**) proved more difficult to make. In these cases, the formation of side products, presumably due to the reactive amino

functionalities were detected by TLC and difficulties associated with recoveries following extraction and purification resulted in low yields (8-20%). The isolated products were analyzed and characterized by a combination of ^{1}H, ^{13}C NMR and mass spectrometry.
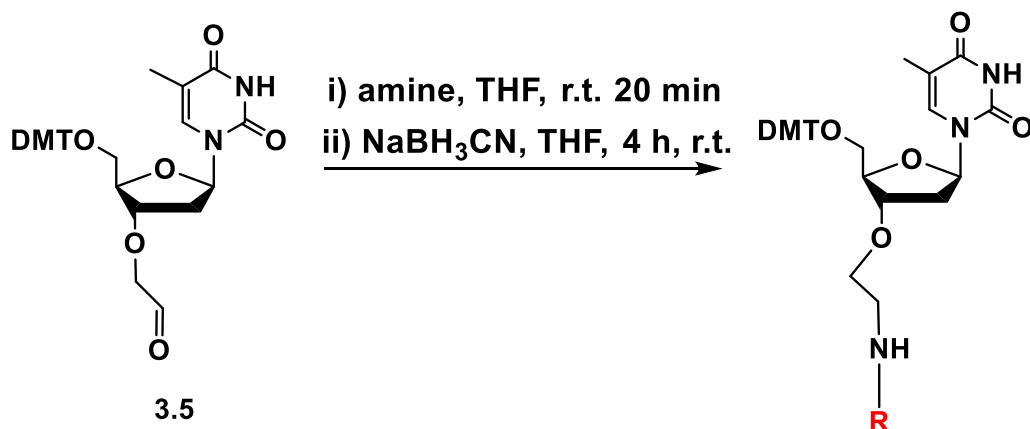
No.	Amine	R	%Yields
3.6	Methylamine	—CH$_3$	32
3.7	Octylamine	(CH$_2$)$_7$CH$_3$	14
3.8	Histamine	(imidazole ethyl)	8
3.9	Spermine	(spermine chain NH$_2$)	20
3.10	1-3, di-amino propane	(propyl)NHBoc	9

Figure 3.5. Diversity oriented synthesis of various nucleolipids by the reductive amination approach.

The diversity oriented synthesis strategy for the various nucleolipids developed in this study is based on the reductive amination approach which ultimately yielded the 5'-carboxy derived nucleolipids **3.16-3.20** (**Scheme 3.1**). Following quantitative removal of the 5'-DMT group using trichloroacetic acid (TCA), a TEMPO-mediated oxidation reaction converted the 5'-hydroxy group to the carboxylic acids, **3.16-3.20**. Each reaction intermediates and the final products were characterized by ^{1}H and ^{13}C NMR, IR spectroscopy and by MS to confirm purities and identities for the incorporation of the 5'-carboxy derived nucleolipids **3.16-3.20** within the killer D-(KLAKLAK)$_2$-AK sequence.
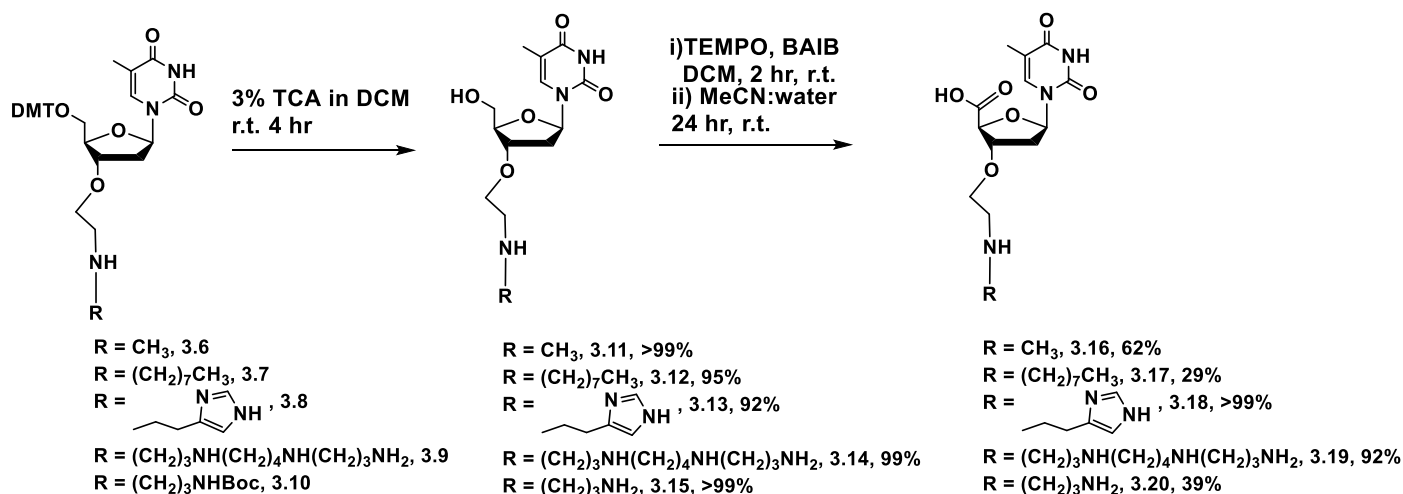
Scheme 3.1. Solution phase synthesis of the 5'-carboxy derived nucleolipids, **3.16-3.20**.

3.4 DESIGN, SOLID PHASE BIOCONJUGATION AND CHARACTERIZATION OF (FITC)-AHX-D-(KLAKLAK)₂-AK-NUCLEOLIPIDS

3.4.1. DESIGN OF NOVEL AHX-D-(KLAKLAK)₂-AK-NUCLEOLIPIDS

The novel peptide nucleolipids consist of trifunctional bioconjugates (**Figure 3.6**). They contain an *N*-terminal AHx-linked FITC fluorophore for fluorescent imaging and detection applications in live cancer cells. The D-(KLAKLAK)$_2$ peptide encompasses the killer peptide sequence while the *C*-terminal AK sequence contains a Lys(Dde) residue that can be removed under orthogonal deprotection conditions to reveal the reactive side chain amino group for bioconjugation. Solid phase bioconjugation of the support-bound D-(KLAKLAK)$_2$-AK sequence with the carboxy derived nucleolipids is anticipated to provide a small library of peptide-nucleolipid conjugates for exploring structure-activity relationships in cancer.
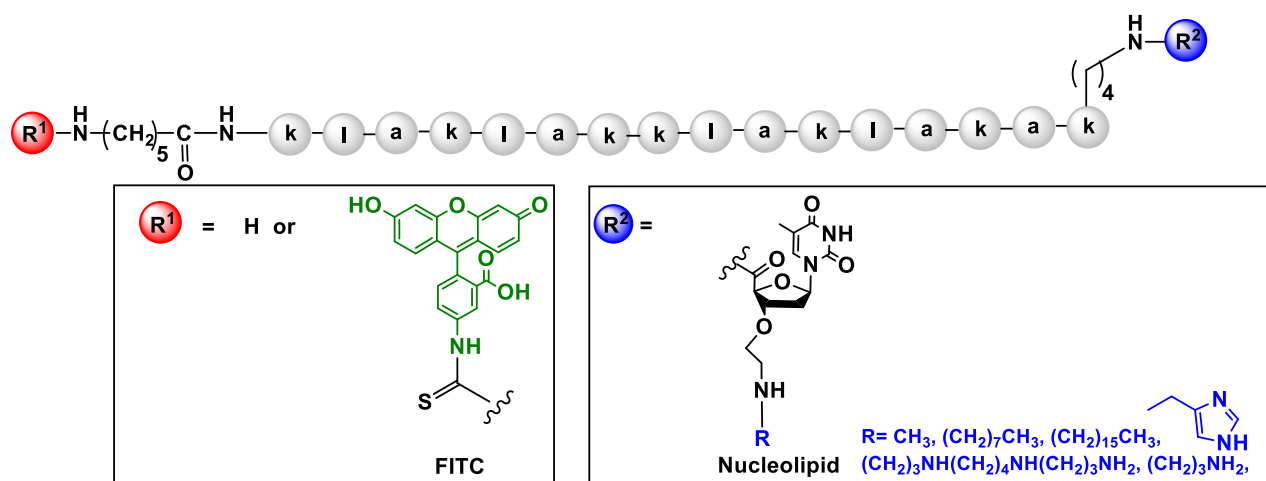
Figure 3.6. Peptide-nucleolipid structures. The D-(KLAKLAK)$_2$-AK peptide scaffold with R^1(red) = H or FITC, R^2(blue) = Nucleolipid where R = CH$_3$, (CH$_2$)$_7$CH$_3$, (CH$_2$)$_{15}$CH$_3$, (CH$_2$)$_3$NH(CH$_2$)$_4$NH(CH$_2$)$_3$NH$_2$, (CH$_2$)$_3$NH$_2$, and histamine. All amino acids are in their D-configuration.

3.4.2. SOLID PHASE BIOCONJUGATION

The solid phase bioconjugation approach has been developed to actively couple potent and reactive drug like molecules or biologicals onto the solid support e.g. resin, bead, or mica surface.

A suitable solid support was first selected based on sequence compatibility and synthetic efficiency. The poly(ethylene glycol) (PEG) based resins have proven to be especially useful in the synthesis of lengthy and hydrophobic peptides that have the tendency to aggregate during the solid phase synthesis procedure. The excellent swelling properties of PEG-based resins in organic solvents such as DMF and acids such TFA have been shown to improve synthetic efficiency and recoveries following solid phase peptide synthesis [24]. In our approach, the D-(KLAKLAK)$_2$-AK sequence was synthesized on the Rink amide PEG resin for generating C-terminal peptide amides. The C-terminal Lys residue contained the Dde protecting group that has been shown to orthogonally deblock using buffered hydroxylamine hydrochloride that promotes the transamination reaction of the support-bound peptide sequence [25]. In our approach, hydroxylamine hydrochloride was buffered and solubilized in imidazole and NMP/DMF, respectively, for selectively unmasking the Lys side chain Dde group. This reaction was closely monitored by LC-MS that produced 60-80% conversions on solid phase. An Fmoc protecting group at the N-terminus directed the coupling of the 5'-carboxy-derived nucleolipids at the C-terminus Lys side chain amino group. A HCTU-mediated coupling reaction (**Scheme 3.2**) was used to couple the nucleolipids to the support-bound peptide sequence. Following solid-phase bioconjugation, Fmoc deprotection using basic piperidine followed by FITC coupling at the N-terminal AHx linker produced the FITC-labeled peptide-nucleolipid bioconjugates on solid phase. Of note, peptide-nucleolipid bioconjugates were also produced without the FITC label. In these cases, a portion of the Fmoc-AHx-D-(KLAKLAK)$_2$-nucleolipid bound resin was Fmoc deblocked followed by cleavage and deprotection of the bioconjugate from solid phase. The TFA-mediated cleavage and deprotection conditions were also employed for isolating the FITC-labeled bioconjugates from solid phase. Control peptides with and without the FITC/nucleolipids were

also produced in order to determine the influence of the modifiers on peptide structure and biological activities. The isolated peptide-nucleolipid bioconjugates were analyzed and purified by RP HPLC (**Table 3.2**). The identities of the pure bioconjugates were confirmed by LC-MS for SAR studies.
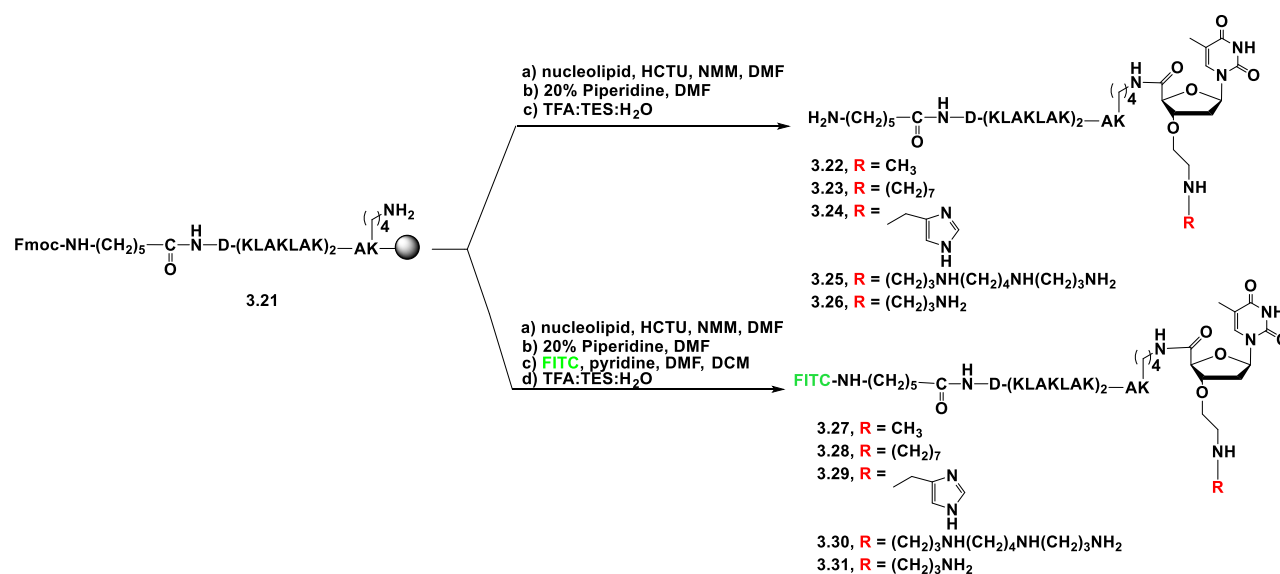
Scheme 3.2. Solid phase synthesis of FITC and non-FITC tagged D-(KLAKLAK)$_2$-AK with nucleolipids.

Entry	Sequence and Number	[a]Crude Purity(%)	[b]Isolated Purity(%)	[c]Isolated Yield(%/mg)	[d]M.W. (g/mol) Actual(e)	[e]Z	[f]RT (min) MeOH	[g]RT (min) MeCN
1	AHx-D-(KLAKLAKKLAKLAK)-AK-Methylamine nucleolipid, **3.22**	70	99	67/10	533.6 (533.1)	4	10.6	9.7
2	AHx-D-(KLAKLAKKLAKLAK)-AK-Octylamine nucleolipid, **3.23**	55	96	80/9	446.3 (446.7)	5	11.2	8.9
3	AHx-D-(KLAKLAKKLAKLAK)-AK-Histamine nucleolipid, **3.24**	78	95	79/12	386.0 (386.2)	6	9.3	5.7
4	AHx-D-(KLAKLAKKLAKLAK)-AK-Spermine nucleolipid, **3.25**	83	96	80/9	576.5 (576.2)	4	12.0	10.1
5	AHx-D-(KLAKLAKKLAKLAK)-AK-1,3-diaminopropane nucleolipid, **3.26**	90	97	54/7.5	544.4 (544.4)	4	11.9	7.4
6	FITC-AHx-D-(KLAKLAKKLAKLAK)-AK-Methylamine nucleolipid, **3.27**	85	>99	45/8	505.0 (505.7)	5	13.2	11.1
7	FITC-AHx-D-(KLAKLAKKLAKLAK)-AK-Octylamine nucleolipid, **3.28**	86	>99	60/9.5	524.8 (524.6)	5	15.0	12.3
8	FITC-AHx-D-(KLAKLAKKLAKLAK)-AK-Histamine nucleolipid, **3.29**	90	>99	71/6	521.8 (521.0)	5	12.3	12.0
9	FITC-AHx-D-(KLAKLAKKLAKLAK)-AK-Spermine nucleolipid, **3.30**	93	98	80/5.5	539.6 (539.2)	5	13.3	9.8
10	FITC-AHx-D-(KLAKLAKKLAKLAK)-AK-1,3-diaminopropane nucleolipid, **3.31**	75	>99	73/7.8	641.4 (641.8)	4	15.0	14.5

Table 3.2. Characterization data of peptide nucleolipid bioconjugates. [a]Crude purities by RP-HPLC at 220 nm. [b]Isolated purities by RP-HPLC at 220 nm using 2-80% MeOH/H_2O with 0.1% FA over 17 min. [c]Isolated yields based on the resin loading. [d]Observed mass (expected mass) as [M+H]+/Z as detected by LCMS. [e]Charged state of the peptides as detected by LCMS in positive

mode. [f]Retention times using 2-80% MeOH/ H$_2$O with 0.1% FA over 17 min. [g]Retention times using 2-80% MeCN/H$_2$O with 0.1% FA over 17 min.

3.4.3. CHARACTERIZATION OF PEPTIDE NUCLEOLIPID BIOCONJUGATES

The hydrophilicities of the peptide bioconjugates were confirmed by RP HPLC (**Figure 3.7**). In our analysis, the histamine-derived peptide nucleolipid bioconjugate (**3.24**) eluted fastest on the C18 RP HPLC column (rt: 9.3 min) during the acidic RP HPLC conditions (i.e. 2-80% MeOH/H$_2$O 0.1% FA). This result suggests that the heterocycle fine-tunes the amphiphilic nature of the nucleolipid. Furthermore, the ionizable imidazole is also anticipated to be protonated during the RP HPLC conditions further contributing to the polar, polycationic nature of the sequence. The polyamine derived peptide-nucleolipid bioconjugates (**3.25** and **3.26**) proved to be most hydrophobic and retained (rt: 12.0 min and 11.9 min, respectively) indicating that the lengthy, aliphatic hydrocarbon polyamine chain of the nucleolipid provided a more non-polar contribution to the bioconjugate. Presumably, this factor outweighs the polar contribution of the polycationic polyamine using the same eluent gradient conditions on the C18 RP column. The methyl- and octyl-amine derived peptide nucleolipids (**3.22,** 10.6 min and **3.23**, 11.2 min, respectively) were also found to be hydrophobic and retained sequences on the C18 RP column, albeit to a lesser extent when compared to the polyamine-derived nucleolipid bioconjugates (**3.25** and **3.26**). Taken together, the nucleolipids contribute variable effects on the polarity of the D-(KLAKLAK)$_2$-AK sequence that may influence their structure, formulation and biological activity in cell culture conditions.
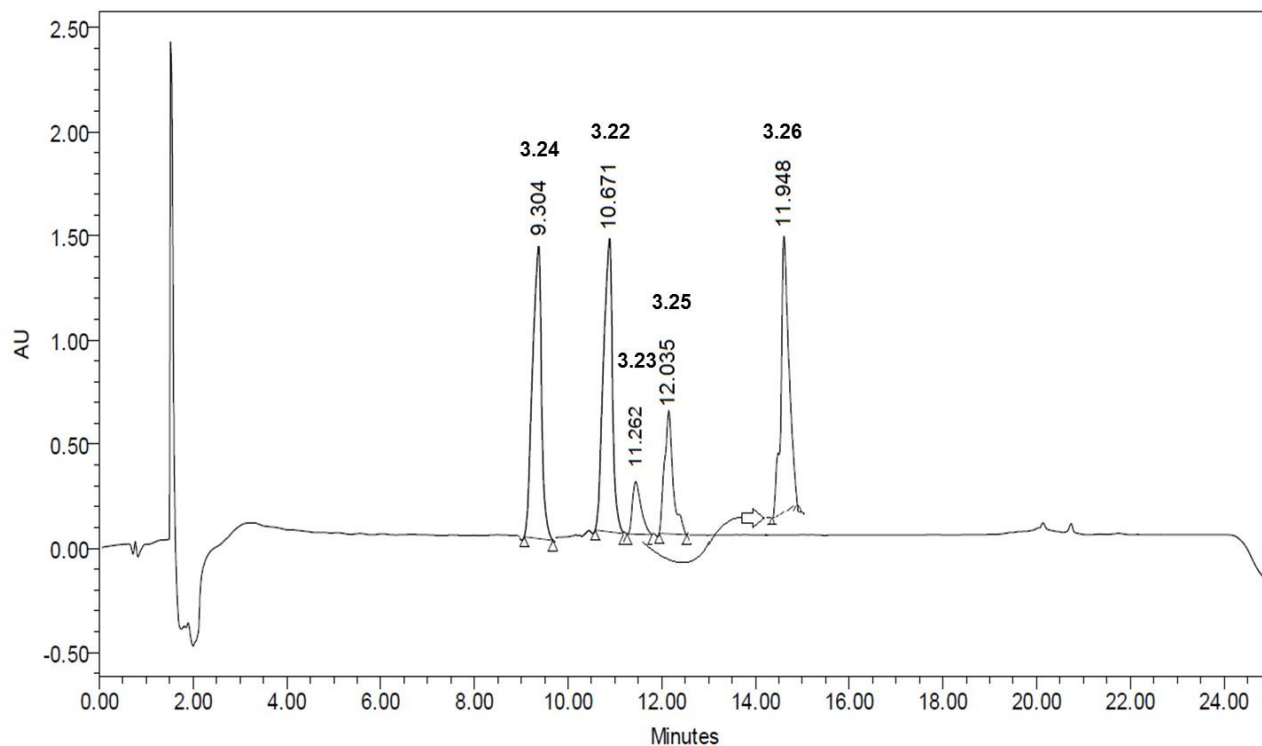
Figure 3.7. Comparative RP HPLC analysis of the nucleolipid-derived D-(KLAKLAK)$_2$-AK, bioconjugates (**3.22-3.26**).

Furthermore, UV-Vis spectroscopy confirmed the characteristic absorption bands of the peptide bonds ($\lambda_{max} \sim 220$ nm), thymine base ($\lambda_{max} \sim 260$ nm) and the FITC label ($\lambda_{max} \sim 450$ nm) corresponding to the nucleolipid-derived D-(KLAKLAK)$_2$-AK, bioconjugates (**Figure 3.8**).
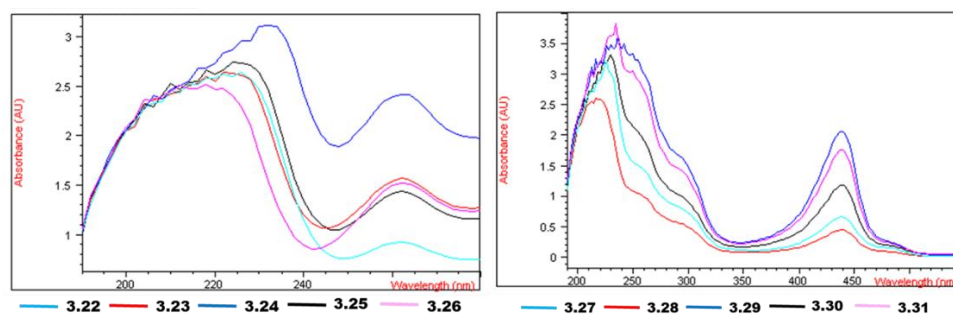
Figure 3.8. Comparative UV-Vis spectroscopy (190-310 nm) of the nucleolipid-derived D-(KLAKLAK)$_2$-AK, bioconjugates (**3.22-3.26**) and (**3.27-3.31**).

CD spectroscopy was then used to evaluate the secondary structures (if any) of the peptides in H_2O:TFE. The combination of H_2O:TFE has served to mimic the amphiphilic lipid bilayer microenvironment that may stabilize peptide secondary structures [26]. In this study, the methyl- and octyl-amine nucleolipid derived D-(KLAKLAK)$_2$-AK sequence, **3.22** and **3.23**, respectively, displayed stable, α-helical secondary structure (40-65% helicity), while the histamine nucleolipid derived D-(KLAKLAK)$_2$-AK, **3.24**, displayed enhanced helicity (65-76%) and the polyamine nucleolipid derived D-(KLAKLAK)$_2$-AK **3.25** and **3.26**, demonstrated a less stable (<40%) α -helical secondary structure (**Figure 3.9**). Many amphiphilic cell-penetrating peptides adopt α-helical secondary structures. This peptide motif may functions as a recognition site with other membrane spanning proteins facilitating cellular permeability [27].
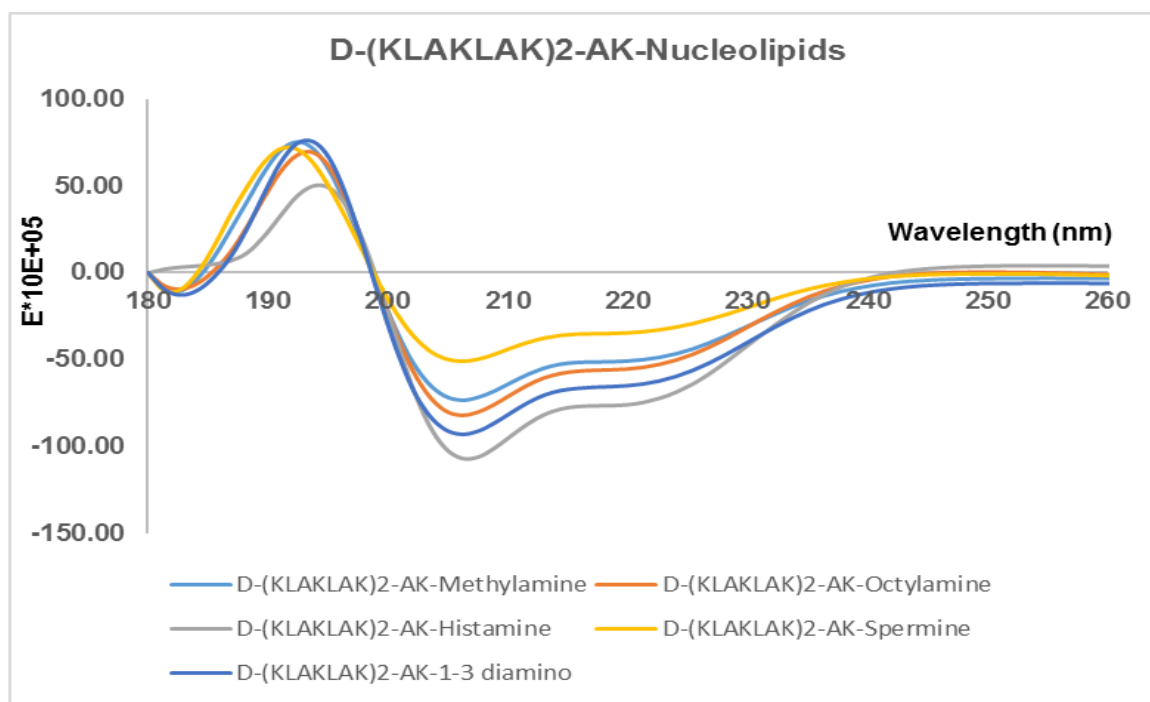
Figure 3.9. CD spectroscopy of the peptide-nucleolipid bioconjugates (**3.22**-**3.26**) in TFE:H_2O (1:1 v/v, 12.5 μM).

3.5. BIOLOGICAL ACTIVITIES OF THE NUCLEOLIPID-PEPTIDE BIOCONJUGATES

3.5.1. CYTOTOXICITIES IN MM1S MELANOMA CANCER CELLS

The cytotoxic activities of the nucleolipid-peptide bioconjugates (**3.22**-**3.26**) were evaluated within the MM.1S human multiple myeloma B cell lymphoblast culture, known to be a clinically relevant tumor model for evaluating the anti-cancer effects of new drug candidates [28]. The MM.1S cell culture and testing of the synthetic bioconjugates was accomplished by Mariana Phillips and Chris Cultrara, PhD students in the laboratory of Dr. David Sabatino (Department of Chemistry and Biochemistry, SHU). A Guava Nexin® Reagent (EMD Millipore) was used to assess early and late-stage apoptosis by flow cytometry [29]. In this assay, the MM.1S cells were incubated for 24 hours with the bioconjugates (**3.22-3.26**, 2.5 μM in PBS buffer). After incubation, the cells were centrifuged, washed and stained with the Guava Nexin® Reagent to determine the MM.1S cells' viability using flow cytometry. The results showed early and late stage apoptotic events for the MM.1S cells when treated with the histamine-derived nucleolipid-peptide bioconjugate **3.24**, (**Figure 3.10**) making it a lead for further biological evaluation. The remaining bioconjugates did not exhibit toxicity in this assay.
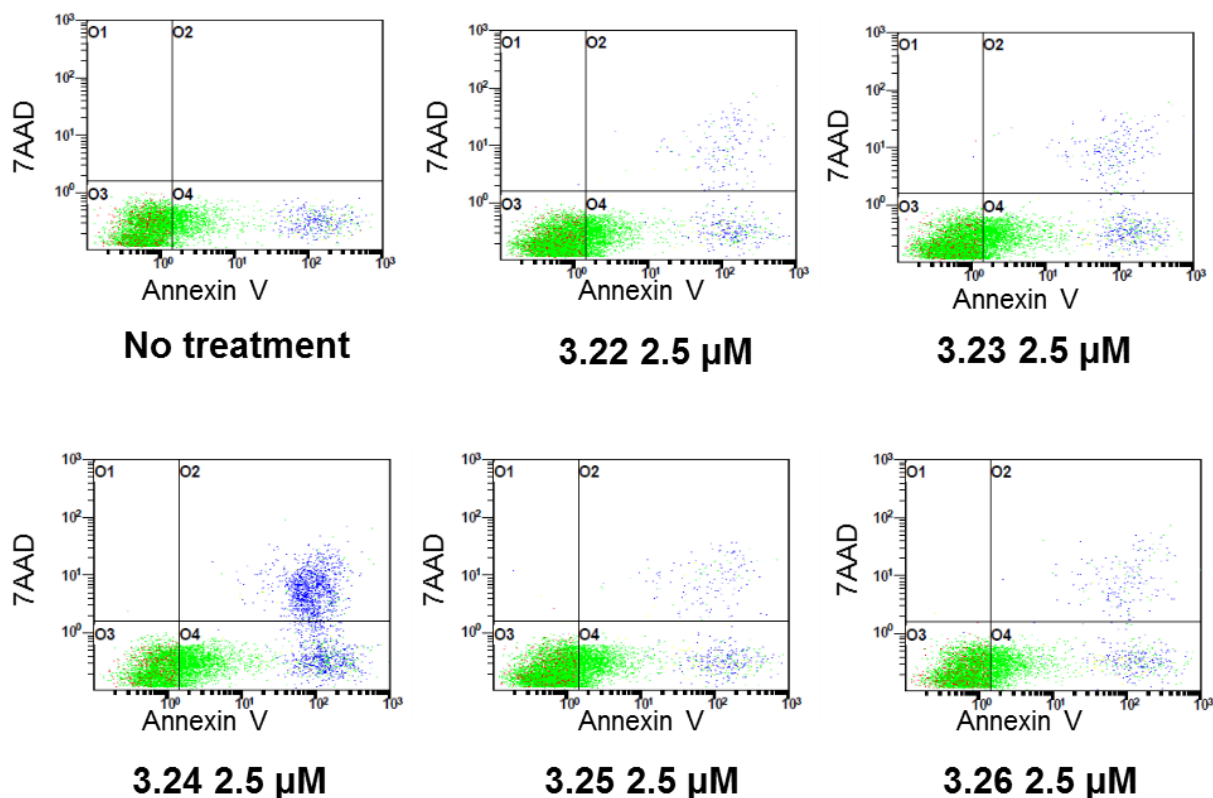
Figure 3.10. Peptide-nucleolipid bioconjugate effects on the MM1S cells' viability according to the Guava Nexin Reagent using flow cytometry.

3.6 CONCLUSIONS

In conclusion, a versatile diversity-oriented synthesis approach for the generation of a small library of novel peptide-nucleolipid bioconjugates is described in this chapter. The methodology underscores a flexible and adaptive reductive amination approach for installing a variety of alkyl, cyclic and polyamines into a nucleoside scaffold for formulating structurally diverse nucleolipids for exploring SAR studies. The nucleolipids were functionalized with a reactive 5'-carboxy group which facilitated bioconjugation on solid support with the cytotoxic D-(KLAKLAK)$_2$-AK sequence. The peptide-nucleolipid bioconjugates were found to exhibit tunable biophysical and structural properties that were influenced by the nature of the nucleolipid group. In general, the

bioconjugates maintained amphiphilic, α-helical characteristics which were anticipated to contribute to their biological activities in live cancer cells. A single dose (2.5 μM) screen against the MM.1S multiple myeloma cancer cells revealed a lead peptide that was contributive towards early and late stage apoptotic events. This lead potentially encompasses a new class of peptide-based anti-cancer drugs.

3.7. EXPERIMENTAL SECTION
3.7.1. SYNTHESIS

5'-*O*-(dimethoxytrityl) 3'-*O*-(methylaminoethyl) thymidine [3.6]: The starting material **3.5** (200 mg, 0.34 mmol) and methylamine (11.2 μL, 0.32 mmol) were dissolved in 3 mL of dry THF. The reaction was stirred for 20 min at room temperature and sodium cyanoborohydride (26 mg, 0.41 mmol, 1.2 equiv) was added to reaction mixture and stirred for 4.5 hrs. The reaction was then concentrated *in vacuo* and purified by flash column chromatography using EtOAc:Petroleum ether (9:1 v/v) to yield a white foamy product **3.6** in 32% yield. m.p. 60 °C. $[\alpha]_{589}^{22}$: +12.11 (c 0.01, DCM). $R_f = 0.60$ (EtOAc–petroleum ether, 9:1 v/v). IR (KBr) υ_{max} (cm^{-1}) = 5994.0, 5978.8, 5966.7, 5948.3, 5937.3, 5920.7, 5913.2, 5895.0, 5886.7, 5871.7, 5863.0, 5833.2, 5843.4, 5773.8, 5757.6, 5743.1, 5579.2, 5467.3, 5317.1, 5205.1, 5161.5, 5155.3, 5077.3, 5025.6, 4960.5, 3750.9, 3744.9, 3737.1, 3712.1, 2376.1, 2347.0, 1507.4, 1275.2, 764.2, 749.5. ^{1}H NMR (499.79 MHz, CD$_2$Cl$_2$): δ = 0.92 (t, *J* = 6.0 Hz, 3H), 1.34 (t, *J* = 12 Hz, 3H) , 1.50 (d, *J* = 12.0 Hz, 3H), 1.57 (s, 1H), 2.27 (m, 1H), 2.40 (t, *J* = 6.0 Hz, 1H), 2.78 (d, *J* = 8.0 Hz, 1H), 2.99 (m, 2H), 3.31 (m, 1H), 3.40 (d, *J* = 11 Hz, 1H), 3.61 (m, 1H), 3.70–3.81 (m, 8H), 4.10 (dd, *J* = 2, 14.5 Hz, 1H), 4.20 (d, *J* = 5.0 Hz, 1H), 6.24 (m, 1H), 6.86 (m, 4H), 7.24-7.33 (m, 7H), 7.41 (d, *J* = 10.0 Hz, 2H), 7.50 (m, 1H). ^{13}C NMR (125.68 MHz, CD$_2$Cl$_2$): δ = 11.6, 37.3, 63.5, 72.3, 80.9, 83.5, 84.6, 84.7, 87.0, 110.9,

111.2, 113.1, 113.3, 127.0, 128.0, 129.9, 130.0, 135.2, 135.2, 135.3, 135.5, 144.4, 144.5, 144.6, 150.3, 158.9, 163.4. ESI MS (m/z) calculated for $C_{34}H_{41}N_3O_7$ [M+H], 602.7; found 602.6.

5'-*O*-(dimethoxytrityl) 3'-*O*-(octylaminoethyl) thymidine [3.7]: The starting material **3.5** (200 mg, 0.340 mmol) and octylamine (54 µL, 0.323 mmol) were dissolved in 3 mL of dry THF. The reaction was stirred for 30 min at room temperature and sodium cyanoborohydride (26 mg, 0.409 mmol, 1.2 equiv) was added to reaction mixture and stirred for 4.5 hrs. The reaction was then concentrated *in vacuo* and purified by flash column chromatography using EtOAc:Petroleum ether (6:4 v/v) to yield a white foamy product **3.7** in 14% yield. m.p. 67 °C. $[\alpha]_{589}^{23.6}$: +38.04 (c 0.01, Acetone). R_f = 0.80 (EtOAc–petroleum ether, 6:4 v/v). IR (KBr) υ_{max} (cm^{-1}) = 2346.8, 1748.4, 1715.1, 1704.9, 1681.9, 1669.4, 1647.0, 1569.5, 1575.6, 1558.0, 1540.3, 1521.1, 1506.7, 1489.3, 1275.3, 1261.1, 764.2, 749.8. ^{1}H NMR (499.84 MHz, CD$_2$Cl$_2$): δ = 1.10 (t, J = 7.0 Hz, 3H), 1.32 (t, J = 10.5 Hz, 16H), 1.52 (d, J = 7.0 Hz, 3H), 1.50 (s, 1H), 2.21 (m, 1H), 2.42 (t, J = 7.0 Hz, 1H), 2.679 (d, J = 2.0 Hz, 1H), 3.00 (m, 2H), 3.33 (m, 1H), 3.42 (d, J = 7 Hz, 1H), 3.62 (m, 1H), 3.71–3.82 (m, 8H), 4.11 (dd, J = 2.0 Hz, 1H), 4.21 (d, J = 5.0 Hz, 1H), 6.29 (t, 1H), 6.90 (d, 4H), 7.22-7.32 (m, 7H), 7.53 (d, J = 10.0 Hz, 2H), 7.43 (s, 1H). ^{13}C NMR (125.6 MHz, CD$_2$Cl$_2$): δ =5.1, 7.7, 11.7, 21.9, 22.6, 25.7, 29.0, 31.6, 37.5, 47.0, 55.2, 62.4, 63.8, 72.2, 80.9, 92.4, 110.0, 111.1, 113.3, 128.0, 129.9, 132.2, 135.2, 143.0, 147.1, 150.2, 154.8, 158.8, 165.3, 178.7, 182.1, 217.6, 231.8. ESI MS (m/z) calculated for $C_{41}H_{54}N_3O_7$ [M+H], 699.8; found 699.9.

5'-*O*-(dimethoxytrityl) 3'-*O*-(histamineoethyl) thymidine [3.8]: The starting material **3.5** (200 mg, 0.340 mmol) and histamine (36 mg, 0.323 mmol) were dissolved in 3 mL of dry THF. The reaction was stirred for 20 min at room temperature and sodium cyanoborohydride (26 mg, 0.409 mmol, 1.2 equiv) was added to reaction mixture and stirred for 4 hrs. The reaction was then concentrated *in vacuo* and purified by flash column chromatography using EtOAc:Petroleum ether

(9:1 v/v) to yield a white foamy product **3.8** in 8% yield. m.p. 90 °C. $[\alpha]_{589}^{23.8}$: +204.4 (c 0.01, DCM). R_f = 0.75 (EtOAc–petroleum ether, 9:1 v/v). IR (KBr) υ_{max} (cm^{-1}) = 3492.2, 2347.5, 2174.8, 1733.8, 1677.5, 1658.7, 1641.8, 1631.3, 1557.4, 1540.8, 1502.6, 1440.0, 1391.0, 1251.7, 1178.4, 1104.9. ^{1}H NMR (499.9 MHz, CD$_2$Cl$_2$): δ = 1.0 (t, J = 4.0 Hz, 3H), 1.35 (m, 4H) , 1.50 (d, J = 12.0 Hz, 3H), 1.57 (s, 1H), 2.23 (m, 1H), 2.46 (t, J = 6.0 Hz, 1H), 2.84 (d, J = 7.9 Hz, 2H), 3.00 (m, 2H), 3.34 (m, 1H), 3.47 (d, J = 11 Hz, 1H), 3.65 (m, 1H), 3.75–3.81 (m, 6H), 4.11 (dd, J = 2, 14.5 Hz, 1H), 4.80 (d, J = 5.0 Hz, 1H), 6.28 (m, 1H), 6.85 (m, 4H), 7.24-7.33 (m, 7H), 7.41 (d, J = 10.0 Hz, 1H), 7.0 (s, 1H), 8.73 (m, 1H), 11.3 (m, 1H), 13.0 (m, 1H). ^{13}C NMR (125.6 MHz, CD$_2$Cl$_2$): δ = 7.7, 11.7, 22.6, 25.7, 29.0, 31.6, 55.2, 55.3, 62.4, 63.8, 80.9, 92.4, 110.0, 111.1, 113.3, 128.0, 129.9, 130.0, 135.2, 150.2, 158.8. ESI MS (m/z) calculated for C$_{38}$H$_{44}$N$_5$O$_7$ [M+H], 681.7; found 681.8.

5'-*O*-(dimethoxytrityl) 3'-*O*-(spermineoethyl) thymidine [3.9]: The starting material **3.5** (200 mg, 0.340 mmol) and spermine (66 mg, 0.323 mmol) were dissolved in 3 mL of dry THF. The reaction was stirred for 20 min at room temperature and sodium cyanoborohydride (26 mg, 0.409 mmol, 1.2 equiv) was added to reaction mixture and stirred for 4 hrs. The reaction was then concentrated *in vacuo* and purified by flash column chromatography using EtOAc:Methanol (9:1 v/v) to yield a white foamy product **3.9** in 20% yield. m.p. 85 °C. $[\alpha]_{589}^{23}$: +35.5 (c 0.01, DCM). R_f = 0.10 (EtOAc–Methanol, 9:1 v/v). IR (KBr) υ_{max} (cm^{-1}) = 5533.1, 5465.0, 3501.1, 3550.3, 3473.4, 3300.0, 2376.6, 2347.0, 1868.4, 1843.9, 1829.5, 1810.3, 1800.3, 1791.7, 1780.1, 1771.0, 1748.3, 1739.8, 1714.1, 1705.6, 1683.1, 1669.8, 1662.4, 1647.0, 1635.6, 1507.3, 1454.6, 1423.6, 1365.6, 1219.5, 1034.9. ^{1}H NMR (499.84 MHz, CD$_2$Cl$_2$): δ = 1.0 (m, 3H), 1.30 (t, J = 10.5 Hz, 2H) , 1.38 (m, 4H), 1.48 (d, J = 10.0 Hz, 3H), 1.57 (s, 1H), 2.23 (m, 1H), 2.46 (t, J = 6.0 Hz, 1H), 2.53 (m, 10H), 2.81 (d, J = 8.0 Hz, 1H), 3.00 (m, 2H), 3.33 (m, 1H), 3.44 (d, J = 11 Hz, 1H), 3.49 (d, J =

6 Hz, 2H), 3.64 (m, 1H), 3.75–3.83 (m, 8H), 4.11 (dd, J = 2, 14.5 Hz, 1H), 4.21 (d, J = 5.0 Hz, 1H), 6.29 (m, 1H), 6.85 (m, 4H), 7.24-7.33 (m, 7H), 7.41 (d, J = 10.0 Hz, 2H), 7.43 (s, 1H). ^{13}C NMR (125.6 MHz, CD$_2$Cl$_2$): δ = 12.4, 25.3, 27.3, 25.3, 38.2, 39.4, 49.6, 49.0, 46.3, 48.1, 55.8, 63.9, 68.8, 82.0, 89.3, 94.8, 110.9, 114.8, 126.2, 127.5, 128.2, 129.2, 136.0, 150.8, 158.1, 163.7, ESI MS (m/z) calculated for C$_{43}$H$_{61}$N$_6$O$_7$ [M+H], 772.4; found 772.5.

5'-*O*-(dimethoxytrityl) 3'-*O*-(*N*-Boc-1,3-diamineoethylpropane) thymidine [3.10]: The starting material **3.5** (200 mg, 0.34 mmol) and *N*-Boc-1,3-diaminopropane (56.2 mg, 0.32 mmol) were dissolved in 3 mL of dry THF. The reaction was stirred for 20 min at room temperature and sodium cyanoborohydride (26 mg, 0.41 mmol, 1.2 equiv) was added to reaction mixture and stirred for 4 hrs. The reaction was then concentrated *in vacuo* and purified by flash column chromatography using EtOAc:Methanol (9:1 v/v) to yield a white foamy product **3.10** in 9% yield. m.p. 80 °C. $[\alpha]_{589}^{23.8}$: +9.16 (c 0.01, DCM). R$_f$ = 0.10 (EtOAc–Methanol, 9:1 v/v). IR (KBr) υ$_{max}$ (cm^{-1}) =3514.2, 1791.0, 1771.6, 1721.0, 1710.6, 1635.6, 1608.6, 1557.9, 1540.9, 1511.6, 1422.5, 1365.6, 1222.6, 1177.7, 1092.6, 831.4. ^{1}H NMR (499.79 MHz, CD$_2$Cl$_2$): δ = 1.42 (t, J = 7.0 Hz, 3H), 1.50 (d, J = 12.0 Hz, 3H), 1.57 (s, 1H), 1.74 (m, 2H), 2.33 (d, J = 11.0 2H), 2.38 (m, 3H), 2.46 (t, J = 6.0 Hz, 1H), 2.53 (t, J = 6.0 Hz, 2H), 2.81 (d, J = 8.0 Hz, 1H), 3.18 (m, 2H), 3.33 (m, 1H), 3.49 (d, J = 11 Hz, 2H), 3.64 (m, 1H), 3.76–3.81 (m, 8H), 4.11 (d, J = 2, 14.5 Hz, 1H), 4.21 (dd, J = 5.0 Hz, 1H), 6.29 (m, 1H), 6.85 (m, 4H), 7.24-7.33 (m, 7H), 7.19 (d, J = 10.0 Hz, 1H), 11.32 (s, J = 5.0 Hz, 1H) ^{13}C NMR (125.6 MHz, CD$_2$Cl$_2$): δ = 22.2, 25.4, 25.9, 26.3, 29.1, 29.3, 29.3, 29.2, 29.6, 31.9, 53.0, 53.1, 53.4, 53.6, 53.8, 55.2, 55.3, 96.0, 97.3, 99.8, 111.1, 113.2, 128.0, 130.0, 131.0, 135.3, 135.4, 158.9, 195.8. ESI MS (m/z) calculated for C$_{41}$H$_{52}$N$_4$O$_9$Na [M+Na], 767.3; found 767.0.

5'-hydroxy 3'-*O*-(methylaminoethyl) thymidine [3.11]: A solution of 3% TCA in DCM (10 mL) was added dropwise at room temperature to **[3.6]** (100 mg, 0.166 mmol). The reaction was continued for 3 hr until complete consumption of starting material was detected by TLC. The crude product was extracted in DCM/water and the aqueous phase was isolated, freeze-dried and lyophilized to dryness. The crude product was purified by silica gel column chromatography (EtOAc:Petroleum ether, 6:4 v/v) to obtain >99% of a white foamy product [**3.11**]. m.p. 67 °C. $[\alpha]_{589}^{25}$ +12.65 (c 0.01, DCM). R_f = 0.10 (EtOAc–Petroleum ether, 6:4). IR (KBr) υ_{max} (cm^{-1}) = 3734.5, 3710.5, 3633.7, 3180.3, 2597.7, 2260.9, 1688.4, 1843.8, 1754.8, 1406.6, 1228.2, 845.6, 683.9 ^{1}H NMR (499.9 MHz, CD$_2$Cl$_2$): δ = 0.82 (t, J = 7.25 Hz, 2H), 1.24 (s, 3H), 1.62 (bs, 1H), 1.80 (s, 3H), 2.23 (d, J = 6.5 Hz, 1H), 2.22-2.25 (m, 1H), 2.52 (s, 2H), 2.70 (d, J = 5.0 Hz, 1H), 2.76 (t, J = 5.25 Hz, 1H), 2.90 (t, J = 7.25 Hz, 1H), 3.60 (s, 1H), 3.70 (s, 1H), 4.0 (m, 1H), 4.10 (d, J = 3.0 Hz, 1H), 6.51 (bs, 1H), 6.14- 6.17 (m, 1H), 7.71 (s, 1H), 11.19 (s, 1H). ^{13}C NMR (126.9 MHz, CD$_2$Cl$_2$): δ = 12.0, 14.7, 22.1, 24.9, 26.8, 28.0, 29.8, 38.6, 52.0, 53.2, 62.0, 64.4, 68.3, 80.0, 80.7, 83.1, 110.0, 136.3, 138.4, 151.0, 164.1, 161.8, 165.2. ESI MS (m/z) calculated for C$_{13}$H$_{22}$N$_3$O$_5$ [M+H], 300.3; found 300.5.

5'-hydroxy 3'-*O*-(octylaminoethyl) thymidine [3.12]: A solution of 3% TCA in DCM (10 mL) was added dropwise at room temperature to **[3.7]** (100 mg, 0.142 mmol). The reaction was continued for 3 hr until complete consumption of starting material was detected by TLC. The crude product was extracted in DCM/water and the aqueous phase was isolated, freeze-dried and lyophilized to dryness. The crude product was purified by silica gel column chromatography (EtOAc:Petroleum ether, 6:4 v/v) to obtain >95% of a white foamy product [**3.12**]. m.p. 70 °C. $[\alpha]_{589}^{22.4}$ +5.5 (c 0.01, DCM). R_f = 0.10 (EtOAc–Petroleum ether, 6:4). IR (KBr) υ_{max} (cm^{-1}) = 3433.3, 2252.7, 2126.7, 1843.9, 1792.0, 1771.9, 1733.7, 1658.7, 1642.1, 1401.5, 1027.5, 824.3,

762.2. ^{1}H NMR (499.9 MHz, CD$_2$Cl$_2$): δ = 1.10 (d, J = 11 Hz, 2H), 1.26 (s, 16H), 1.61 (bs, 1H), 1.79 (s, 3H), 2.14 (d, J = 6.5 Hz, 1H), 2.22-2.25 (d, J = 7.25 Hz, 1H), 2.52 (s, 1H), 2.69 (d, J = 5.0 Hz, 1H), 2.76 (t, J = 5.25 Hz, 1H), 2.90 (t, J = 4.25 Hz, 2H), 3.60 (s, 1H), 3.70 (s, 1H), 4.2 (bs, 1H), 4.4 (bs, J = 3.0 Hz, 1H), 6.89 (bs, 1H), 6.5 (m, 1H), 7.98 (s, 1H), 11.56 (s, 1H). ^{13}C NMR (126.9 MHz, CD$_2$Cl$_2$): δ = 11.9, 12.2, 22.5, 24.2, 25.0, 29.0, 29.1, 31.1, 36.6, 51.0, 52.2, 62.0, 63.4, 80.2, 80.1, 84.1, 84.6, 115.0, 138.9, 151.0, 165.2. ESI MS (m/z) calculated for C$_{20}$H$_{36}$N$_3$O$_5$ [M+H], 398.2; found 398.9.

5'-hydroxy 3'-*O*-(histaminoethyl) thymidine [3.13]: A solution of 3% TCA in DCM (10 mL) was added dropwise at room temperature to **[3.8]** (100 mg, 0.146 mmol). The reaction was continued for 3 hr until complete consumption of starting material was detected by TLC. The crude product was extracted in DCM/water and the aqueous phase was isolated, freeze-dried and lyophilized to dryness. The crude product was purified by silica gel column chromatography (EtOAc:Petroleum ether, 6:4 v/v) to obtain >92% of a white foamy product [**3.13**]. m.p. 75 °C. $[\alpha]_{589}^{22.5}$ +147.4 (c 0.01, DCM). R$_f$ = 0.10 (EtOAc–Petroleum ether, 6:4). IR (KBr) υ_{max} (cm^{-1}) = 3523.1, 3500.2, 3129.5, 2900.3, 2692.4, 2529.6, 2319.3, 1843.9, 1754.1, 1631.5, 1348.3, 1254.3, 1083.4, 844.3, 677.9 ^{1}H NMR (499.84 MHz, CD$_2$Cl$_2$): δ = 0.99 (s, J = 4.0 Hz, 3H), 1.25 (m, 4H) ,1.53 (d, J = 11 Hz, 3H), 1.59 (s, 1H), 2.24 (m, 1H), 2.46 (t, J = 6.0 Hz, 1H), 2.84 (d, J = 7.9 Hz, 2H), 3.00 (m, 1H), 3.34 (m, 1H), 3.47 (d, J = 11 Hz, 1H), 3.65 (m, 1H), 3.75–3.81 (m, 2H), 4.11 (dd, J = 2, 14.5 Hz, 1H), 4.15 (m, 1H), 6.42 (m, 1H), 6.95 (m, 1H), 7.55(m, 1H), 8.73 (m, 1H), 11.5 (m, 1H). ^{13}C NMR (126.9 MHz CD$_2$Cl$_2$): δ = 11.9, 14.3, 14.4, 22.5, 24.9, 26.8, 29.0, 29.1, 36.6, 52.0, 53.2, 62.0, 64.4, 68.0, 80.2, 80.2, 80.3, 84.2, 84.3, 84.8, 84.9, 85.0, 115.0, 138.4, 151.0, 164.1, 165.2, 200.0, 220.1, 220.8.ESI MS (m/z) calculated for C$_{17}$H$_{26}$N$_5$O$_5$ [M+H], 379.1; found 379.0.

5' hydroxy 3'-*O*-(spermineoethyl) thymidine [3.14]: A solution of 3% TCA in DCM (10 mL) was added dropwise at room temperature to **[3.9)]** (100 mg, 0.129 mmol). The reaction was continued for 3 h until complete consumption of starting material was detected by TLC. The crude product was extracted in DCM/water and the aqueous phase was isolated, freeze-dried and lyophilized to dryness. The crude product was purified by silica gel column chromatography (EtOAc:Petroleum ether, 6:4 v/v) to obtain >99% of a white foamy product. m.p. 79 °C. $[\alpha]_{589}^{22.8}$ +29.5 (c 0.01, DCM). R_f = 0.10 (EtOAc–Petroleum ether, 6:4). IR (KBr) υ_{max} (cm^{-1}) = 2836.3, 2730.4, 2450.5, 1744.8, 1631.1, 1335.8, 1249.5, 832.6, 741.6, 675.7. ^{1}H NMR (499.9 MHz, CD$_2$Cl$_2$): δ = 0.99 (m, 3H), 1.30 (t, J = 10.5 Hz, 3H) , 1.38 (m, 8H), 1.48 (d, J = 10.0 Hz, 3H), 1.57 (s, 1H), 2.23 (m, 2H), 2.46 (t, J = 6.0 Hz, 1H), 2.53 (m, 8H), 2.81 (d, J = 8.0 Hz, 3H), 3.91 (m, 1H), 3.99 (d, J = 11 Hz, 2H), 4.11 (dd, J = 2, 12.5 Hz, 2H), 4.21 (d, J = 5.0 Hz, 2H), 6.28 (m, 1H), 6.95 (m,1H), 11.2 (s, J = 12.5 Hz, 1H), ^{13}C NMR (126.9 MHz, CD$_2$Cl$_2$): δ = 15.4, 60.7, 61.0, 65.9, 65.8, 77.71, 79.6, 81.1, 92.8, 97.7, 107.2, 110.0, 110.9, 112.7, 113.5, 227.3. ESI MS (m/z) calculated for C$_{22}$H$_{43}$N$_6$O$_5$ [M+H], 470.3; found 469.3.

5'-hydroxy 3'-*O*-(1,3-diamineoethylpropane) thymidine [3.15]: A solution of 90% TFA in DCM (3 mL) was added dropwise at room temperature to **[3.10]** (100 mg, 0.134 mmol). The reaction was continued for 40 min, until complete consumption of starting material was detected by TLC. The crude product was extracted in DCM/water and the aqueous phase was isolated, freeze-dried and lyophilized to dryness. The crude product was purified by silica gel column chromatography (EtOAc:Petroleum ether, 6:4 v/v) to obtain 56% of a white foamy product. m.p. 80 °C. $[\alpha]_{589}^{22.6}$ -4.4 (c 0.01, DCM). R_f = 0.10 (EtOAc–Petroleum ether, 6:4). IR (KBr) υ_{max} (cm^{-1})

= 3514.2, 1791.0, 1771.6, 1721.0, 1710.6, 1678.3, 1635.6, 1608.6, 1557.9, 1540.9, 1511.6, 1422.5, 1365.6, 1222.6, 1177.7, 1092.6, 831.4, 766.2, 549.8. ^{1}H NMR (499.9 MHz, CD$_2$Cl$_2$): δ = 1.22 (t, J = 7 Hz, 2H), 1.24 (s, 4H), 1.60 (bs, 2H), 2.1 (s, 3H), 2.14 (d, J = 12.5 Hz, 1H), 2.82 (s, 3H), 3.50 (s, 1H), 3.71 (s, 1H), 4.25 (m, 6H), 4.20 (d, J = 4.0 Hz, 1H), 5.98 (t, J = 12.5 Hz, 1H), 10.0 (s, 1H), 11.6 (s, 1H). ^{13}C NMR (126.9 MHz, CD$_2$Cl$_2$): δ = 13.1, 13.2, 22.5, 24.2, 26.9, 29.0, 29.3, 30.9, 36.6, 52.1, 53.2, 62.0, 65.0, 80.0, 80.5, 84.2, 84.3, 84.8, 84.9, 99.2, 100.0, 110.0, 138.3, 145.4, 162.0, 198.1, 206.2, 208.9, 210.7. ESI MS (m/z) calculated for C$_{15}$H$_{27}$N$_4$O$_5$ [M+H], 343.1; found 343.2.

5'-carboxy 3'-*O*-(methylaminoethyl) thymidine [3.16]: To a solution of **[3.11]** (500 mg, 1.67 mmol) in CH$_2$Cl$_2$ (1 mL) was added 2,2,6,6-tetramethyl-1-piperidinyloxy (TEMPO) (45.4 mg, 0.241 mmol), and iodobenzene diacetate (BAIB) (682 mg, 2.29 mmol) at room temperature. After the mixture was stirred for 2 h, MeCN:H$_2$O (1:1 v/v, 530 µL) was added to the reaction mixture and stirred for 24 h. The crude product was extracted in DCM/water and the aqueous phase was isolated, freeze-dried and lyophilized to dryness. The crude product was purified by flash chromatography (CHCl$_3$:MeOH 9:1 v/v). The pure product was obtained as white powder in 62% yield. M.p= 79°C. $[\alpha]_{589}^{22.6}$ = 143.5 (c 0.01, DCM), R$_f$ = 0.10 (CHCl$_3$: MeOH 9:1 v/v). IR (KBr) υ_{max} (cm^{-1})= 2951.0, 2586.9, 1868.5, 1843.9, 1754.1, 1643.0, 1471.3, 1368.0, 1343.1, 1252.1, 1117.6, 839.9, 743.7, 679.1. ^{1}H NMR (499.9 MHz, DMSO): δ= 1.19 (t, J = 14.0 Hz, 3H), 1.56 (t, J = 4 Hz, 3H), 2.70-2.81 (m, 7H), 3.30-3.35 (m, 1H), 3.52 (bs, 1H), 3.98-4.05 (m, 2H), 4.42-4.47 (m, 1H), 4.49 (d, J = 2 Hz, 1H), 6.23 (m, 1H), 9.10 (s, 1H), 11.24 (bs, 1H). ^{13}C NMR (129.69 MHz, DMSO-d_6): δ= 11.0, 12.3, 21.5, 39.7, 56.7, 60.1, 62.3, 74.6, 80.1, 82.6, 83.9, 110.1, 113.6, 116.8, 128.8, 129.7, 136.7, 144.1, 150.2, 159.8, 162.6, 170.1, 201.9. ESI MS (m/z) calculated for C$_{13}$H$_{19}$N$_3$O$_6$ [M+], 313.1; found 313.0.

5'-carboxy 3'-*O*-(octylaminoethyl) thymidine [3.17]: To a solution of **[3.12]** (500 mg, 1.26 mmol) in CH_2Cl_2 (1 mL) was added 2,2,6,6-tetramethyl-1-piperidinyloxy (TEMPO) (36.2 mg, 0.241 mmol), and iodobenzene diacetate (BAIB) (742 mg, 2.30 mmol) at room temperature. After the mixture was stirred for 2 h, a mixture of $MeCN:H_2O$ (1:1 v/v, 530 µL) was added to the reaction mixture and stirred for 24 h. The crude product was extracted in DCM/water and the aqueous phase was isolated, freeze-dried and lyophilized to dryness. The crude product was purified by flash chromatography ($CHCl_3$:MeOH 9:1 v/v). The pure product was obtained as white powder in 29% yield. M.p= 82°C. $[\alpha]_{589}^{22.6}$ = -8.25 (c 0.01, DCM), R_f = 0.10 ($CHCl_3$: MeOH 9:1 v/v). IR (KBr) υ_{max} (cm^{-1})= 2934.3, 1791.6, 1658.7, 1456.3, 1364.5, 1270.7, 1133.2, 894.9, 825.1, 733.7, 669.1. ^{1}H NMR (499.9 MHz, DMSO): δ= 1.20 (t, J = 11.0 Hz, 1H), 1.60 (m, 17H), 2.40-2.56 (m, 4H), 2.60-2.90 (m, 3H), 3.28-3.59 (m, 1H), 3.63 (d, J = 12 Hz, 1H), 4.01-4.05 (m, 2H), 4.44-4.45 (m, 1H), 6.23 (s, 1H), 6.82 (s, 1H), 9.37 (s, 1H), 11.25 (bs, 1H). ^{13}C NMR (125.69 MHz, DMSO-d_6): δ= 13.2, 39.5, 39.6, 58.2, 62.1, 64.8, 80.2, 83.2, 84.4, 109.0, 112.8, 115.6, 117.8, 131.8, 134.8, 139.0, 142.6, 162.8, 171.4, 179.9, 175.8, 194.2, 198.2, 204.8. ESI MS (m/z) calculated for $C_{14}H_{33}N_3O_6$ [M+], 411.2; found 411.9.

5'-carboxy 3'-*O*-(histamineoethyl) thymidine [3.18]: To a solution of **[3.13]** (500 mg, 1.32 mmol) in CH_2Cl_2 (1 mL) was added 2,2,6,6-tetramethyl-1-piperidinyloxy (TEMPO) (36.2 mg, 0.241 mmol), and iodobenzene diacetate (BAIB) (742 mg, 2.298 mmol) at room temperature. After the mixture was stirred for 2 h, a mixture of $MeCN:H_2O$ (1:1 v/v, 530 µL) was added to the reaction mixture and stirred for 24 h. The crude product was extracted in DCM/water and the aqueous phase was isolated, freeze-dried and lyophilized to dryness. The crude product was purified by flash chromatography ($CHCl_3$:MeOH 9:1 v/v) in >99% yield. M.p= 85°C. $[\alpha]_{589}^{22.6}$ = -7.69 (c 0.01,

DCM), R_f = 0.10 (CHCl$_3$: MeOH 9:1 v/v). IR (KBr) υ_{max} (cm^{-1})= 2950.5, 1843.9, 1758.3, 1665.3, 1471.5, 1388.3, 1339.4, 1230.7, 1118.7, 1014.6, 835.9, 737.4, 676.3. ^{1}H NMR (499.84 MHz, DMSO- d_6): δ = 0.89 (t, J = 4.0 Hz, 1H), 1.25 (m, 3H) , 1.60 (s, 1H), 2.22 (m, 1H), 2.83 (d, J = 5 Hz, 2H), 3.02 (m, 1H), 3.34 (m, 1H), 3.72 (m, 7H), 4.14 (dd, J = 14.5 Hz, 1H), 4.19 (m, 1H), 6.15 (m, 1H), 7.25 (m, 1H), 9.0 (s, 1H), 11.18 (bs, 1H). ^{13}C NMR (125.69 MHz, DMSO-d_6): δ= 10.9, 37.3, 54.6, 63.9, 69.7, 79.0, 83.7, 84.4, 86.6, 110.2, 113.2, 116.1, 126.9, 127.9, 128.2, 130.1, 135.0, 135.5, 135.7, 135.8, 145.0, 150.4, 151.7, 158.9, 163.4, 179.2, 204.8. ESI MS (m/z) calculated for C$_{17}$H$_{23}$N$_5$O$_6$ [M-H], 393.4; found 392.1.

5'-carboxy 3'-*O*-(spermineoethyl) thymidine [3.19]: To a solution of **[3.14]** (500 mg, 1.06 mmol) in CH$_2$Cl$_2$ (1 mL) was added 2,2,6,6-tetramethyl-1-piperidinyloxy (TEMPO) (36.2 mg, 0.241 mmol), and iodobenzene diacetate (BAIB) (742 mg, 2.23 mmol) at room temperature. After the mixture was stirred for 2 h, a mixture of MeCN:H$_2$O (1:1 v/v, 530 µL) was added to the reaction mixture and stirred for 24 h. The crude product was extracted in DCM/water and the aqueous phase was isolated, freeze-dried and lyophilized to dryness. The crude product was purified by flash chromatography (CHCl$_3$:MeOH 9:1 v/v). The pure product was obtained as white powder in 92% yield. M.p= 89°C. $[\alpha]_{589}^{25}$ = +63.25 (c 0.01, DCM), R_f = 0.10 (CHCl$_3$: MeOH 9:1 v/v). IR (KBr) υ_{max} (cm^{-1})= 2949.0, 1868.5, 1843.9, 1665.7, 1472.0, 1366.5, 1332.4, 1231.5, 1118.7, 1089.1, 1059.2, 1014.5, 975.8, 635.8, 734.7, 678.1. ^{1}H NMR (499.8 MHz, DMSO-d_6): δ = 0.98 (m, 1H), 1.30 (t, J = 10.5 Hz, 2H) , 1.38 (m, 4H), 1.48 (d, J = 10.0 Hz, 3H), 1.57 (s, 1H), 2.23 (m, 1H), 2.46 (t, J = 6.0 Hz, 1H), 2.53 (m, 7H), 2.81 (d, J = 8.0 Hz, 1H), 3.91 (m, 4H), 3.99 (d, J = 11 Hz, 3H), 4.11 (dd, J = 12.5 Hz, 4H), 4.21 (d, J = 5.0 Hz, 2H), 6.28 (m, 1H), 6.95 (m,3H), 11.2 (s, J = 12.5 Hz, 1H), 13.0 (m, 1H). ^{13}C NMR (125.70 MHz, DMSO-d_6): δ= 12.1, 14.5, 21.2, 55.5, 60.2, 64.2, 74.7, 80.4, 83.3, 84.1, 84.2, 86.5, 110.2, 113.75, 128.1, 128.4, 130.2, 135.6, 135,8, 136.0,

145.1, 150.8, 158.6, 164.1, 170.8, 201.1ESI MS (m/z) calculated for $C_{22}H_{40}N_6O_6$ [M-H], 484.3; found 483.3.

5'-carboxy 3'-*O*-(1,3-diamineoethylpropane) thymidine [3.20]: To a solution of **[3.15]** (500 mg, 1.46 mmol) in CH_2Cl_2 (1 mL) was added 2,2,6,6-tetramethyl-1-piperidinyloxy (TEMPO) (36.2 mg, 0.241 mmol), and iodobenzene diacetate (BAIB) (742 mg, 2.298 mmol) at room temperature. After the mixture was stirred for 2 h, a mixture of MeCN:H_2O (1:1 v/v, 530 µL) was added to the reaction mixture and stirred for 24 h. The crude product was extracted in DCM/water and the aqueous phase was isolated, freeze-dried and lyophilized to dryness. The crude product was purified by flash chromatography (CHCl$_3$:MeOH 9:1 v/v). The pure product was obtained as white powder in 90% yield. M.p= 80°C. $[\alpha]_{589}^{22.8}$ = -4.4 (c 0.01, DCM), R_f = 0.10 (CHCl$_3$: MeOH 9:1 v/v). IR (KBr) υ_{max} (cm^{-1})= 2933.9, 1678.2, 1365.8, 1179.3, 1131.2 ^{1}H NMR (499.9 MHz, DMSO-d_6): δ = 1.25 (t, J = 11.5 Hz, 1H), 1.24-1.59 (m, 8H), 2.15 (s, 3H), 2.19 (d, J = 6 Hz, 1H), 2.80 (bs, 2H), 3.51 (s, 2H), 3.70 (s, 1H), 4.15-4.20 (m, 1H), 4.42 (bs, 2H), 6.0 (t, J = 8 Hz, 1H), 11.62 (s, 1H), 13.25 (bs, 1H). ^{13}C NMR (125.70 MHz, DMSO-d_6): δ= 12.9, 14.3, 22.5, 26.2, 26.6, 29.1, 29.5, 31.7, 83.2, 84.4, 85.9, 108.9, 108.9, 138.6, 150.9, 164.4, 173.4. ESI MS (m/z) calculated for $C_{15}H_{24}N_4O_6Na$ [M+Na], 379.1; found 379.0.

Solid phase bioconjugation.

Solid-phase bioconjugation of peptide nucleolipids (**3.22-3.31**) were performed on an oil bath reaction apparatus with a stirring block. The peptide-bound Rink amide poly (ethylene glycol) resin (Nova PEG, 0.47 mmol/g) **3.21**, was added into a microglass tube and slowly agitated with DMF (500 µL) at 60 ºC. Nucleolipids (**3.16-3.20**, 3 eq.) were added in DMF (500 µL) along with NMM (6 eq.) and HCTU (3 eq.). The reaction mixture was preactivated for 7 min before being slowly added to the resin-bound peptide and agitated for 14 h at 60 ºC. Following coupling, the

resin was washed with MeOH, DMF and DCM (3x15 mL) followed by deprotection of the Fmoc protecting group (30 min) with 20% piperidine in DMF. The resin was then washed (MeOH, DMF and DCM) and dried with $N_{2(g)}$. Labeling of the Ahx-peptide *N*-terminus with fluorescein isothiocyanate (FITC, 1.1 eq.) in pyridine:DMF:DCM (12:7:5 v/v/v) was accomplished in the dark, overnight at room temperature. Following synthesis, peptide cleavage from the solid support and deprotection of the side-chain protecting groups were accomplished with concentrated trifluoroacetic acid (TFA, 95%) with minimal addition (5%) of reaction scavengers (*i.e.* H_2O, triethylsilane). The cleavage and deprotection reaction was completed in 2 hrs at room temperature. Peptide-nucleolipid samples (**3.22-3.31**) were concentrated, precipitated in cold ether, and isolated as white pellets for LC/MS analyses and purification.

Characterization of peptides by LC/MS:

Crude peptide-nucleolipid samples were dissolved in MeOH/H_2O for LCMS analyses. Sample analyses were performed on an Agilent 1100 series ESI-LCMS with single quadrupole mass analyzer and LC conditions which used a linear binary gradient (2-80% MeOH/H_2O, 0.1% FA, over 25min). Analytical RP-HPLC was performed using a Waters 2695 Symmetry® C18 column (3.9 x 150 mm, 5 μm particle size) using a linear binary gradient, 20-80% or 2-82% MeCN/H_2O, 0.1%FA, over 17 min at 25°C, with a 1 mL/min flow rate and detection at 220 nm and 260 nm. Samples collected after purification were lyophilized to a white solid and re-dissolved in 50:50 v/v H_2O:MeOH to confirm purity and identity by LCMS analyses.

Circular Dichroism (CD) Spectroscopy:

Samples were prepared 12-16 hr. ahead of time in H_2O:TFE (50:50, v/v) and stored at 5 ºC. CD spectra were collected as an average of 3 scans on an Olis Circular Dichroism (CD)

Spectrophotometer (Model: 24994 Rapid Scanning Monochromator, online instrument system) from 260-190 nm, using 1 nm bandwidth and 0.5 min step size at 25 °C. Samples were blank corrected, the data was smoothed and converted to molar ellipticity values from the equation $[\theta] = \theta/cl$, where θ is the molar ellipticity (mdeg), c is the molar concentration of the peptides (12.5 μM) and l is the path length of the cell (1 cm). The data was imported into Microsoft Excel and the CD spectra were plotted in terms of molar ellipticity *vs* wavelength.

UV/Vis Spectroscopy.

The final concentrations of the peptide solutions was determined by UV/Vis spectrophotometry at 214 nm (ε value of peptides and calculated from the equation:

$$\varepsilon_{214} = (\varepsilon_{peptidebond})(n_{peptidebonds}) + \Sigma \, (\varepsilon_{aminoacid(i)})(n_{aminoacid(i)}).$$

The analyses were conducted on an 8452A Diode Array Spectrophotometer from OLIS, with wavelength range set from 190 – 600 nm with maximum absorption collected at 220 and 260 nm in addition to 490 nm for the FITC-labeled peptides. Peptide concentrations were standardized at 12.5 μM.

Cell Viability.

To evaluate the MM1S cells' viability following treatment with the synthetic peptide-nucleolipid bioconjugates, **3.22-3.31**, the MM1S cells were incubated for 24 h in a 24 well plate, at 50,000 viable cells/well. MM1S cells were left untreated, and treated with the synthetic peptide-nucleolipid bioconjugates, **3.22-3.31**, (2.5 μM) at 37°C in 5% CO_2 humidified air. Cells were then collected and washed with FACS buffer, centrifuged, and suspended in Guava Nexin Reagent® (100 μL/tube, from EMD Millipore). Following incubation (20 min) at room temperature in the

dark, the MM1S cells were analyzed for early and late apoptotic events by flow cytometry following the vendor instructions.

3.8 REFERENCES:

1) Allain, V.; Bourgaux, C.; Couvreur, P. *Nucleic Acids Res.* **2012**, *40*, 1891-1903.

2) Gissot, A.; Camplo, M.; Grinstaff, M.W.; Barthélémy, P. *Org. Biomol. Chem.* **2008**, *6*, 1324-1333.

3) Rosemeyer, H. *Chem. Biodiv*., **2005**, *2*, 977-1063.

4) Patel, P.; Hanawa, E.; Yadav, R.; Samuni, U.; Marzabadi, C.; Sabatino, D. *Bioorg. Med. Chem. Lett.*, **2013**, *23*, 5086-5090.

5) Simeone, L.; Milano, D.; De Napoli, L.; Irace, C.; Di Pascale, A.; Boccalon, M.; Tecilla, P.; Montesarchio, D. *Chemistry* **2011**, *17*, 13854-13865.

6) Simeone, L.; Irace, C.; Di Pascale, A.; Ciccarelli, D.; D'Errico, G.; Montesarchio, D. *Eur. J. Med. Chem.* **2012**, *57*, 429-440.

7) Patil, S.P.; Yi, J.W.; Bang, E.K.; Jeon, E.M.; Kim, B.H. *Med. Chem. Commun.*, **2011**, *2*, 505-508.

8) Yang, H.W.; Yi, J.W.; Bang, E.K.; Jeon, E. M.; Kim, B. H. *Org. Biomol. Chem*., **2011**, *9*, 291-296.

9) Latxague, L.; Dalila, M.J.; Patwa, A.; Ziane, S.; Chassande, O.; Godeau, G.; Barthelemy, P. *Chimie*, **2012**, *15*, 29-36.

10) Campins, N.; Dieudonne, P.; Grinstaff, M.W.; Barthelemy, P. *New J. Chem*., **2007,** *31*, 1928–1934.

11) Moreau, L.; Barthelemy, P.; El Maataoui, M.; Grinstaff, M.W. *J. Am. Chem. Soc.*, **2004**, *126*, 7533–7539.

12) Chabaud, P.; Camplo, M.; Payet, D.; Serin, G.; Moreau, L.; Barthelemy, P.; Grinstaff, M.W.; *Bioconjug. Chem*., **2006**, *17*, 466–472.

13) Moreau, L.; Barthelemy, P.; Li, Y.; Luo, D.; Prata, C. A. H.; Grinstaff, M.W. *Mol. BioSyst.,* **2005***, 1,* 260–264.

14) Barthelemy, P.; Prata, C. A. H.; Filocamo, S. F.; Immoos, C. E.; Maynor, B. W.; Hashmi, S. A. N.; Lee, S. J.; Grinstaff, M.W. *Chem. Comm.*, **2005**, *10*, 1261–1263.

15) Arigon, J.; Prata, C. A. H., Grinstaff, M. W.; Barthelemy, P. *Bioconjug. Chem.*, **2005**, *16*, 864–872.

16) Milani, S.; Bombelli, F.B.; Berti, D.; Hauss, T.; Dante, S.; Baglioni, P. *Biophys. J.*, **2006**, *90*, 1260–1269.

17) Khiati, S.; Pierre, N.; Andriamanarivo, S.; Grinstaff, M.W.; Arazam, N.; Nallet, F.; Navailles, L.; Barthelemy, P. *Bioconjug. Chem.*, **2009**, *20*, 1765–1772.

18) Bombelli, F.B.; Berti, D.; Almgren, M.; Karlsson, G.; Baglioni, P. *J. Phys. Chem,* **2006**, *110*, 17627–17637.

19) Yanagawa, H.; Ogawa, Y.; Furuta, H.; Tsuno, K. *J. Am. Chem. Soc*. **1989**, *111*, 4567–4570.

20) Horton, K.L.; Stewart, K.M.; Fonseca, S.B.; Guo, Q.; Kelley, S.O. *Chem. Biol.* **2008**, *15*, 375-382.

21) Andersen, H.H.; Elberling, J.; Arendt-Nielsen, L. *Acta. Derm. Venereol.*, **2015**, *95*, 771–775.

22) Julian, M.; Hernandez, A.; Maurras, A.; Puget, K.; Amblard, M.; Martinez, J.; Subra, G. *Tetrahedron Lett.* **2009**, *50*, 260-263.

23) Rana, N., Huang, S.; Patel, P.; Samuni, U.; Sabatino, D. *Bioorg. Med. Chem. Lett.*, **2016**, *26*, 3567–3571.

24) García-Ramos, Y.; Paradís-Bas, M.; Tulla-Puche, J.; Albericio, F.; *J. Pept. Sci.* **2010**, *16*, 675-678.

25) Dıaz-Mochon, J. J.; Bialy, L.; Bradley, M. *Org. Lett.*, **2004,** *6*, 1127–1129.

26) Ozdirekcan, S.; Nyholm, T. K.; Raja, M.; Rijkers, D. T.; Liskamp, R. M.; Killian, *J. A. Biophys. J.* 2008, **94**, 1315-1325.

27) Epand, R.; Shai, Y.; Segrest, J. P.; Anantharamaiah, G. M. *Pept. Sci*. **1995**, *37*, 319-338.

28) Greenstein, S.; Krett, N.L.; Kurosawa, Y.; Ma, C.; Chauhan, D.; Hideshima, T.; Anderson, K.C.; Rosen, S.T. *Exp. Hematol*. **2003**, *31*, 271-282.

29) Demo, S.D.; Masuda, E.; Rossi, A.B.; Throndset, B.T.; Gerard, A.L.; Chan, E.H.; Armstrong, R.J.; Fox, B.P.; Lorens, J.B.; Payan, D.G.; Scheller, R.H.; Fisher, J.M. *Cytometry* **1999**, *36*, 340–348.

CHAPTER 4. CONCLUSIONS, FUTURE WORK AND CONTRIBUTIONS TO KNOWLEDGE

4.1 CONCLUSIONS MADE IN THIS THESIS
4.1.1 SYNTHESIS, CHARACTERIZATION AND ANTI-CANCER ACTIVITY OF A PEPTIDE-NUCLEOLIPID BIOCONJUGATE

In Chapter 2, the design, synthesis and characterization of a new class of "killer" peptide nucleolipid bioconjugate was described for anti-cancer applications. These research objectives were accomplished by developing a solution-phase synthesis strategy for making the requisite 5'-carboxy 3'-hexadecylamine thymidine nucleolipid (**Scheme 2.1**). The key step in this synthetic approach was based on a reductive amination reaction which condensed hexadecylamine onto the 3'-aldehyde-derived thymidine building block. This strategy was envisioned as an entry point for coupling a variety of alkyl, aryl and heterocyclic amines in order to generate functionally diverse nucleolipids. In this proof-of-concept study, the 3'-hexadecylamine-derived nucleolipid was synthesized in good yields and converted to the 5'-carboxy-derived nucleolipid following 5-detritylation and oxidation reactions. The final nucleolipid product was characterization by NMR, IR spectroscopy and mass spectrometry in order to validate identity and compound purity.

This thymidine-derived nucleolipid was rationally designed and developed for conjugation with the pro-apoptotic peptide D-(KLAKLAK)$_2$ sequence (**Figure 2.1**). This so-called "killer" peptide has shown the ability to induce bacterial cell death, with limited toxicity observed in mammalian cells [1]. In order to improve the cytotoxic activity of the D-(KLAKLAK)$_2$ sequence towards malignant mammalian cell types, such as cancer, the amphiphilic nucleolipid was anticipated to enhance cell permeability and mitochondria localization of the D-(KLAKLAK)$_2$-AK sequence for potentiating its anti-cancer activity. The native D-(KLAKLAK)$_2$-AK and palmitamide derived sequences were made as controls using solid phase peptide synthesis. In the case of the palmitamide-derived sequence, an orthogonally protected Lys(Dde) was unmasked

using buffered hydroxylamine and the liberated ε-amino group was reacted with palmitic acid using HCTU coupling conditions to afford the *C*-terminal palmitamide derived D-(KLAKLAK)$_2$-AK. The HCTU-based coupling conditions were also used to generate the nucleolipid derived D-(KLAKLAK)$_2$-AK sequence. These sequences also contained *N*-terminal modifications, including the incorporation of the Ahx linker and FITC. The peptide bioconjugates were isolated in sufficient yields (10-33%) and purities (≥96%) for structure-activity relationship studies.

Comparison of retention times of the peptide conjugates with the native sequence indicated that conjugation of the D-(KLAKLAK)$_2$-AK sequence with palmitic acid and nucleolipid produced more hydrophobic, retained sequences on the C18 reverse-phase HPLC column (**Figure 2.2. B**). Moreover, UV-Vis absorption studies validated the characteristics absorptions for the peptide (220 nm) and nucleolipid (260 nm) (**Figure 2.2 C**). CD spectroscopy was used to study the secondary structures of the conjugates in comparison to the native sequence. Distinct α-helical secondary structures were observed for all samples in a H$_2$O:TFE solvent system indicating that conjugation retains the helical peptide character of the sequence (**Figure 2.2D** and **Table 2.2**). DLS and TEM studies were used to confirm the self-assembly of the peptide high-ordered nanostructures, presumably due to the amphiphilic nature of the sequence (**Figure 2.3**). Thus, the amphiphilic peptide bioconjugates were found to retain the structure (α-helix) characteristics of the native sequences, while fine-tuning its polar properties for biological action in malignant cancer cells. We hypothesized that the positively charged, amphiphilic α-helical peptide conjugates would display enhanced cell permeability and mitochondria localization leading to toxicity in cancer cells. In order to test this hypothesis, the anti-cancer activity of the peptide conjugates were examined relative to the native sequence.

A 60 cancer cell line screen was performed at the National Cancer Institute, testing the anti-proliferative properties of the peptides dosed at a single concentration. In this screen, the amphiphilic peptide bioconjugates were found to be more active than the native D-(KLAKLAK)$_2$-AK sequence, especially in a selected panel of non-small cell lung carcinoma (**Table 2.3, Figures 2.4-2.7**). The A549 lung cancer cell line was found to be the most sensitive, with the nucleolipid-derived sequence exhibiting the greatest cytotoxicity followed by the palmitamide and the native peptide sequence. Thus, conjugation of the D-(KLAKLAK)$_2$-AK sequence with the amphiphilic nucleolipid has served to potentiate the anti-cancer activity of the so-called "killer" peptide sequence [2]. A structure-activity relationship study was developed in Chapter 3 in order to explore the influence of nucleolipid modifications on the anti-cancer activity of the D-(KLAKLAK)$_2$-AK sequence.

4.1.2   DIVERSITY ORIENTED SYNTHESIS OF PEPTIDE NUCLEOLIPID BIOCONJUGATES FOR STRUCTURE-ACTIVITY RELATIONSHIP STUDIES

In Chapter 3, a new diversity oriented synthesis approach is described for the generation of modified nucleolipids and their incorporation within the native D-(KLAKAK)$_2$-AK sequence. These methods are important for the generation of new peptide nucleolipid bioconjugates that may serve as bifunctional probes for exploring the influence of nucleolipid modification on the anti-cancer activity of the D-(KLAKAK)$_2$-AK sequence. The diversity oriented synthesis approach described in chapter 3 is based on our existing reductive amination methodology [2]. Extension of the substrate scope related to this method allowed for the condensation of alkylamines, polyamines, and heterocyclic amines onto the 3'-aldehyde derived thymidine precursor (**Figure 3.5**). This two-step one pot reaction allowed for the generation of structurally diverse nucleolipids

which were subsequently converted into their reactive 5'-carboxy derived nucleolipids following our previously described detritylation and oxidation conditions [2]. Each nucleolipid was characterized by a combination of ^{1}H, ^{13}C NMR, IR spectroscopy and mass spectrometry in order to confirm identities and purities. The isolated 5'-carboxy derived nucleolipids were incorporated at the Lys *C*-terminus of the D-(KLAKAK)$_2$-AK sequence by the HCTU-mediated coupling conditions previously described [2]. Furthermore, peptides were generated with and without the *N*-terminal FITC for exploring structure-activity relationships against cellular tumor targets (**Figure 3.6**).

The isolated peptide-nucleolipid bioconjugates were analyzed and purified by RP HPLC. The identities of the pure bioconjugates were confirmed by LC-MS for exploring our structure-activity relationship studies. The amphiphilic properties of the peptide-nucleolipid bioconjugates were initially explored by RP-HPLC (**Figure 3.7**). In this study, the alkylamine and polyamine derived nucleolipids were found to impart greater hydrophobicity onto the D-(KLAKAK)$_2$-AK sequence when compared to the histamine-derived nucleolipids. CD spectroscopy was then used to evaluate the secondary structures (if any) of the peptides in H$_2$O:TFE. The combination of H$_2$O:TFE served to mimic the amphiphilic lipid bilayer microenvironment that may stabilize peptide secondary structures. The structurally diverse nucleolipids were found to retain α-helical peptide secondary structures, albeit, with varying effects on (Percentage of) helical character (**Figure 3.9**).

The biological evaluation of the small library of peptide nucleolipid bioconjugates has been tested on the HepG2 hepatoblastoma cell culture. In this assay, a Guava Nexin® Reagent (EMD Millipore) was used to assess early and late-stage apoptosis by flow cytometry [3]. The results revealed no signifncant populations in early and late stage apoptotic events for the HepG2 cells

when treated with the synthetic bioconjugates, (**Figure 3.10**). These results are preliminary and additional biological testing is anticipated to confirm the capabilities of structurally diverse nucleolipids to potentiate the cancer cell death effects of the D-(KLAKAK)$_2$-AK sequence. Furthermore, the FITC-labeled bioconjugates may provide important mechanistic information related to cell permeability and mitochondrial localization for anti-cancer activity. In a related study, the lead nucleolipid-derived D-(KLAKAK)$_2$-AK sequence may be extended with cancer-targeting peptide sequences in order to facilitate selective anti-cancer activity. The latter is a current focus of our on-going research work for generating potent and selective anti-cancer peptides.

4.2 PRELIMINARY STUDIES AND FUTURE WORK TOWARDS THE DEVELOPMENT OF A CANCER-TARGETING PEPTIDE-NUCLEOLIPID BIOCONJUGATE

4.2.1 RATIONAL DESIGN

The Pep42 cancer-targeting peptide has been a cornerstone sequence in our research group for the development of selective anti-cancer approaches [4]. Pep42, was selected by Janda and co-workers as a short, cyclic peptide sequence capable of binding to and internalizing within cancer cells that express GRP78 on the cell surface [5]. Considering that GRP78 functions as an oncoprotein signaling tumor initiation, proliferation, invasion and drug resistance, it has been classified as a therapeutically relevant biomarker in cancer [6]. Furthermore, GRP78 is overexpressed on the cell surface of many transformed primary tumors, but not on normal, healthy cells making the identification of cell surface GRP78 ligands of critical importance for the development of cancer-targeting strategies. In our approach, a lead nucleolipid-derived D-(KLAKAK)$_2$-AK sequence is extended at the *N*-terminus with the Pep42 sequence, CTVALPGGYVRVC,, followed by the incorporation of the aminohexanoic acid linker (AHx) and

116

fluorescein isothiocyanate (FITC). Additionally, poly(ethylene) glycol spacers (0, 3, 6, 12) may be introduced in between the Pep42 and D-(KLAKAK)$_2$ sequence to provide spatial control in between the bifunctional peptide sequences and to also help promote aqueous solubility and biocompatibility. A structure representation of a first generation FITC-Ahx-Pep42-D-(KLAKAK)$_2$-AK-nucleolipid conjugate is described in **Figure 4.1**.
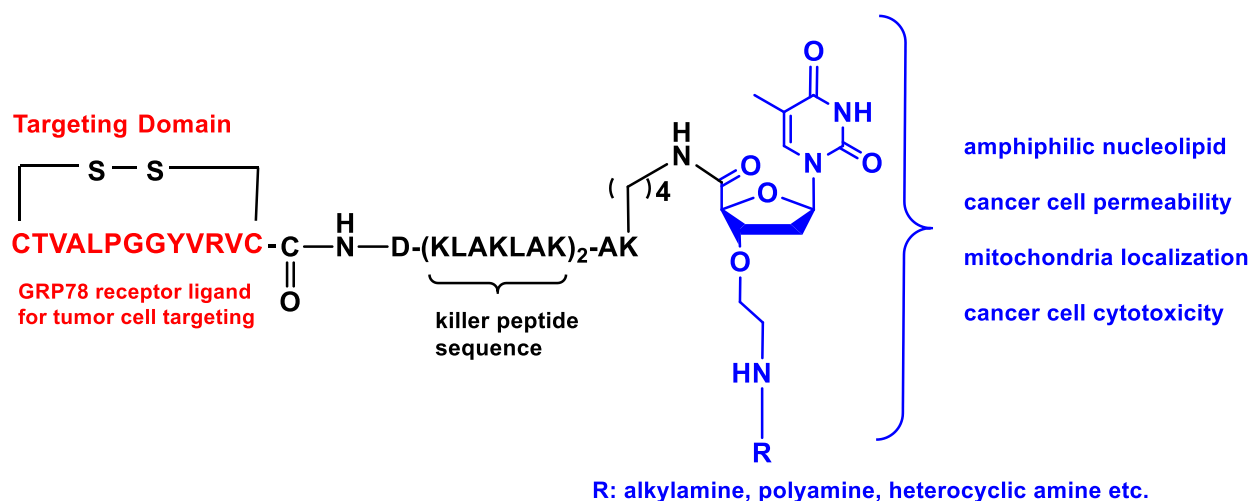
Figure 4.1. Rational design of the GRP78-targeting FITC-Ahx-Pep42-D-(KLAKAK)$_2$-AK-nucleolipid conjugate.

4.2.2. SYNTHESIS

Working alongside Adah Beck, a first year undergraduate student working in the laboratory of Dr. David Sabatino in the Department of Chemistry and Biochemsitry, a synthesis strategy for the desired bioconjugate was designed and developed. Fmoc-based solid phase peptide synthesis was used for the preparation of the GRP78-targeting FITC-Ahx-Pep42-D-(KLAKAK)$_2$-AK-nucleolipid conjugate. The peptide sequence was generated on a Rink Amide NovaPEG resin. At the *C*-terminus, the Lys(Dde) residue was incorporated and selectively deprotected on solid phase for the coupling of the carboxy-derived nucleolipid. HCTU-coupling conditions were once again

used to effectively couple the nucleolipd and the Fmoc-amino acids on solid phase. The first representative example of the Pep42- D-(KLAKAK)$_2$-AK-nucleolipid conjugate was synthesized without a PEG spacer, however, the Ahx linker was incorporated at the *N*-terminus for FITC incorporation. In this final synthetic step, a portion of the peptide bound support was cleaved and deprotected without the FITC label, whereas, another portion of the resin was used to couple FITC at the *N*-terminus. Following cleavage and deprotection, the crude peptide bioconjugates were analyzed by LCMS to confirm identities and purities. Our synthetic strategy for making the GRP78-targeting FITC-Ahx-Pep42-D-(KLAKAK)$_2$-AK-nucleolipid conjugate proved fruitful (**Scheme 4.1 and Figures 4.2, 4.3**) and sets the stage for making a small library of Pep42- D-(KLAKAK)$_2$-AK-nucleolipid bioconjugates for exploring selective and potent anti-cancer activities in tumors that overexpress GRP78 at the cell surface. The latter is a focal point of our current studies aimed towards the development of potent GRP78-targeting ligands.
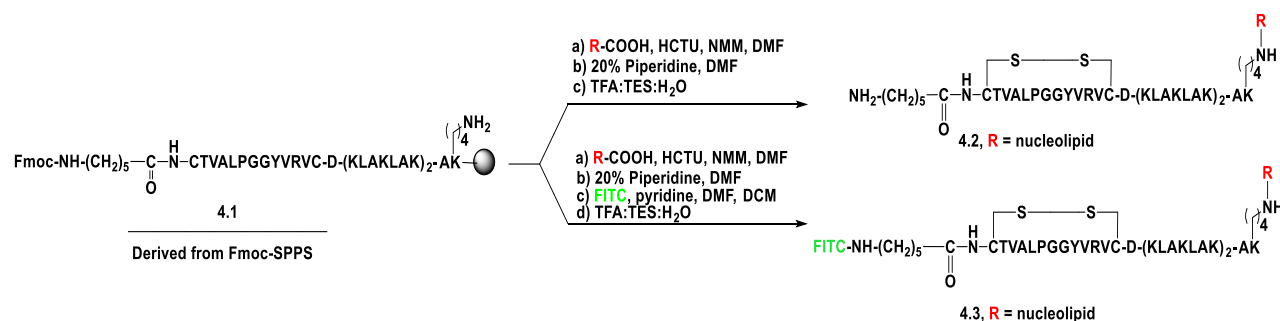
Scheme 4.1. Fmoc-solid phase peptide synthesis of Pep42-D-(KLAKAK)$_2$-AK-nucleolipid bioconjugates.
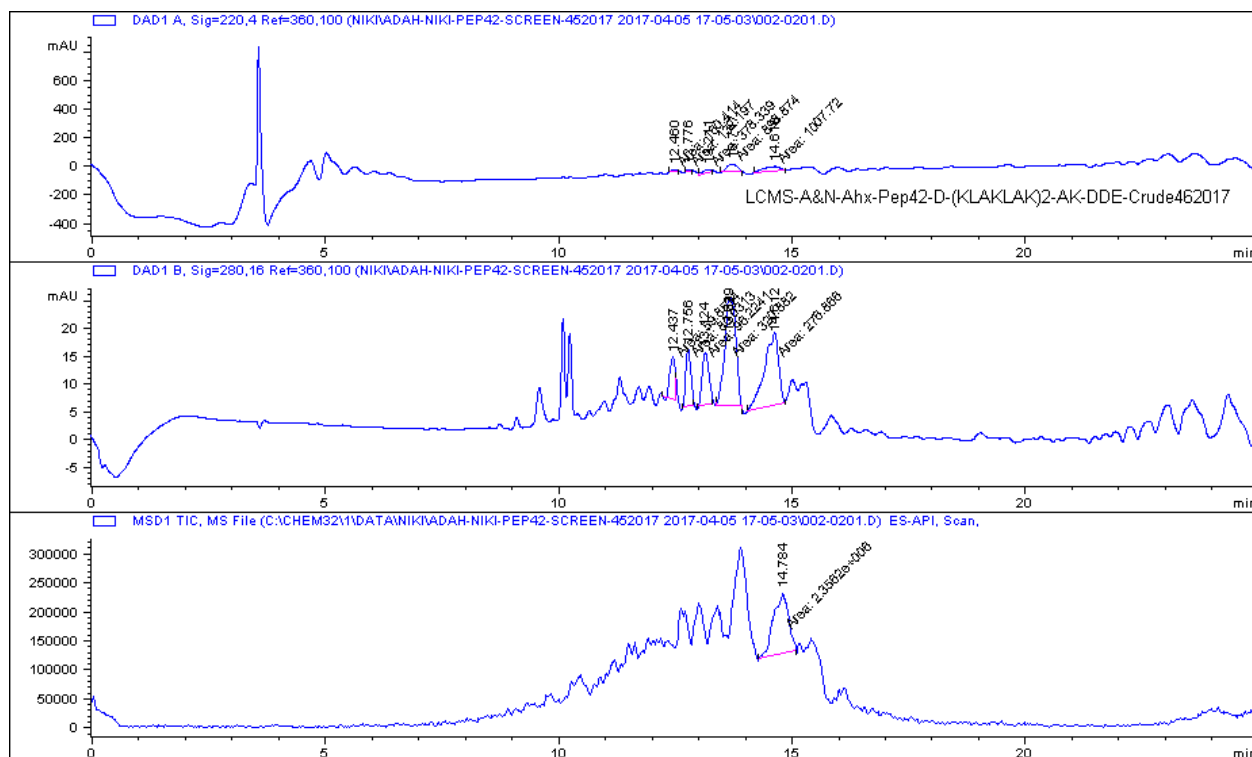
Figure 4.2. LC-MS analysis of crude AHx-CTVALPGGYVRVC-D-(KLAKLAKKLAKLAK)-AK-Dde using a linear gradient 20-80% MeOH/H$_2$O (0.1% FA) over 17 min using a Waters 2695 Symmetry® C18 column (3.9 x 150 mm, 5 μm particle size) set at a temperature of 25 °C at a flow rate of 1.0 mL/min with detection at 220 nm.
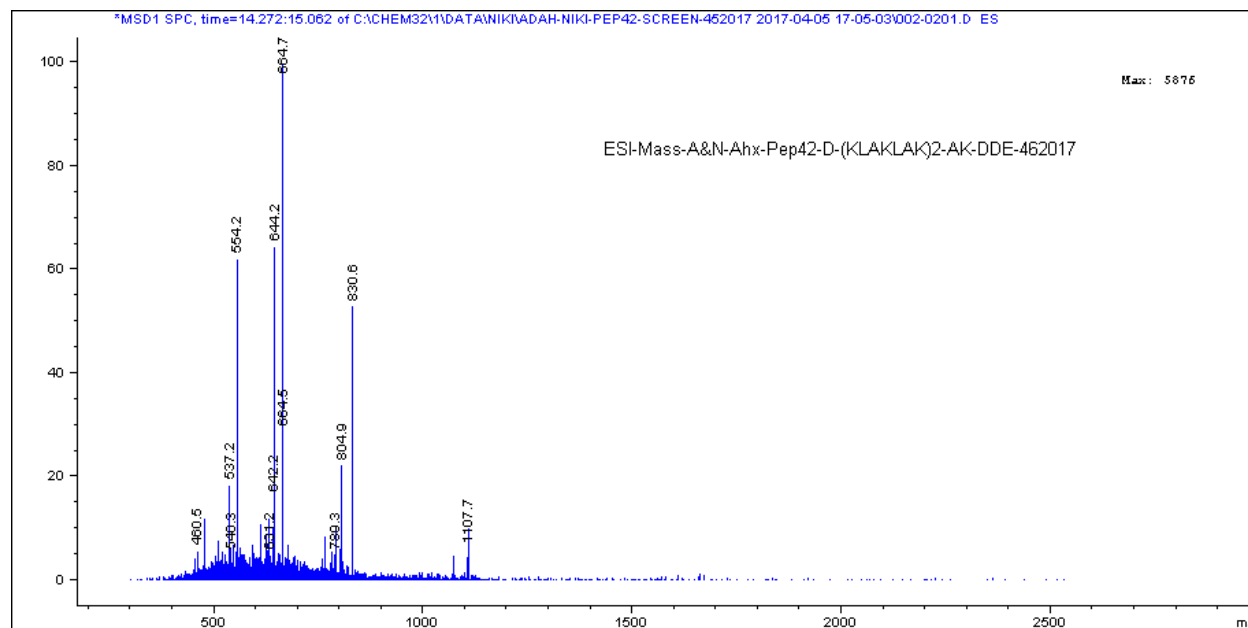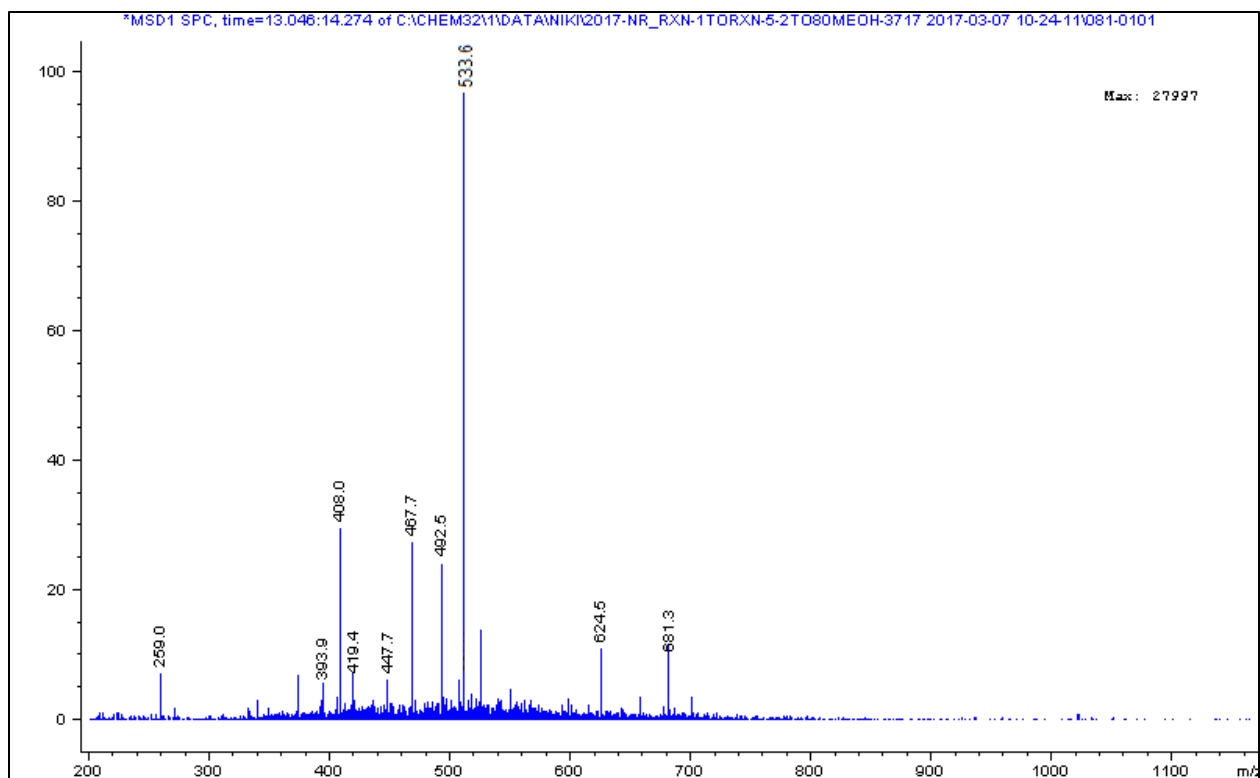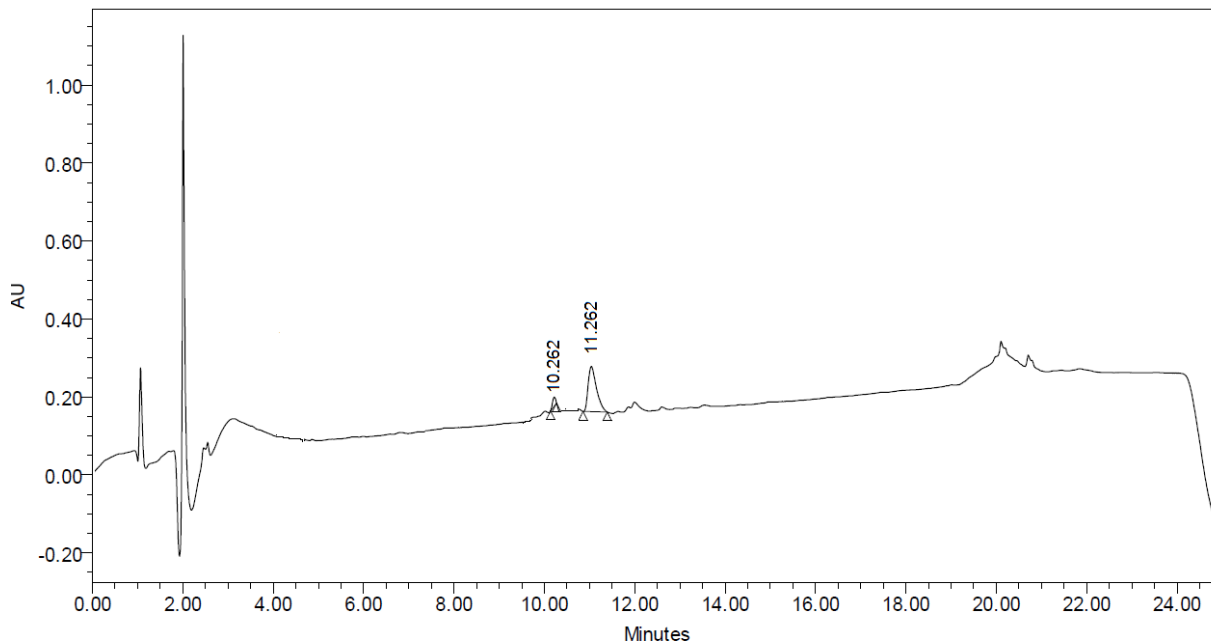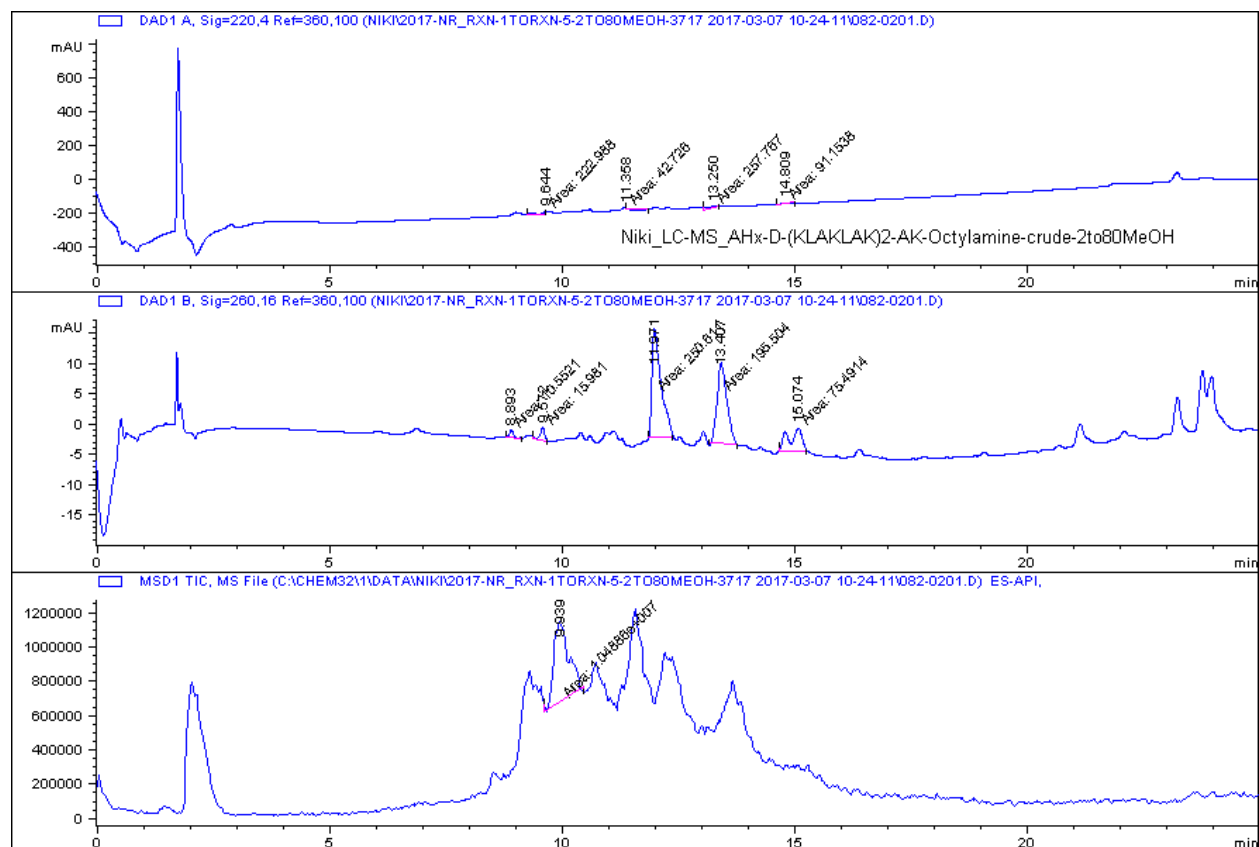
Figure 4.3. ESI-MS analysis of crude AHx-CTVALPGGYVRVC-D-(KLAKLAKKLAKLAK)-AK-Dde using a linear gradient 20-80% MeOH/H₂O (0.1% FA) over 17 min using a Waters 2695 Symmetry® C18 column (3.9 x 150 mm, 5 µm particle size) set at a temperature of 25 °C at a flow rate of 1.0 mL/min with detection at 220 nm.

4.3. REFERENCES

1) Javadpour, M. M.; Juban, M. M.; Lo, W. C.; Bishop, S. M.; Alberty, J. B.; Cowell, S. M.; Becker, C. L.; McLaughlin, M. L. *J. Med. Chem.* **1996**, *39*, 3107.

2) Rana, N.; Huang, S.; Patel, P.; Samuni, U.; Sabatino, D. *Bioorg. Med. Chem. Lett.* **2016**, *26,* 3567-3571.

3) Ryan, E.; Blake, A.J.; Benoit, A.; David, M.F.; Robert, A.K. *Invest. New Drugs*. **2013**, *31*, 285-292.

4) Joseph, S.C.; Blackman, B.A.; Kelly, M.L.; Phillips, M.; Beaury, M.W.; Martinez, I.; Parronchi, C.J.; Bitsaktsis, C.; Blake, A.D.; Sabatino, D. J. Pept. Sci. **2014**, *20*, 736-745.

5) Kim, Y.; Lillo, A.M.; Steiniger, S.C.; Liu, Y.; Ballatore, C.; Anichini, A.; Mortarini, R.; Kaufmann, G.F.; Zhou, B.; Felding-Habermann, B.; Janda, K.D. *Biochemistry*. **2006**, *45*, 9434-9444.

6) Li, J.; Lee, A.S.; *Curr. Mol. Med*. **2006**, *6*, 45-54.

4.4. PUBLICATIONS, INVENTION DISCLOSURES AND CONFERENCE PRESENTATIONS

Manuscripts accepted for publication

1) Rana, N., Huang, S., Patel, P., Samuni, U., Sabatino, D. **Synthesis, Characterization and Anti-Cancer Activity of a Peptide-Nucleolipid Bioconjugate.** *Bioorg. Med. Chem. Lett*., **2016,** *26*, 3567-3571.

2) Rana, N., Patel, P., Patel, M., Kozuch, S., Sabatino, D. **Nucleic Acid Bioconjugates in Cancer Detection and Therapy. ChemMedChem**, **2016**, *11*, 252-269.

3) Rana, N., Sabatino, D. **Solid-Phase Peptide Synthesis and Structural Analyses by Circular Dichroism Spectroscopy of the Cytotoxic D-(KLAKLAK)$_2$ Sequence**. Proceedings of the 24th American Peptide Symposium. American Peptide Society, June 10, **2015.**

Manuscripts accepted for publication

1) Rana, N., Phillips, M., Beck, A., Sabatino, D. **Diversity Oriented Synthesis of Peptide Nucleolipid Bioconjugates for Structure-Activity Relationship Studies.** *Manuscript in preparation.*

Poster Presentations

Selected presentation

1) Rana, N., Patel, P., Patel, H., Borland, E., Yadav, R., Hanawa, E., Goldman, D., Marzabadi, C., Samuni, U., Gorun, S.M., Sabatino, D. **Nucleic Acid Bioconjugates in Anti-Cancer Applications.** 248th ACS National Meeting & Exposition, San Francisco, CA, United States, Aug 10-14, (**2014**), MEDI-27766 (Sci-Mix)

Conference Presentations

1) <u>Rana, N.,</u> Sabatino, D. **Diversity Oriented Synthesis of Peptide Nucleolipid Bioconjugates for Structure-Activity Relationship Studies,** TIDES:Oligonucleotide and Peptides**,** SHMS, The New York Academy of Sciences, April 29-May 24, **2017.**

2) <u>Rana, N.,</u> Huang, S., Patel, P., Samuni, U., Sabatino, D. **Structure-Activity Relationship Studies of the Cytotoxic D-(KLAKLAK)$_2$ Peptide Sequence And Its Related Analogs**, The New York Academy of Sciences, May 25, **2016.**

3) <u>Rana, N</u>., Huang, S., Patel, P., Samuni, U., Sabatino, D. **Structure-Activity Relationship Studies of the Cytotoxic D-(KLAKLAK)$_2$ Peptide Sequence And Its Related Analogs**, The 61st annual New Jersey Academy of Sciences meeting, April 30, **2016.**

4) <u>Rana, N</u>., Huang, S., Patel, P., Samuni, U., Sabatino, D. **Structure-Activity Relationship Studies of the Cytotoxic D-(KLAKLAK)$_2$ Peptide Sequence And Its Related Analogs**, The 27th annual Dr. George Perez research colloquium, School of health and medical sciences, Seton Hall University, April 22, **2016.**

5) <u>Rana, N</u>., Huang, S., Patel, P., Samuni, U., Sabatino, D. **Structure-Activity Relationship Studies of the Cytotoxic D-(KLAKLAK)$_2$ Peptide Sequence And Its Related Analogs**, 20th Annual Petersheim Academic Expositions, Seton Hall University, April 19, **2016**.

6) <u>Rana, N</u>., Sabatino, D. **Solid-Phase Peptide Synthesis and Structural Analyses by Circular Dichroism Spectroscopy of the Cytotoxic D-(KLAKLAK)$_2$ Sequence**, 24th American Peptide Symposium. American Peptide Society, June 10, **2015**.

7) <u>Rana, N</u>., Sabatino, D. **Solid-Phase Peptide Synthesis and Structural Analyses by Circular Dichroism Spectroscopy of the Cytotoxic D-(KLAKLAK)$_2$ Sequence**, The New York Academy of Sciences, May 25, **2015**.

8) <u>Rana, N</u>., Sabatino, D. **Solid-Phase Peptide Synthesis and Structural Analyses by Circular Dichroism Spectroscopy of the Cytotoxic D-(KLAKLAK)$_2$ Sequence**, 19th Annual Petersheim Academic Expositions, Seton Hall University, April 21, **2015**.

9) <u>Rana, N</u>., Patel, P., Patel, M., Goldman, D., Maina, A., Carrion, E., Kozuch, S., Patel, H., Borland, E., Cultrara, C., Yadav, R., Hanawa, E., Blackman, B., Samuni, U., Marzabadi, C., Blake, A., Gorun, S.M., Sabatino, D. **Modifying the sizes and shape of nucleic acids by chemical synthesis**. April 22, (**2014**), 20th Annual Petersheim Academic Expositions, Seton Hall University, April 21, **2014**.

10) <u>Rana, N</u>., Patel, P., Patel, H., Borland, E., Yadav, R., Hanawa, E., Goldman, D., Marzabadi, C., Samuni, U., Gorun, S.M., Sabatino, D. **Nucleic Acid Bioconjugates in Anti-Cancer Applications**. 248th ACS National Meeting & Exposition, San Francisco, CA, United States, Aug 10-14, (**2014**)

11) <u>Rana, N</u>., Patel, P., Patel, M., Goldman, D., Maina, A., Carrion, E., Kozuch, S., Patel, H., Borland, E., Cultrara, C., Yadav, R., Hanawa, E., Blackman, B., Samuni, U., Marzabadi, C., Blake, A., Gorun, S.M., Sabatino, D. **Modifying the sizes and shape of nucleic acids by chemical synthesis**. June 5, (**2014**), the New York Academy of Sciences.

12) <u>Rana, N</u>., Patel, P., Patel, H., Borland, E., Sabatino, D. **Nucleic Acid Bioconjugates in Anticancer Application**. New York Academy of Science, December 11, **2013**.

13) <u>Rana, N</u>., Patel, P., Sabatino, D. **Applications of an amino acyl Nucleolipid Bio-conjugate in Medicinal Chemistry**. 17th Annual Petersheim Academic Expositions, Seton Hall University, April 18, **2013**.

14) <u>Rana, N</u>., Mistry, B., **Spectroscopy Methods and Application**s, Department of Chemistry. Spectroscopy Conference. South Gujarat University, India, April 1, **2010**

Book Chapter Contribution

1) <u>Rana, N</u>., Phillips, M., Luisi, G., Carrion, E., Sabatino, D. **Development of peptide biomarkers**, Wiley online library, **2017.** (*In press)*

TABLE OF CONTENTS

Sequence: AHx-D-(KLAKLAKKLAKLAK)-AK-Methylamine nucleolipid, **3.22**

Solvent: 2-80% MeOH (0.1% FA) over 17 min

Detection: PDA 220nm

Results and analysis:

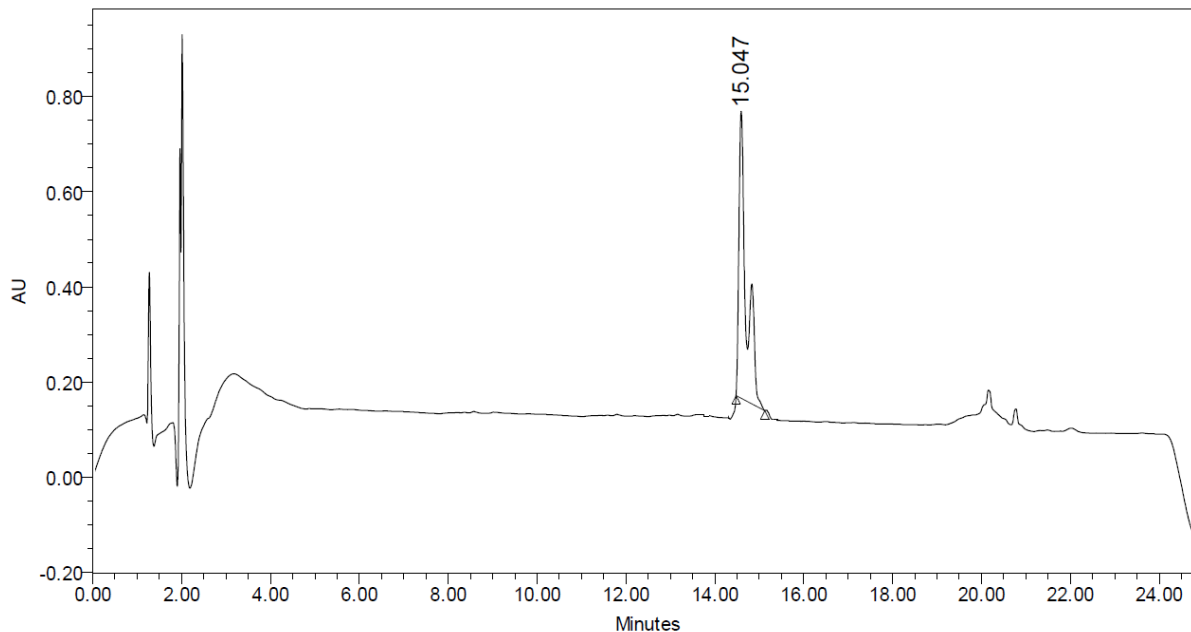|	Retention Time	Area	% Area	Height
1	10.671	395043	98.95	133547
2	11.608	71105	1.05	4450

Figure A1. RP-HPLC analysis of purified AHx-D-(KLAKLAKKLAKLAK)-AK-Methylamine nucleolipid, **3.22** using a linear gradient 2-80% MeOH/H_2O (0.1% FA) over 17 min using a Waters 2695 Symmetry® C18 column (3.9 x 150 mm, 5 μm particle size) set at a temperature of 25 °C at a flow rate of 1.0 mL/min with detection at 220 nm.
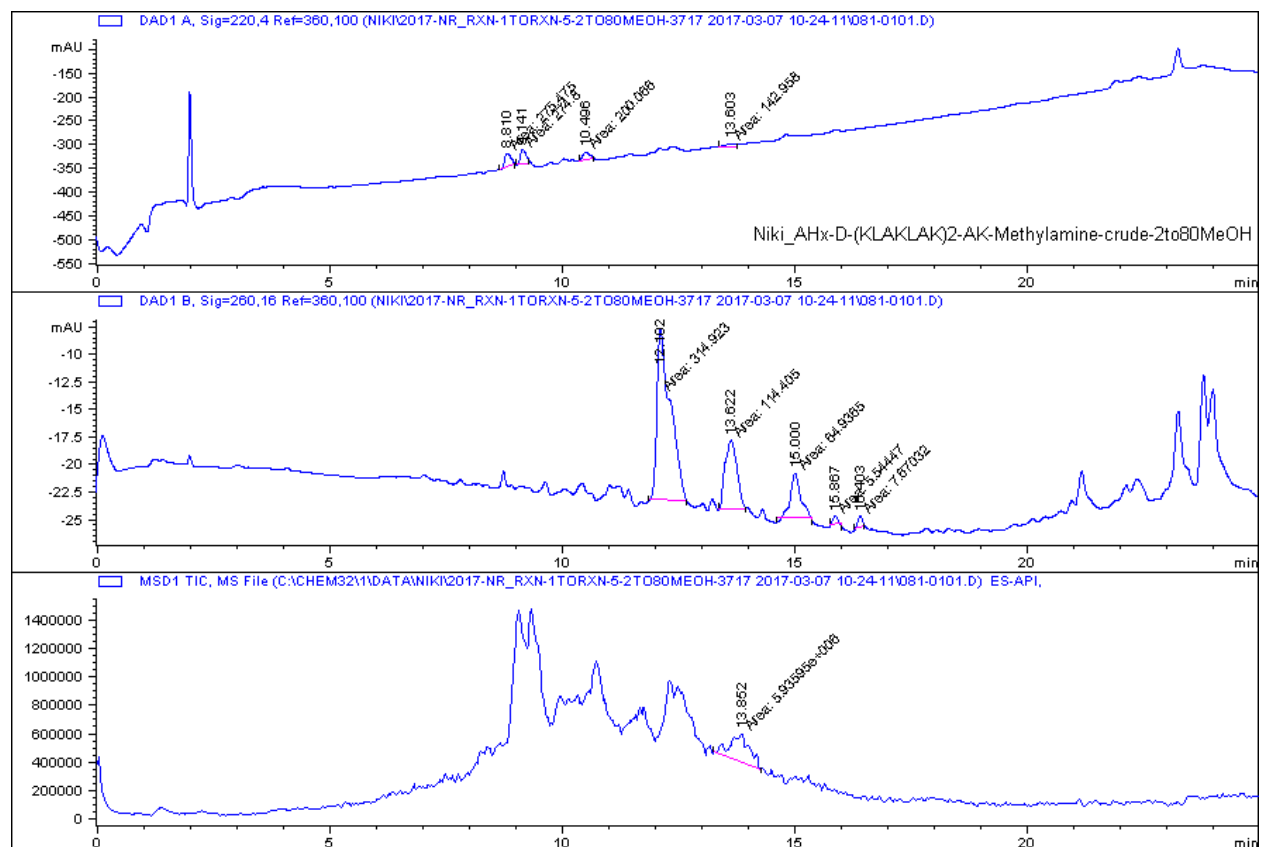
Figure A2. LC-MS analysis of crude AHx-D-(KLAKLAKKLAKLAK)-AK-Methylamine nucleolipid, **3.22** using a linear gradient 2-80% MeOH/H$_2$O (0.1% FA) over 17 min using a Waters 2695 Symmetry® C18 column (3.9 x 150 mm, 5 μm particle size) set at a temperature of 25 °C at a flow rate of 1.0 mL/min with detection at 220 nm.
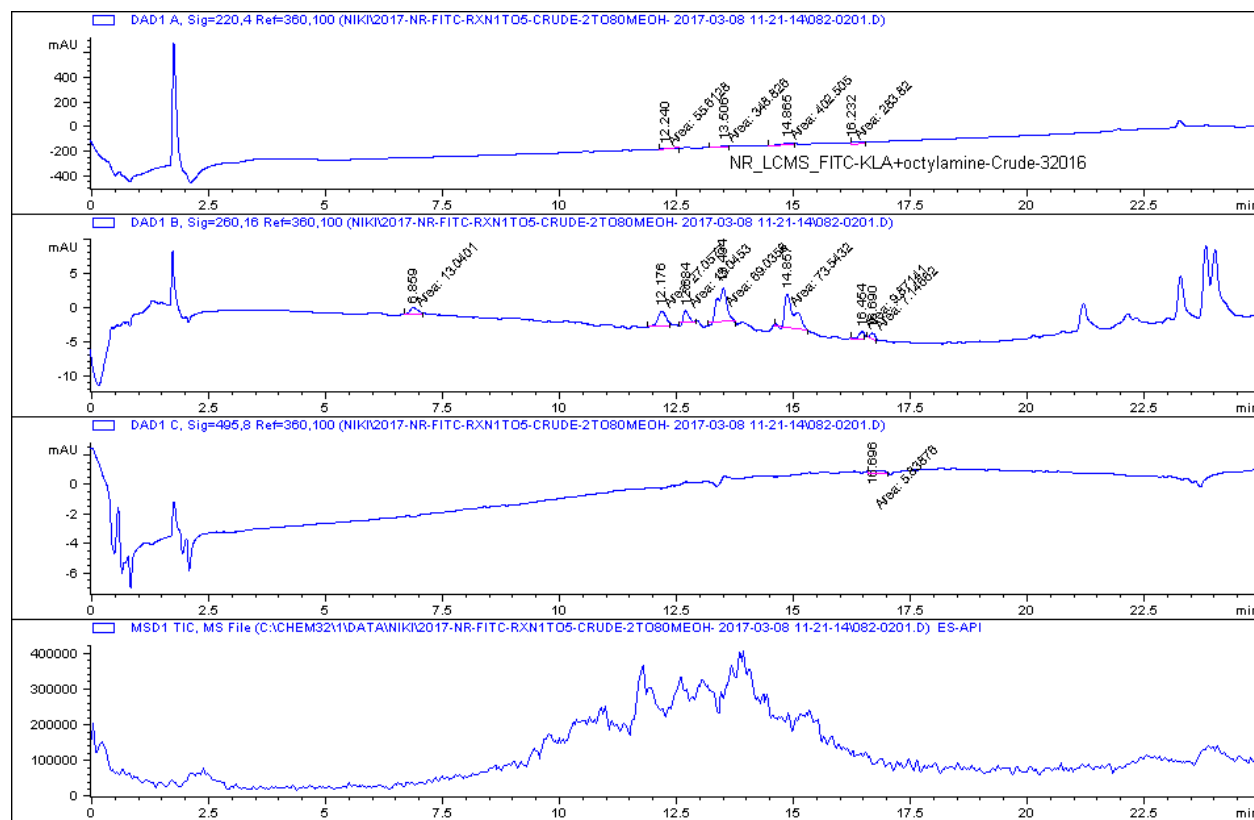
Figure A3. ESI-LCMS analysis of purified AHx-D-(KLAKLAKKLAKLAK)-AK-Methylamine nucleolipid, **3.22** using a linear gradient 2-80% MeOH/H$_2$O (0.1% FA) over 17 min using a Waters 2695 Symmetry® C18 column (3.9 x 150 mm, 5 μm particle size) set at a temperature of 25 °C at a flow rate of 1.0 mL/min with detection at 220 nm.
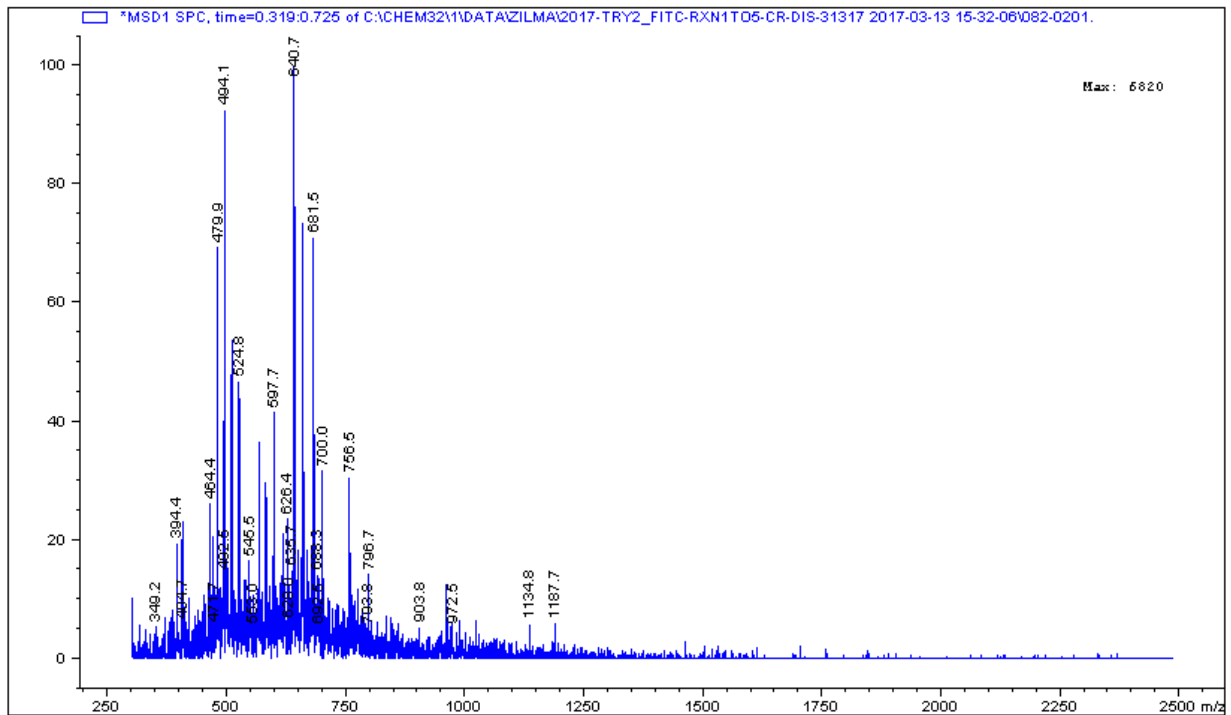
Sequence: AHx-D-(KLAKLAKKLAKLAK)-AK-Octylamine nucleolipid, **3.23**

Solvent: 2-80% MeOH (0.1% FA) over 17 min

Detection: PDA 220nm

Results and analysis:

	Retention Time	Area	% Area	Height
1	10.262	1797	4.05	23666
2	11.262	108567	95.95	33003

Figure A4. RP-HPLC analysis of purified AHx-D-(KLAKLAKKLAKLAK)-AK-Octylamine nucleolipid, **3.23** using a linear gradient 2-80% MeOH/H$_2$O (0.1% FA) over 17 min using a Waters 2695 Symmetry® C18 column (3.9 x 150 mm, 5 μm particle size) set at a temperature of 25 °C at a flow rate of 1.0 mL/min with detection at 220 nm.
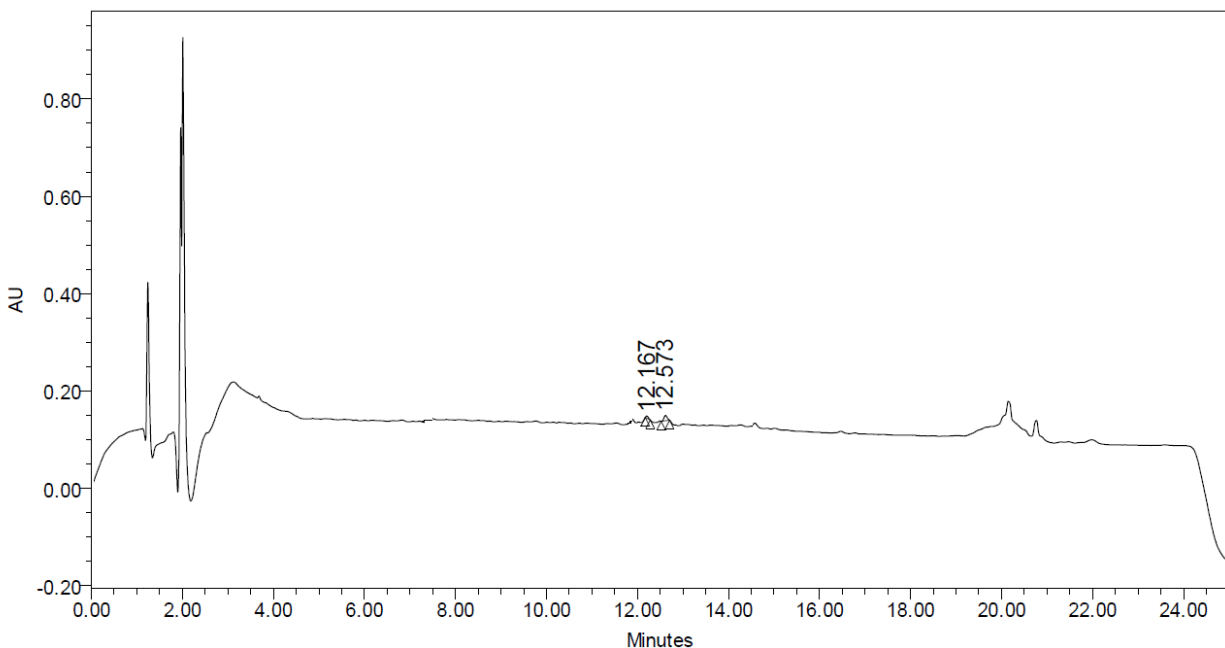
Figure A5. LCMS analysis of crude AHx-D-(KLAKLAKKLAKLAK)-AK-Octcylamine nucleolipid, **3.23** using a linear gradient 2-80% MeOH/H_2O (0.1% FA) over 17 min using a Waters 2695 Symmetry® C18 column (3.9 x 150 mm, 5 μm particle size) set at a temperature of 25 °C at a flow rate of 1.0 mL/min with detection at 220 nm.
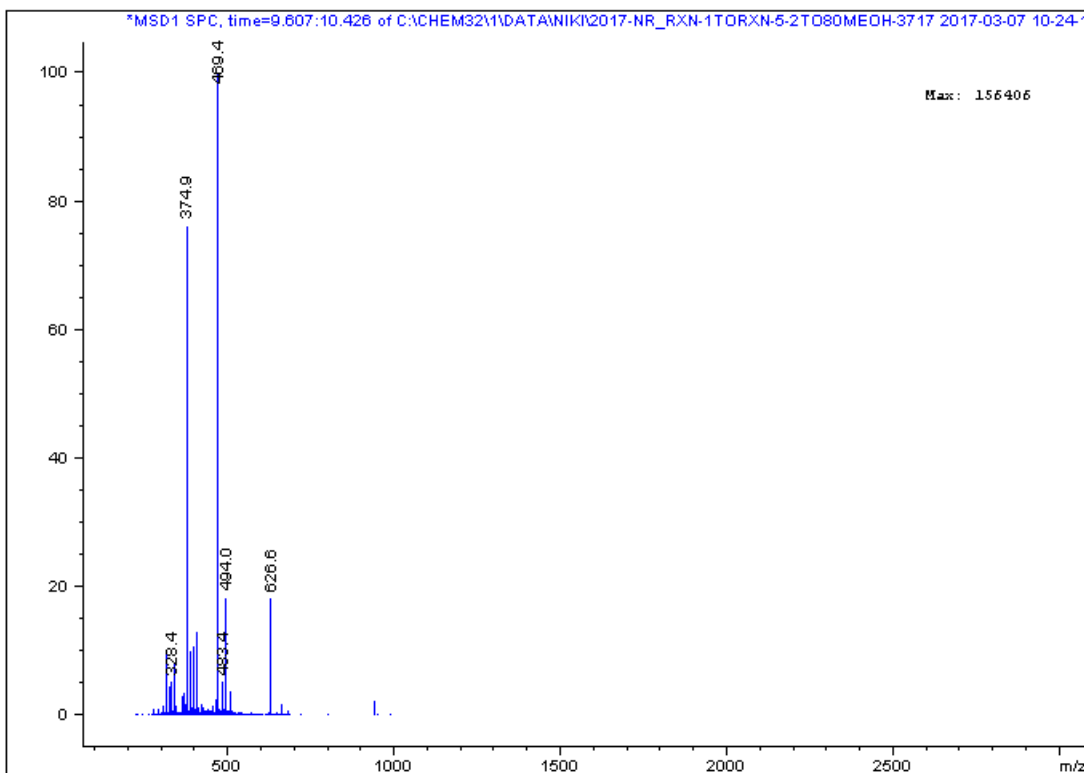
Figure A6. ESI-LCMS analysis of purified AHx-D-(KLAKLAKKLAKLAK)-AK-Octylamine nucleolipid, **3.23** using a linear gradient 2-80% MeOH/H$_2$O (0.1% FA) over 17 min using a Waters 2695 Symmetry® C18 column (3.9 x 150 mm, 5 μm particle size) set at a temperature of 25 °C at a flow rate of 1.0 mL/min with detection at 220 nm.
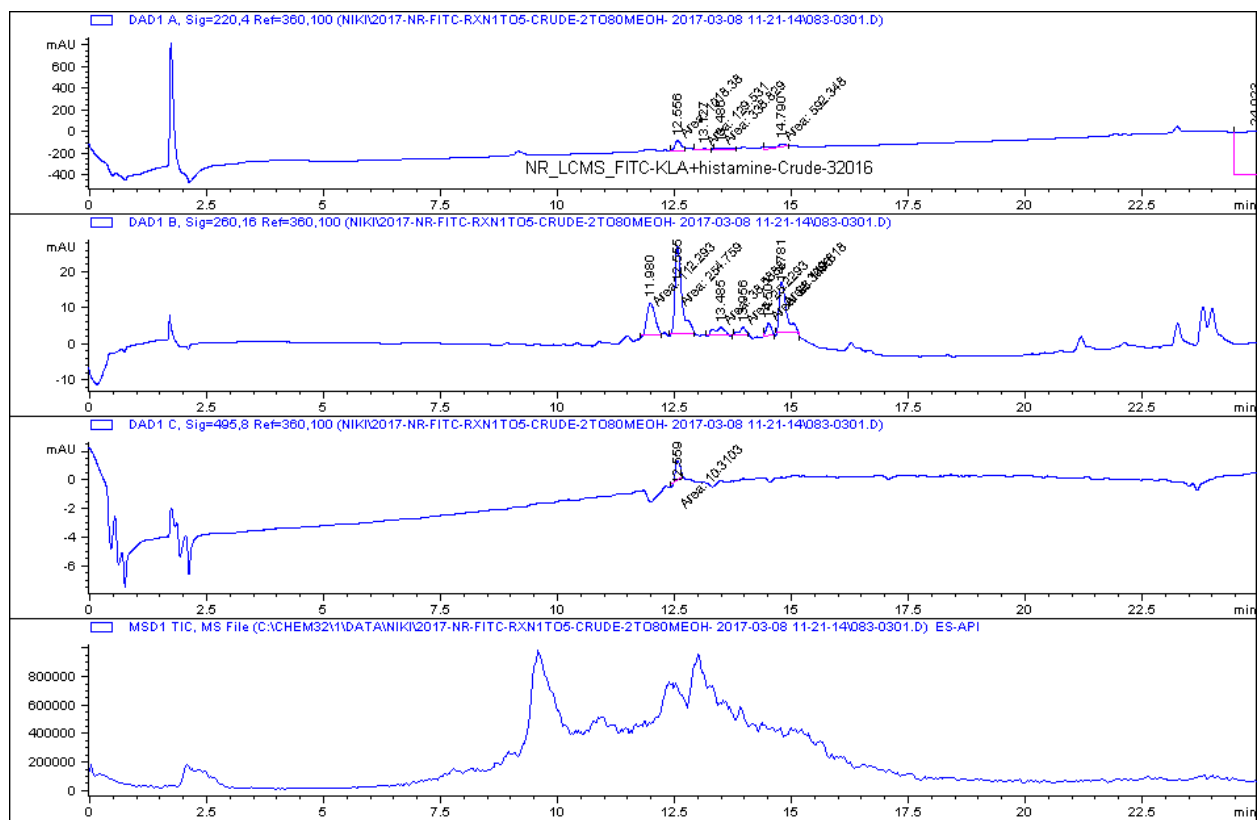
Sequence: AHx-D-(KLAKLAKKLAKLAK)-AK-Histamine nucleolipid, **3.24**

Solvent: 2-80% MeOH (0.1% FA) over 17 min

Detection: PDA 220nm
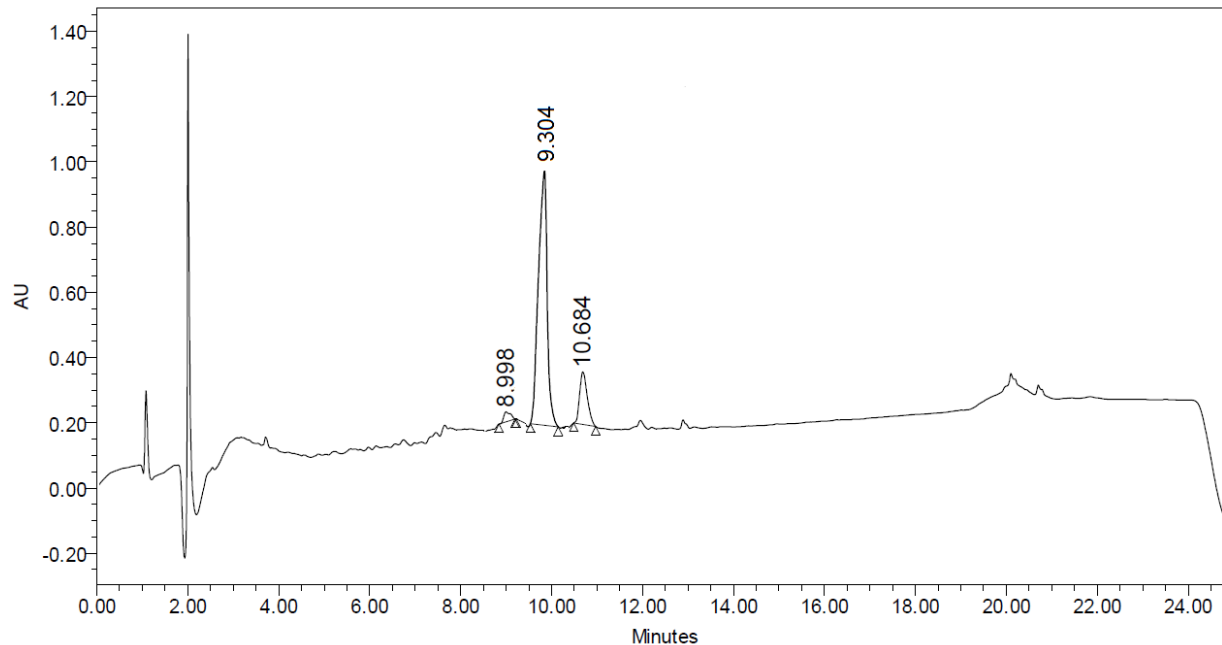
Results and analysis:

	Retention Time	Area	% Area	Height
1	8.998	31396	1.34	30778
2	9.304	573102	95.01	123665
3	10.684	188451	3.65	161128

Figure A7. RP-HPLC analysis of purified AHx-D-(KLAKLAKKLAKLAK)-AK-Histamine nucleolipid, **3.24** using a linear gradient 2-80% MeOH/H_2O (0.1% FA) over 17 min using a Waters 2695 Symmetry® C18 column (3.9 x 150 mm, 5 μm particle size) set at a temperature of 25 °C at a flow rate of 1.0 mL/min with detection at 220 nm.
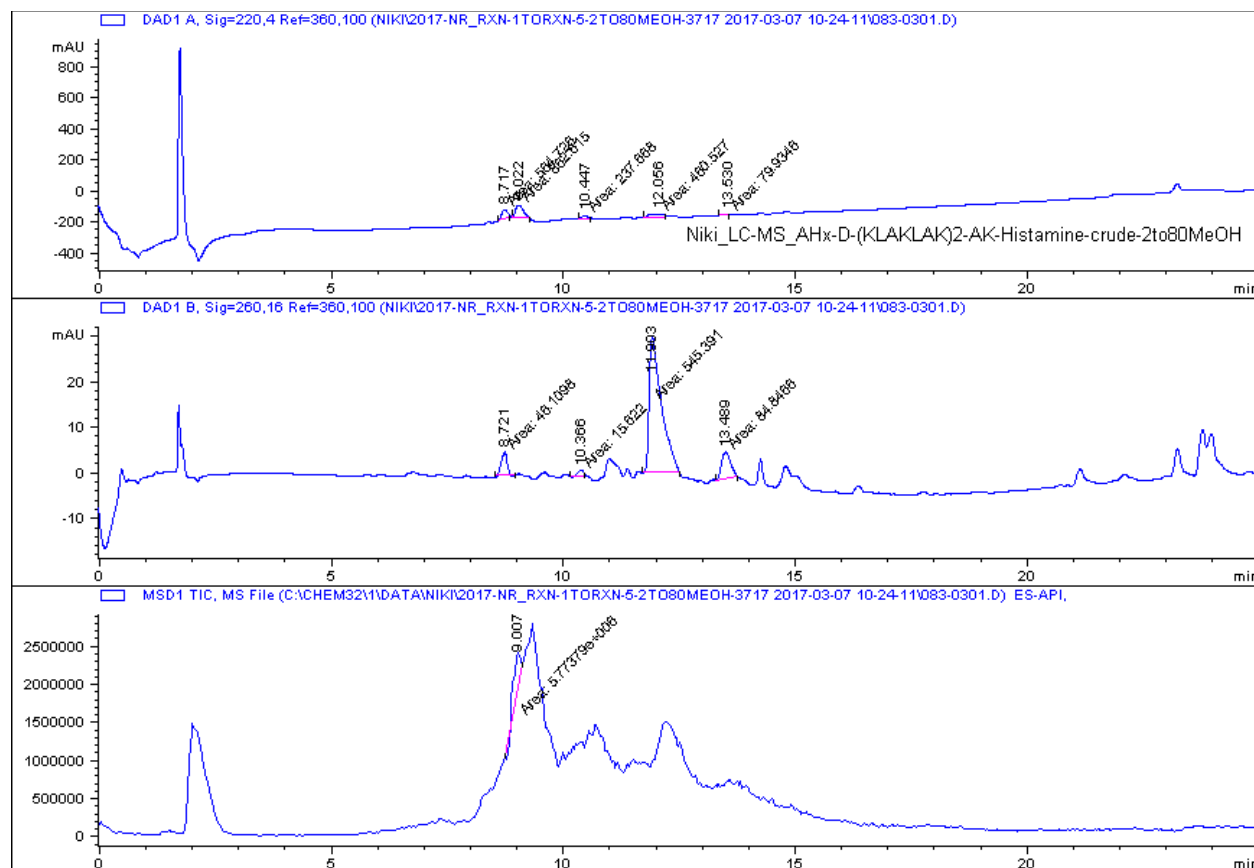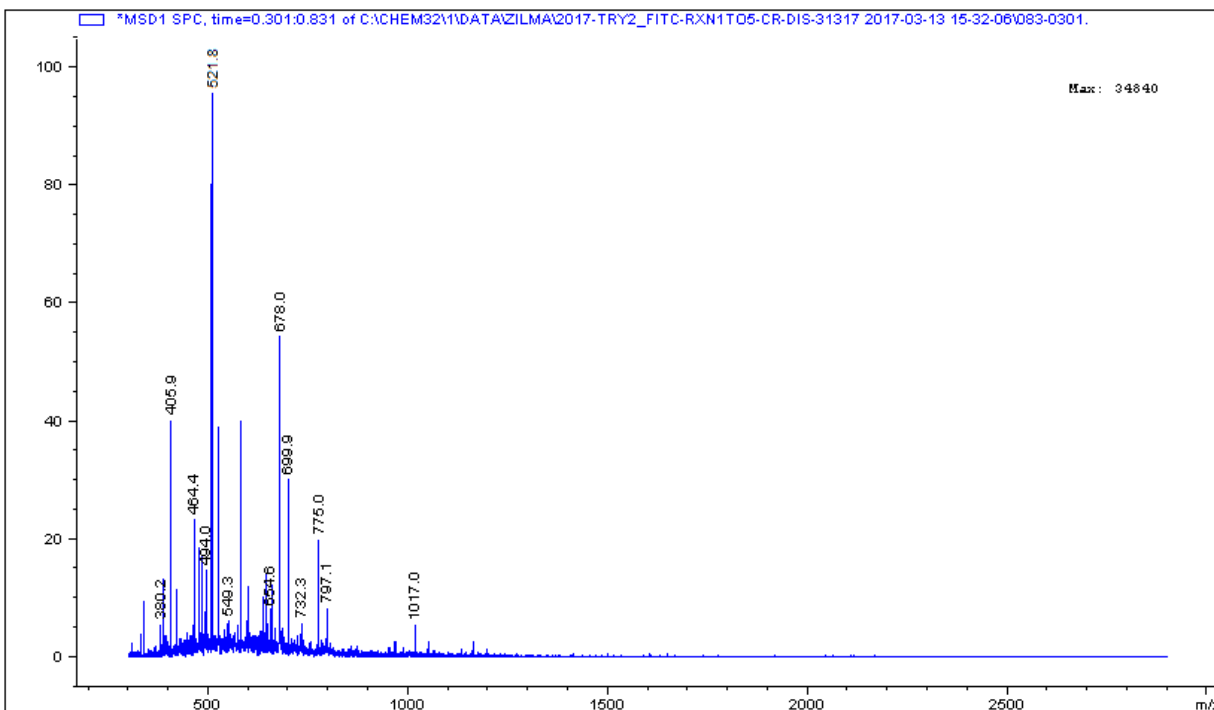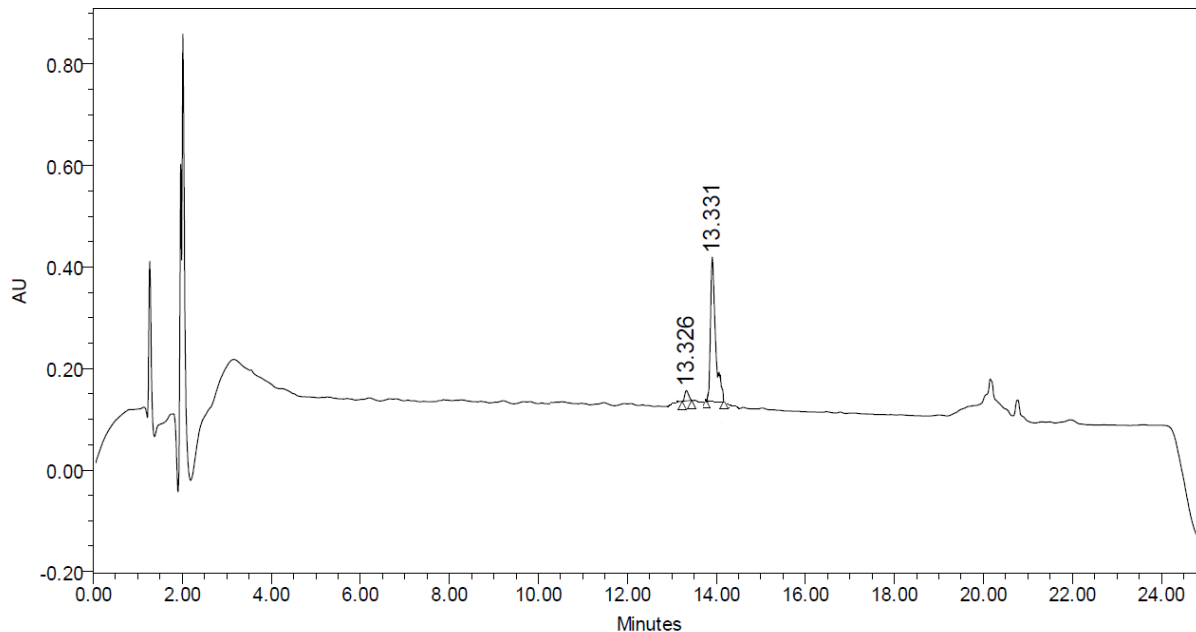
Figure A8. LCMS analysis of crude AHx-D-(KLAKLAKKLAKLAK)-AK-Histamine nucleolipid, **3.24** using a linear gradient 2-80% MeOH/H$_2$O (0.1% FA) over 17 min using a Waters 2695 Symmetry® C18 column (3.9 x 150 mm, 5 μm particle size) set at a temperature of 25 °C at a flow rate of 1.0 mL/min with detection at 220 nm.
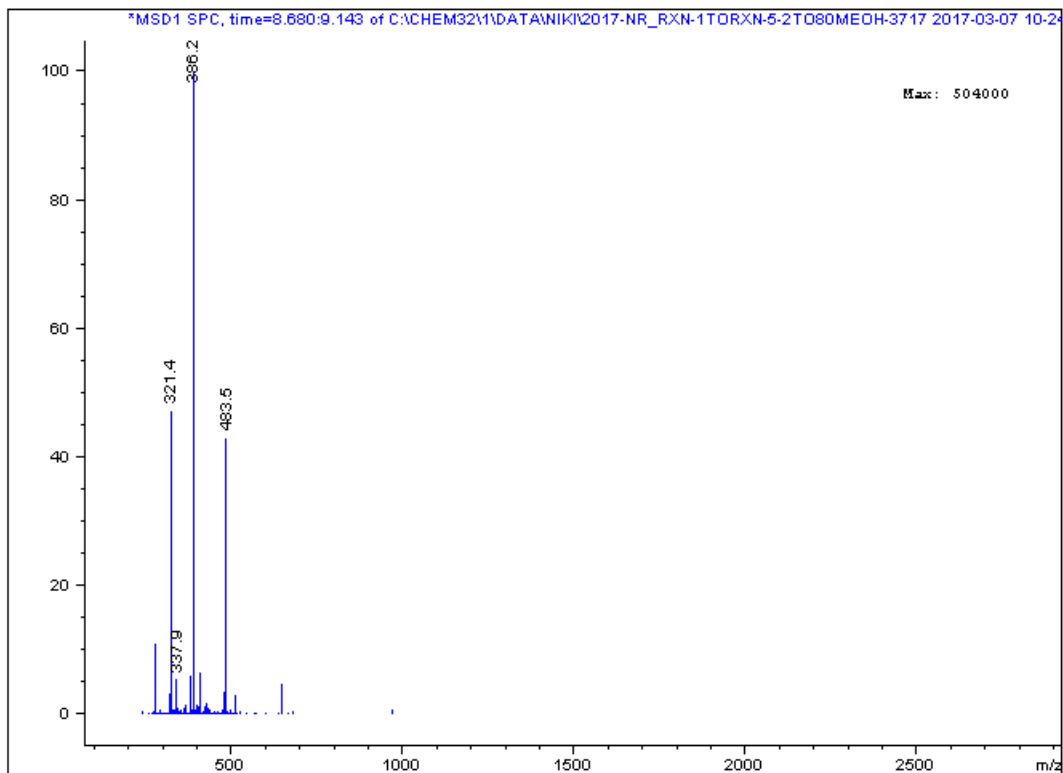
Figure A9. ESI-LCMS analysis of purified AHx-D-(KLAKLAKKLAKLAK)-AK-Histamine nucleolipid, **3.24** using a linear gradient 2-80% MeOH/H_2O (0.1% FA) over 17 min using a Waters 2695 Symmetry® C18 column (3.9 x 150 mm, 5 µm particle size) set at a temperature of 25 °C at a flow rate of 1.0 mL/min with detection at 220 nm.
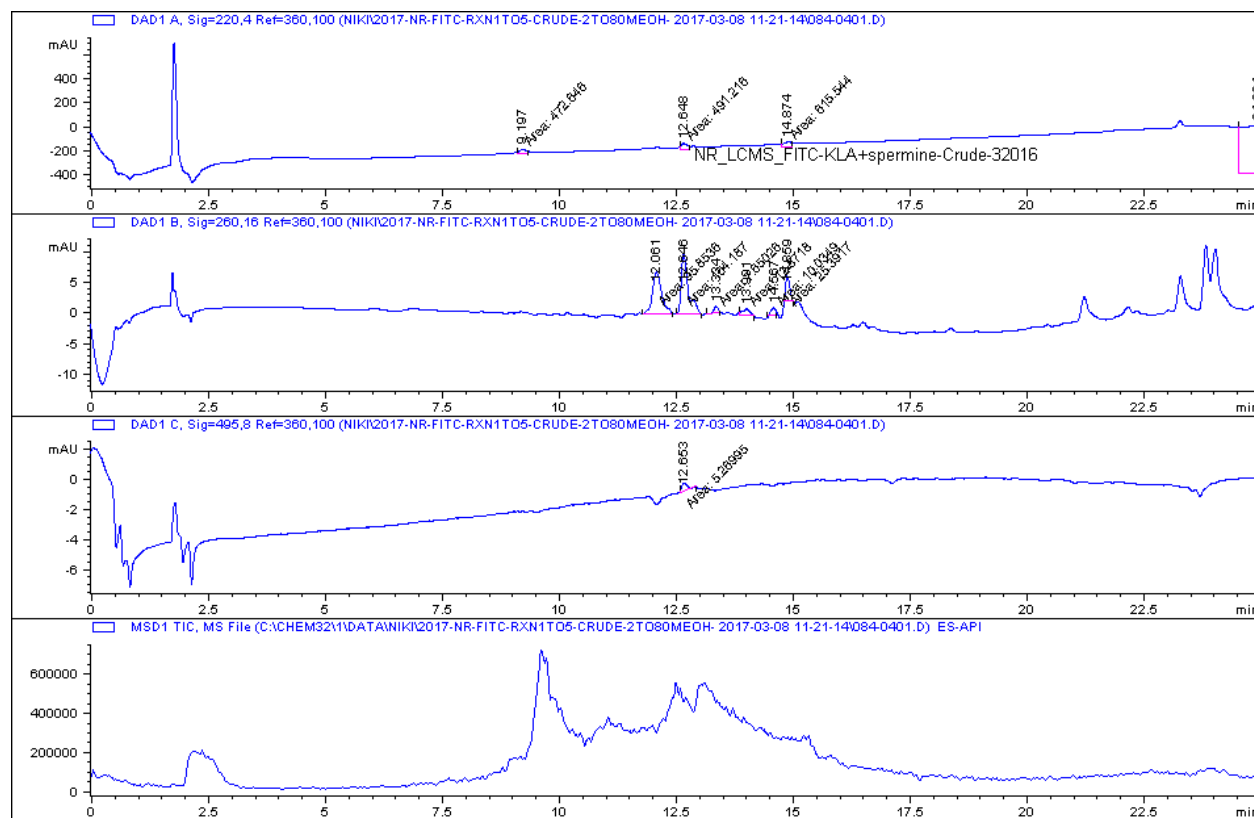
Sequence: AHx-D-(KLAKLAKKLAKLAK)-AK-Spermine nucleolipid, **3.25**

Solvent: 2-80% MeOH (0.1% FA) over 17 min

Detection: PDA 220nm
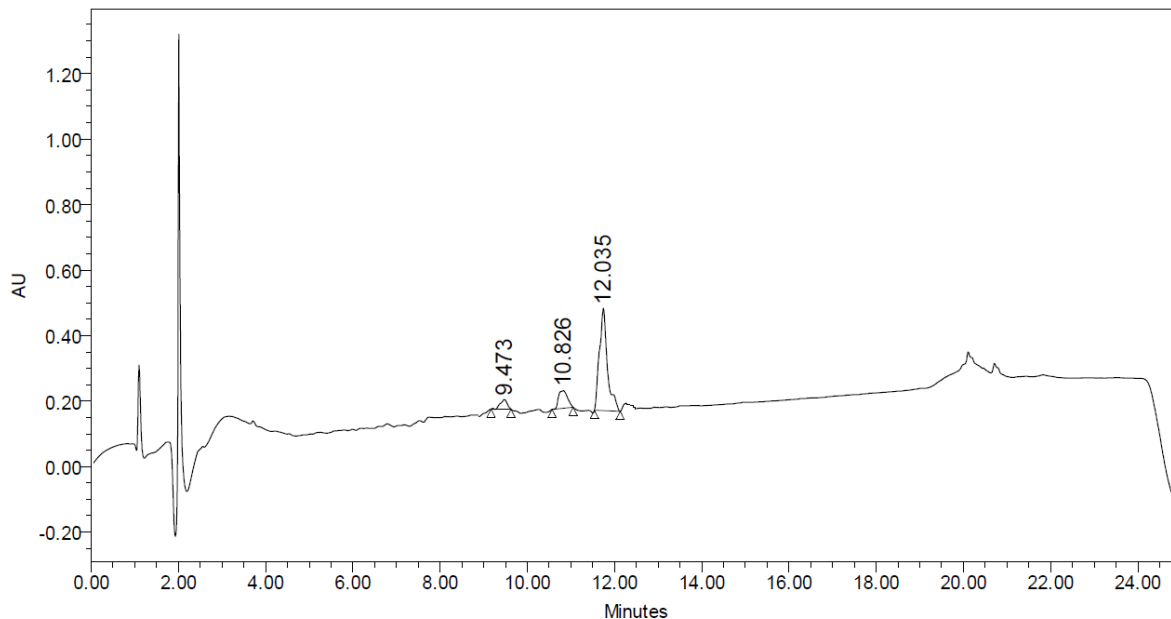
Results and analysis:

	Retention Time	Area	% Area	Height
1	9.473	318468	1.20	1141
2	10.826	763932	2.46	53514
3	12.035	1193838	96.34	95167

Figure A10. RP-HPLC analysis of purified AHx-D-(KLAKLAKKLAKLAK)-AK-Spermine nucleolipid, **3.25** using a linear gradient 2-80% MeOH/H_2O (0.1% FA) over 17 min using a Waters 2695 Symmetry® C18 column (3.9 x 150 mm, 5 μm particle size) set at a temperature of 25 °C at a flow rate of 1.0 mL/min with detection at 220 nm.
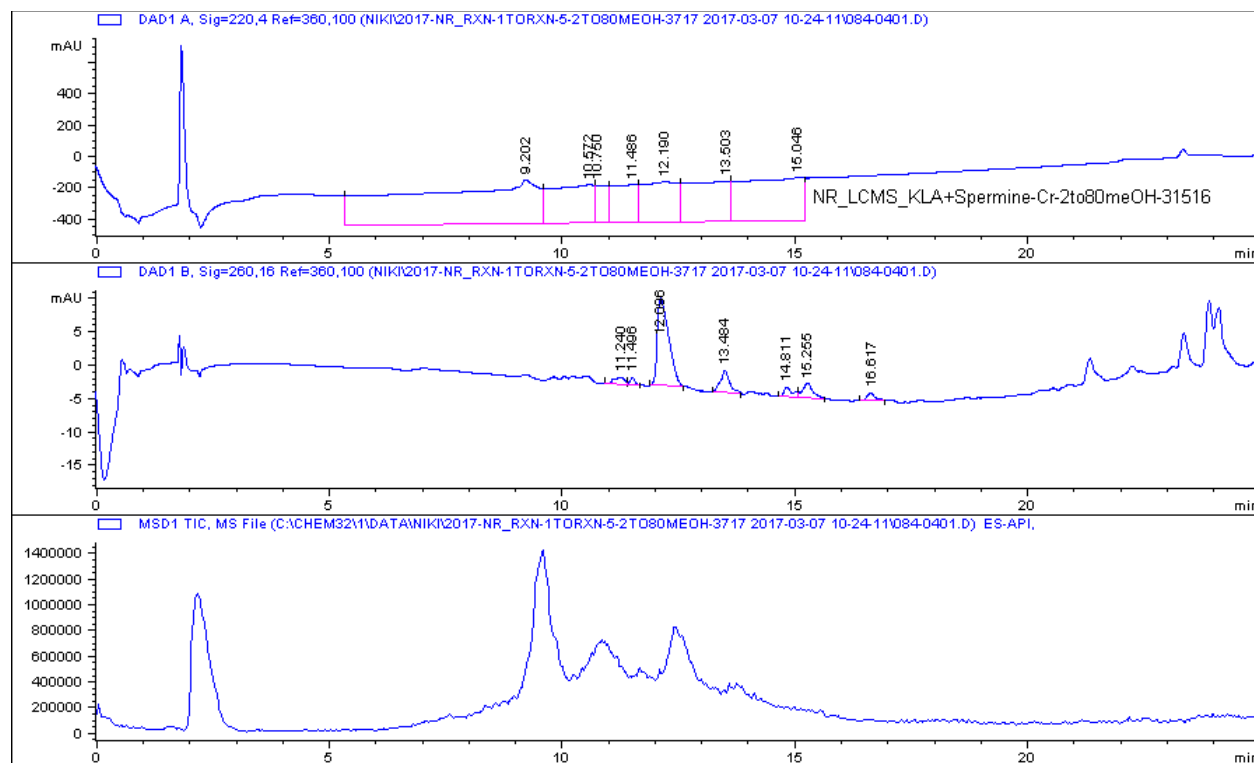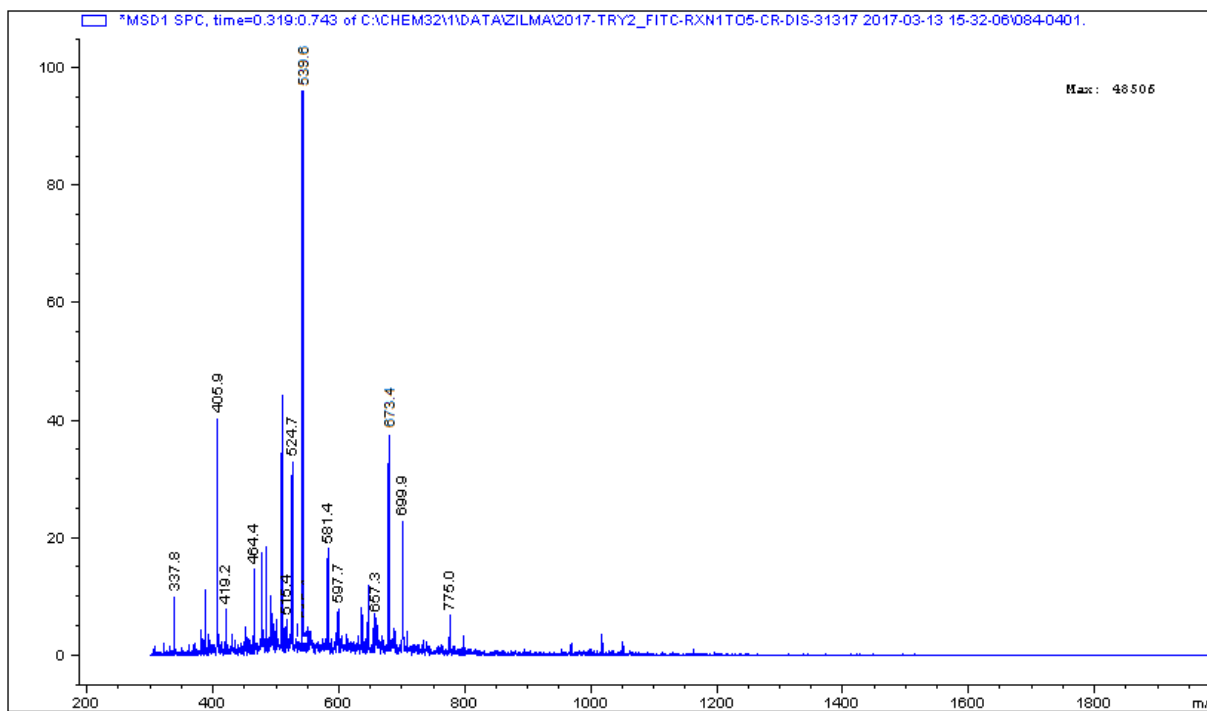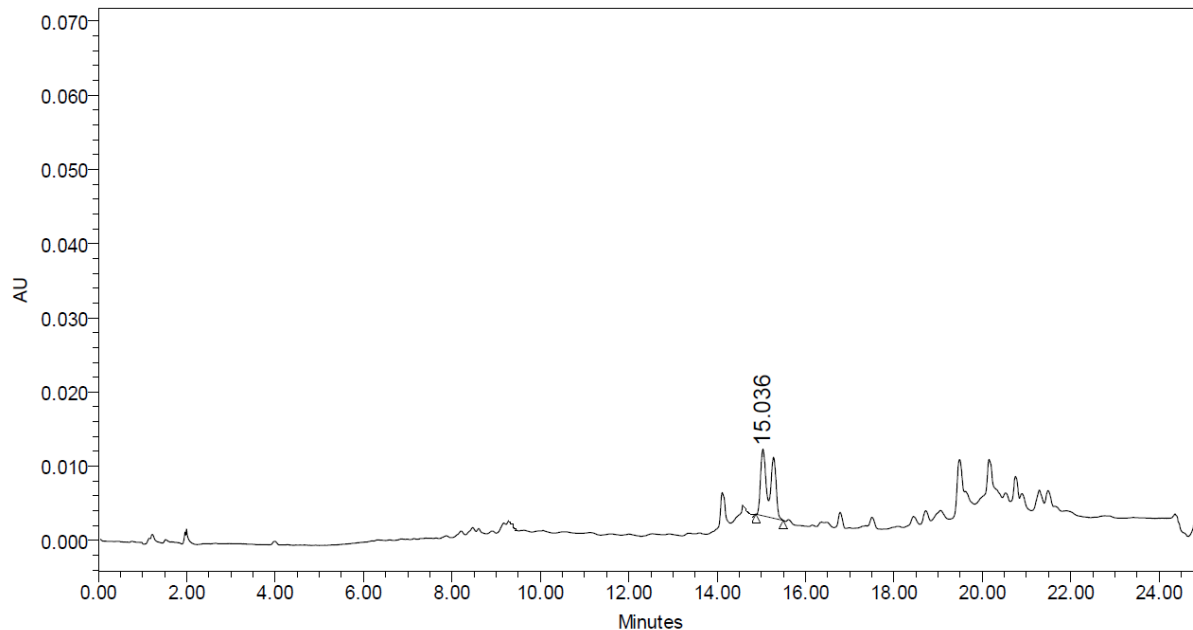
Figure A11. LCMS analysis of purified AHx-D-(KLAKLAKKLAKLAK)-AK-Spermine nucleolipid, **3.25** using a linear gradient 2-80% MeOH/H$_2$O (0.1% FA) over 17 min using a Waters 2695 Symmetry® C18 column (3.9 x 150 mm, 5 μm particle size) set at a temperature of 25 °C at a flow rate of 1.0 mL/min with detection at 220 nm.
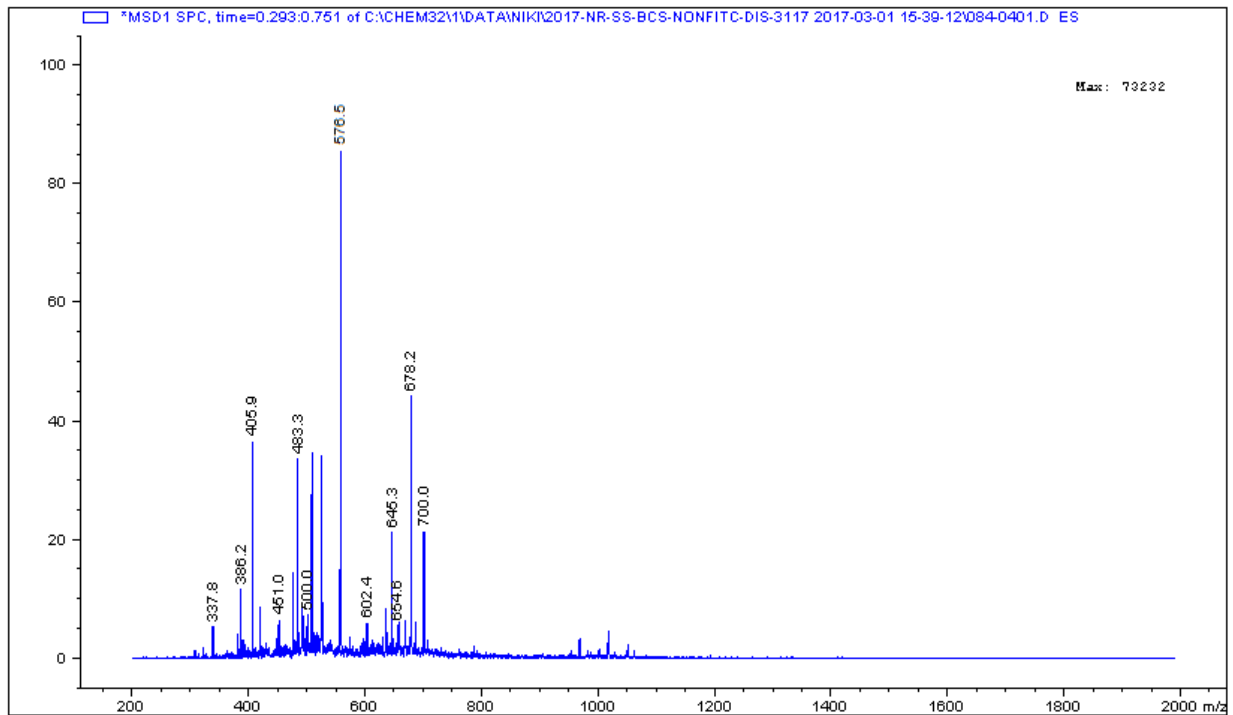
Figure A12. ESI-LCMS analysis of purified AHx-D-(KLAKLAKKLAKLAK)-AK-Spermine nucleolipid, **3.25** using a linear gradient 2-80% MeOH/H$_2$O (0.1% FA) over 17 min using a Waters 2695 Symmetry® C18 column (3.9 x 150 mm, 5 μm particle size) set at a temperature of 25 °C at a flow rate of 1.0 mL/min with detection at 220 nm.

Sequence: AHx-D-(KLAKLAKKLAKLAK)-AK-1,3-diaminopropane nucleolipid, **3.26**

Solvent: 2-80% MeOH (0.1% FA) over 17 min

Detection: PDA 220nm
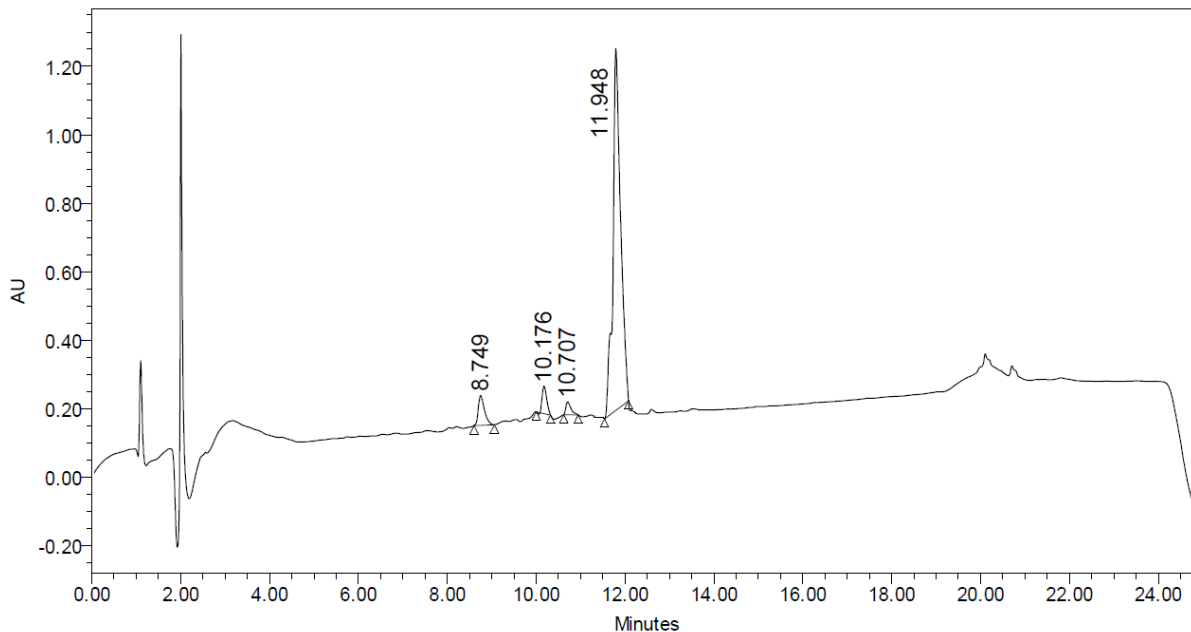
Results and analysis:

	Retention Time	Area	% Area	Height
1	8.749	38426	0.86	86646
2	10.176	586519	1.20	79560
3	10.707	296971	0.91	36979
4	11.948	857782	97.03	97567

Figure A13. RP-HPLC analysis of purified AHx-D-(KLAKLAKKLAKLAK)-AK-1,3-diaminopropane nucleolipid, **3.26** using a linear gradient 2-80% MeOH/H_2O (0.1% FA) over 17 min using a Waters 2695 Symmetry® C18 column (3.9 x 150 mm, 5 μm particle size) set at a temperature of 25 °C at a flow rate of 1.0 mL/min with detection at 220 nm.
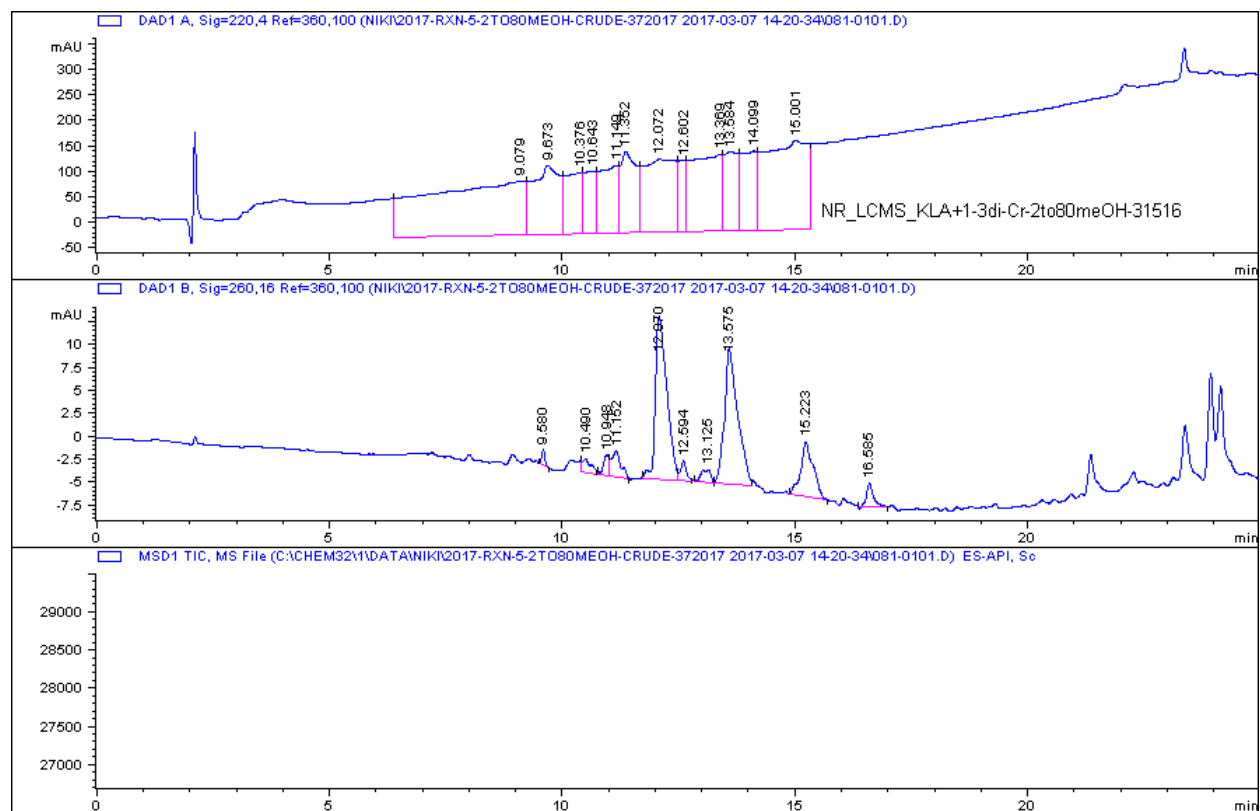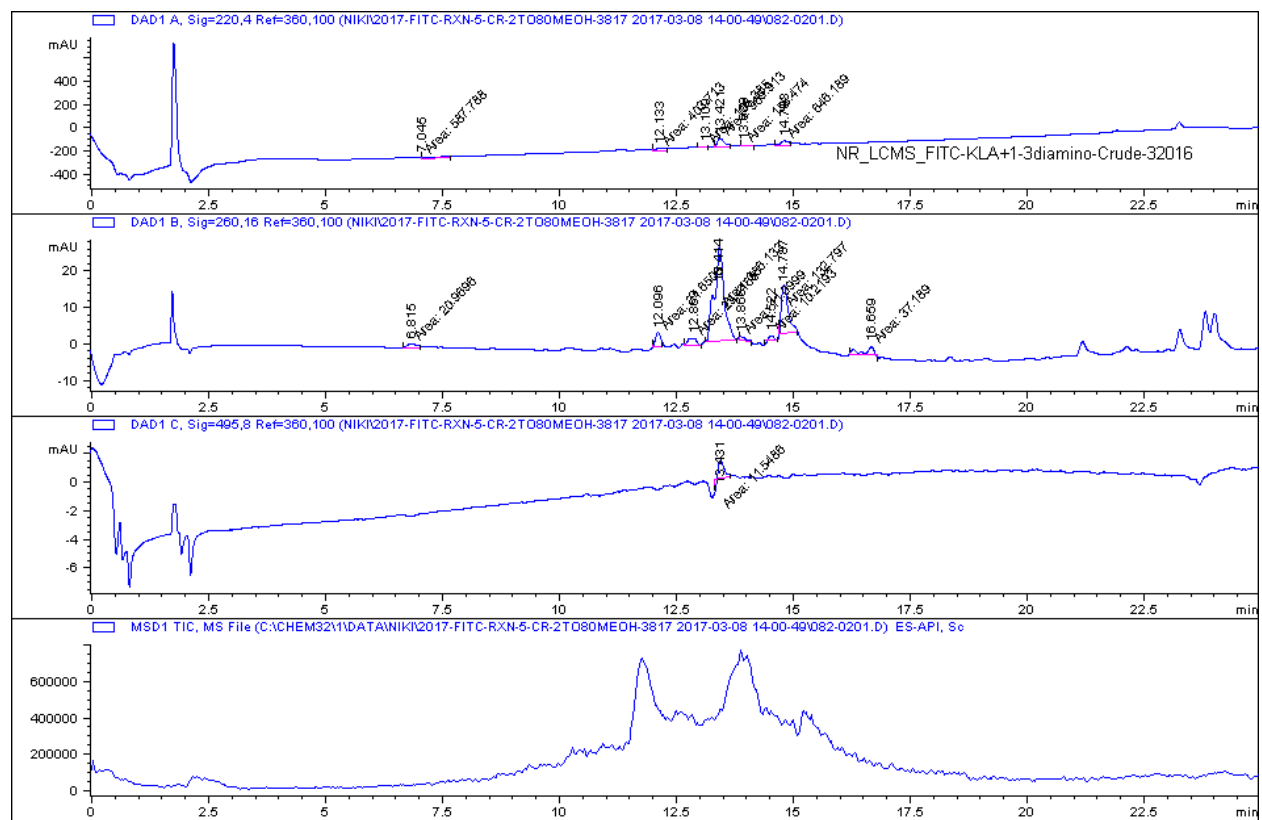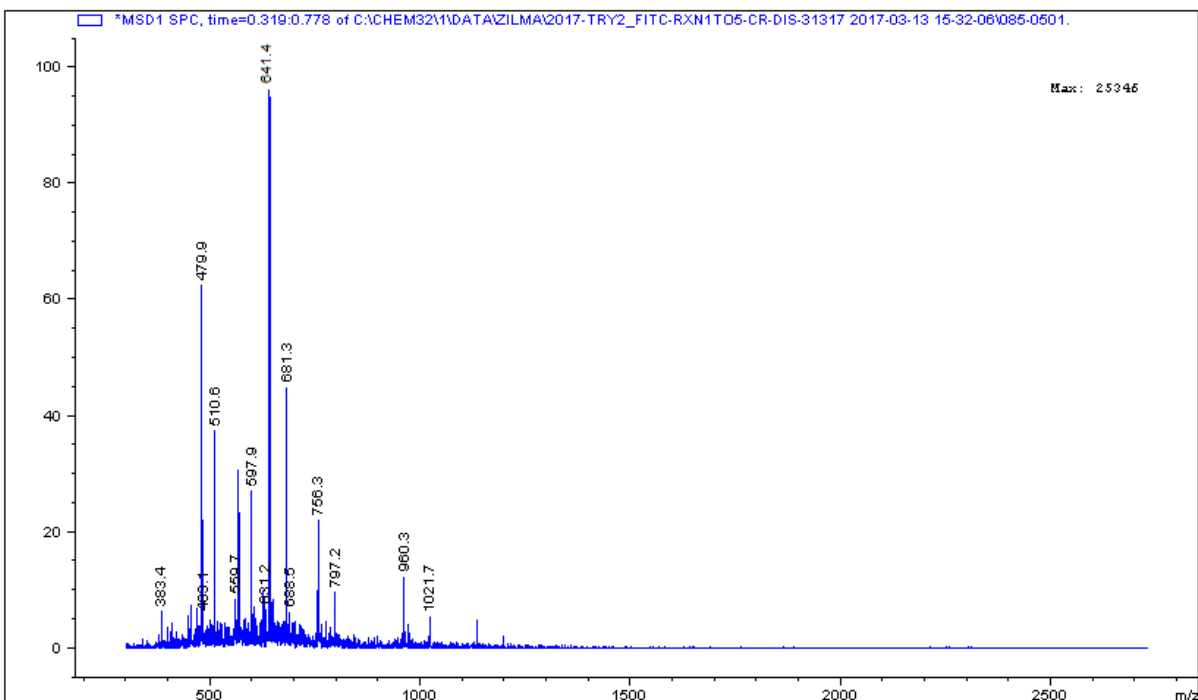
Figure A14. LCMS analysis of purified AHx-D-(KLAKLAKKLAKLAK)-AK-1,3-diaminopropane nucleolipid, **3.26** using a linear gradient 2-80% MeOH/H_2O (0.1% FA) over 17 min using a Waters 2695 Symmetry® C18 column (3.9 x 150 mm, 5 µm particle size) set at a temperature of 25 °C at a flow rate of 1.0 mL/min with detection at 220 nm.
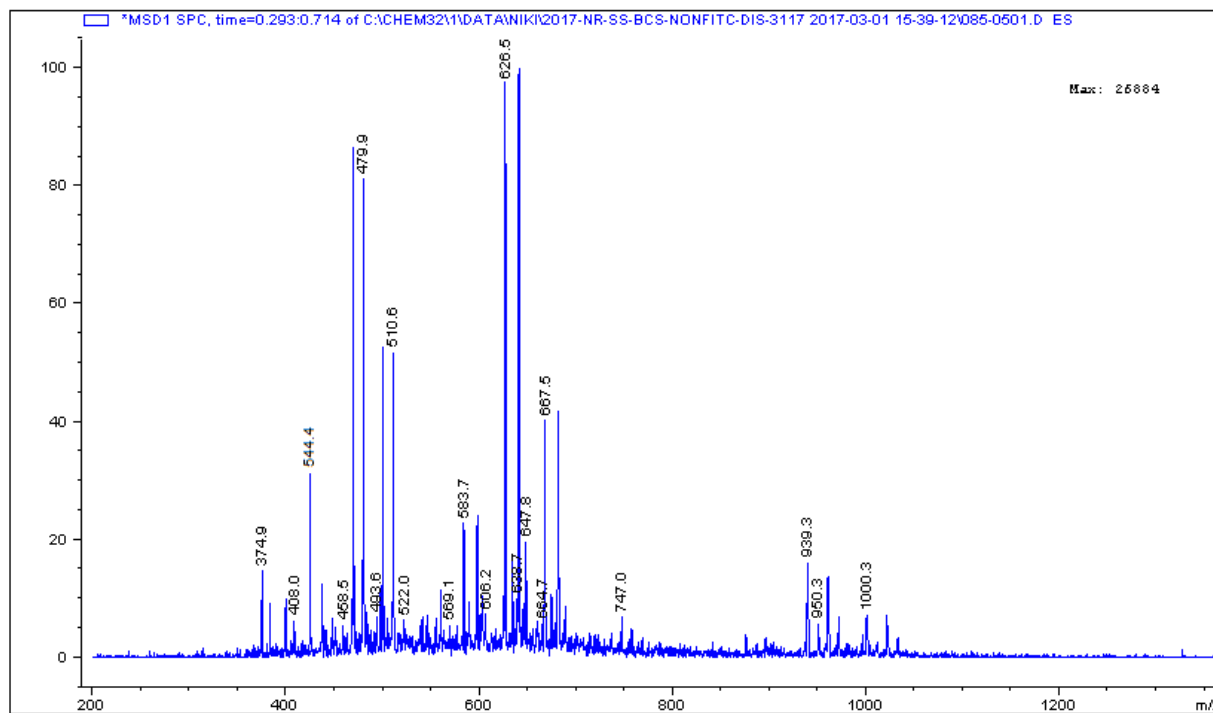
Figure A15. ESI-LCMS analysis of purified AHx-D-(KLAKLAKKLAKLAK)-AK-1,3-diaminopropane nucleolipid, **3.26** using a linear gradient 2-80% MeOH/H_2O (0.1% FA) over 17 min using a Waters 2695 Symmetry® C18 column (3.9 x 150 mm, 5 μm particle size) set at a temperature of 25 °C at a flow rate of 1.0 mL/min with detection at 220 nm.

Sequence: FITC-AHx-D-(KLAKLAKKLAKLAK)-AK-Methylamine, **3.27**

Solvent: 2-80% MeOH (0.1% FA) over 17 min

Detection: PDA 495nm
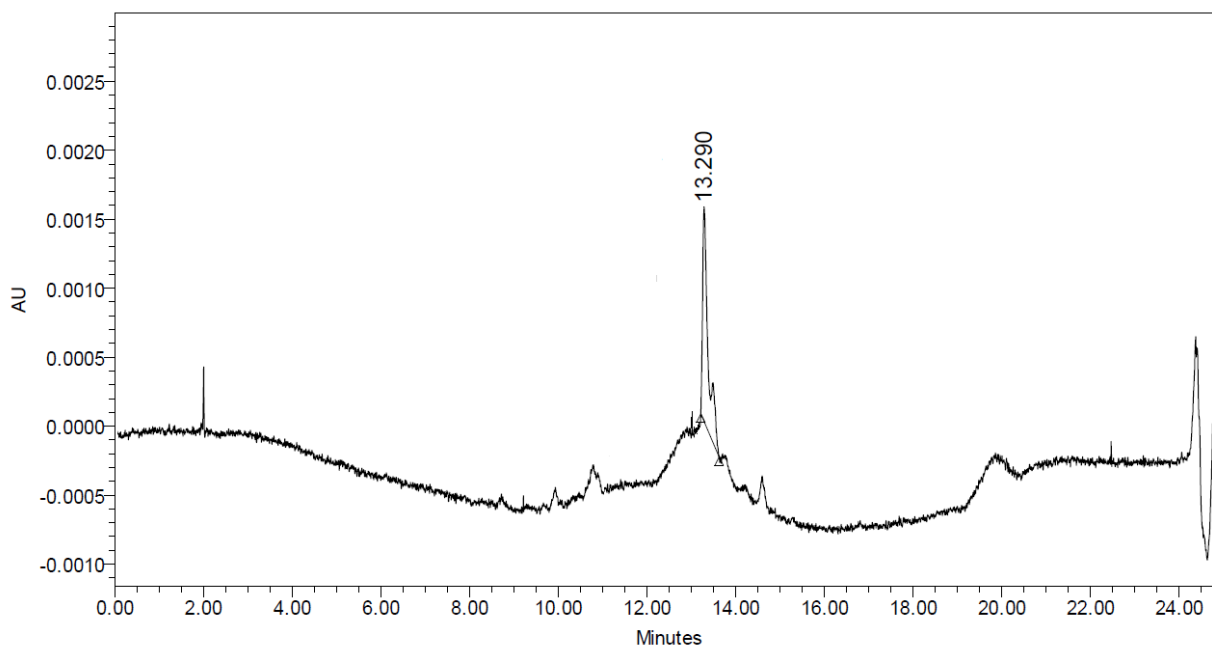
Results and analysis:

	Retention Time	Area	% Area	Height
1	13.290	32452	100	1232

Figure A16. RP-HPLC analysis of purified FITC-AHx-D-(KLAKLAKKLAKLAK)-AK-Methylamine nucleolipid, **3.27** using a linear gradient 2-80% MeOH/H$_2$O (0.1% FA) over 17 min using a Waters 2695 Symmetry® C18 column (3.9 x 150 mm, 5 μm particle size) set at a temperature of 25 °C at a flow rate of 1.0 mL/min with detection at 495 nm.
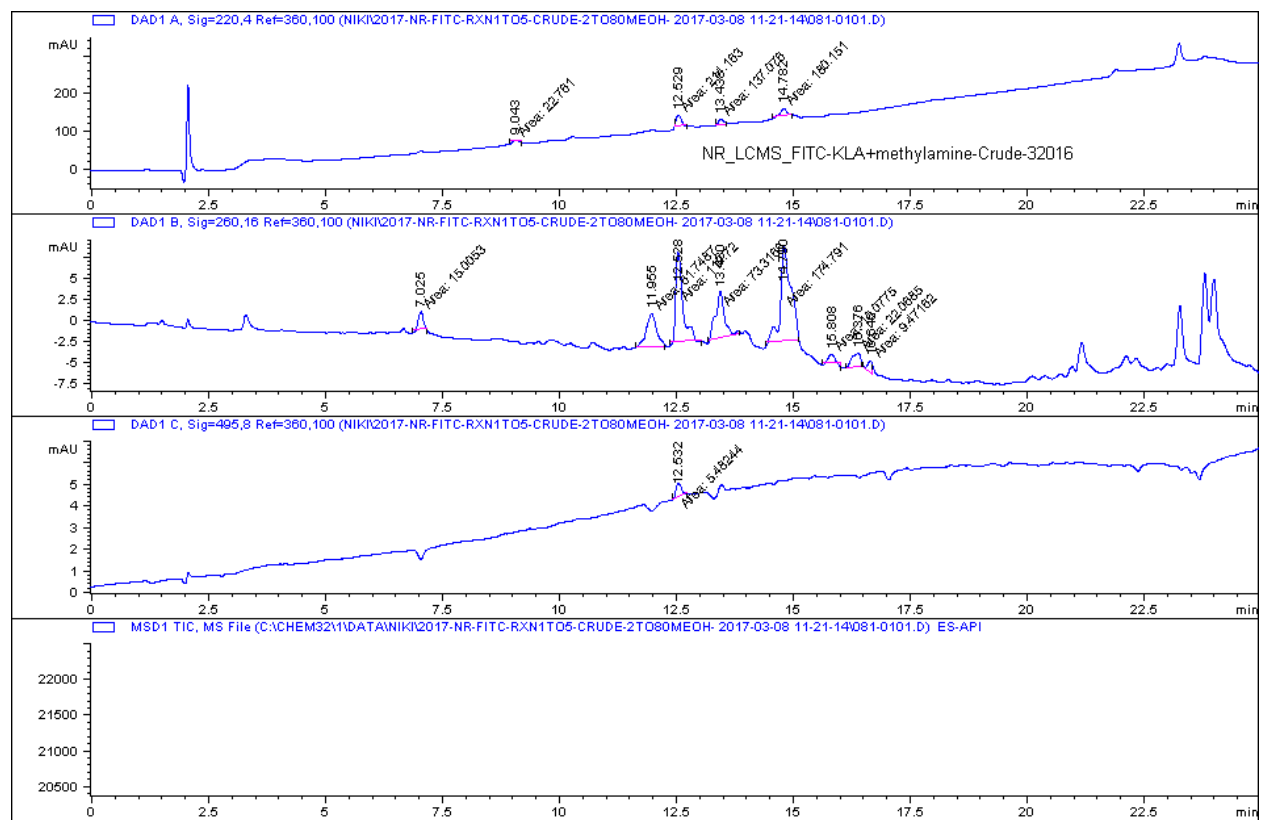
Figure A17. LCMS analysis of crude FITC-AHx-D-(KLAKLAKKLAKLAK)-AK-Methylamine nucleolipid, **3.27** using a linear gradient 2-80% MeOH/H$_2$O (0.1% FA) over 17 min using a Waters 2695 Symmetry® C18 column (3.9 x 150 mm, 5 μm particle size) set at a temperature of 25 °C at a flow rate of 1.0 mL/min with detection at 495 nm.
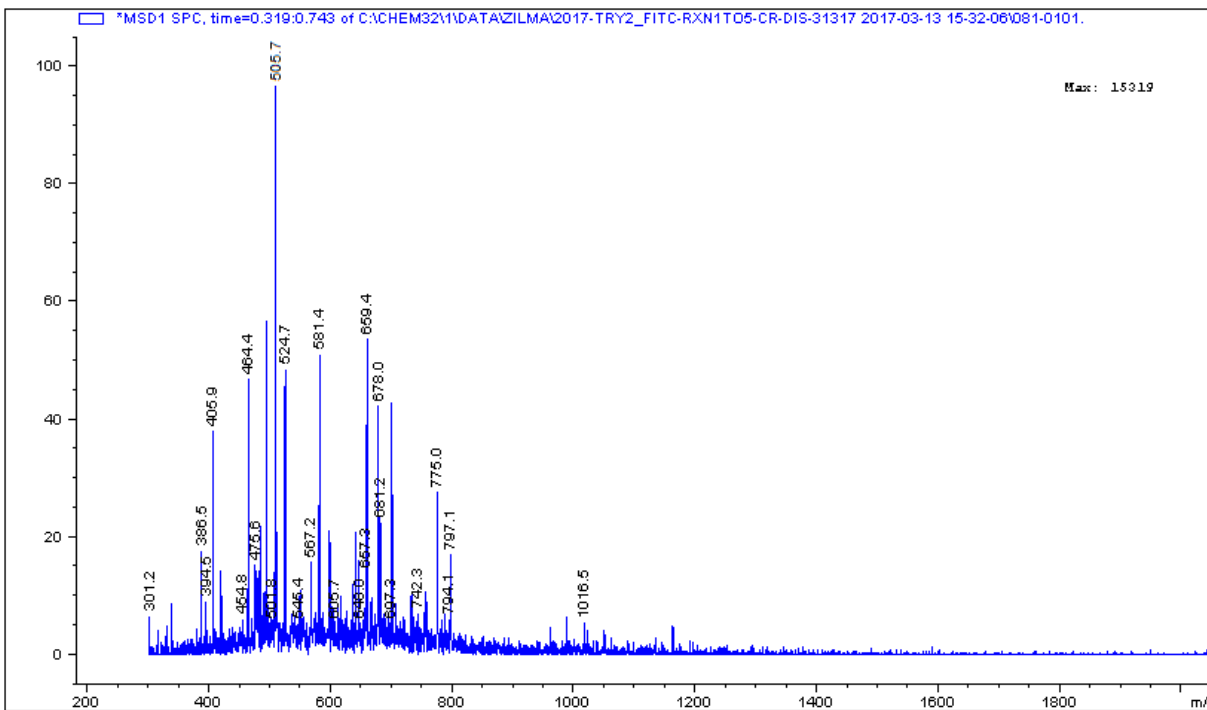
Figure A18. ESI-LCMS analysis of purified FITC-AHx-D-(KLAKLAKKLAKLAK)-AK-Methylamine nucleolipid, **3.27** using a linear gradient 2-80% MeOH/H$_2$O (0.1% FA) over 17 min using a Waters 2695 Symmetry® C18 column (3.9 x 150 mm, 5 μm particle size) set at a temperature of 25 °C at a flow rate of 1.0 mL/min with detection at 495 nm.

Sequence: FITC-AHx-D-(KLAKLAKKLAKLAK)-AK-Octylamine, **3.28**

Solvent: 2-80% MeOH (0.1% FA) over 17 min

Detection: PDA 220 nm

Results and analysis:

	Retention Time	Area	% Area	Height
1	15.047	108239	100	9432

Figure A19. RP-HPLC analysis of purified FITC-AHx-D-(KLAKLAKKLAKLAK)-AK-Octylamine nucleolipid, **3.28** using a linear gradient 2-80% MeOH/H_2O (0.1% FA) over 17 min using a Waters 2695 Symmetry® C18 column (3.9 x 150 mm, 5 μm particle size) set at a temperature of 25 °C at a flow rate of 1.0 mL/min with detection at 220 nm.

Figure A20. LCMS analysis of purified FITC-AHx-D-(KLAKLAKKLAKLAK)-AK-Octylamine nucleolipid, **3.28** using a linear gradient 2-80% MeOH/H$_2$O (0.1% FA) over 17 min using a Waters 2695 Symmetry® C18 column (3.9 x 150 mm, 5 μm particle size) set at a temperature of 25 °C at a flow rate of 1.0 mL/min with detection at 220 nm.

Figure A21. ESI-LCMS analysis of purified FITC-AHx-D-(KLAKLAKKLAKLAK)-AK-Octylamine nucleolipid, **3.28** using a linear gradient 2-80% MeOH/H$_2$O (0.1% FA) over 17 min using a Waters 2695 Symmetry® C18 column (3.9 x 150 mm, 5 μm particle size) set at a temperature of 25 °C at a flow rate of 1.0 mL/min with detection at 220 nm.

Sequence: FITC-AHx-D-(KLAKLAKKLAKLAK)-AK-Histamine, **3.29**

Solvent: 2-80% MeOH (0.1% FA) over 17 min

Detection: PDA 220 nm

Results and analysis:

	Retention Time	Area	% Area	Height
1	12.167	108239	50.0	2873
2	12.573	199388	49.5	3127

Figure A22. RP-HPLC analysis of purified FITC-AHx-D-(KLAKLAKKLAKLAK)-AK-Histamine nucleolipid, **3.29** using a linear gradient 2-80% MeOH/H$_2$O (0.1% FA) over 17 min using a Waters 2695 Symmetry® C18 column (3.9 x 150 mm, 5 μm particle size) set at a temperature of 25 °C at a flow rate of 1.0 mL/min with detection at 220 nm.

Figure A23. LCMS analysis of purified FITC-AHx-D-(KLAKLAKKLAKLAK)-AK-Histamine nucleolipid, **3.29** using a linear gradient 2-80% MeOH/H$_2$O (0.1% FA) over 17 min using a Waters 2695 Symmetry® C18 column (3.9 x 150 mm, 5 μm particle size) set at a temperature of 25 °C at a flow rate of 1.0 mL/min with detection at 220 nm.

Figure A24. ESI-LCMS analysis of purified FITC-AHx-D-(KLAKLAKKLAKLAK)-AK-Histamine nucleolipid, **3.29** using a linear gradient 2-80% MeOH/H$_2$O (0.1% FA) over 17 min using a Waters 2695 Symmetry® C18 column (3.9 x 150 mm, 5 μm particle size) set at a temperature of 25 °C at a flow rate of 1.0 mL/min with detection at 220 nm.

Sequence: FITC-AHx-D-(KLAKLAKKLAKLAK)-AK-Spermine, **3.30**

Solvent: 2-80% MeOH (0.1% FA) over 17 min

Detection: PDA 220 nm

Results and analysis:

	Retention Time	Area	% Area	Height
1	13.326	8348	1.4	454
2	13.331	121470	98.6	946

Figure A25. RP-HPLC analysis of purified FITC-AHx-D-(KLAKLAKKLAKLAK)-AK-Spermine nucleolipid, **3.30** using a linear gradient 2-80% MeOH/H_2O (0.1% FA) over 17 min using a Waters 2695 Symmetry® C18 column (3.9 x 150 mm, 5 μm particle size) set at a temperature of 25 °C at a flow rate of 1.0 mL/min with detection at 220 nm.
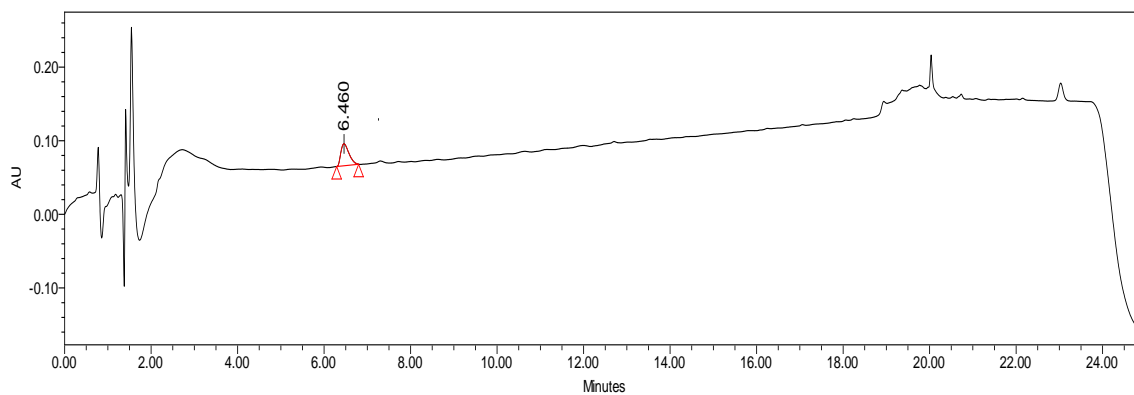
Figure A26. LCMS analysis of purified FITC-AHx-D-(KLAKLAKKLAKLAK)-AK-Spermine nucleolipid, **3.30** using a linear gradient 2-80% MeOH/H$_2$O (0.1% FA) over 17 min using a Waters 2695 Symmetry® C18 column (3.9 x 150 mm, 5 μm particle size) set at a temperature of 25 °C at a flow rate of 1.0 mL/min with detection at 220 nm.

Figure A27. ESI-LCMS analysis of purified FITC-AHx-D-(KLAKLAKKLAKLAK)-AK-Spermine nucleolipid, **3.30** using a linear gradient 2-80% MeOH/H$_2$O (0.1% FA) over 17 min using a Waters 2695 Symmetry® C18 column (3.9 x 150 mm, 5 μm particle size) set at a temperature of 25 °C at a flow rate of 1.0 mL/min with detection at 220 nm.

Sequence: FITC-AHx-D-(KLAKLAKKLAKLAK)-AK-1,3-diaminopropane, **3.31**

Solvent: 2-80% MeOH (0.1% FA) over 17 min

Detection: PDA 220 nm

Results and analysis:

	Retention Time	Area	% Area	Height
1	15.036	100	140525	8938

Figure A28. RP-HPLC analysis of purified FITC-AHx-D-(KLAKLAKKLAKLAK)-AK-1,3-diaminopropane nucleolipid, **3.31** using a linear gradient 2-80% MeOH/H_2O (0.1% FA) over 17 min using a Waters 2695 Symmetry® C18 column (3.9 x 150 mm, 5 μm particle size) set at a temperature of 25 °C at a flow rate of 1.0 mL/min with detection at 220 nm.

Figure A29. LCMS analysis of purified FITC-AHx-D-(KLAKLAKKLAKLAK)-AK-1,3-diaminopropane nucleolipid, **3.31** using a linear gradient 2-80% MeOH/H$_2$O (0.1% FA) over 17 min using a Waters 2695 Symmetry® C18 column (3.9 x 150 mm, 5 μm particle size) set at a temperature of 25 °C at a flow rate of 1.0 mL/min with detection at 220 nm.

Figure A30. LCMS analysis of purified FITC-AHx-D-(KLAKLAKKLAKLAK)-AK-1,3-diaminopropane nucleolipid, **3.31** using a linear gradient 2-80% MeOH/H$_2$O (0.1% FA) over 17 min using a Waters 2695 Symmetry® C18 column (3.9 x 150 mm, 5 µm particle size) set at a temperature of 25 °C at a flow rate of 1.0 mL/min with detection at 220 nm.
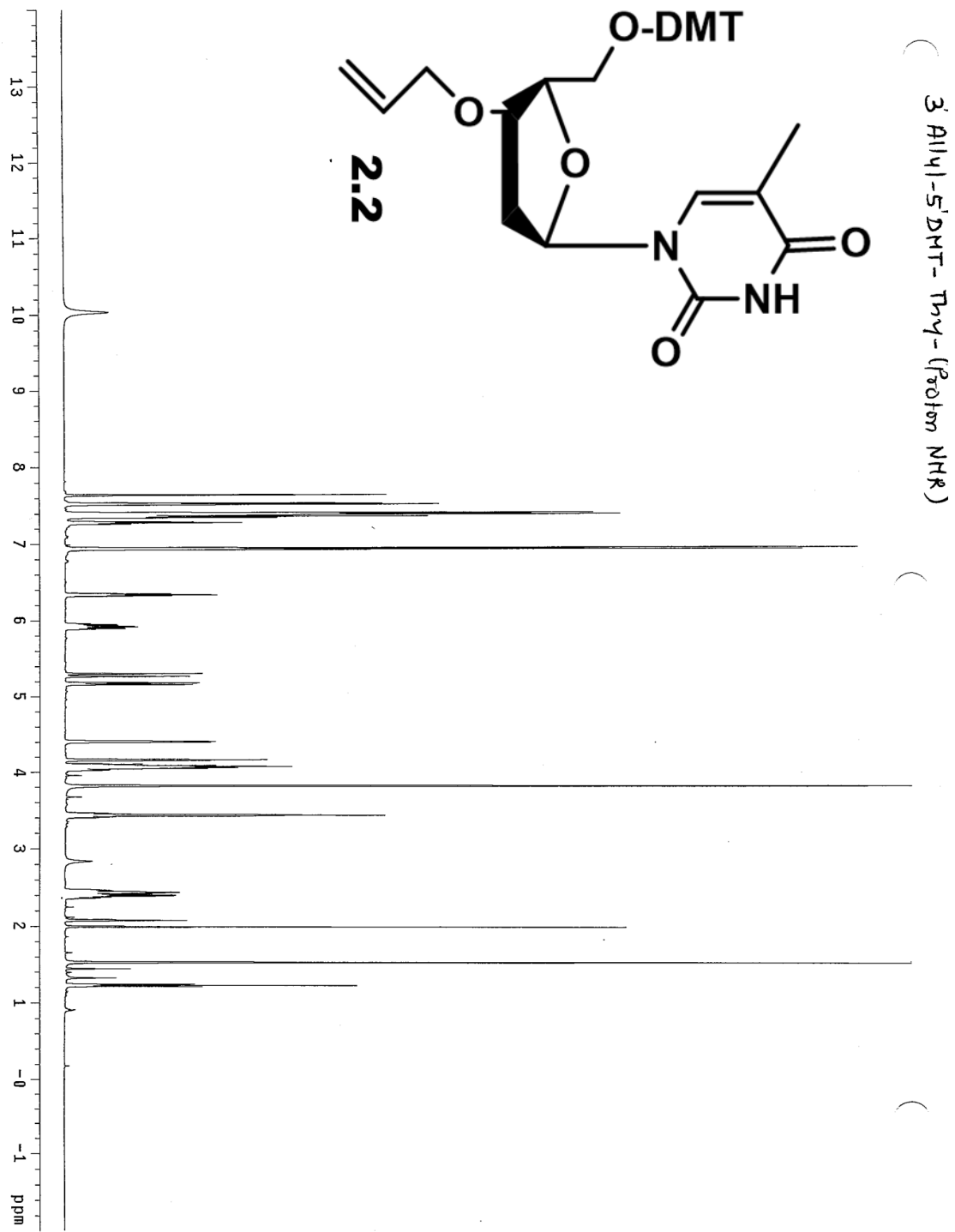
Figure A31. ^{1}H NMR spectrum of **2.2**
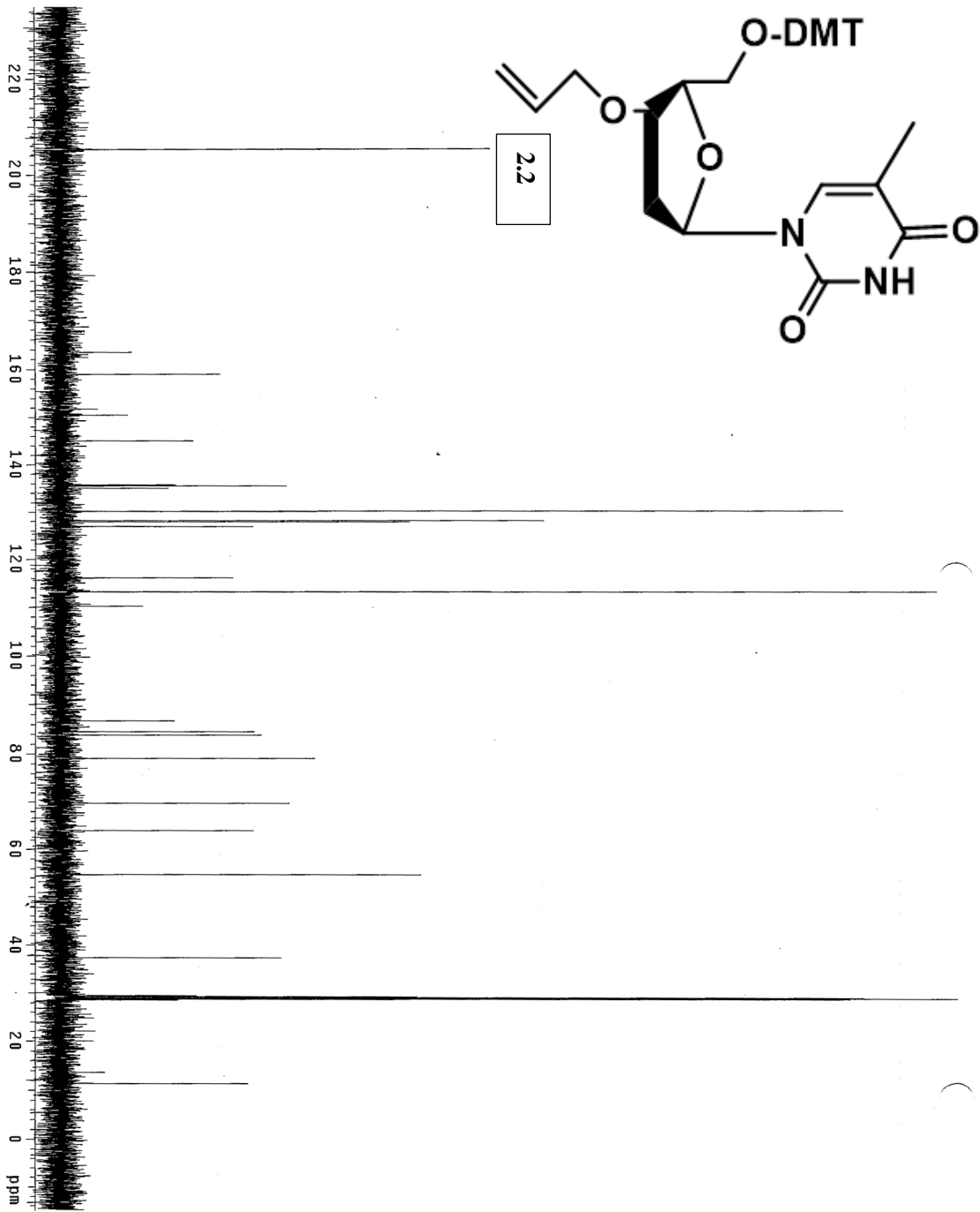
Figure A32. ^{13}C NMR spectrum of **2.2**
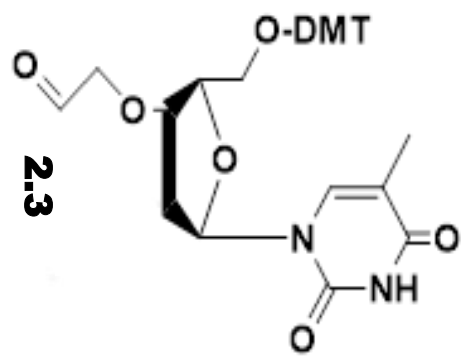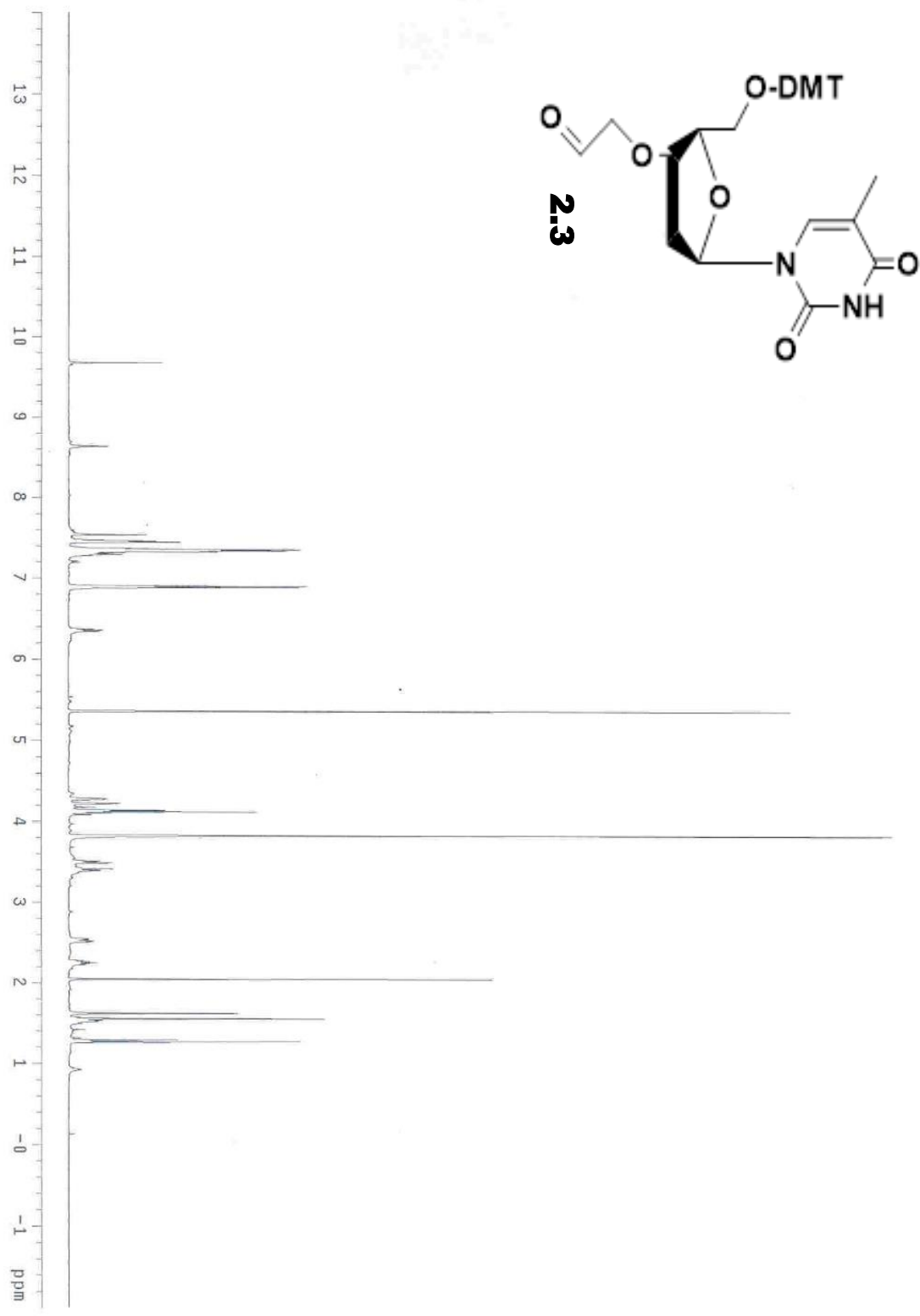
Figure A33. ¹HNMR spectrum of **2.3**
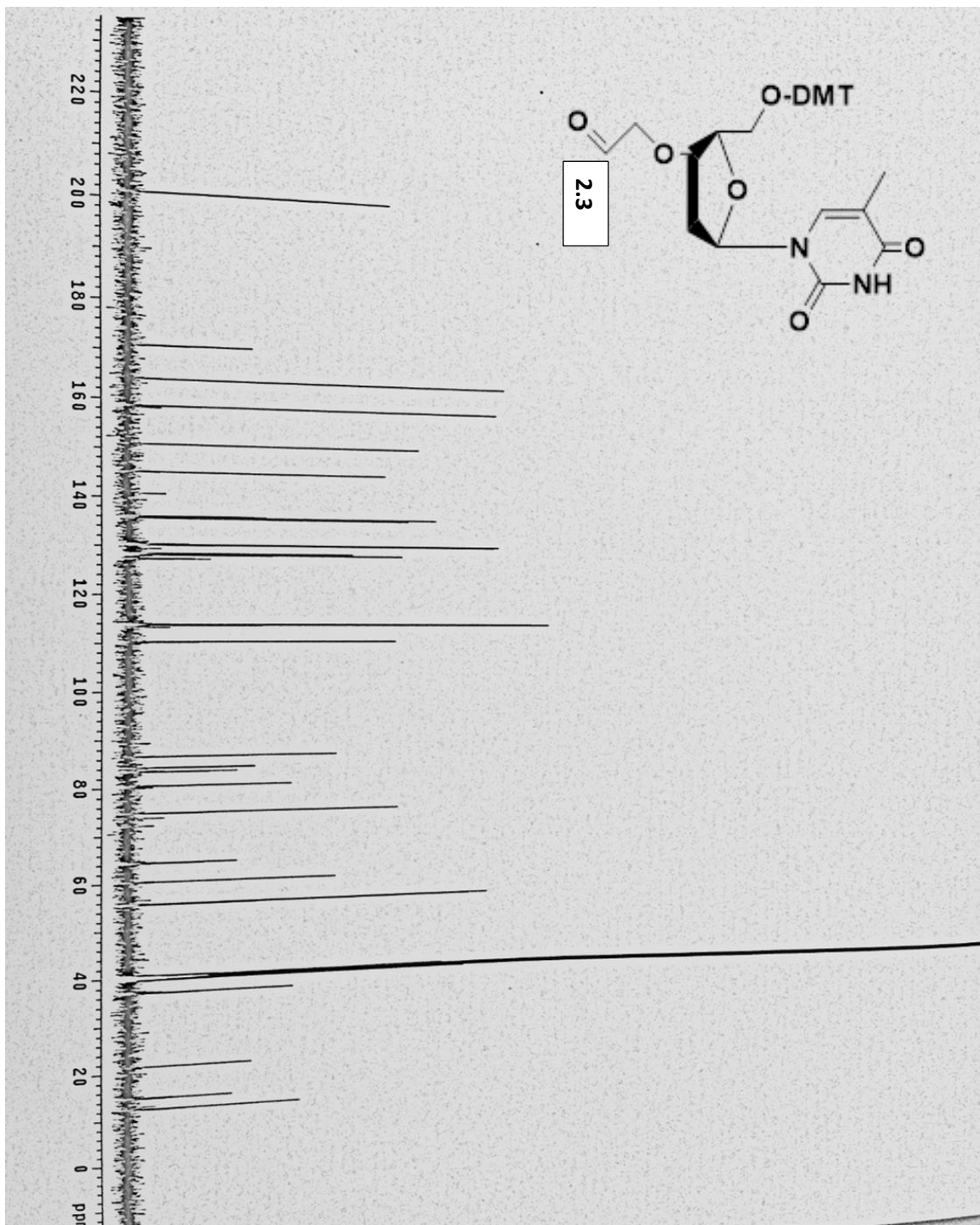
Figure A34. ^{13}CNMR spectrum of **2.3**
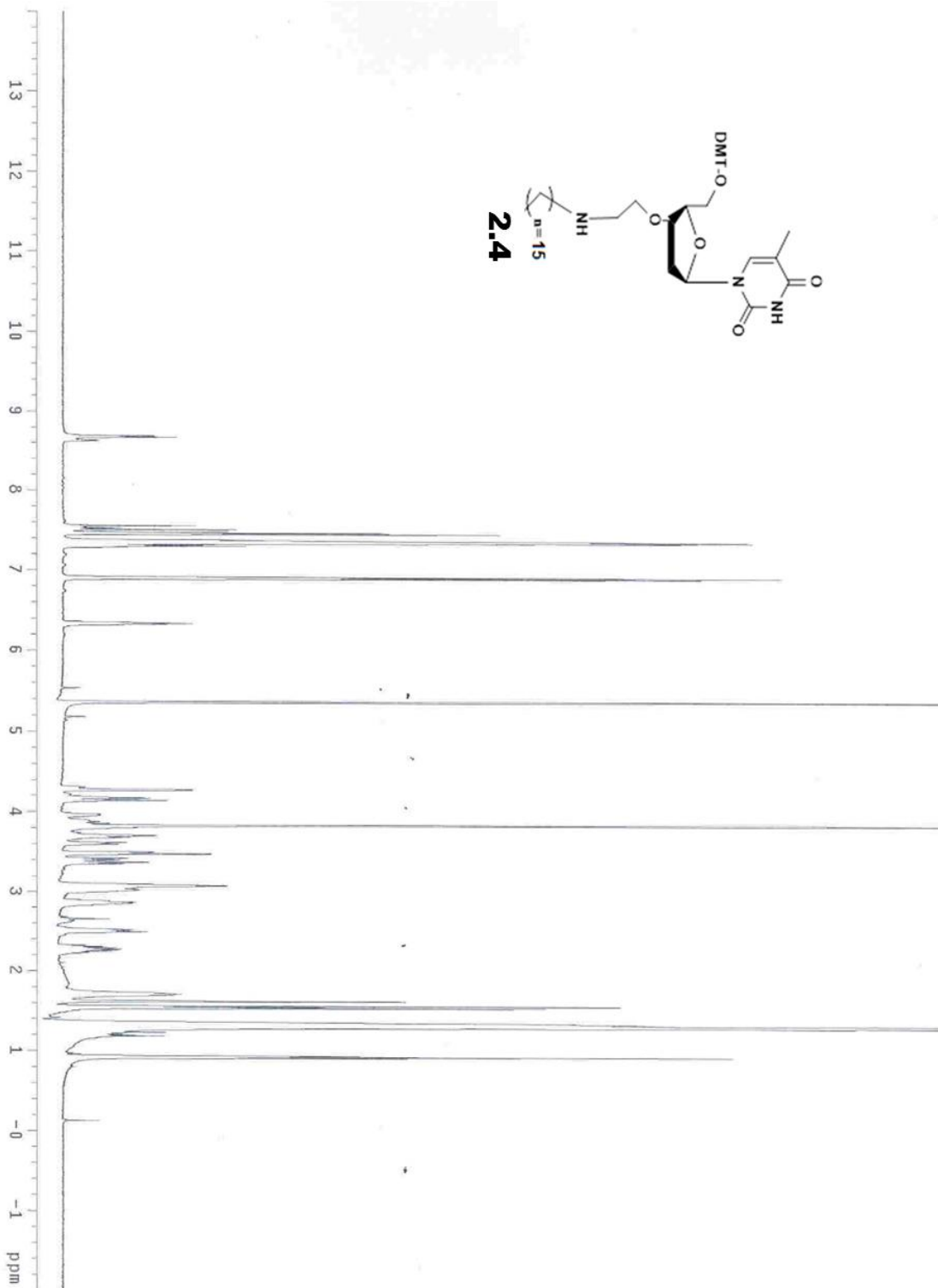
Figure A35. ^{1}H-NMR spectrum of **2.4**
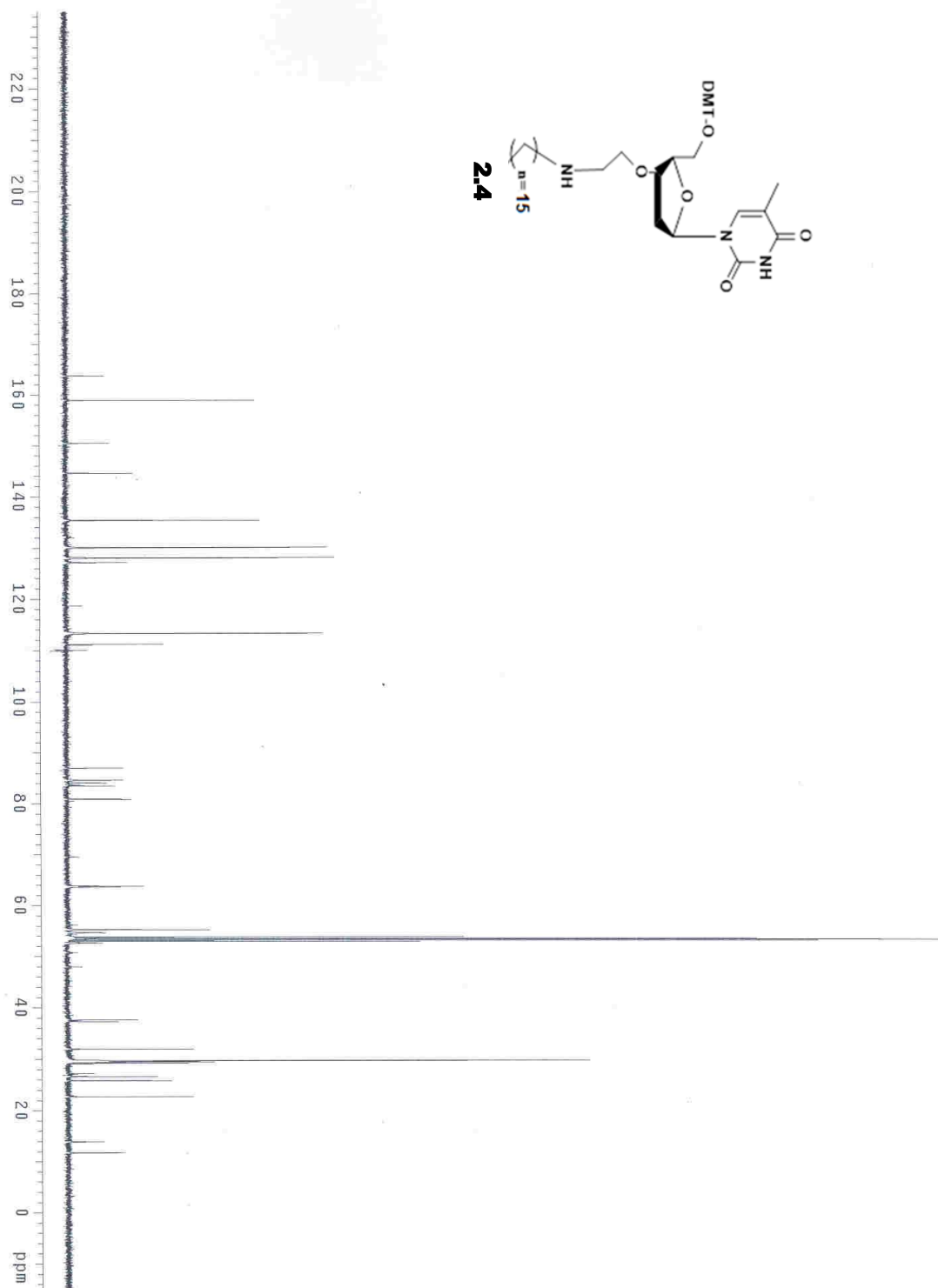
Figure A36. ^{13}C-NMR spectrum of **2.4**
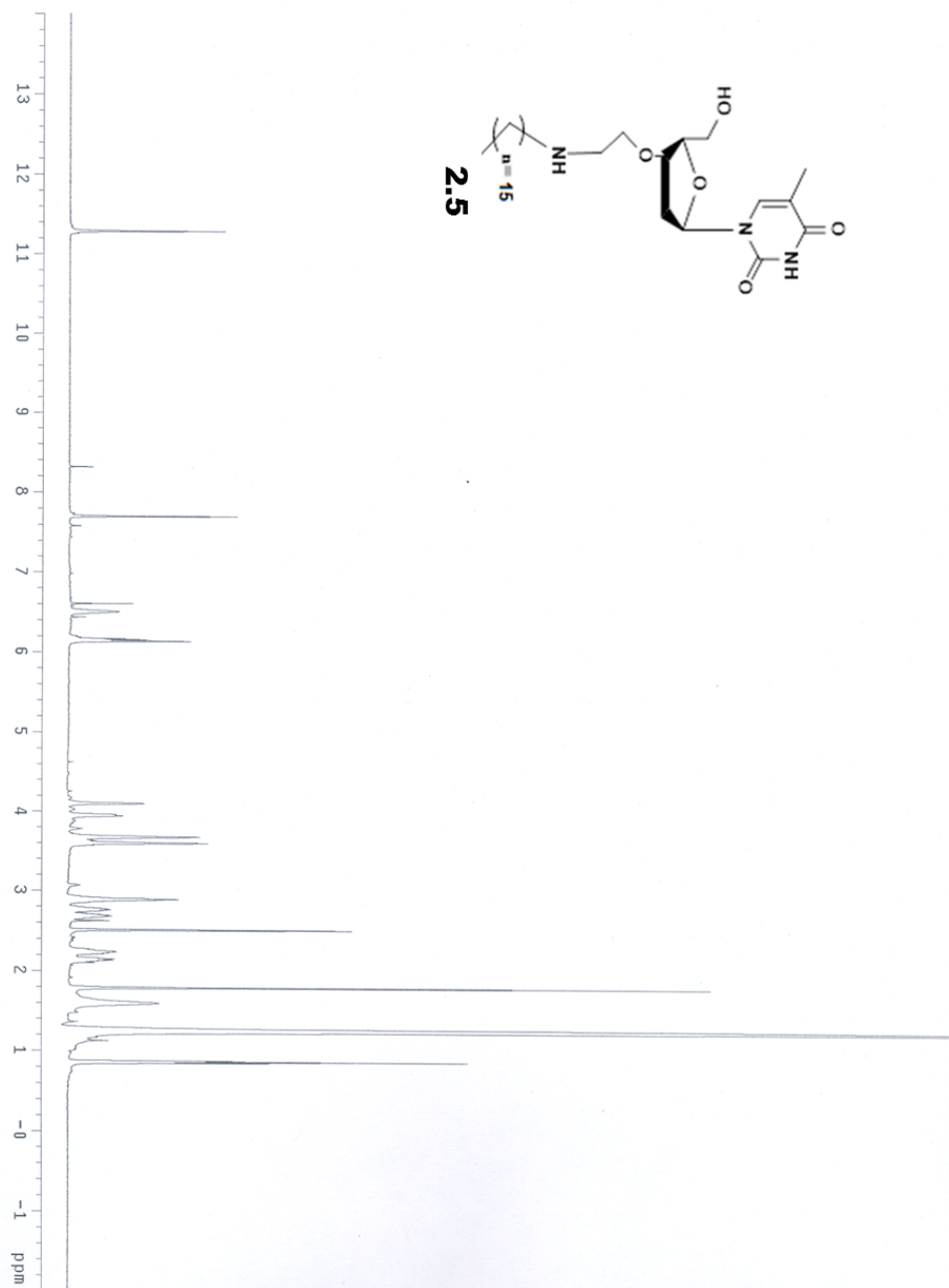
Figure A37. ^{1}H-NMR spectrum of **2.5**
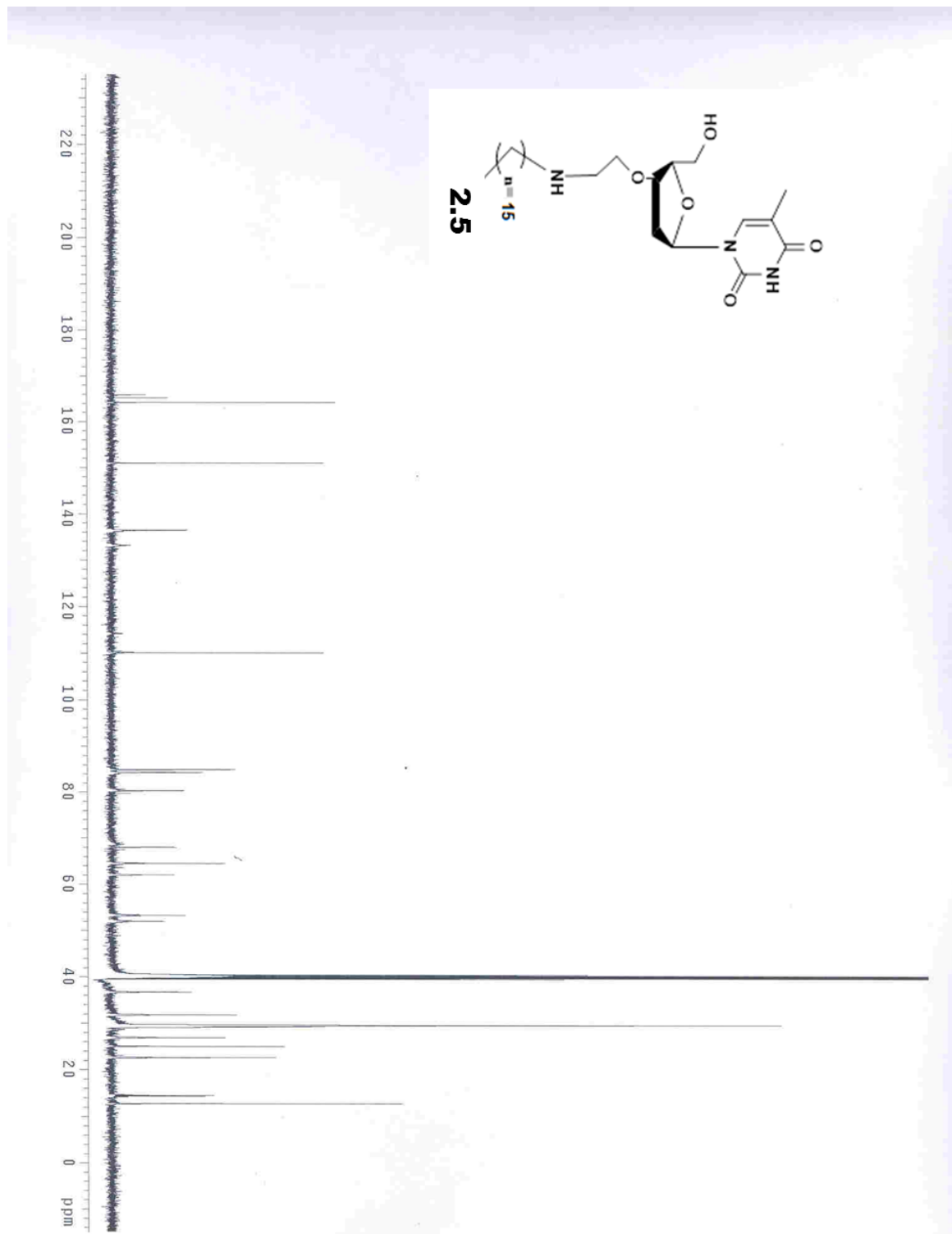
Figure A38. ^{13}C-NMR spectrum of **2.5**
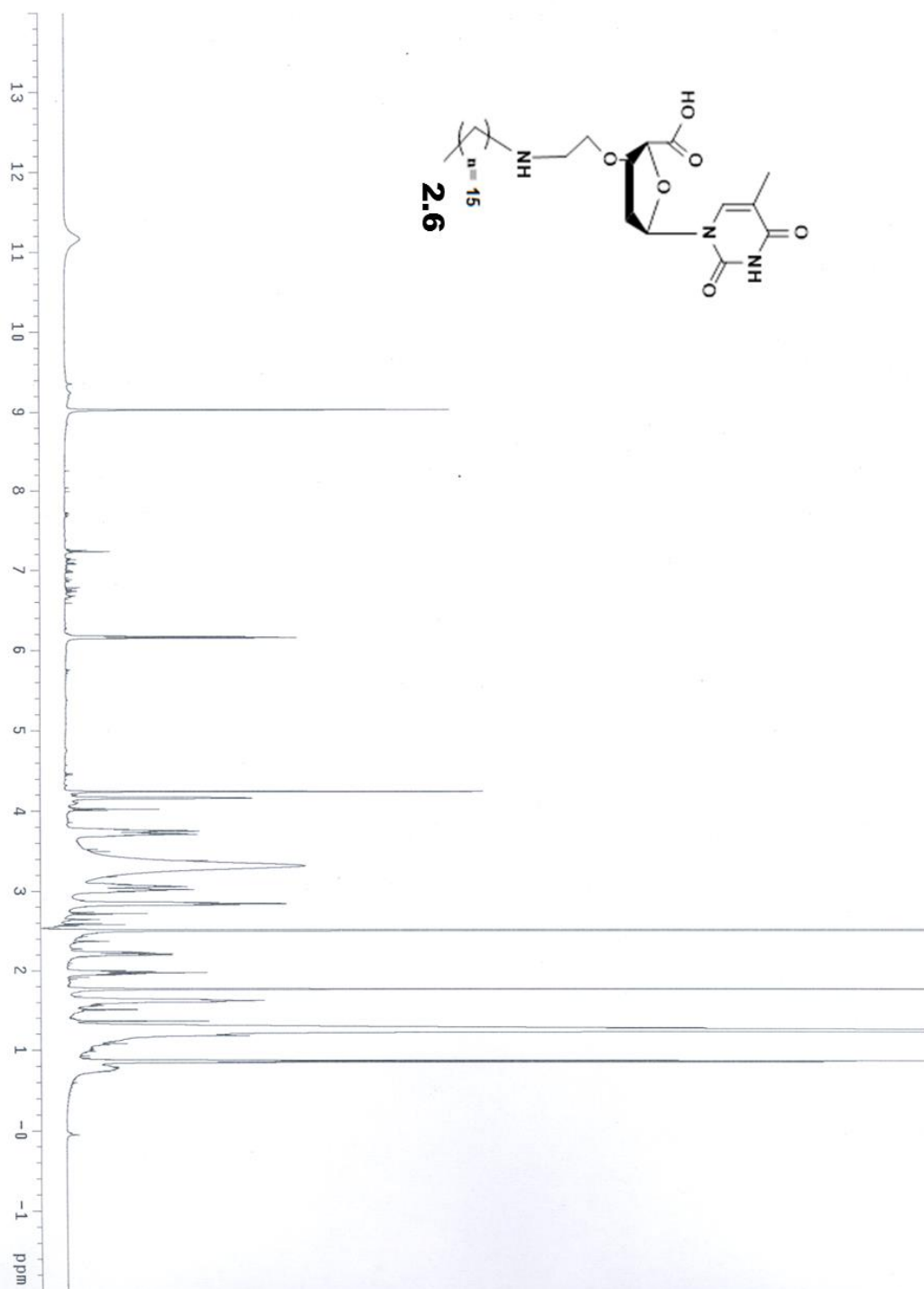
Figure A39. ^{1}H-NMR spectrum of **2.6**
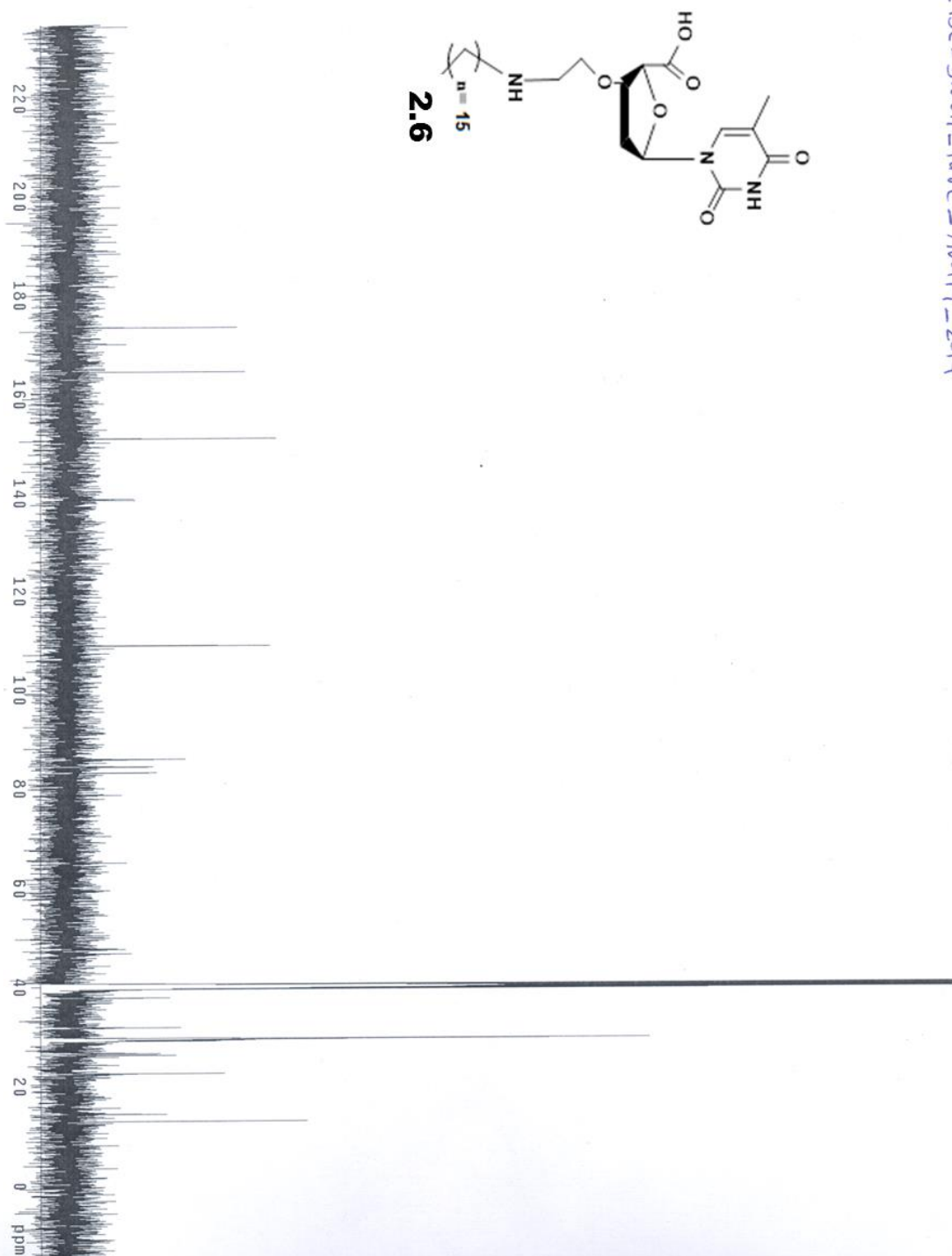
Figure A40. ^{13}C-NMR spectrum of **2.6**
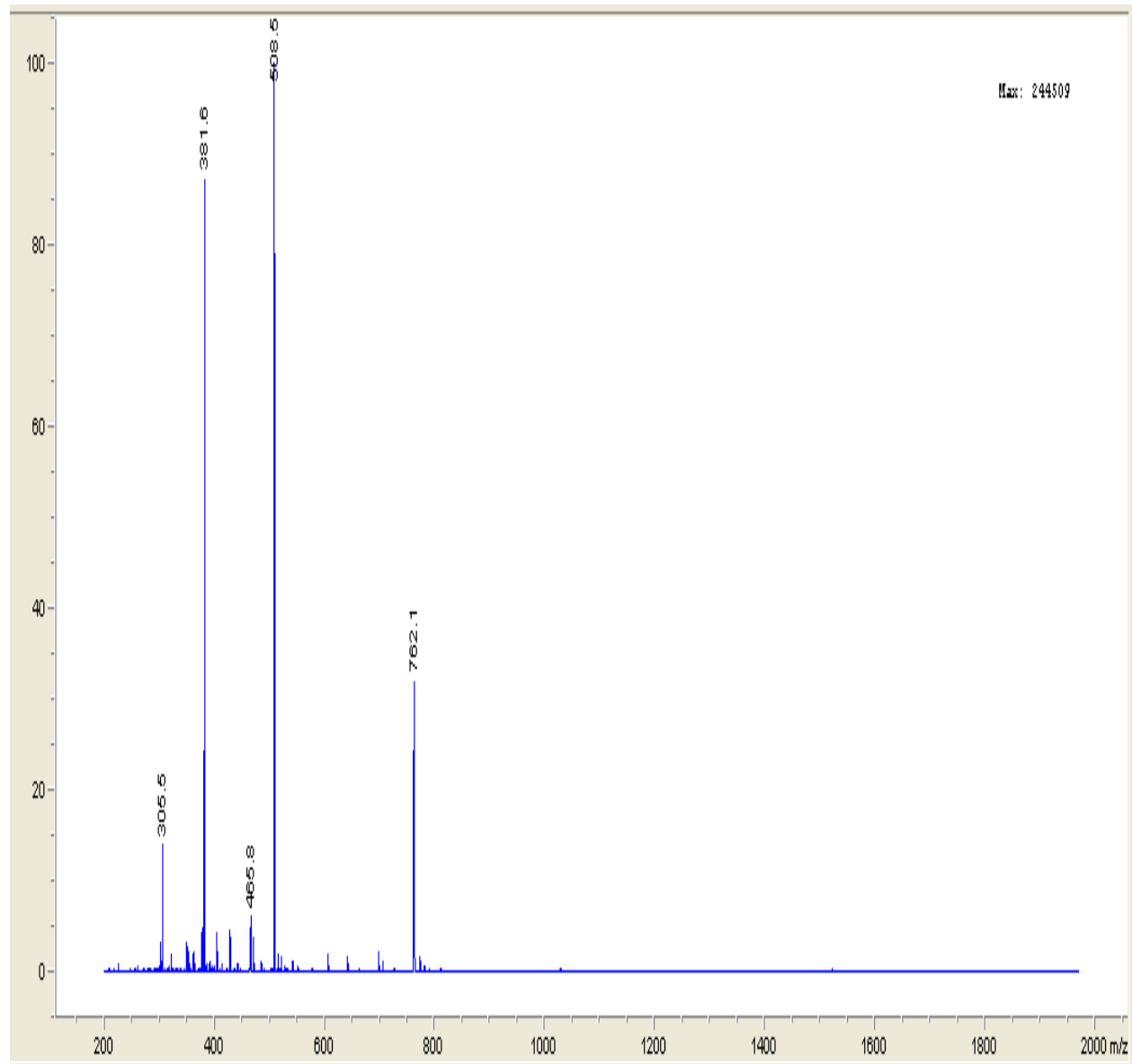
Figure A41. ESI-MS spectra of D-(KLAKLAKKLAKLAK)
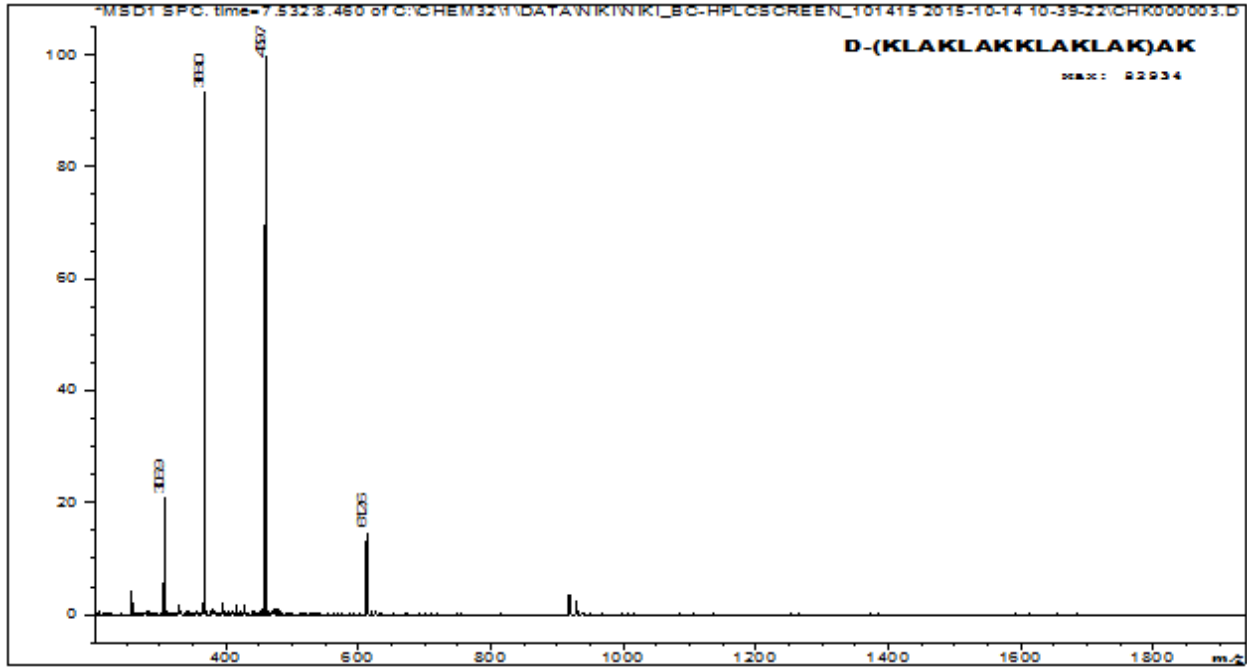
Figure A42. ESI-MS spectra of D-(KLAKLAKKLAKLAK)-AK
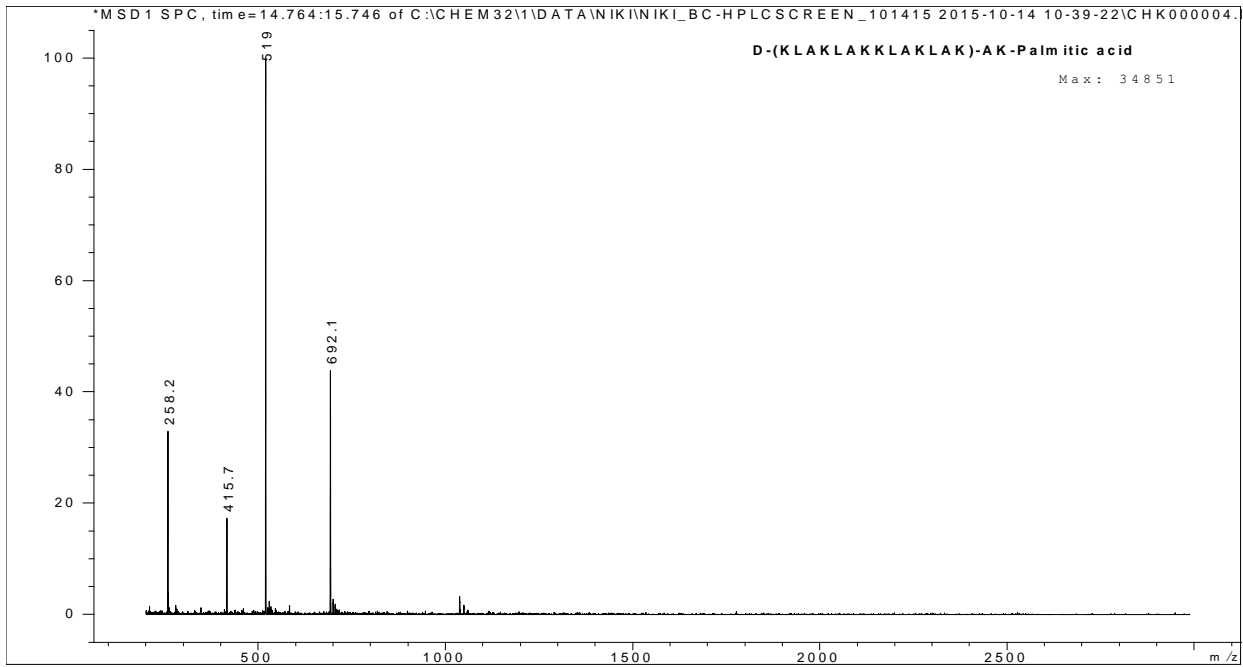
Figure A43. ESI-MS spectra of D-(KLAKLAKKLAKLAK)-AK-Palmitamide
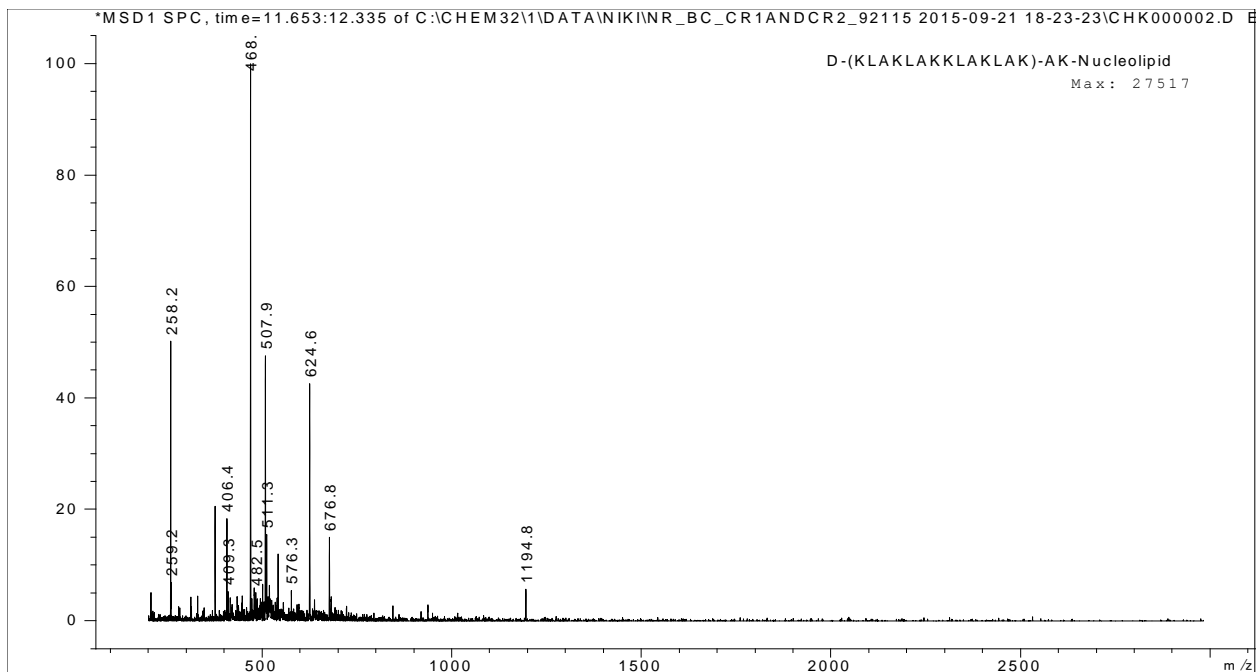
Figure A44. ESI-MS spectra of D-(KLAKLAKKLAKLAK)-AK-Nucleolipid
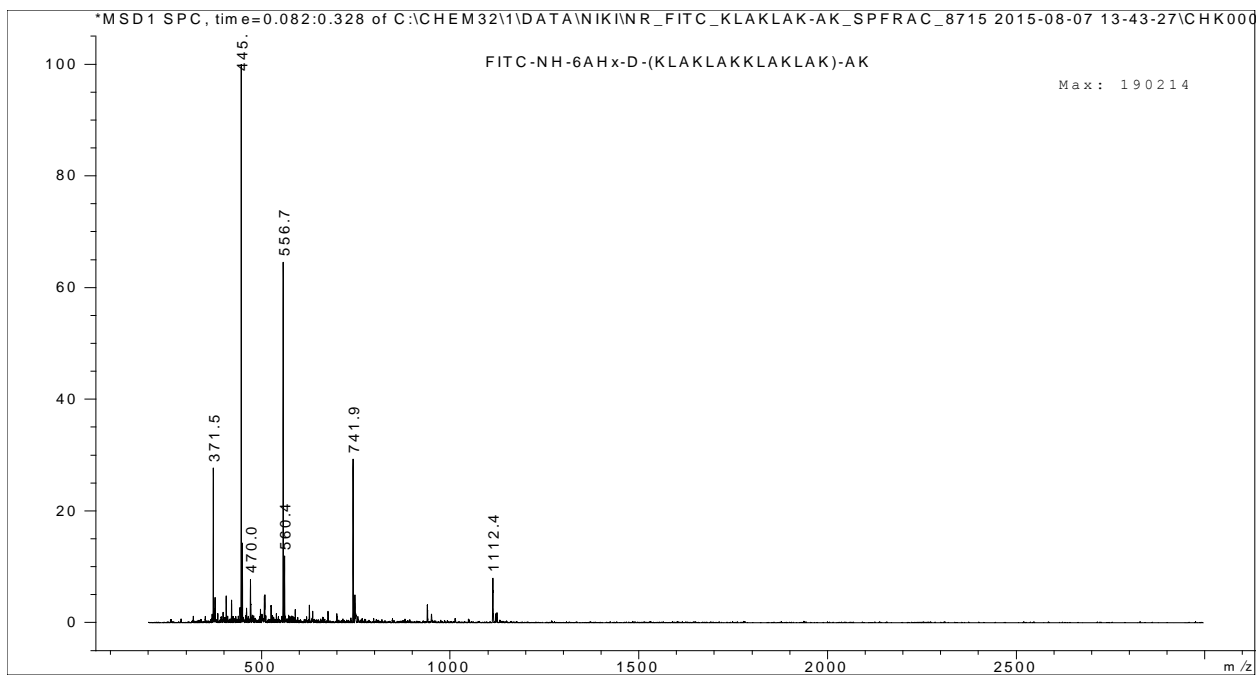
Figure A45. ESI-MS spectra of FITC-Ahx-D-(KLAKLAKKLAKLAK)-AK
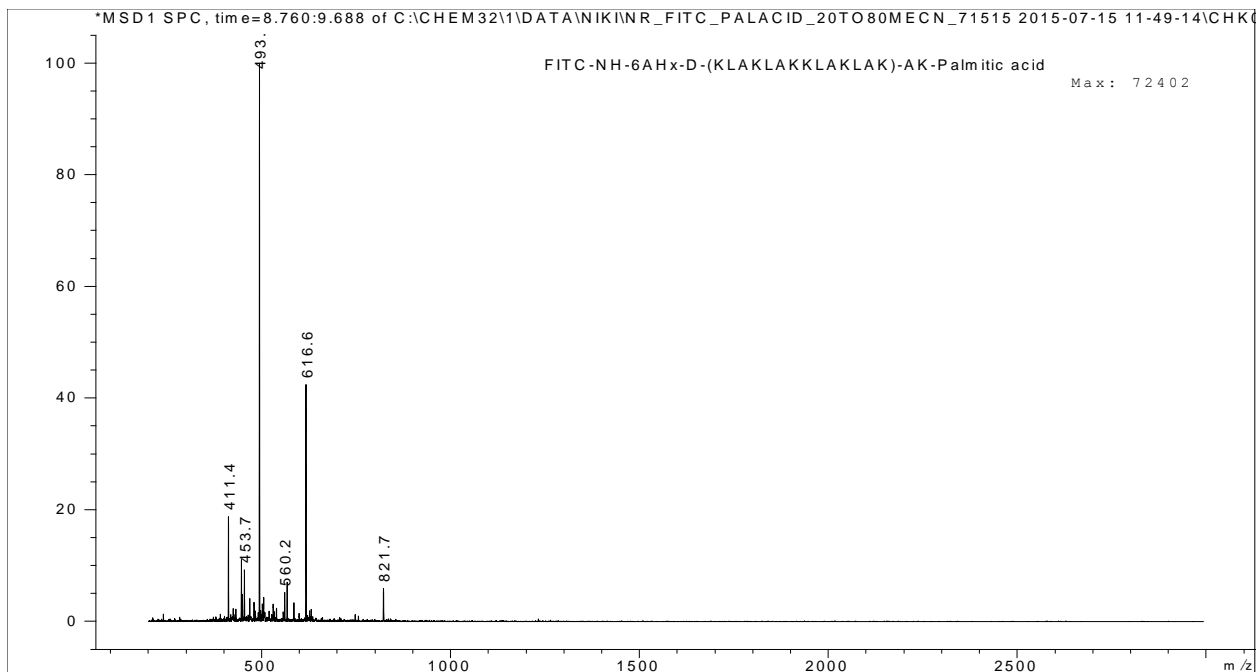
Figure A46. ESI-MS spectra of FITC-Ahx-D-(KLAKLAKKLAKLAK)-AK-Palmitamide.
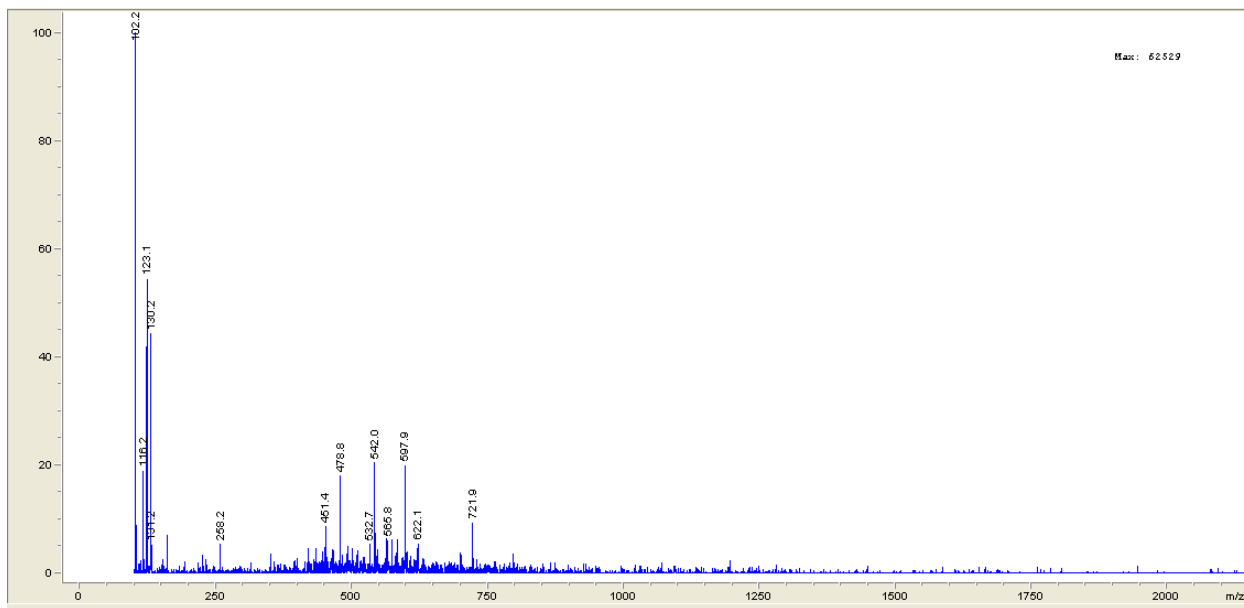
Figure A47. ESI-MS spectra of FITC-Ahx-D-(KLAKLAKKLAKLAK)-AK-Hexadecyl Nucleolipid

173

Sequence: Purified Crude D-(KLAKLAKKLAKLAK)

Solvent: 2-83% MeCN (0.1% TFA) over 18 min
Detection: PDA 220nm
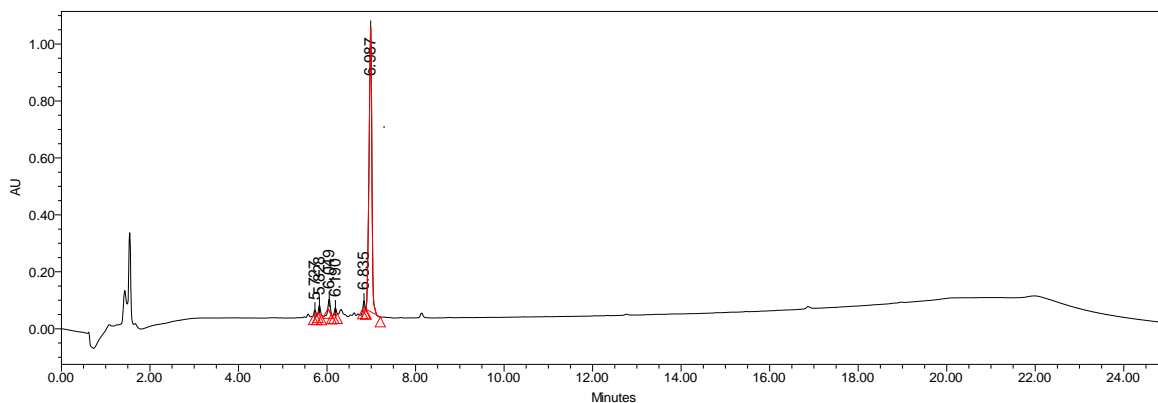
Results and analysis:

	Retention Time	Area	% Area	Height
1	5.727	40407	0.84	16862
2	5.828	71105	1.49	28974
3	6.049	108374	2.26	40163
4	6.190	51206	1.07	20630
5	6.835	65376	1.37	28942
6	6.987	4448515	92.97	998144

Figure A48. RP-HPLC analysis of purified D-(KLAKLAKKLAKLAK) using a linear gradient 2-83% MeCN/H$_2$O (0.1% FA) over 17 min using a Waters 2695 Symmetry® C18 column (3.9 x 150 mm, 5 μm particle size) set at a temperature of 25 °C at a flow rate of 1.0 mL/min with detection at 220 nm.
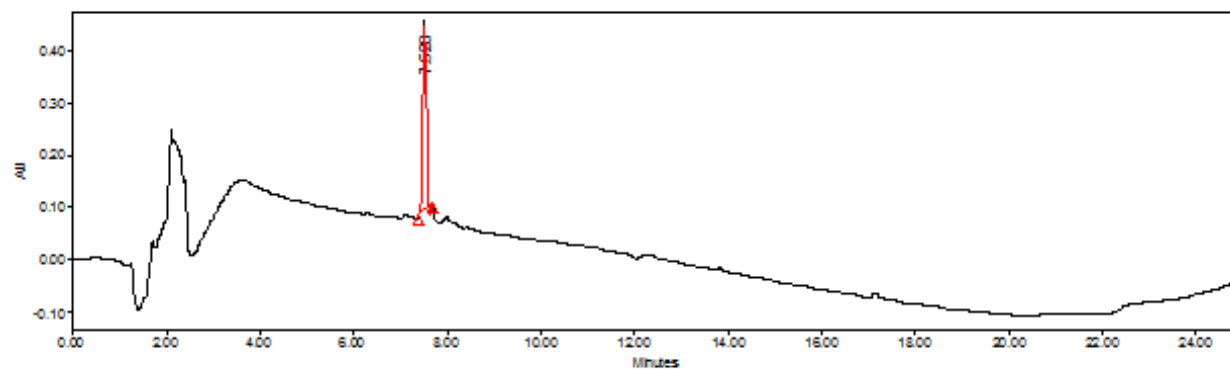
Result and analysis:

	Retention Time	Area	% Area
1	7.528	1965904	100.00

Figure A49. RP-HPLC analysis of purified D-(KLAKLAKKLAKLAK) using a linear gradient 2-83% MeCN/H_2O (0.1% FA) over 17 min using a Waters 2695 Symmetry® C18 column (3.9 x 150 mm, 5 μm particle size) set at a temperature of 25 °C at a flow rate of 1.0 mL/min with detection at 220 nm.

Sequence: NH$_2$-AHx-D-(KLAKLAK)$_2$-AK

Solvent: 2to80MeOH (0.1%FA) over 17 min

Detection: PDA 220nm

Results and analysis:

	Retention Time	Area	% Area
1	6.460	391097	100.00

Figure A50. RP-HPLC analysis of purified D-(KLAKLAKKLAKLAK)-AK using a linear gradient 2-80% MeOH/H$_2$O (0.1% FA) over 17 min using a Waters 2695 Symmetry® C18 column (3.9 x 150 mm, 5 µm particle size) set at a temperature of 25 °C at a flow rate of 1.0 mL/min with detection at 220 nm.

Sequence: NH$_2$-AHx-D-(KLAKLAK)$_2$-AK

Solvent: 2-80% MeCN (0.1% FA) over 17 min

Detection: PDA 220nm
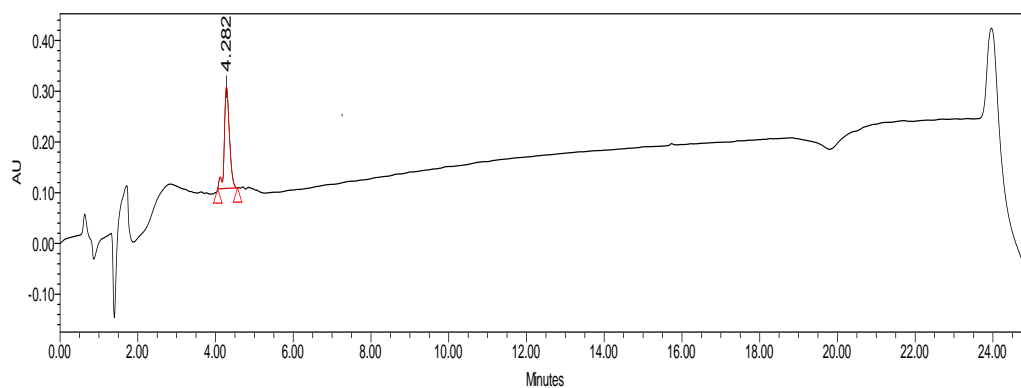
Results and analysis:

	Retention Time	Area	% Area	Height
1	4.282	1837039	100.00	200442

Figure A51. RP-HPLC analysis of purified D-(KLAKLAKKLAKLAK)-AK using a linear gradient 2-80% MeCN/H$_2$O (0.1% FA) over 17 min using a Waters 2695 Symmetry® C18 column (3.9 x 150 mm, 5 μm particle size) set at a temperature of 25 °C at a flow rate of 1.0 mL/min with detection at 220 nm.

Sequence: FITC-NH$_2$-AHx-D-(KLAKLAK)$_2$-AK

Solvent: 2to80MeOH (0.1%FA) over 17 min

Detection: PDA 220nm
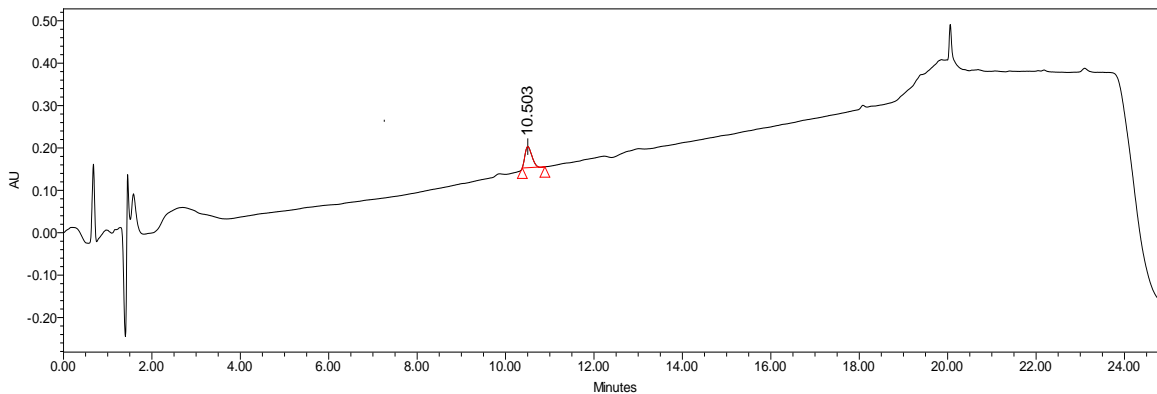
Results and analysis:

	Retention Time	Area	% Area	Height
1	10.503	536682	100.00	49875

Figure A52. RP-HPLC analysis of purified FITC-NH$_2$-AHx-D-(KLAKLAK)$_2$-AK using a linear gradient 2-80% MeOH/H$_2$O (0.1% FA) over 17 min using a Waters 2695 Symmetry® C18 column (3.9 x 150 mm, 5 μm particle size) set at a temperature of 25 °C at a flow rate of 1.0 mL/min with detection at 220 nm.

Sequence: FITC-NH$_2$-AHx-D-(KLAKLAK)$_2$-AK

Solvent: 2to80 MeCN (0.1%FA) over 17 min
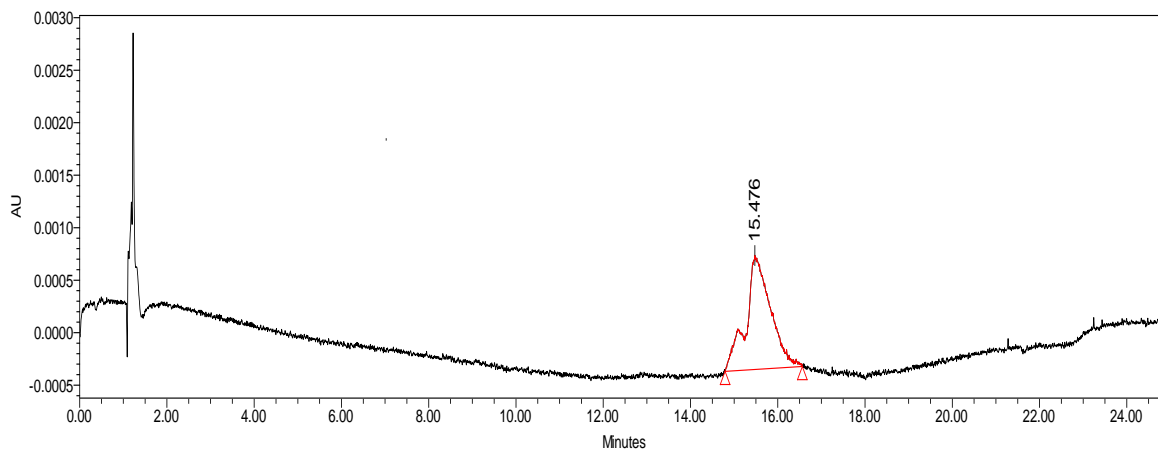
Detection: PDA 220nm
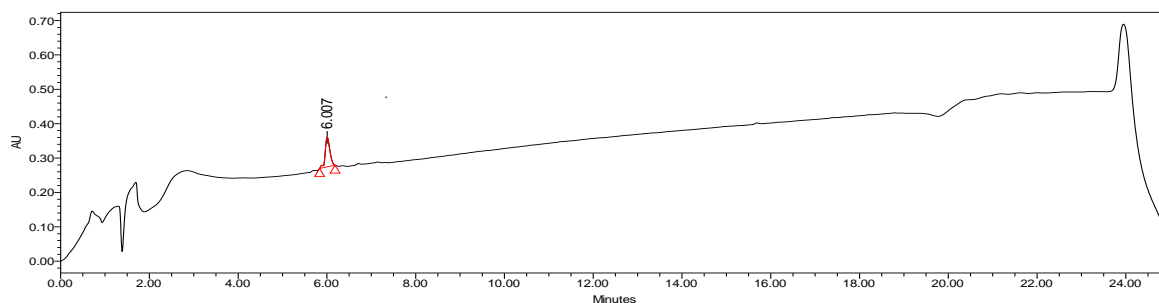
Results and analysis:

	Retention Time	Area	% Area	Height
1	6.007	625007	100.00	85771

Figure A53. RP-HPLC analysis of purified FITC-NH$_2$-AHx-D-(KLAKLAK)$_2$-AK using a linear gradient 2-80% MeCN/H$_2$O (0.1% FA) over 17 min using a Waters 2695 Symmetry® C18 column (3.9 x 150 mm, 5 μm particle size) set at a temperature of 25 °C at a flow rate of 1.0 mL/min with detection at 220 nm.

Sequence: Purified Crude D-(KLAKLAK)₂-AK-Nucleolipid

Solvent: 2to80 MeOH (0.1%FA) over 17 min

Detection: PDA 260nm

Note: After 17min, column contains impurities that are also found in the blank that has not been integrated.
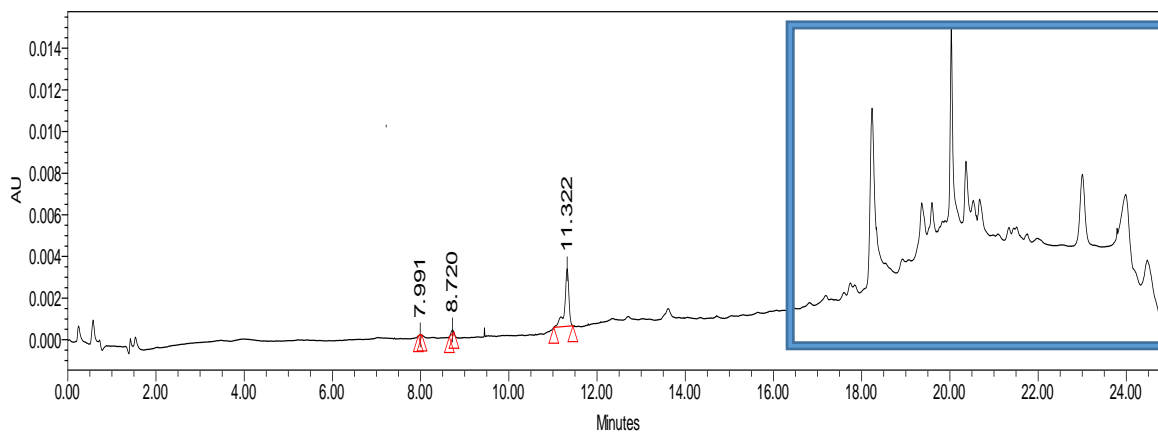
Results and analysis:

	Retention Time	Area	% Area
1	7.991	69	0.36
2	8.720	669	3.49
3	11.322	18443	96.15

Figure A54. RP-HPLC analysis of purified NH₂-AHx-D-(KLAKLAK)₂-AK-Hexadecylamine nucleolipid using a linear gradient 2-80% MeOH/H₂O (0.1% FA) over 17 min using a Waters 2695 Symmetry® C18 column (3.9 x 150 mm, 5 μm particle size) set at a temperature of 25 °C at a flow rate of 1.0 mL/min with detection at 220 nm.

Sequence: Purified Crude D-(KLAKLAK)₂-AK-Nucleolipid

Solvent: 2to80 MeCN (0.1%FA) over 17 min

Detection: PDA 220nm
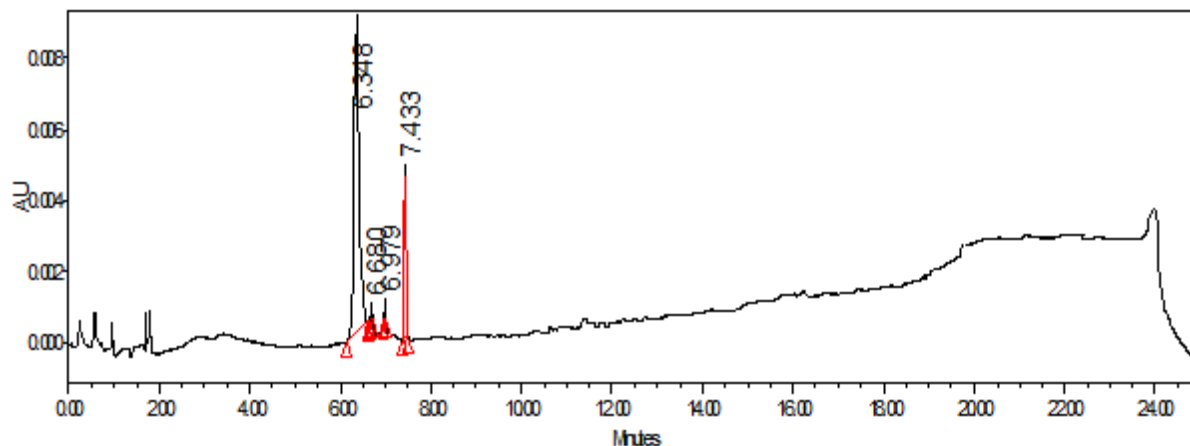
Results and analysis:

	Retention Time	Area	% Area
1	6.348	70359	84.12
2	6.680	376	0.45
3	6.979	574	0.69
4	7.433	12333	14.75

Figure A55. RP-HPLC analysis of purified NH₂-AHx-D-(KLAKLAK)₂-AK-hexadecylamine nucleolipid using a linear gradient 2-80% MeCN/H₂O (0.1% FA) over 17 min using a Waters 2695 Symmetry® C18 column (3.9 x 150 mm, 5 μm particle size) set at a temperature of 25 °C at a flow rate of 1.0 mL/min with detection at 220 nm.

Sequence: Pure FITC-D-(KLAKLAK)$_2$-AK-Nucleolipid (FITC isomer used)

Solvent: 20to80 MeOH (0.1%FA) over 17 min

Detection: PDA 220 nm
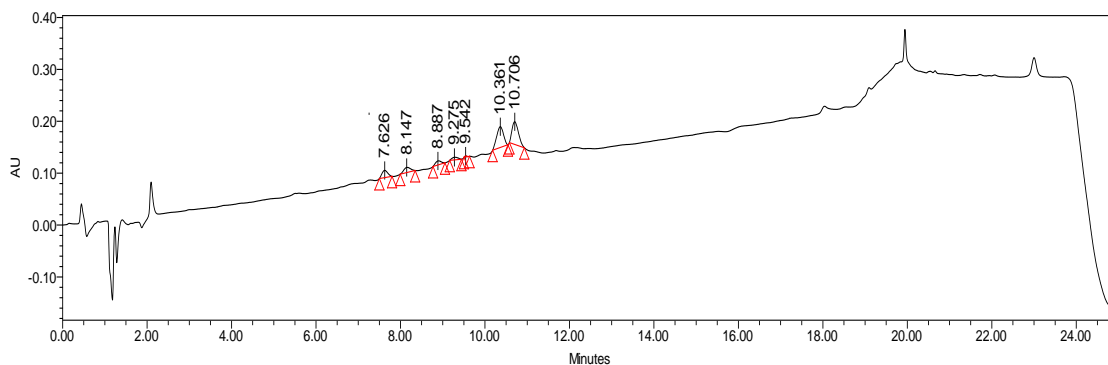
Results and analysis:

	Retention Time	Area	% Area
1	7.626	131930	10.30
2	8.147	110919	8.66
3	8.887	71872	5.61
4	9.275	49954	3.90
5	9.542	6980	0.55
6	10.361	445885	34.82
7	10.706	462856	36.15

Figure A56. RP-HPLC analysis of purified FITC-NH$_2$-AHx-D-(KLAKLAK)$_2$-AK-hexadecylamine nucleolipid using a linear gradient 2-80% MeOH/H$_2$O (0.1% FA) over 17 min using a Waters 2695 Symmetry® C18 column (3.9 x 150 mm, 5 µm particle size) set at a temperature of 25 °C at a flow rate of 1.0 mL/min with detection at 220 nm.

Sequence: Pure FITC-D-(KLAKLAK)₂-AK-Nucleolipid (FITC isomer used)

Solvent: 20to80 MeCN (0.1%FA) over 17 min

Detection: PDA 220 nm
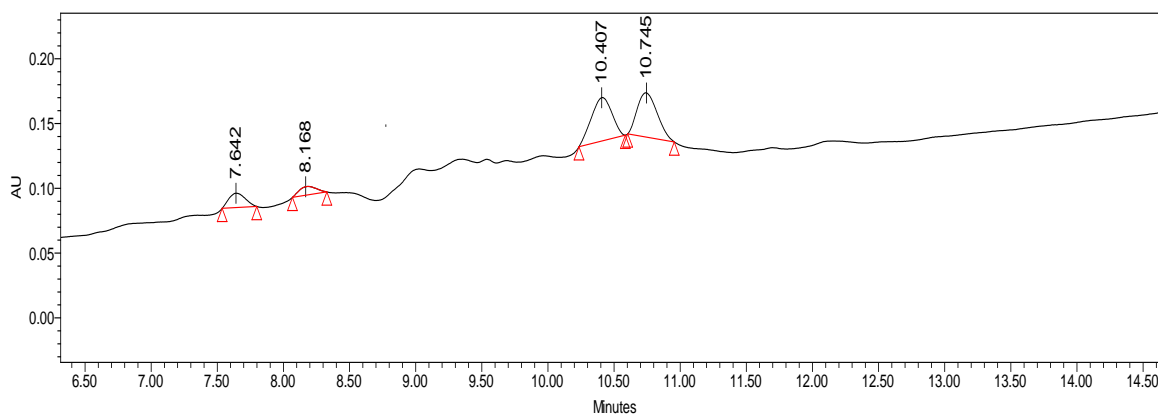
Results and analysis:

	Retention Time	Area	% Area
1	7.642	96124	10.93
2	8.168	59638	6.78
3	10.407	362857	41.25
4	10.745	360942	41.04

Figure A57. RP-HPLC analysis of purified FITC-NH₂-AHx-D-(KLAKLAK)₂-AK-hexadecylamine nucleolipid using a linear gradient 2-80% MeCN/H₂O (0.1% FA) over 17 min using a Waters 2695 Symmetry® C18 column (3.9 x 150 mm, 5 μm particle size) set at a temperature of 25 °C at a flow rate of 1.0 mL/min with detection at 220 nm.

Sequence: Pure D-(KLAKLAK)₂-AK-Palmitamide

Solvent: 20to80 MeCN (0.1%FA) over 17 min

Detection: PDA 220 nm
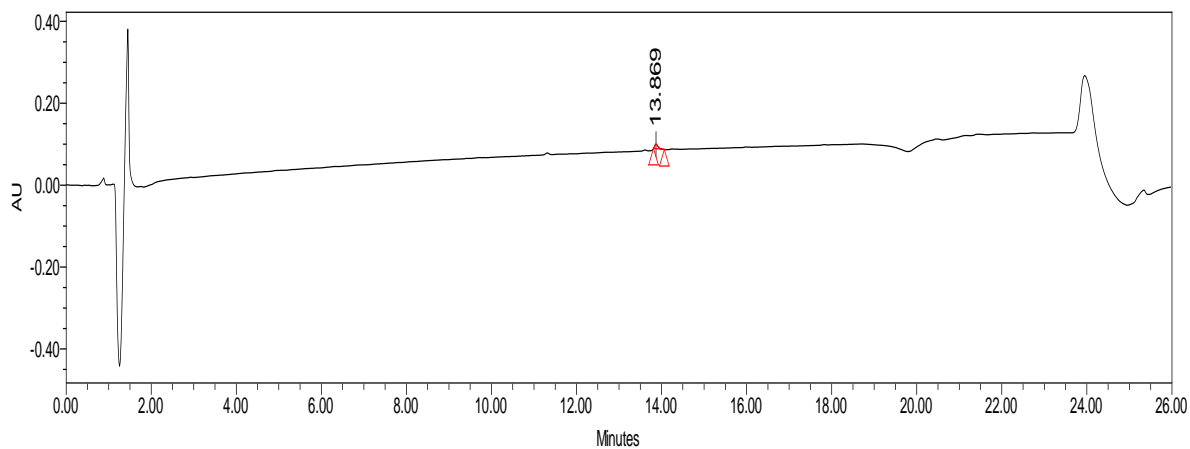
Results and analysis:

	Retention Time	Area	% Area	Height
1	13.869	58123	100.00	10727

Figure A58. RP-HPLC analysis of purified NH_2-AHx-D-(KLAKLAK)₂-AK-Palmitamide using a linear gradient 20-80% MeCN/H_2O (0.1% FA) over 17 min using a Waters 2695 Symmetry® C18 column (3.9 x 150 mm, 5 μm particle size) set at a temperature of 25 °C at a flow rate of 1.0 mL/min with detection at 220 nm.

Sequence: D-(KLAKLAK)$_2$-AK-Palmitamide

Solvent: 20to80 MeOH (0.1%FA) over 17 min

Detection: PDA 220 nm
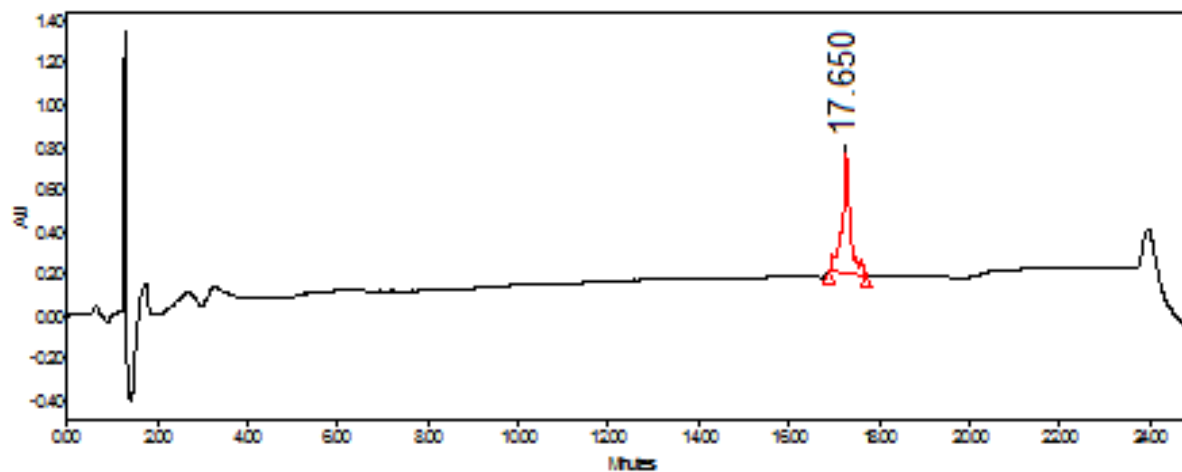
Results and analysis:

	Retention Time	Area	% Area
1	17.650	7418305	100.00

Figure A59. RP-HPLC analysis of purified NH$_2$-AHx-D-(KLAKLAK)$_2$-AK-Palmitamide using a linear gradient 20-80% MeOH/H$_2$O (0.1% FA) over 17 min using a Waters 2695 Symmetry® C18 column (3.9 x 150 mm, 5 μm particle size) set at a temperature of 25 °C at a flow rate of 1.0 mL/min with detection at 220 nm.

Sequence: FITC-D-(KLAKLAK)$_2$-AK-Palmitamide

Solvent: 20to80 MeOH (0.1%FA) over 17 min

Detection: PDA 495 nm

Results and analysis:

	Retention Time	Area	% Area	Height
1	15.476	42560	100.00	1086

Figure A60. RP-HPLC analysis of purified FITC-D-(KLAKLAK)$_2$-AK-Palmitamide using a linear gradient 20-80% MeOH/H$_2$O (0.1% FA) over 17 min using a Waters 2695 Symmetry® C18 column (3.9 x 150 mm, 5 μm particle size) set at a temperature of 25 °C at a flow rate of 1.0 mL/min with detection at 220 nm.

Sequence: FITC-D-(KLAKLAK)₂-AK-Palmitamide

Solvent: 20to80 MeCN (0.1%FA) over 17 min

Detection: PDA 495 nm
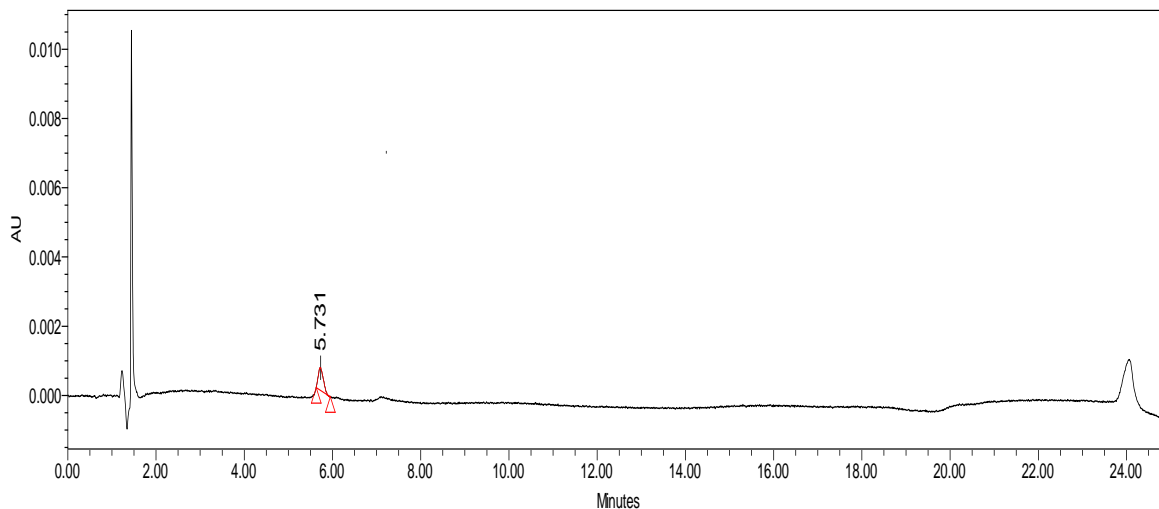
Results and analysis:

	Retention Time	Area	% Area
1	5.731	5215	100.00

Figure A61. RP-HPLC analysis of purified FITC-D-(KLAKLAK)₂-AK-Palmitamide using a linear gradient 20-80% MeCN/H₂O (0.1% FA) over 17 min using a Waters 2695 Symmetry® C18 column (3.9 x 150 mm, 5 μm particle size) set at a temperature of 25 °C at a flow rate of 1.0 mL/min with detection at 220 nm.
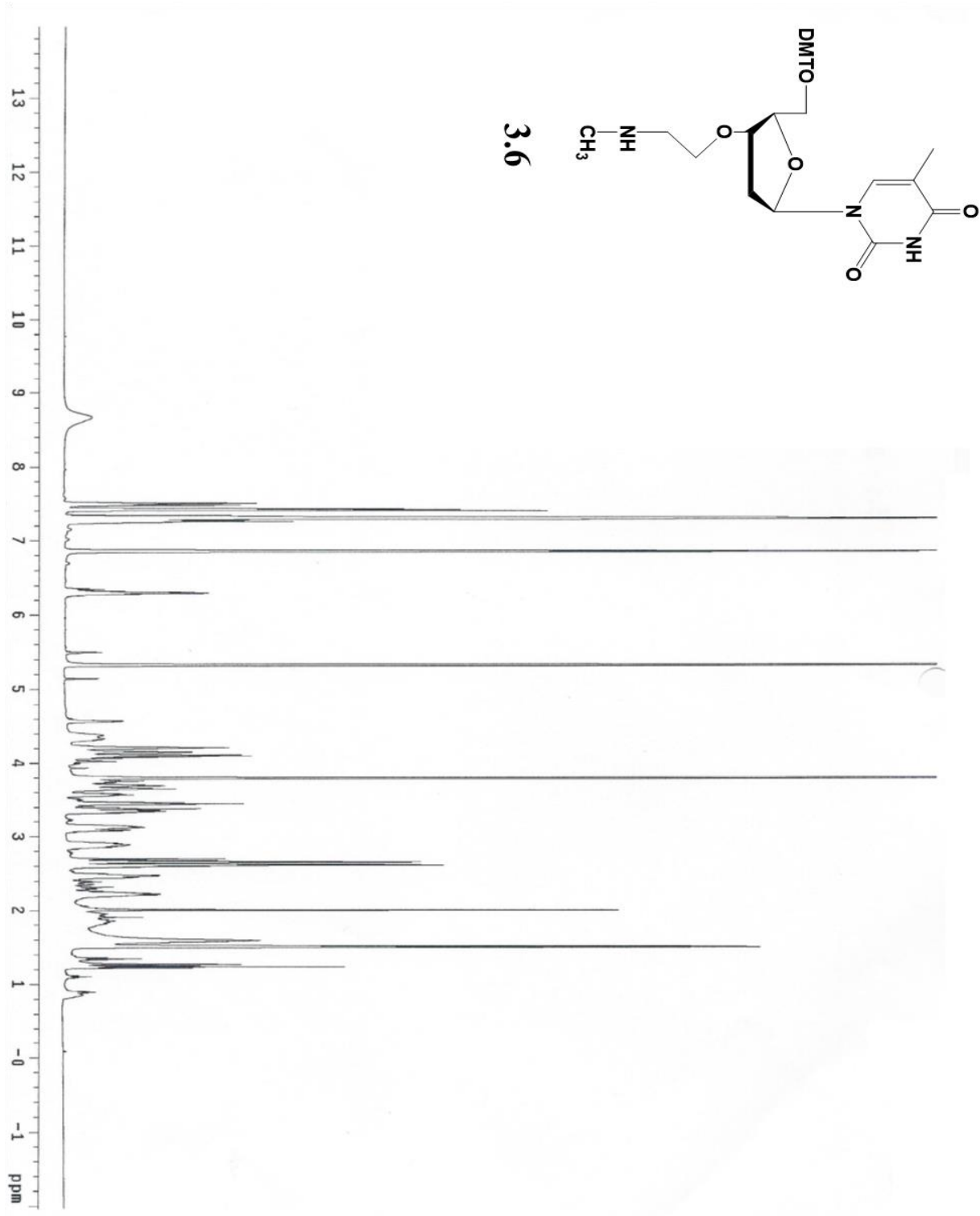
Figure A62. ^{1}H-NMR spectrum of **3.6**
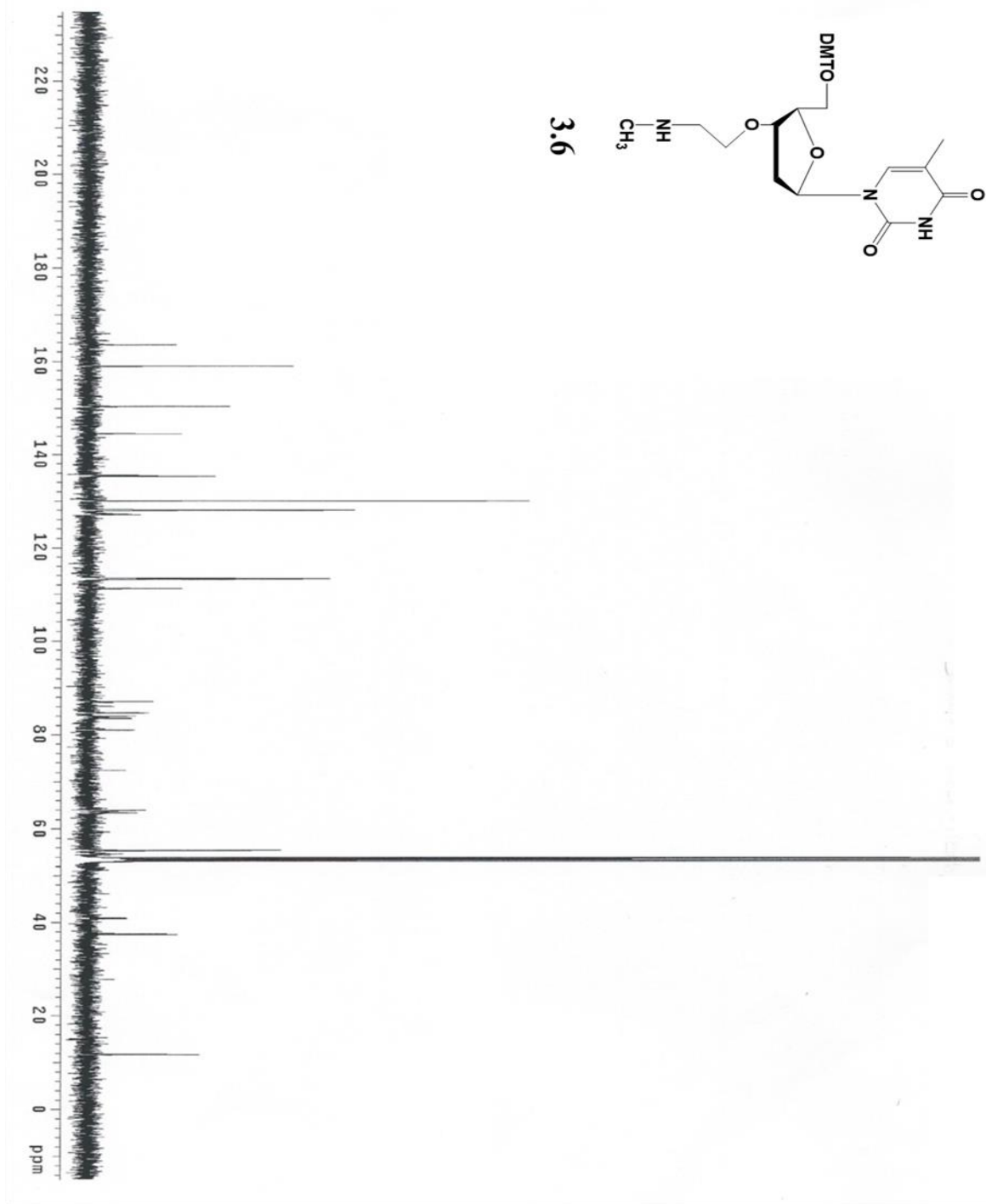
Figure A63. ^{13}C-NMR spectrum of **3.6**
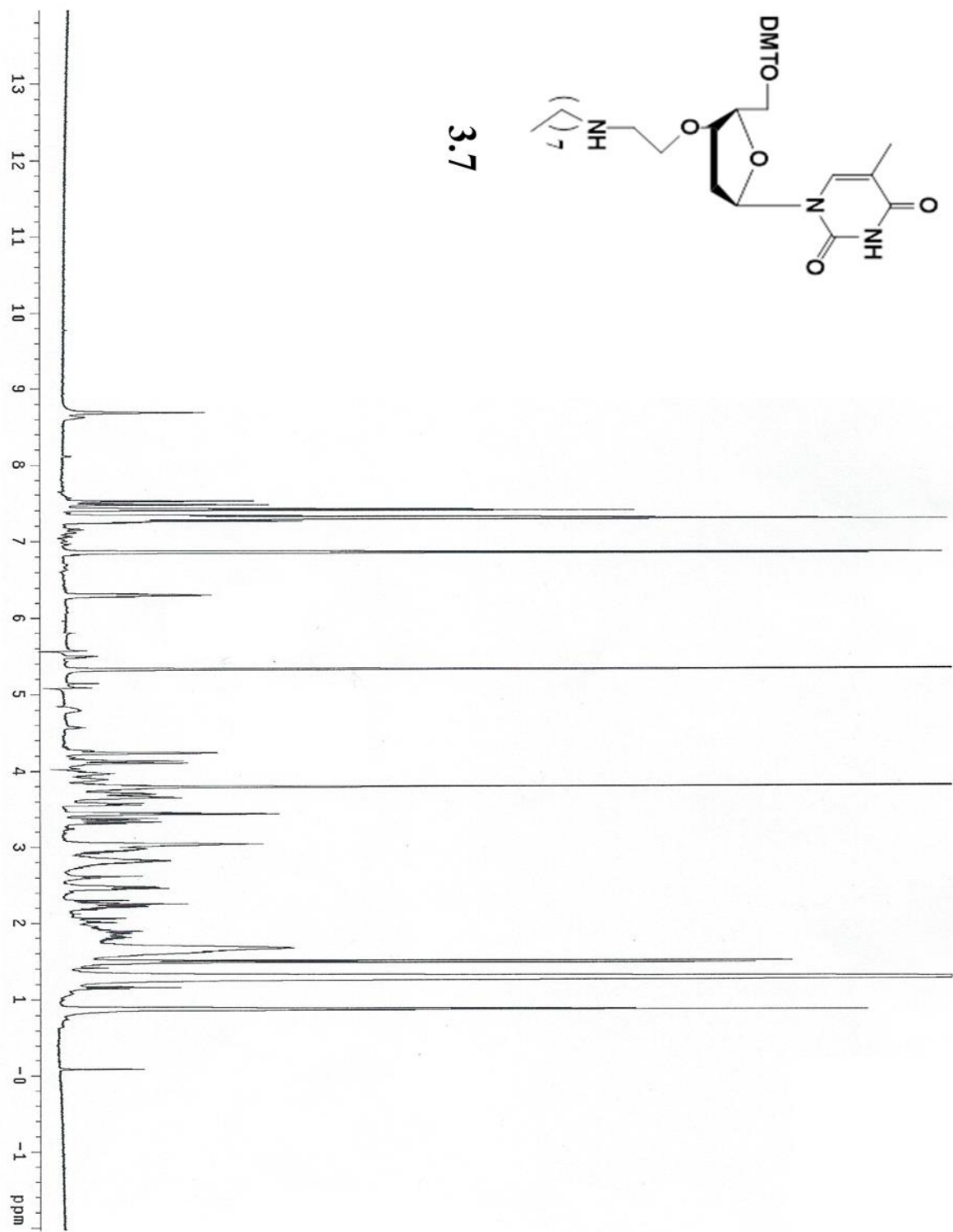
Figure A64. ^{1}H-NMR spectrum of **3.7**
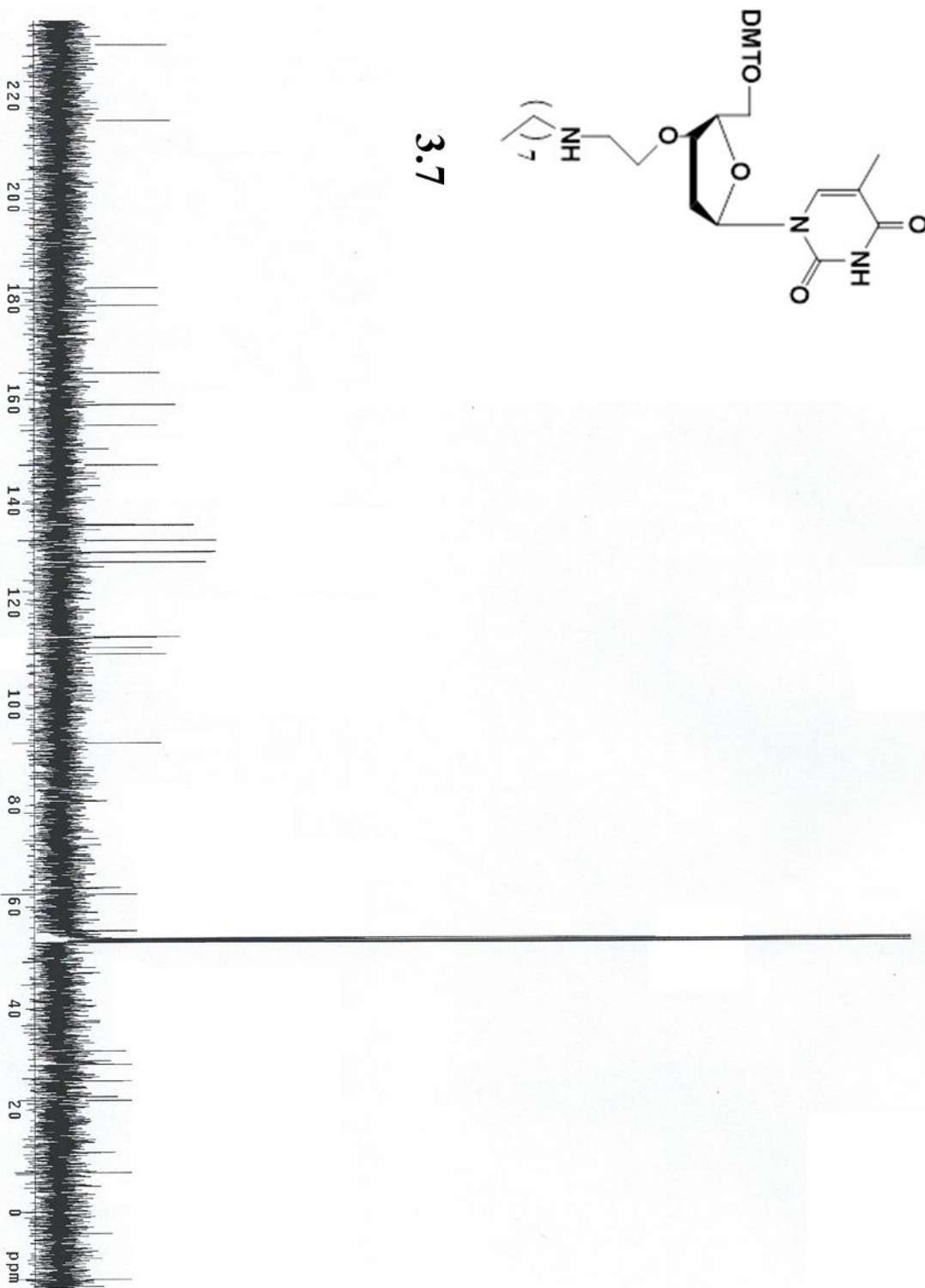
Figure A65. ^{13}C-NMR spectrum of **3.7**
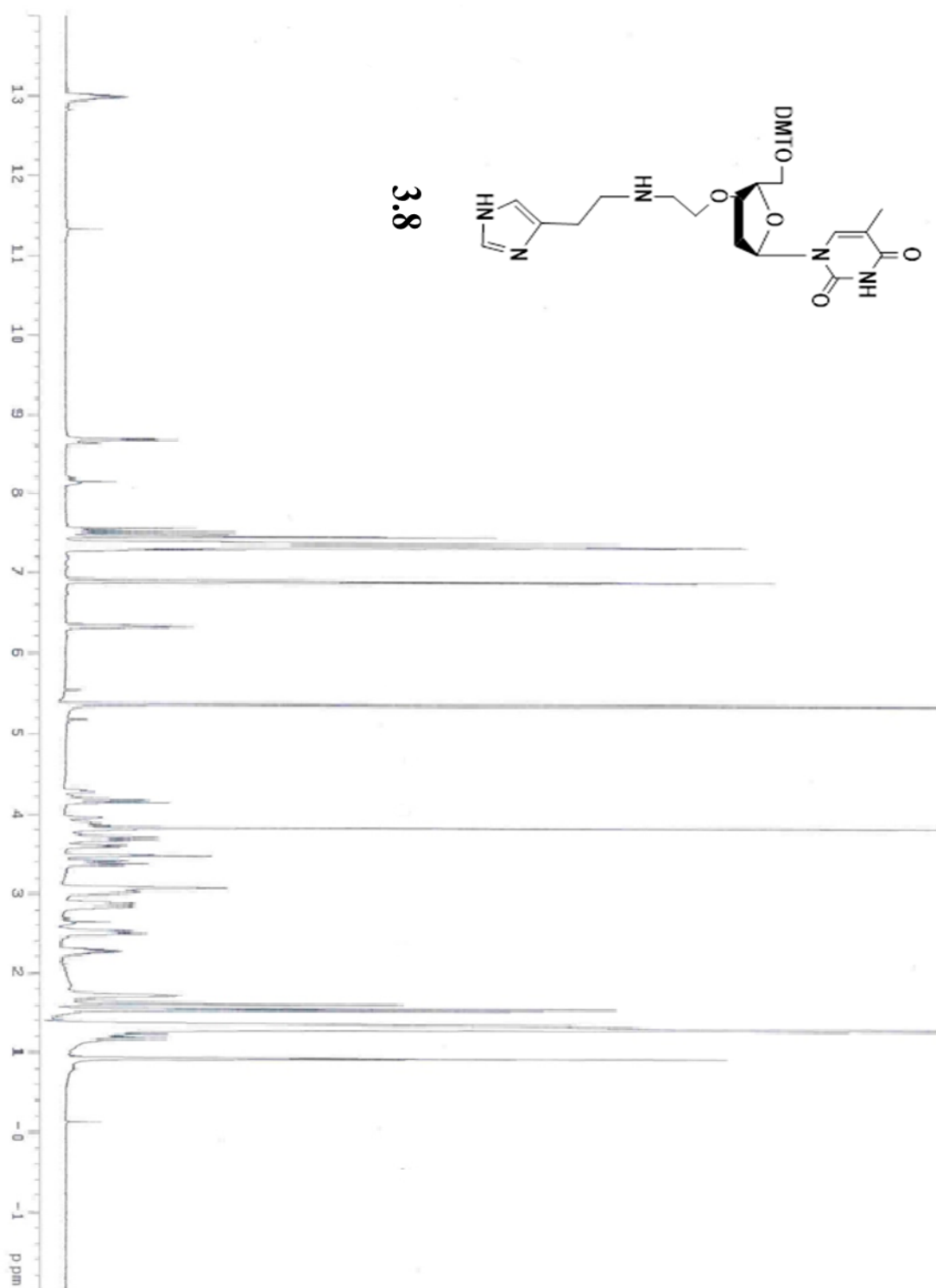
Figure A66. ^{1}H-NMR spectrum of **3.8**
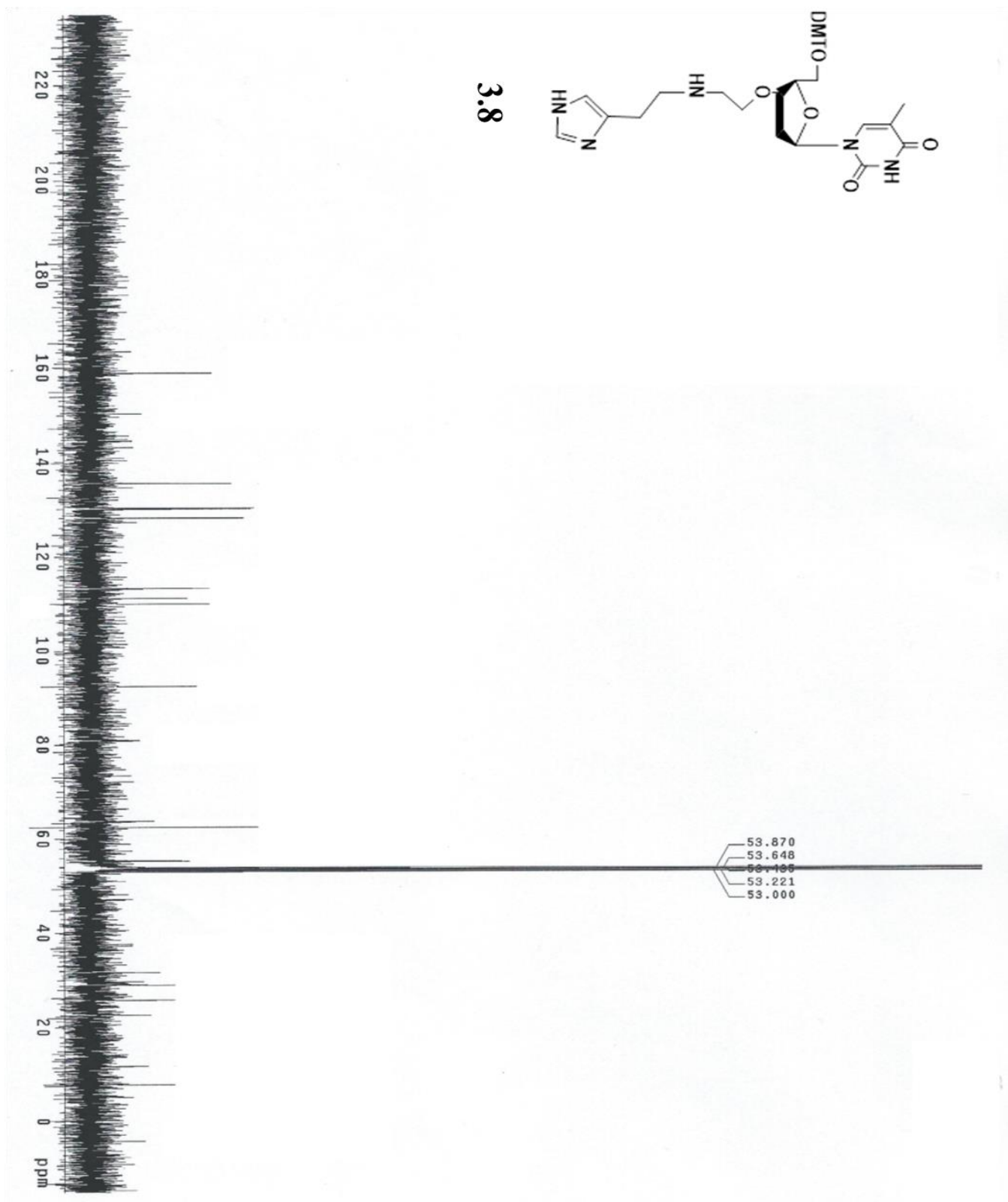
Figure A67. ^{13}C-NMR spectrum of **3.8**
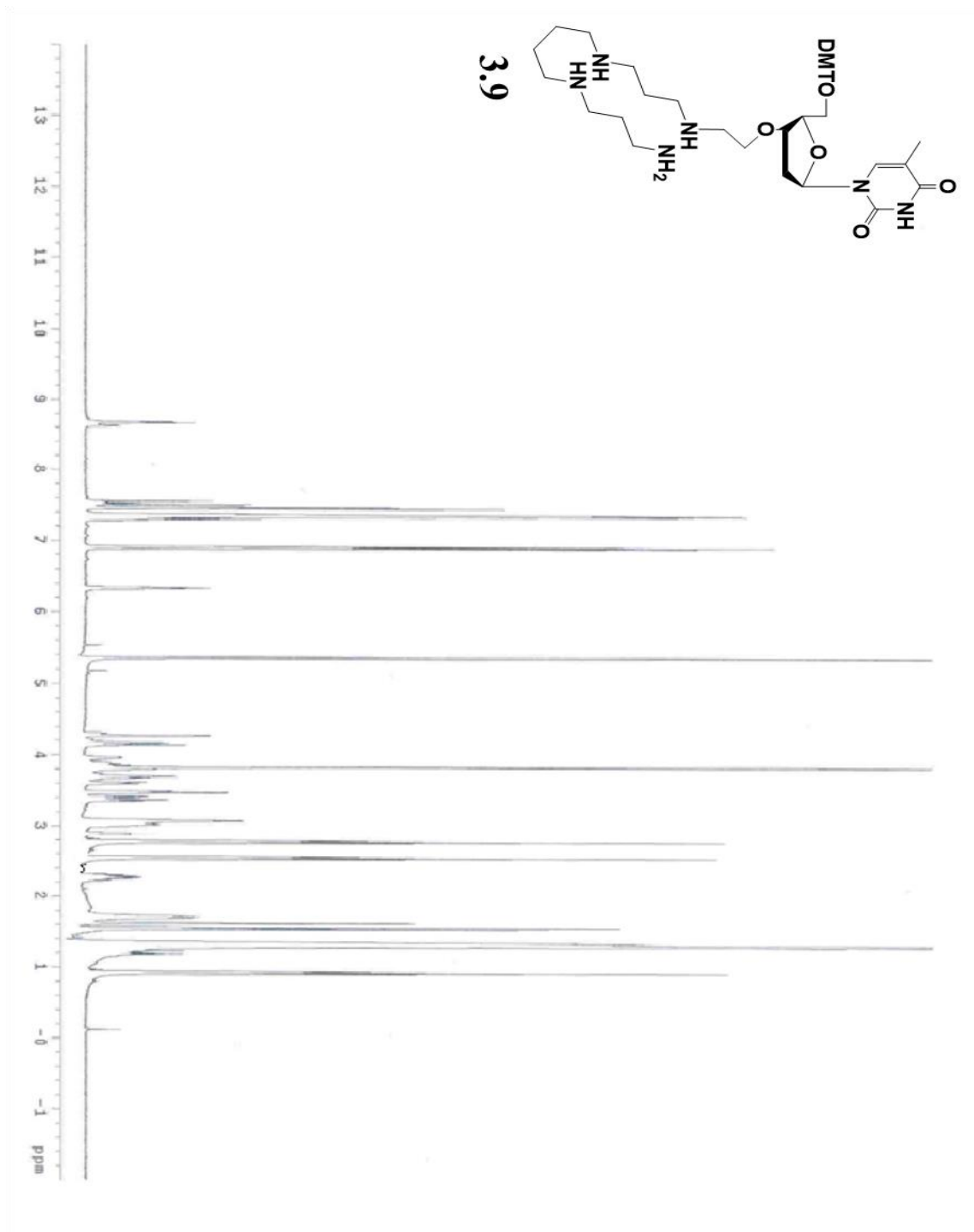
Figure A68. ^{1}H-NMR spectrum of **3.9**
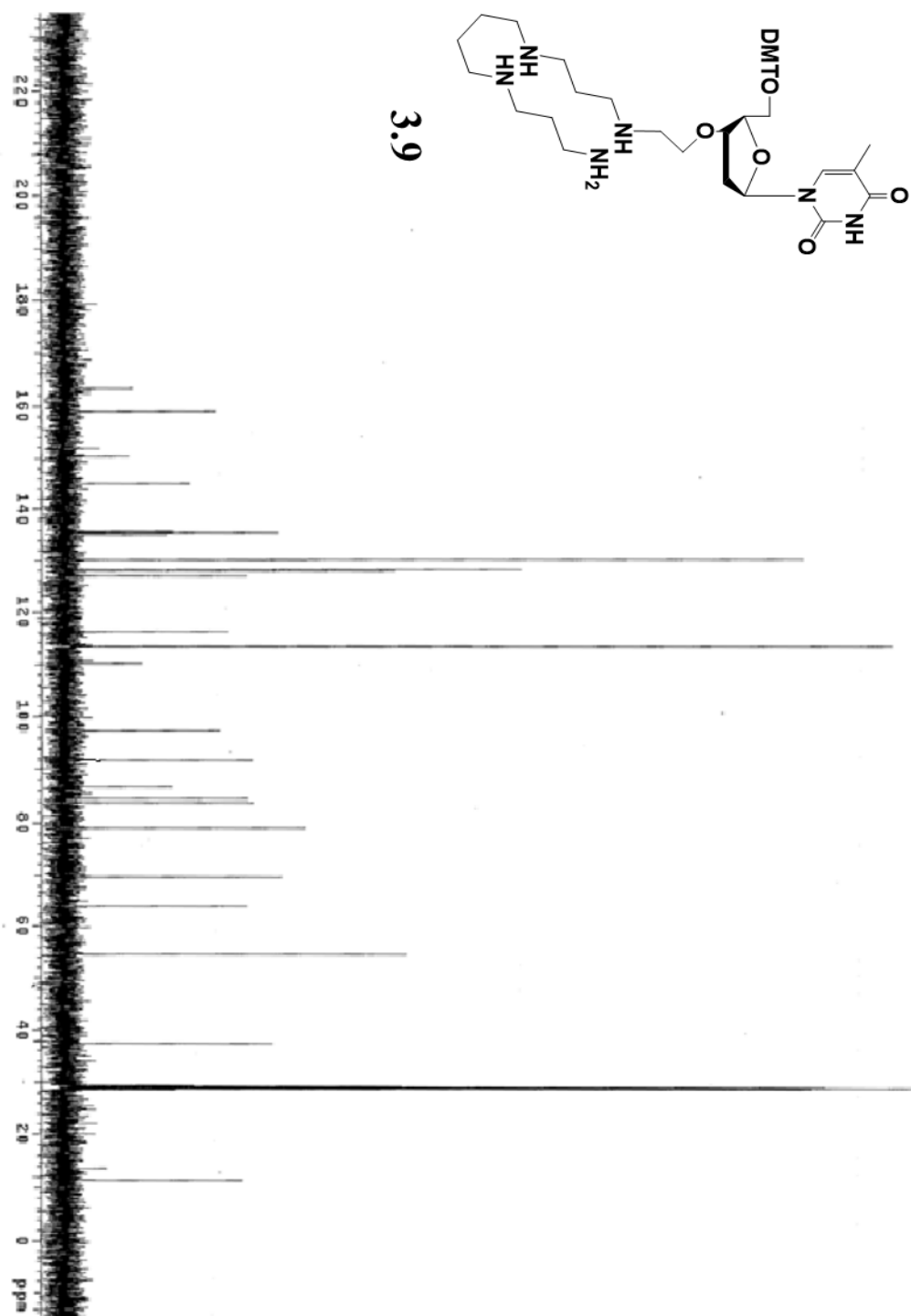
Figure A69. ^{13}C-NMR spectrum of **3.9**
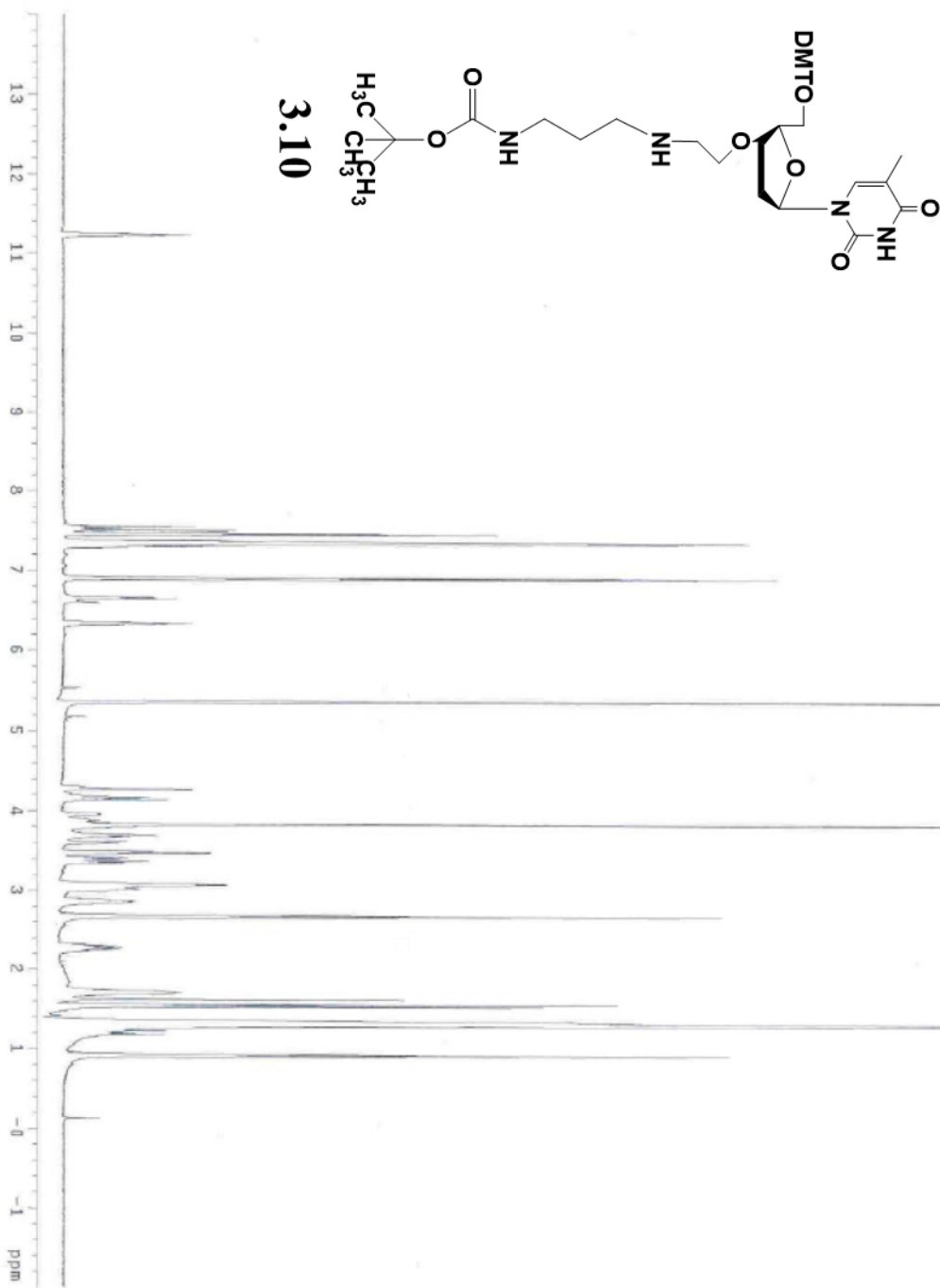
Figure A70. ¹H-NMR spectrum of **3.10**
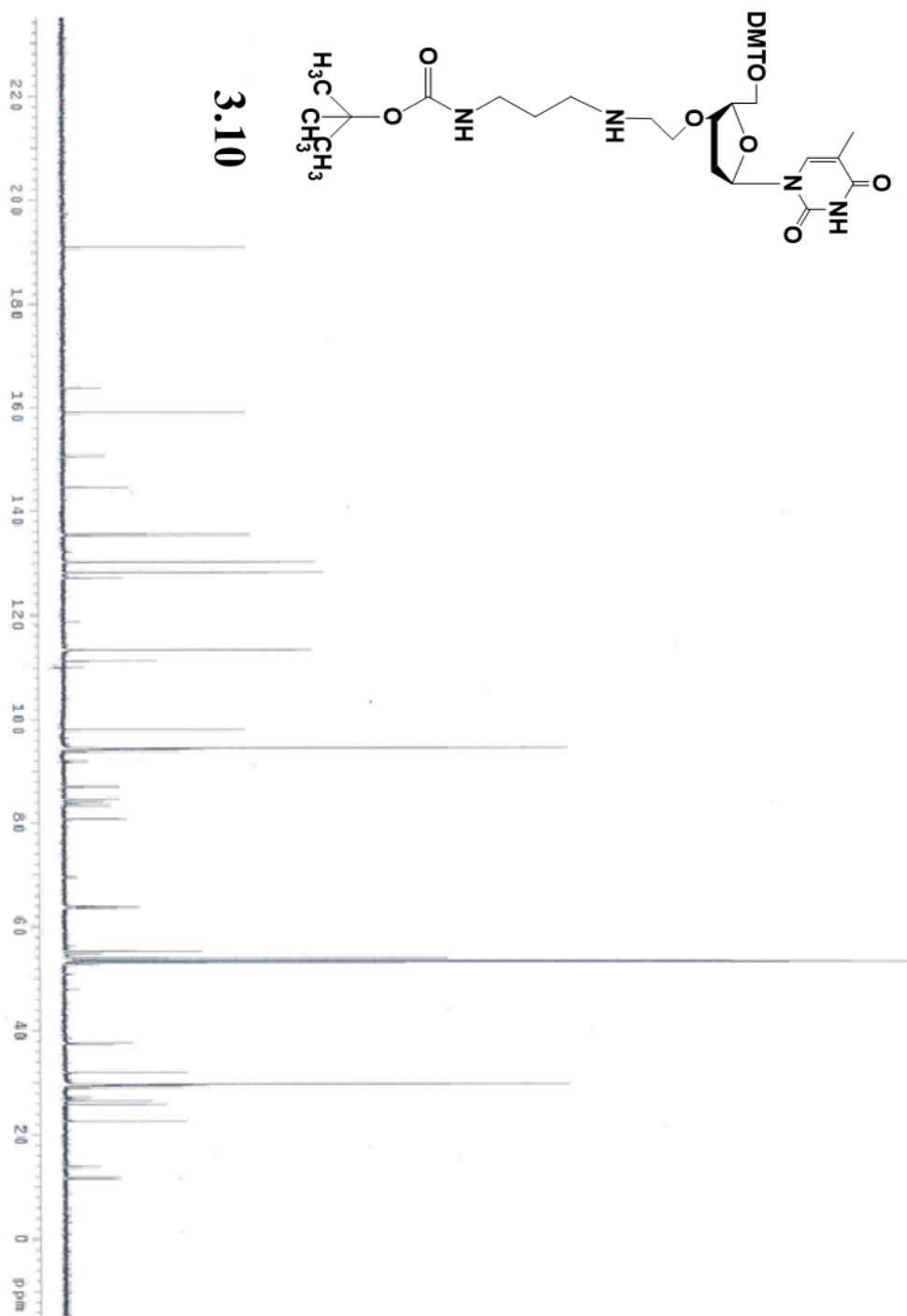
Figure A71. ^{13}C-NMR spectrum of **3.10**
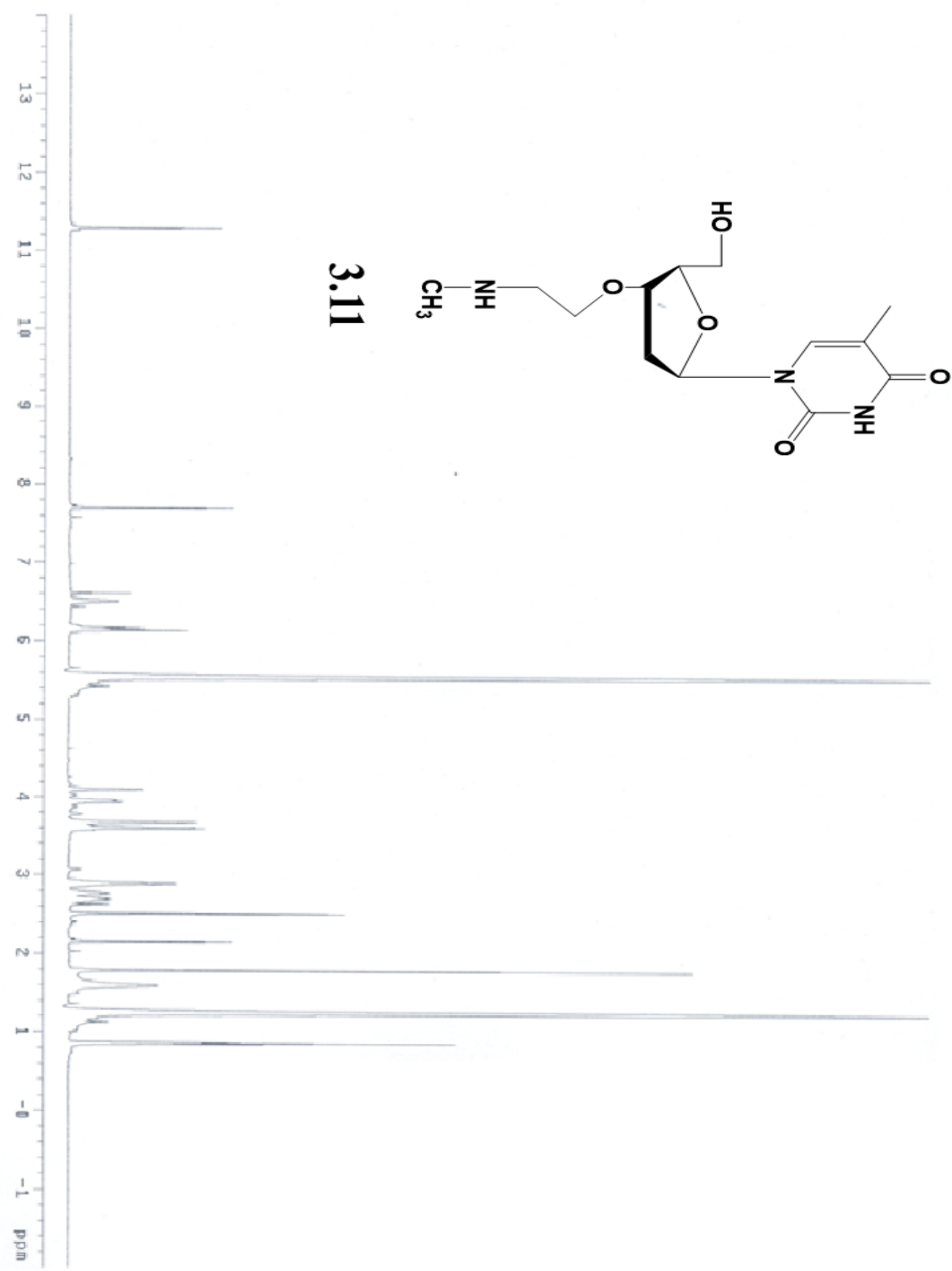
Figure A72. ^{1}H-NMR spectrum of **3.11**
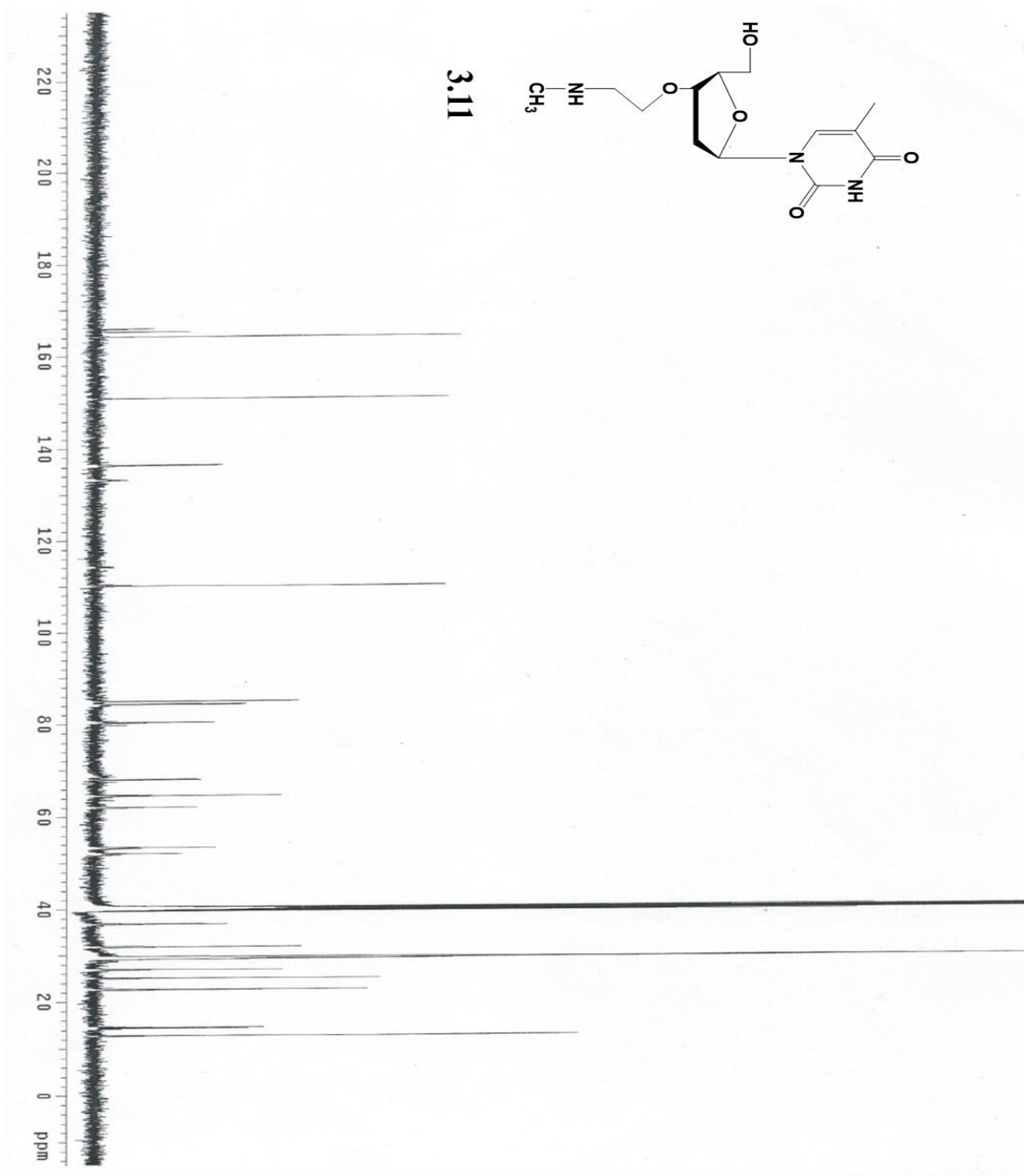
Figure A73. ^{13}C-NMR spectrum of **3.11**
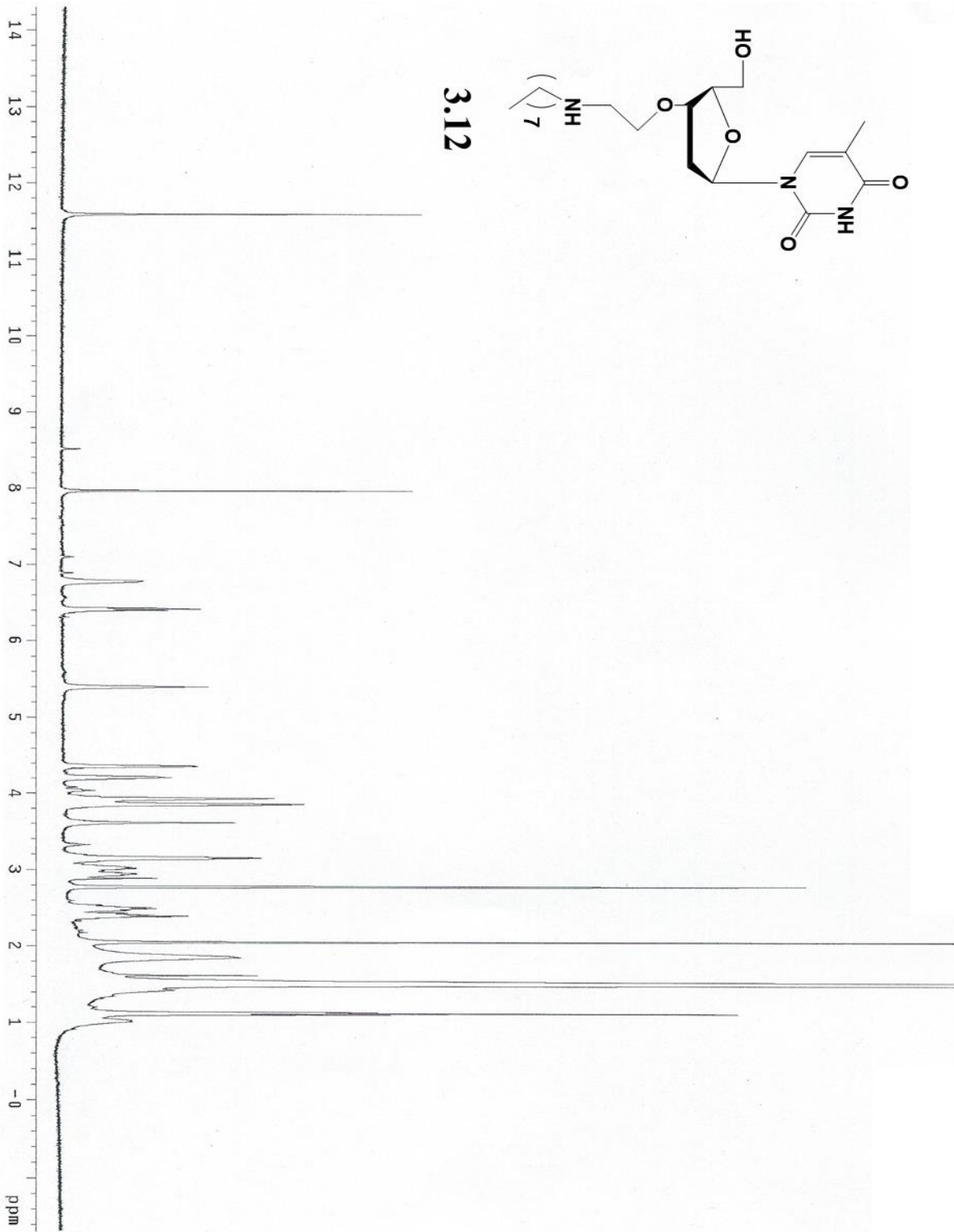
Figure A74. ^{1}H-NMR spectrum of **3.12**
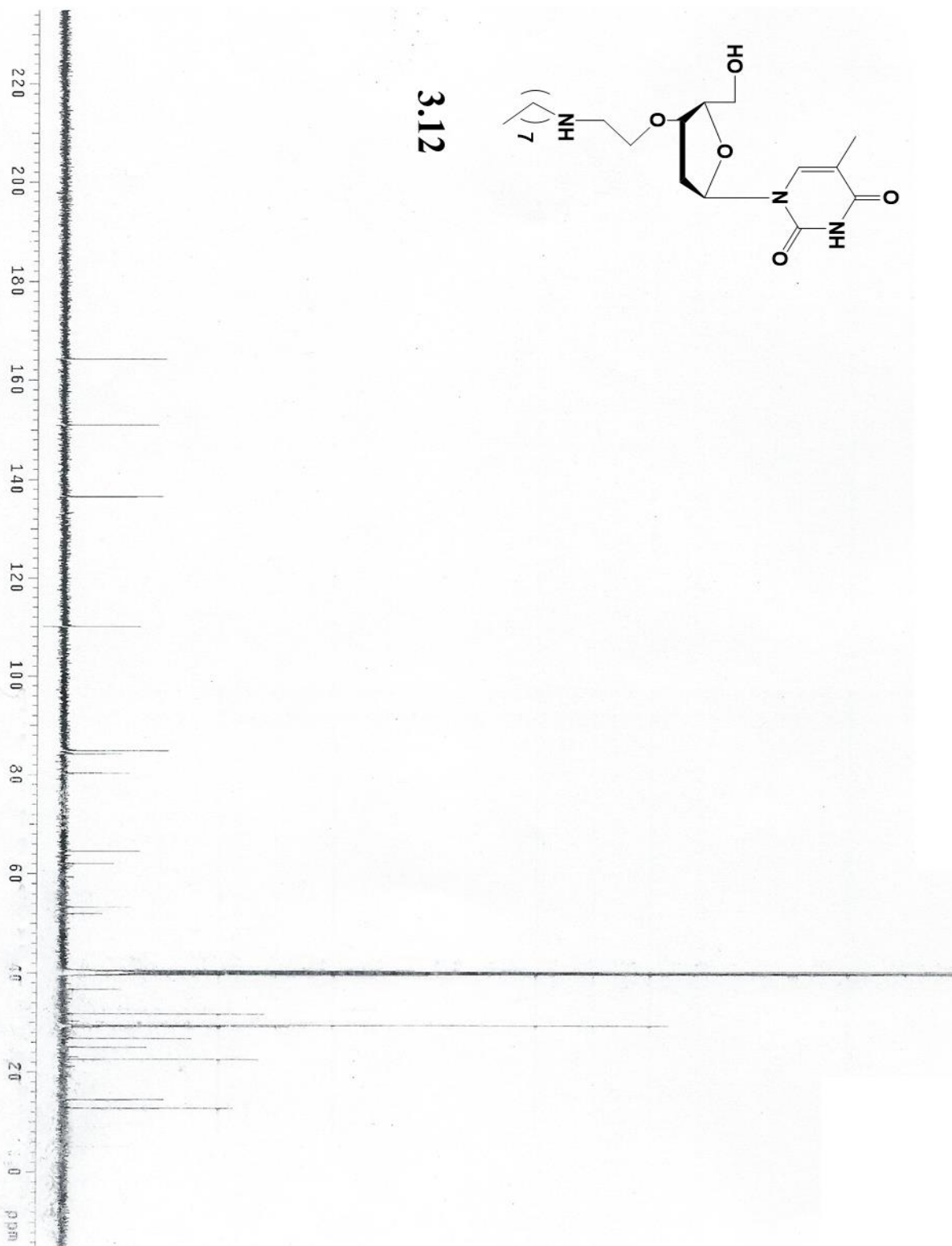
Figure A75. ^{13}C-NMR spectrum of **3.12**
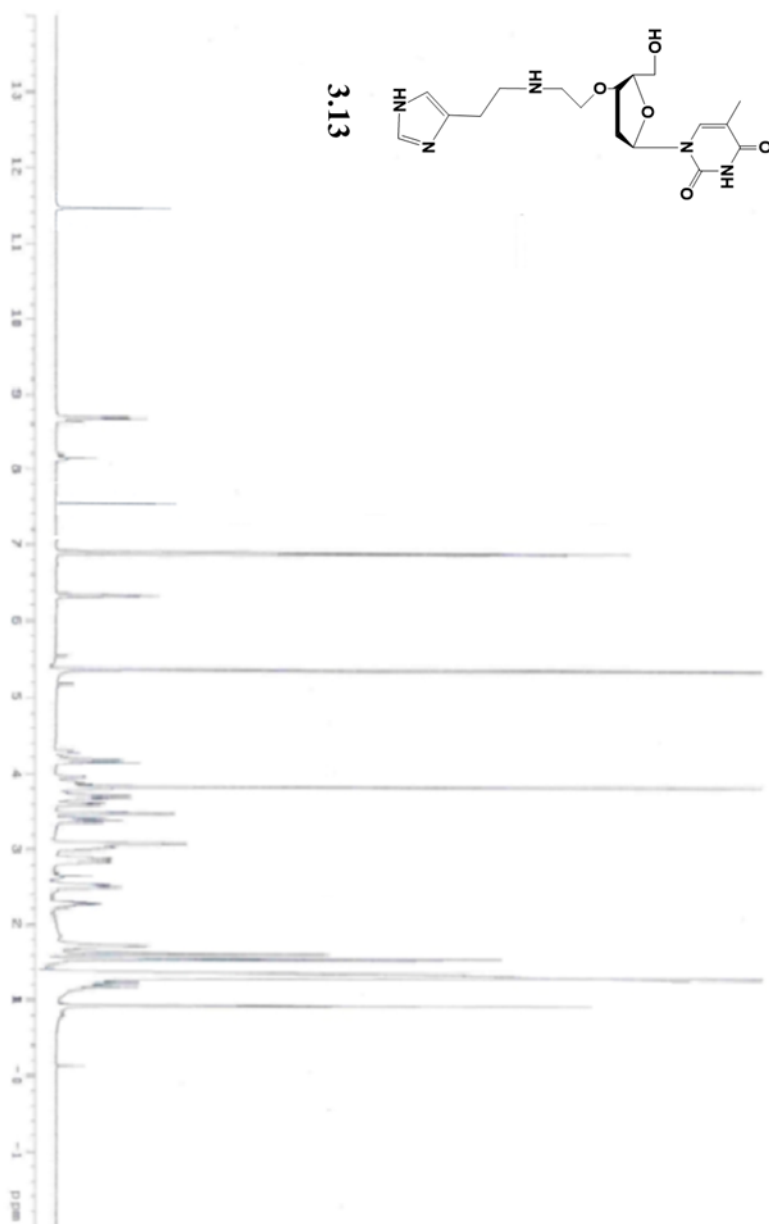
Figure A76. ^{1}H-NMR spectrum of **3.13**
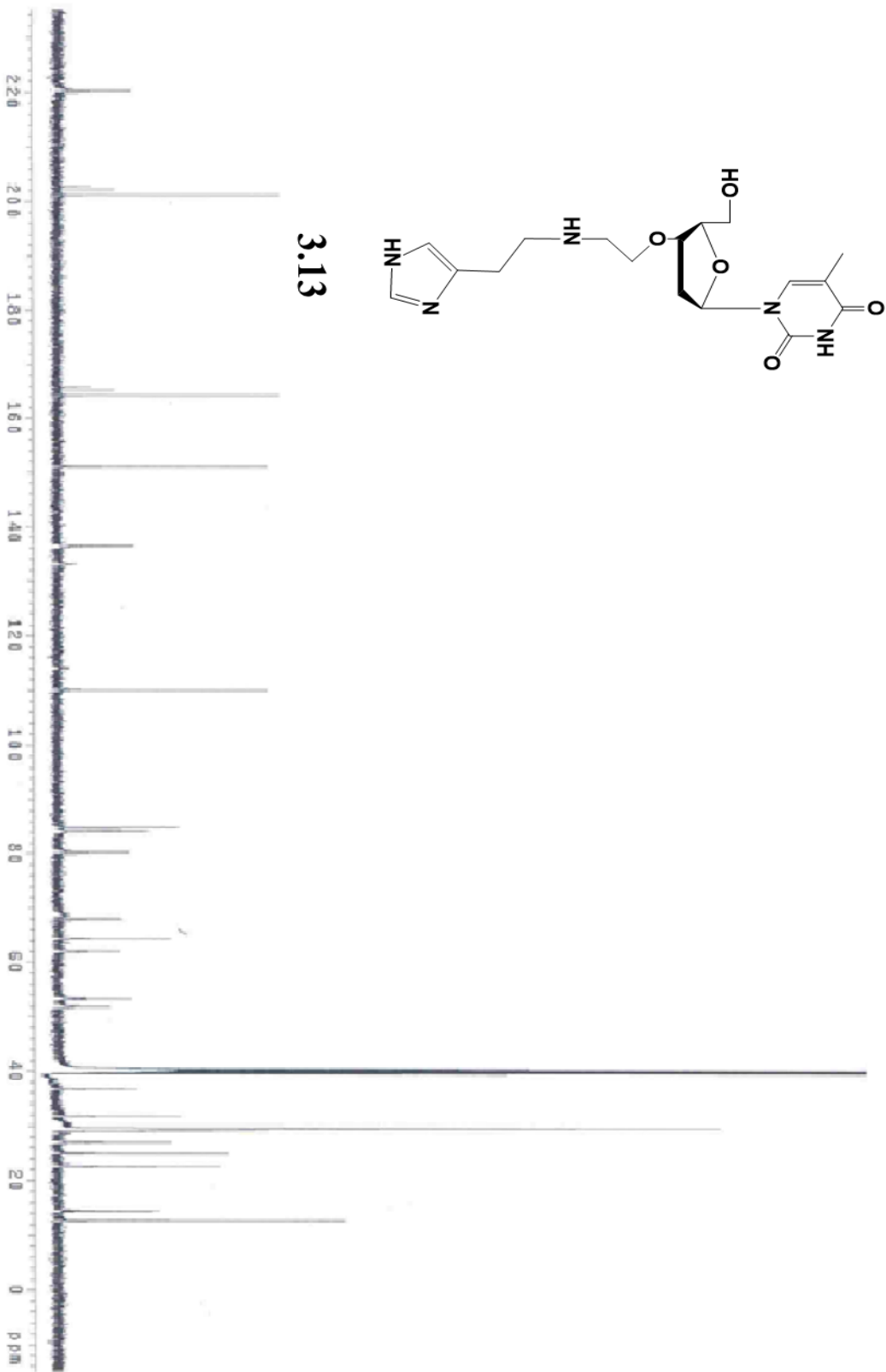
Figure A77. ¹³C-NMR spectrum of **3.13**
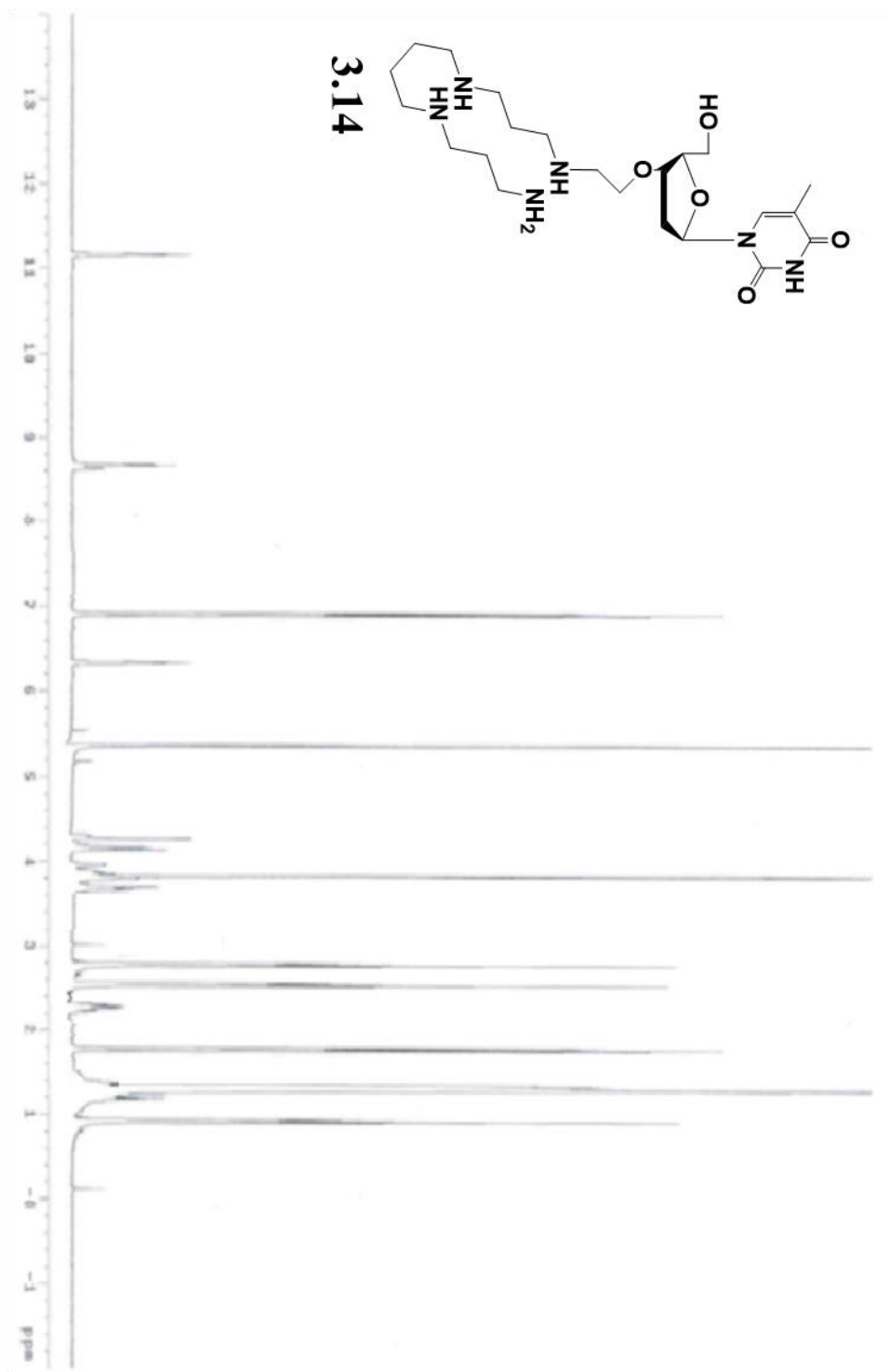
Figure A78. ^{1}H-NMR spectrum of **3.14**
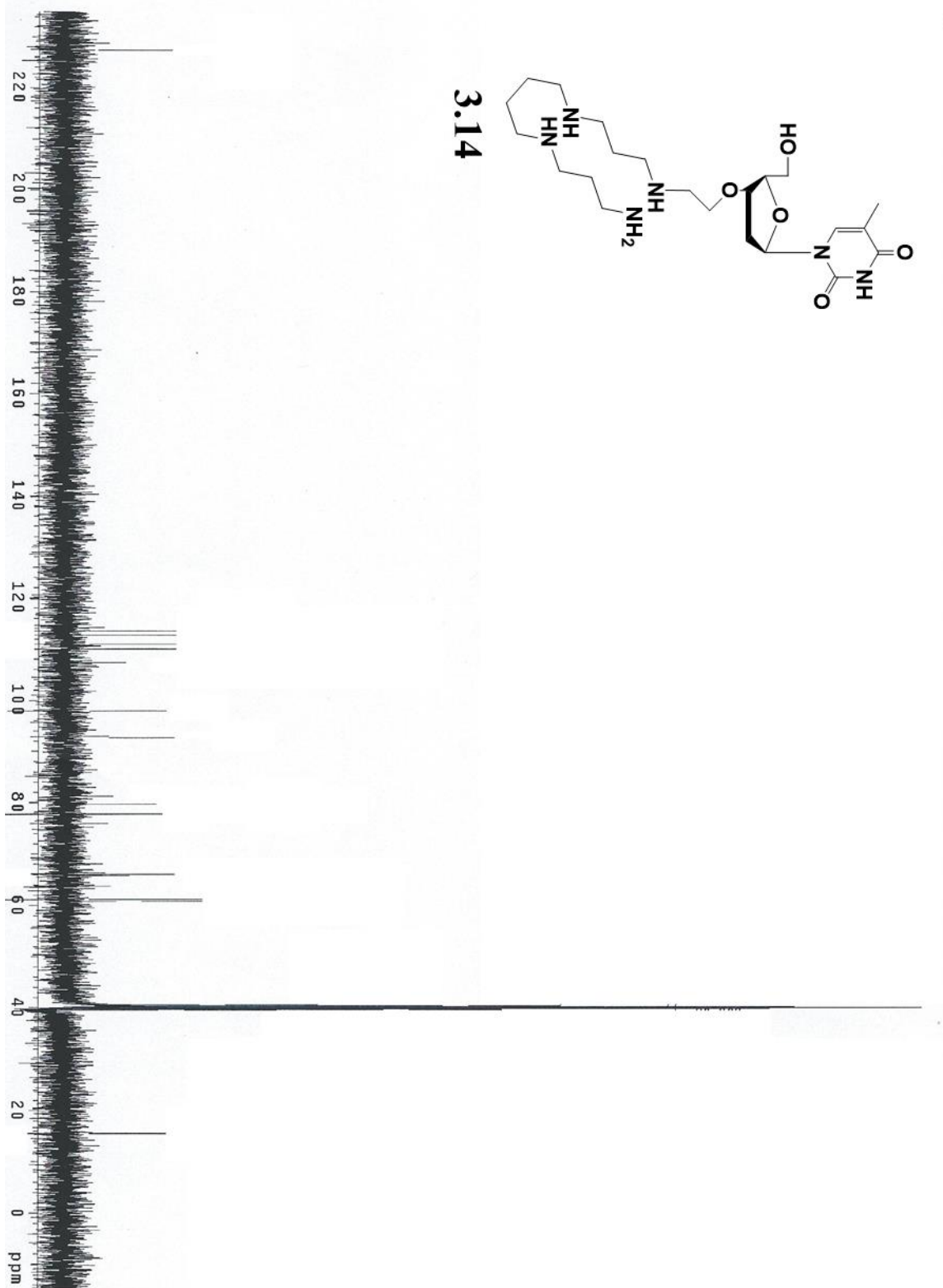
Figure A79. ^{13}C-NMR spectrum of **3.14**
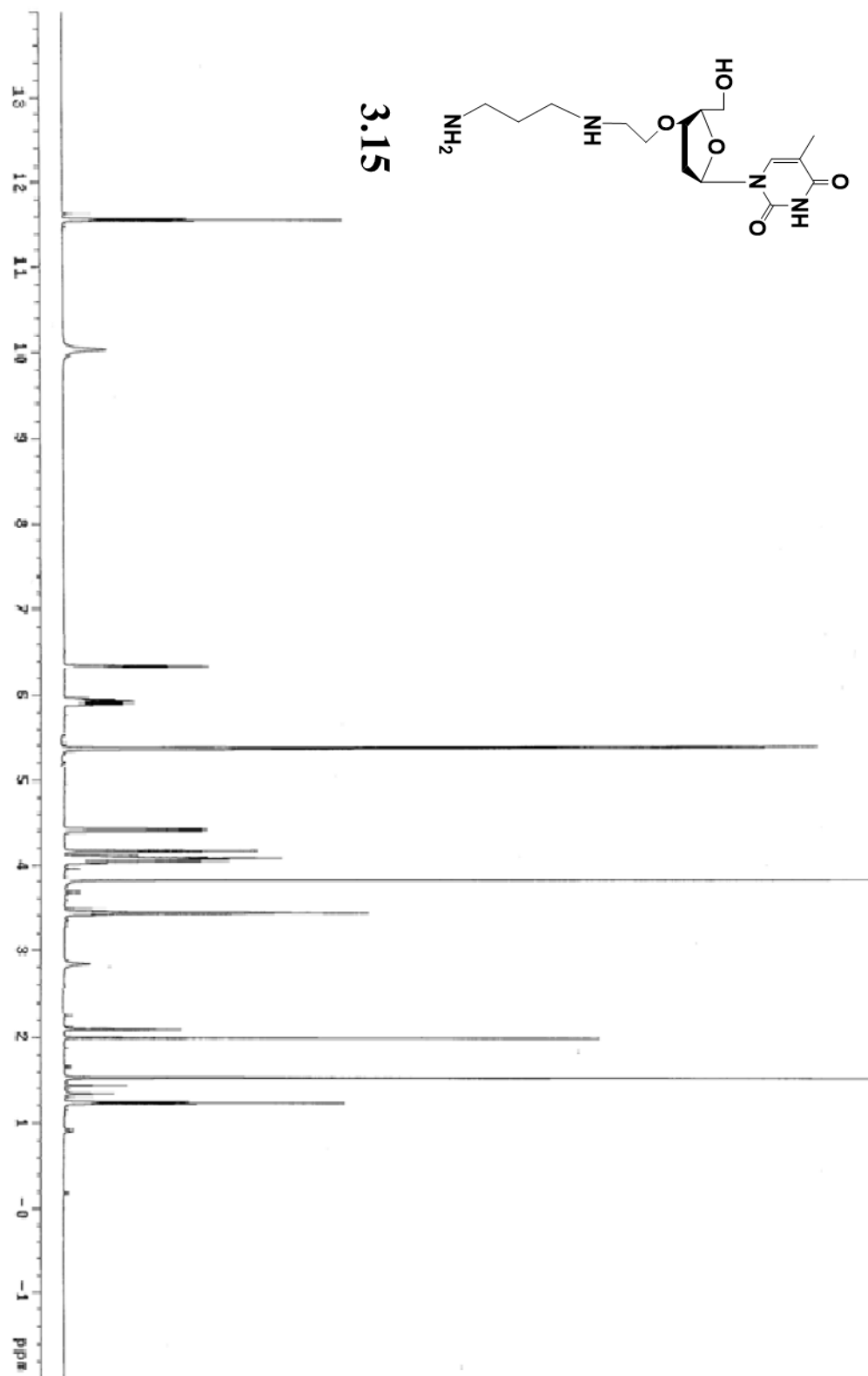
Figure A80. ^{1}H-NMR spectrum of **3.15**
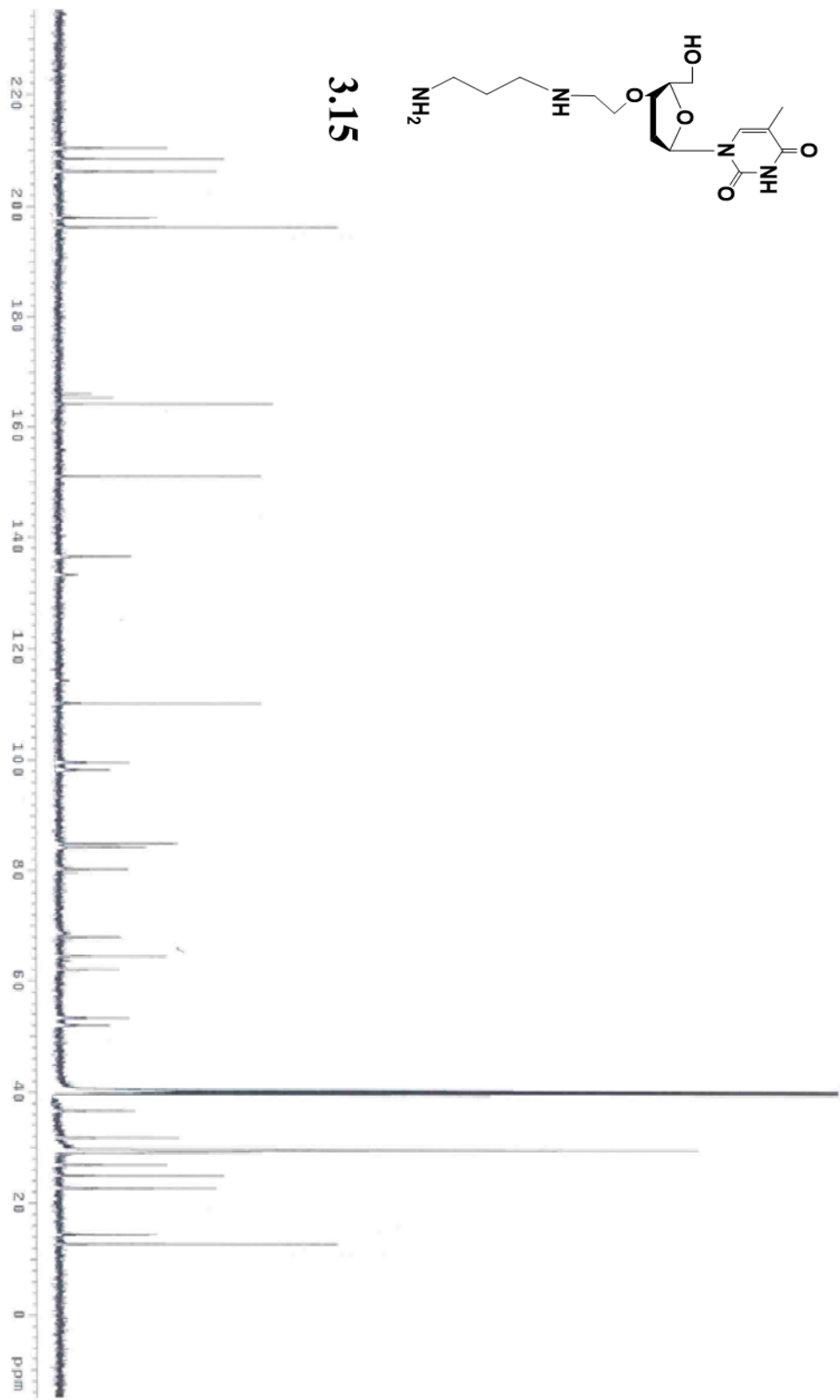
Figure A81. ^{13}C-NMR spectrum of **3.15**
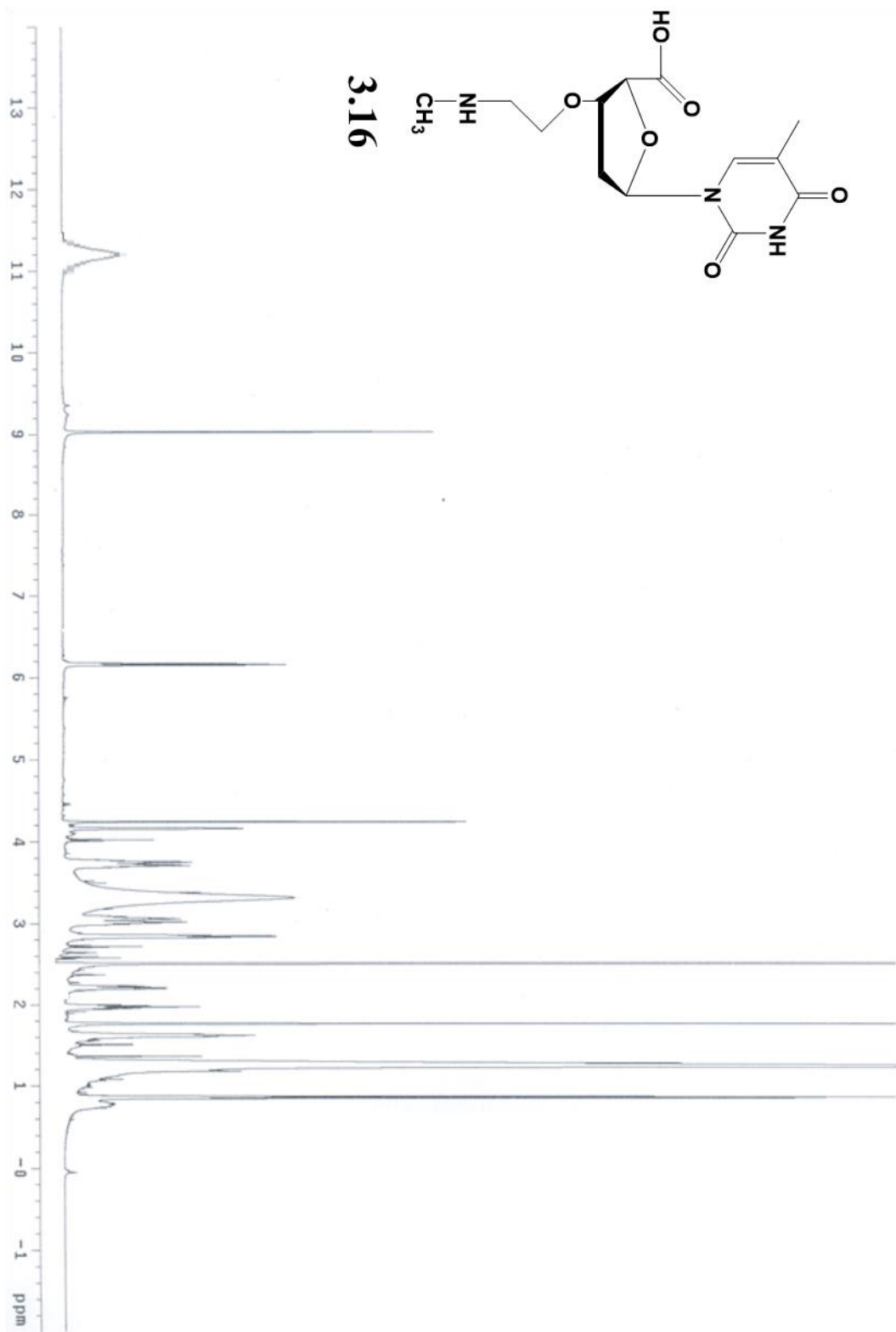
Figure A82. ^{1}H-NMR spectrum of **3.16**
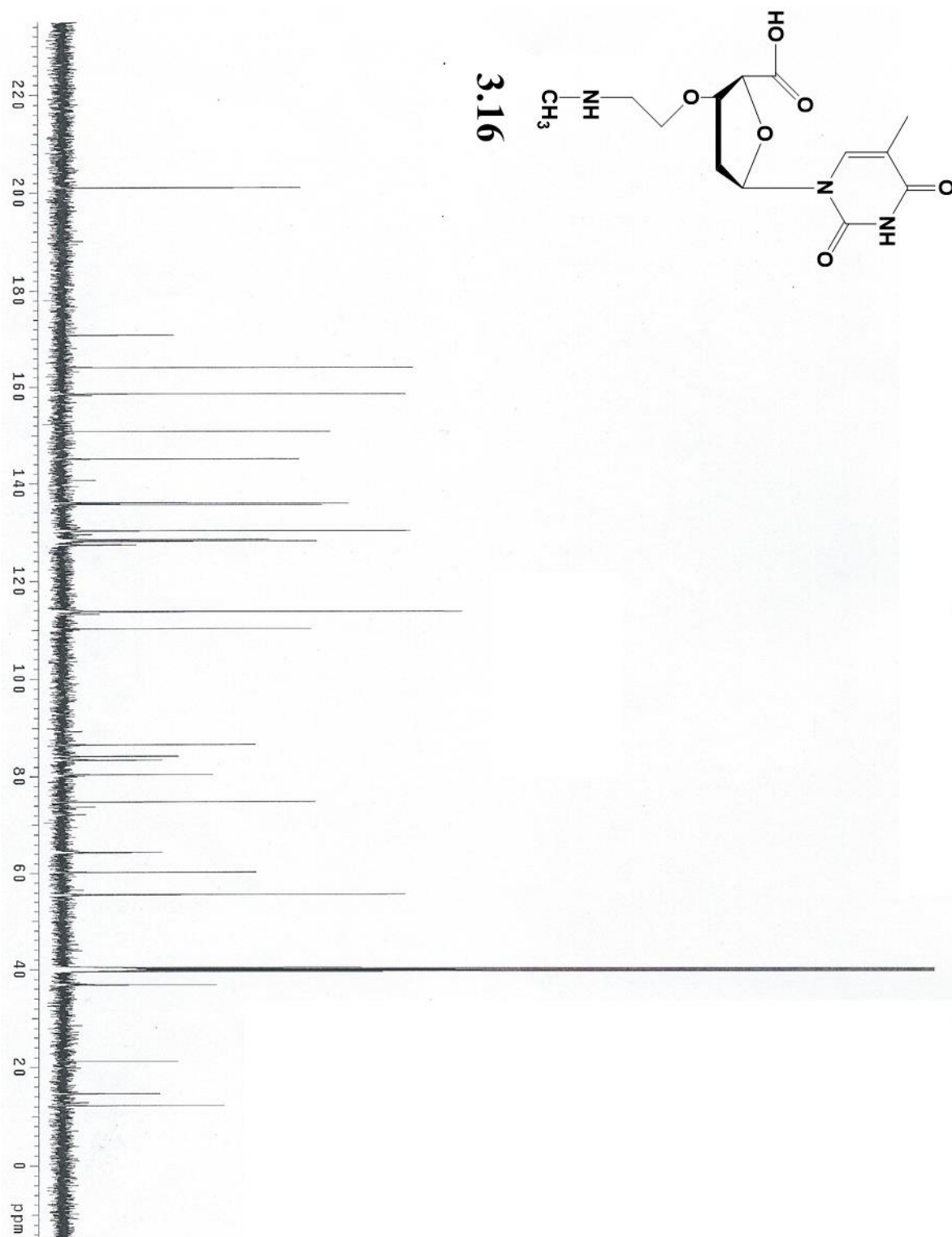
Figure A83. ^{13}C-NMR spectrum of **3,16**
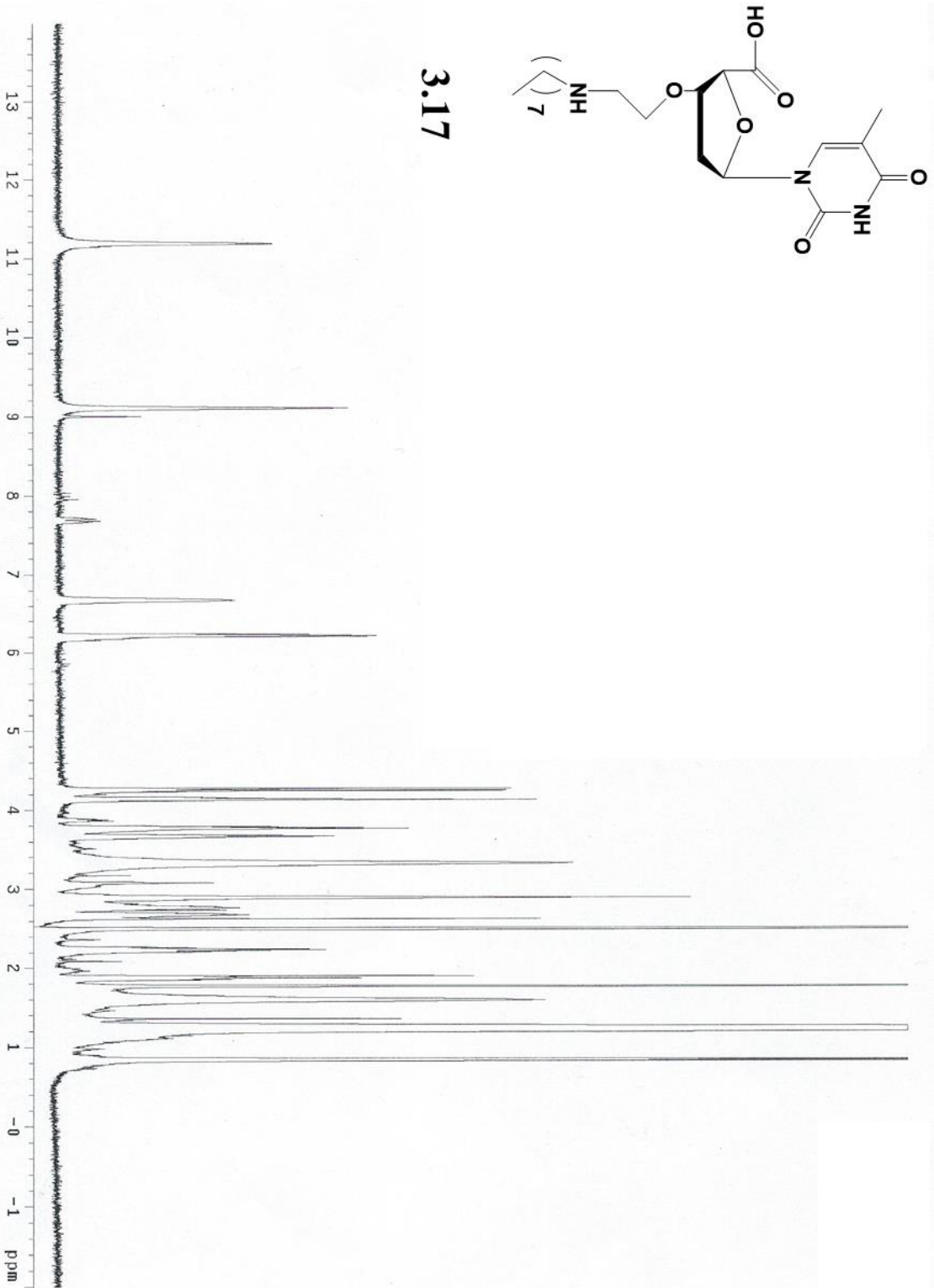
Figure A84. ^{1}H-NMR spectrum of **3.17**
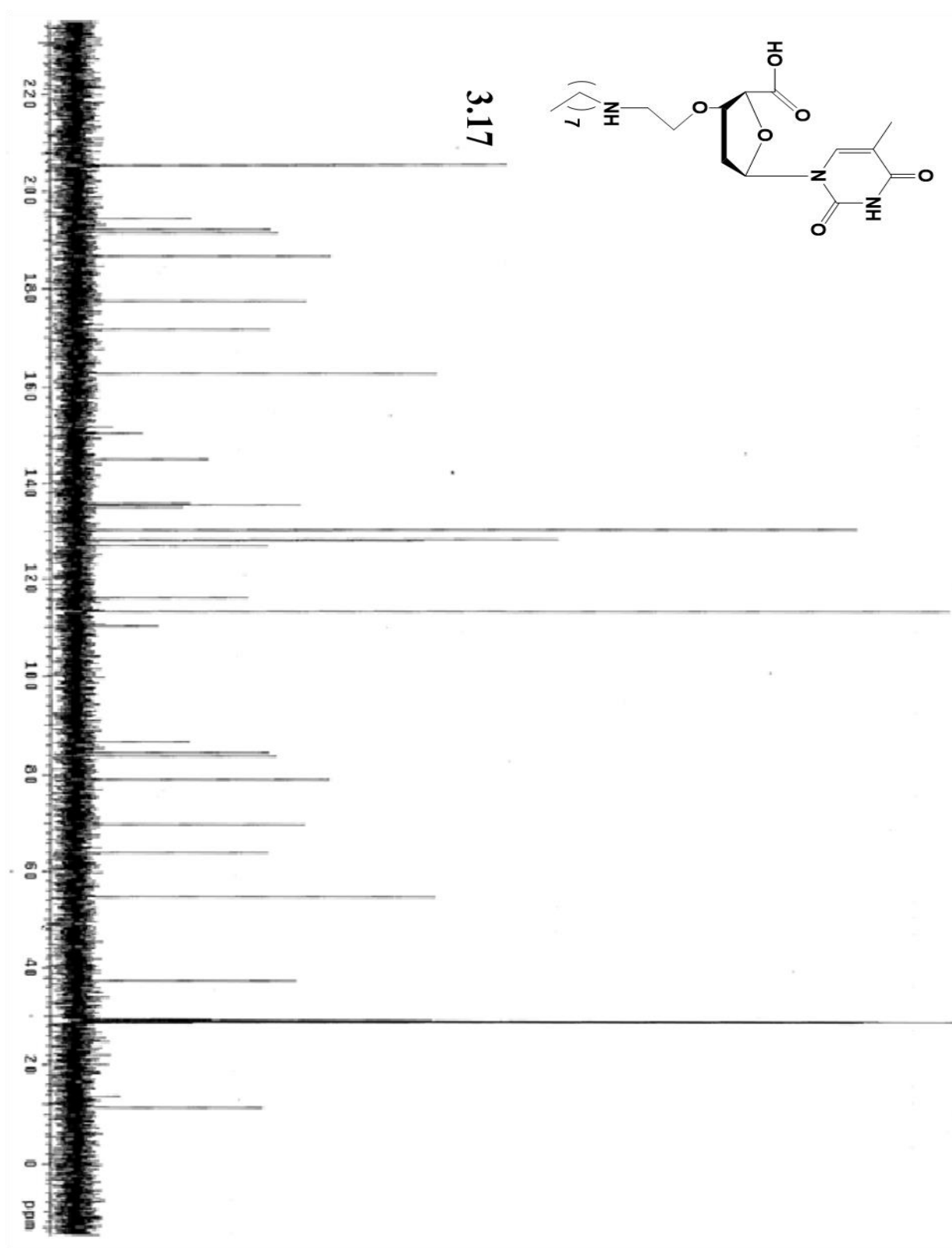
Figure A85. ^{13}C-NMR spectrum of **3.17**
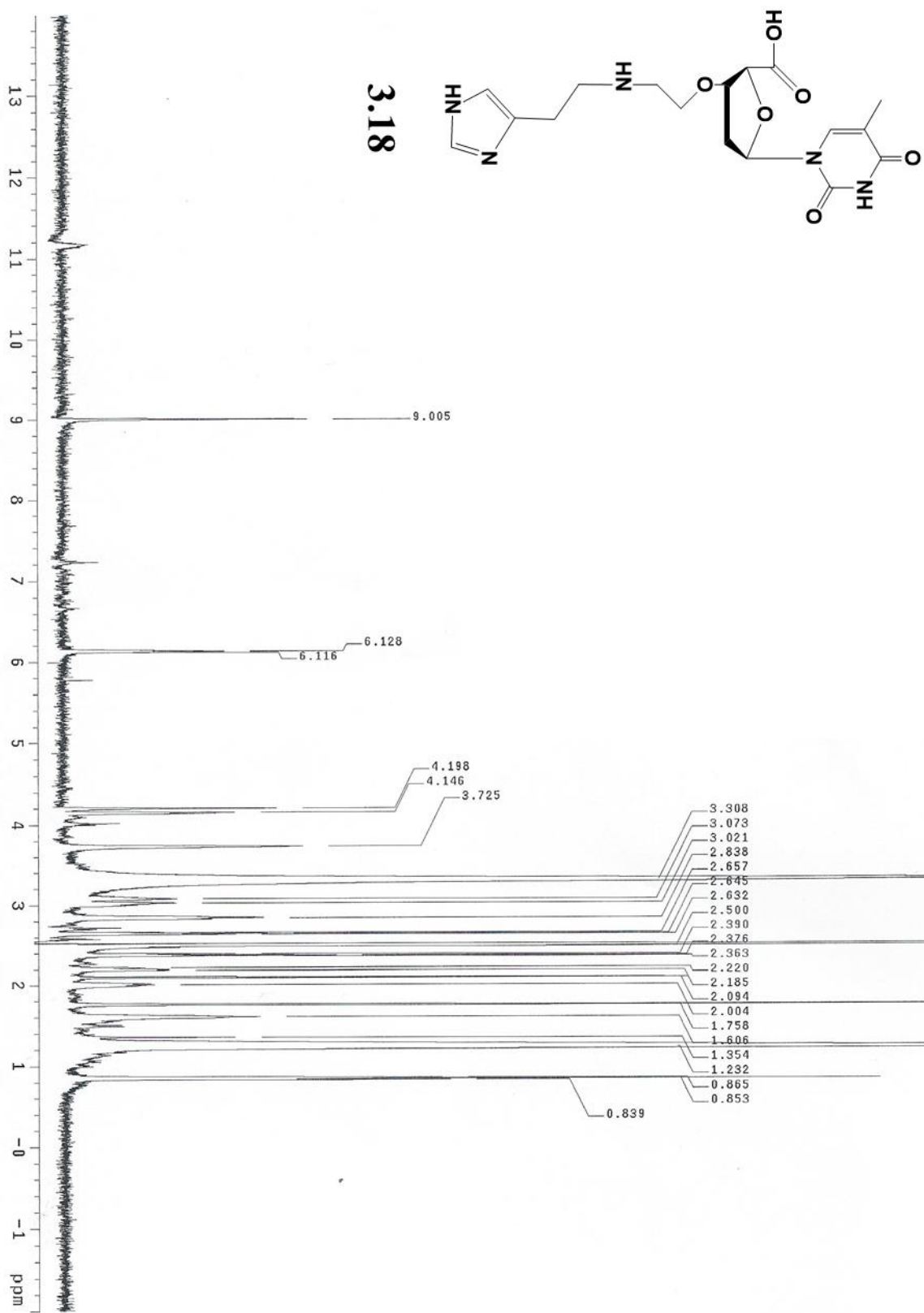
Figure A86. ^{1}H-NMR spectrum of **3.18**

Figure A87. ^{13}C-NMR spectrum of **3.18**

Figure A88. ^{1}H-NMR spectrum of **3.19**
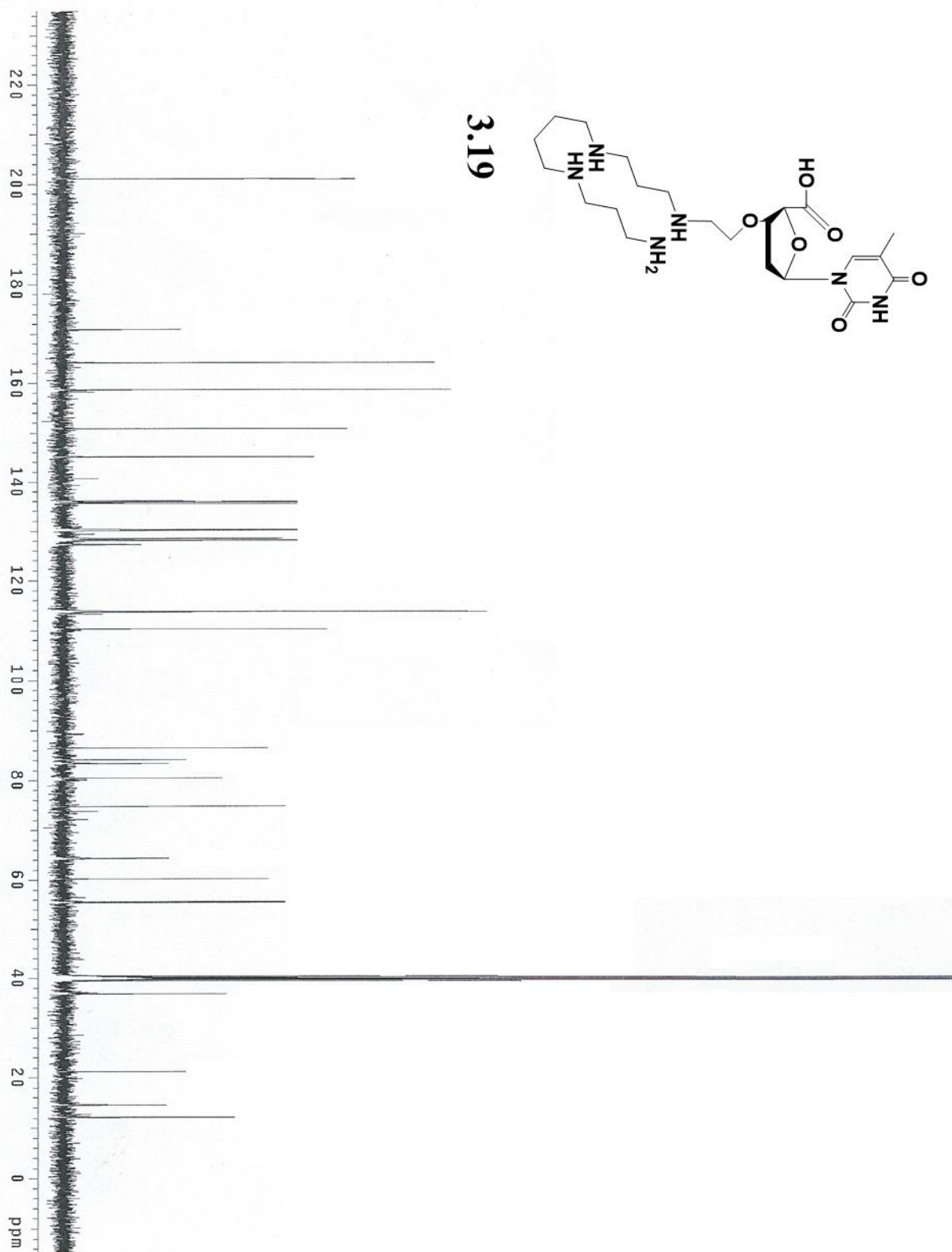
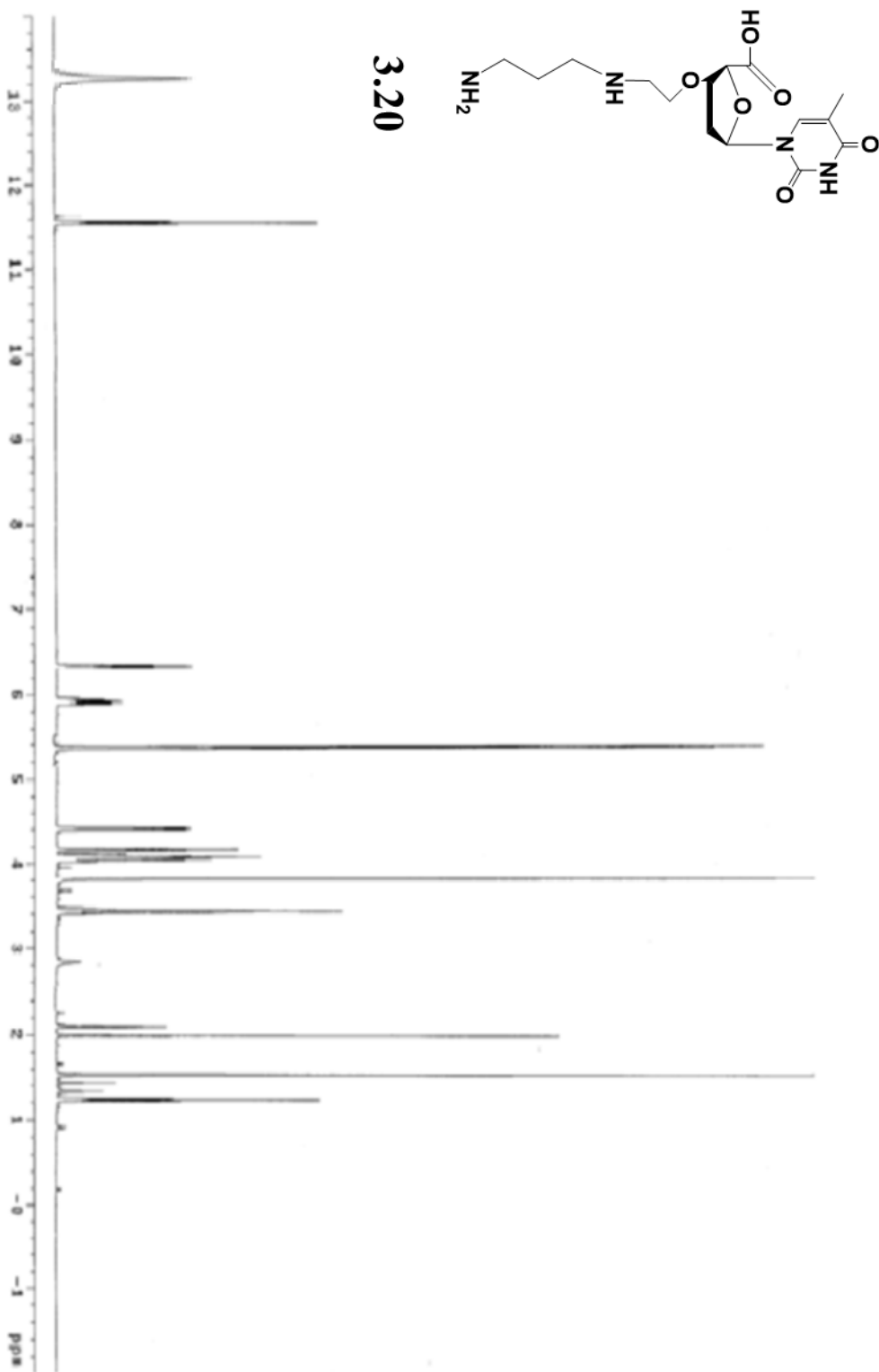**Figure A89.** ^{13}C-NMR spectrum of **3.19**
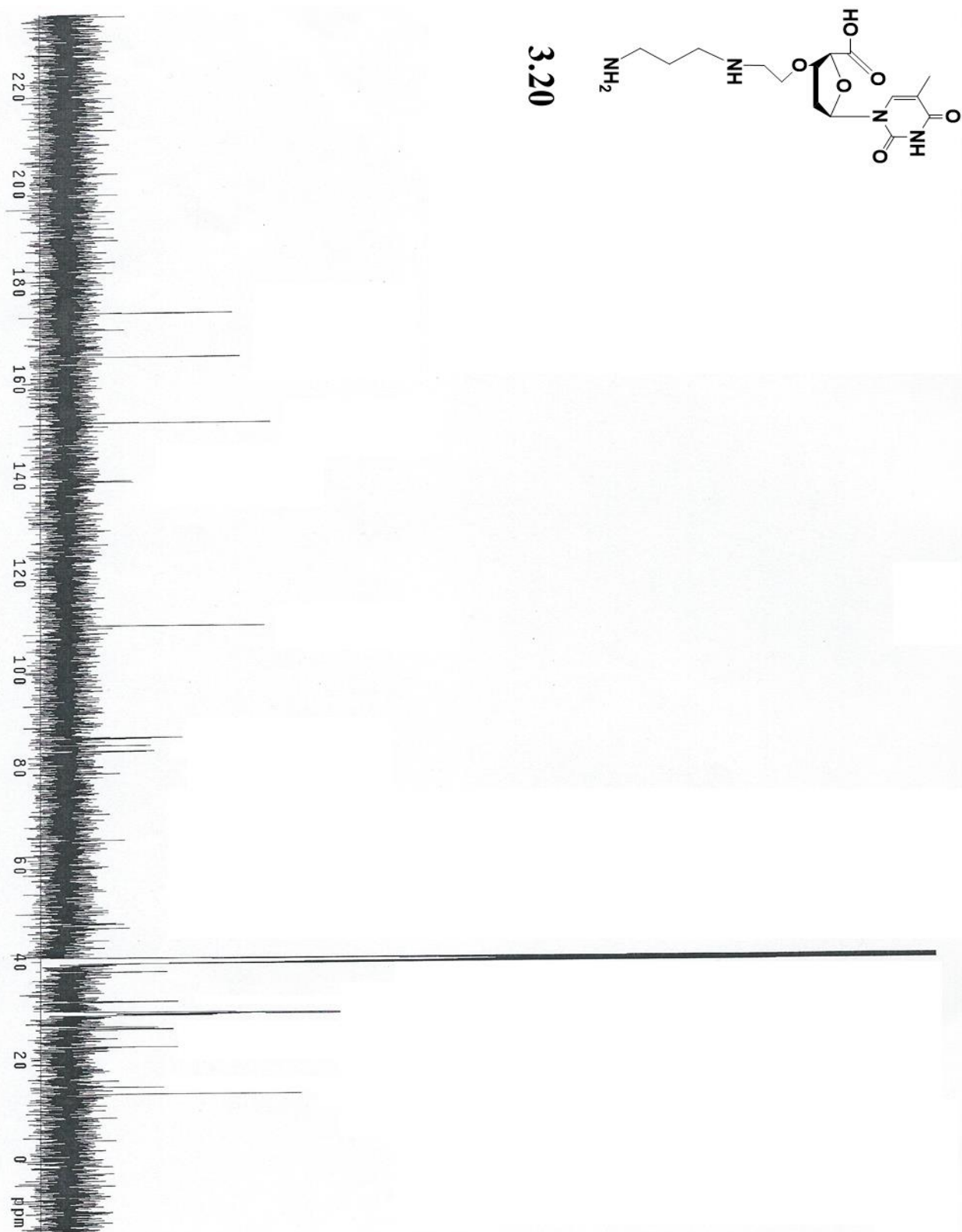
Figure A90. ^{1}H-NMR spectrum of **3.20**

Figure A91. ^{13}C-NMR spectrum of **3.20**